

Investigations on immune sensing of *Staphylococcus aureus* in allergic and inflammatory bowel diseases

Dissertation

der Mathematisch-Naturwissenschaftlichen Fakultät
der Eberhard Karls Universität Tübingen
zur Erlangung des Grades eines
Doktors der Naturwissenschaften
(Dr. rer. nat.)

vorgelegt von

Doğan Doruk Demircioğlu

Tübingen

2014

Tag der mündlichen Qualifikation:

25.02.2015

Dekan:

Prof. Dr. Wolfgang Rosenstiel

1. Berichterstatter:

Prof. Dr. Friedrich Götz

2. Berichterstatter:

Prof. Dr. Andreas Peschel

Table of Contents

Table of Contents	I
Abbreviations	II
Zusammenfassung	1
Summary	3
Publications of the current thesis	5
General introduction	7
1. Staphylococcaceae	7
2. The innate immune system	8
Part I: Innate immune sensing of staphylococcal peptidoglycan	9
Introduction	9
3. Toll-like receptors	9
4. NOD-like receptors	11
5. Dendritic cells, Monocytes and Macrophages	11
6. Peptidoglycan	13
7. Inflammatory Bowel Diseases.....	14
Aim of this study	15
Results	16
Discussion	26
Part II: Adaptive immune response against staphylo-coccal lipoproteins in the context of atopic dermatitis	28
Introduction	28
8. Adaptive immunity.....	28
9. Lipoproteins.....	29
Aim of this study	30
Results	31
Discussion	35
Part III: The role of PGN in the development of food allergies in humans	37
Introduction	37
10. Allergies	37
Aim of this study	38
Results	40
Outlook.....	43
References	45
List of publications	58

Abbreviations

aa	Amino acid
AD	Atopic dermatitis
APC	Antigen presenting cells
Approx.	Approximately
BMDC	Bone marrow-derived dendritic cell
bp	Base pair
BrdU	5-bromo-2'-deoxyuridine
CHS	(T cell-mediated) contact hypersensitivity
CA-MRSA	Community-acquired methicillin-resistant <i>Staphylococcus aureus</i>
CARD	Caspase-recruitment domain
CD	Cluster of Differentiation
DNA	Deoxyribonucleic acid
DSS	Dextran sodium sulfate
Fig.	Figure
FITC	Fluorescein isothiocyanate
FnBPB	Fibronectin binding protein B
GALT	gut associated lymphoid tissue
GlcNAc	N-acetylglucosamine
h	Hour
HA-MRSA	Hospital-acquired methicillin-resistant <i>Staphylococcus aureus</i>
HF	Hydrofluoric acid
iE-DAP	D-γ-glutamyl-meso-DAP dipeptide+
IL	Interleukin
kb	Kilobase
kD	Kilodalton
lip	Lipase
LPP	Lipoprotein
MAMP	Microbial-associated molecular pattern
MALT	Mucosa-associated lymphoid tissue
MD	Morbus Crohn
mDC	Myeloid DC
MDP	Muramyl dipeptide
MDSC	Myeloid-derived suppressor cell

MHC	Major histocompatibility complex
MM6	Mono-Mac-6
MSSA	Methicillin-sensitive <i>Staphylococcus aureus</i>
MurNAc	N-acetylmuramic acid
NF- κ B	Nuclear factor kappa-light-chain-enhancer of activated B cells
NOD	Nucleotide-binding oligomerization domain
OD	Optical density
Ova	Ovalbumin
PAMP	Pathogen-associated molecular pattern
PBP	Penicillin-binding protein
pDC	Plasmacytoid DC
PGN	Peptidoglycan
PGN _{pol}	Polymeric wildtype PGN
PGN _{polΔlgt}	Polymeric PGN derived from the <i>lgt</i> mutant
PP	Propeptide
PRR	Pattern recognition receptor
SP	Signal peptide
Spa	Protein A
T _h	T helper cell
TLR	Toll-like receptor
TNF	Timor necrosis factor
TSLP	Thymic stromal lymphopoietin
UC	Ulcerative colitis
Vs.	versus
WT	Wild type
μ m	Micrometer

Symbols

Δ	Deletion
$^{\circ}$ C	Grad Celsius
μ	Micro
α	Alpha
\emptyset	Mean

Zusammenfassung

Die Erkennung von Bakterien, wie z.B. von *Staphylococcus aureus* (*S. aureus*), durch unser Immunsystem wird durch spezielle keimbahn-codierte „*pattern recognition receptors*“ (PRRs) des angeborenen Immunsystems vermittelt. Diese sogenannten Toll-like-Rezeptoren (TLRs) und NOD-Rezeptoren („*Nucleotide-binding oligomerization domain-containing proteins*“) werden fast ubiquitär auf und innerhalb vieler Zelltypen exprimiert, wie z.B. Epithel- und Immunzellen. Diese Rezeptoren sind in der Lage unterschiedliche und hoch konservierte bakterielle Moleküle zu erkennen, wie z.B. das Lipopolysaccharid (LPS über TLR4), Lipoproteine (LPPs über TLR 2/1 und 2/6 TLR) und, basierend auf der Literatur, auch das Peptidoglycan (PGN über TLR2, PGN-Fragmente über NOD2), welches den Hauptbestandteil der bakteriellen Zellwand darstellt. Das Ziel dieser Arbeit war es die Rolle des PGNs in der Aktivierung des Immunsystems und einen möglichen Einfluss auf Krankheiten, wie atopischer Dermatitis, Morbus Crohn, ulcerativer Colitis und Nahrungsmittelallergien zu eruieren.

Dazu wurde ein neuartiges Verfahren zur Isolierung von hochreinem PGN in ausreichenden Mengen entwickelt und das isolierte PGN und dessen Fragmente, sowie synthetische Lipopeptide, in in-vitro-Zellassays getestet. Wir konnten zeigen, dass beispielsweise reines, polymeres PGN (> 5mer, PGN_{pol}), isoliert aus einer LPP-defizienten *S. aureus* SA113-Mutante (*SA113Δlgt*), keine Immunantwort und Reifung von dendritischen Zellen (DCs) induzierte. Eine Kostimulation von polymerem PGN mit einem TLR2-Liganden, bei dem es sich um LPP-Rückstände innerhalb des PGNs aus einem Wildtyp *S. aureus* (SA113) handelte, führte dahingegen zu einem signifikanten Anstieg der IL-6-, als auch der IL-12p40-Sekretion und der jeweiligen DC-Reifungsmarker (MHC-II, CD40). Eine ähnliche Reaktion konnte auch bei der Stimulation einer Monozyten-Zelllinie (Mono-Mac-6-Zellen) und einer Makrophagen-Zelllinie (J774-Zellen) beobachtet werden.

Nur eine Kostimulation führte zu einer signifikanten IL-8 bzw. TNF- α -Induktion. Ferner führte die kutane *in-vivo*-Applikation von lebenden *S. aureus*-Zellen bei Mäusen zur Inhibierung einer adaptiven Immunantwort durch die Expression von IL-6 und der damit verbundenen Rekrutierung Gr1⁺CD11b⁺ myeloider Suppressorzellen (MDSCs) an die Infektionsstelle. Bedeutender war jedoch, dass die Applikation eines TLR2/6-Liganden (Pam2Cys oder diacylierte LPPs), und nicht die Applikation eines TLR2/1-Liganden (Pam3Cys oder triacylierte LPPs), zur Migration von MDSCs an den Ort der Infektion führte.

Diese MDSC-Rekrutierung reduzierte zudem den Grad der mit der Infektion einhergehenden Schwellung der Ohren der infizierten Mäuse. Diese Ergebnisse liefern eine Erklärung, wie Bakterien in der Lage sein können unsere Haut zu kolonisieren, ohne dabei eine Immunantwort zu induzieren.

Darüber hinaus wurden Ovalbumin-exprimierende Staphylokokken-Stämme (intrazelluläre vs. extrazelluläre Expression) kloniert. Dazu wurde ein xylose-induzierbares Expressionssystem (basierend auf pTX-Vektoren) genutzt und die resultierenden Expressionsvektoren in mehrere Staphylokokken-Stämme transformiert (SA113 Δ *spa*, SA113 Δ *lgt*, SA113 Δ *oatA*, SA113 Δ *tagO*, *S. carnosus* TM300), welche u.a. in der Veränderungen in der Zellwand aufweisen. Die resultierenden Stämme wurden sequenziert und die Ovalbumin-Expression durch Western Blot-Analysen unter Verwendung eines monoklonalen Anti-Ovalbumin-Antikörpers und eines T-Zell-Proliferations-Assays verifiziert.

Summary

Sensing bacteria, such as *Staphylococcus aureus* (*S. aureus*), is based on the ability to recognize them via special germline encoded pattern recognition receptors (PRRs) of the innate immune system, so called Toll-like receptors (TLRs) and Nucleotide-binding oligomerization domain-containing proteins (NODs). These receptors are expressed almost ubiquitously on and inside of several cells types, e.g. epithelial and immune cells. They are able to recognize distinct and highly conserved bacterial molecules, such as lipopolysaccharides (LPS via TLR4), lipoproteins (LPPs via TLR 2/1 and TLR 2/6) and, according to previous literature, peptidoglycan (PGN via TLR2, PGN fragments via NOD2), which is the main constituent of the bacterial cell wall.

The aim of this work was to elucidate the role of PGN in activating the immune system and to investigate its putative role in diseases, such as atopic dermatitis, Morbus Crohn, ulcerative colitis and food allergies.

Therefore, we developed a new method for isolating highly pure PGN in sufficient amounts and tested this molecule and its fragments, along with synthetic lipopeptides, in several *in-vitro* cell assays. For instance, we could show that pure polymeric PGN (>5mer, PGN_{pol}), isolated from a LPP-deficient *S. aureus* SA113 mutant strain (SA113 Δ *lgt*), did not induce an immune response or maturation of murine dendritic cells (DCs). In contrast, co-stimulation of polymeric PGN with a TLR2 ligand, namely LPPs residing within the PGN meshwork of isolated PGN from a wildtype *S. aureus* strain (SA113), led to a significant increase in IL-6, as well as IL-12p40 and the respective maturation markers (MHC-II, CD40). A similar response was observed for stimulation of a monocytic cell line (Mono-Mac-6 cells) and a macrophage cell line (J774 cells), where application of PGN_{pol} alone did not induce the expression and secretion of IL-8 and TNF- α , respectively.

Furthermore, the cutaneous application of *S. aureus in-vivo* suppressed an adaptive immune response by expressing IL-6, which in turn induced and recruited Gr1⁺CD11b⁺ myeloid derived suppressor cells (MDSCs) to the site of infection. More importantly, application of a TLR2/6 ligand (Pam2Cys or diacylated LPPs) elicited the same response *in vivo*, but a TLR2/1 ligand (Pam3Cys or triacylated LPPs) could not achieve the same effect. MDSC recruitment also reduced the degree of ear swelling. These findings provide an explanation for why and how certain bacteria are able to colonize on our skin without inducing an immune response.

In addition, to clarify a putative role of PGN in inducing allergies, ovalbumin-expressing staphylococcal strains (intracellular vs. extracellular expression) have been cloned, using a xylose-inducible expression system (staphylococcal pTX vectors). These constructs were transformed into several staphylococcal strains (SA113 Δ *spa*, SA113 Δ *lgt*, SA113 Δ *oatA*, SA113 Δ *tagO*, *S. carnosus* TM300), which differ in their cell wall composition. The resulting strains were sequenced and the ovalbumin-expression was verified by westernblot analysis using a monoclonal anti-ovalbumin antibody and in T cell proliferation assays. With these strains, we will be able to elucidate a putative role of PGN recognition in inducing or inhibiting allergic responses *in-vitro* and *in-vivo*.

Publications of the current thesis

Paper I:

Daniel Kühner, Mark Stahl, **Doğan D. Demircioğlu**, Ute Bertsche

From cells to muropeptide structures in 24 h: Peptidoglycan mapping by ULPC-MS

Sci Rep. 2014 Dec 16;4:7494. doi: 10.1038/srep07494

Paper II:

Holger Schäffler*; **Doğan D. Demircioğlu***; Daniel Kühner; Sarah Menz; Annika Bender; Ingo B Autenrieth; Peggy Bodammer; Georg Lamprecht; Friedrich Götz; Julia-Stefanie S. Frick

NOD2 Stimulation by Staphylococcus aureus-Derived Peptidoglycan Is Boosted by Toll-Like Receptor 2 Costimulation with Lipoproteins in Dendritic Cells.

Infect. Immun. November 2014 vol. 82 no. 11 4681-4688

*H.S. and D.D.D. contributed equally to this article.

Paper III:

Yuliya Skabytska, Florian Wölbing, Claudia Günther, Martin Köberle, Susanne Kaesler, Ko-Ming Chen, Emmanuella Guenova, **Doruk Demircioğlu**, Wolfgang E. Kempf, Thomas Volz, Hans-Georg Rammensee, Martin Schaller, Martin Röcken, Friedrich Götz and Tilo Biedermann

Cutaneous Innate Immune Sensing of Toll-like Receptor 2-6 Ligands Suppresses T Cell Immunity by Inducing Myeloid-Derived Suppressor Cells

Immunity Volume 41, Issue 5, p762–775, 20 November 2014,

<http://dx.doi.org/10.1016/j.immuni.2014.10.009>

Contributions to publications

Paper I:

From cells to muropeptide structures in 24 h: Peptidoglycan mapping by ULPC-MS

Daniel Kühner invented this method and discussed preliminary results with me. In addition, I did HPLC analysis with different bacterial strains to reproduce and verify this method. Daniel Kühner transferred it to the UPLC and Mark Stahl did the MS and TIC analysis. Finally, I contributed to the manuscript by writing and proof reading.

Paper II:

NOD2 Stimulation by Staphylococcus aureus-Derived Peptidoglycan Is Boosted by Toll-Like Receptor 2 Costimulation with Lipoproteins in Dendritic Cells

The initial idea for this work came from Holger Schäffler. We designed the study, in close agreement with Julia Frick and Friedrich Götz, and wrote the manuscript. I isolated pure and LPS-free PGN and its fragments and performed several MM6 assays, whereas Holger Schäffler was responsible for DC assays and FACS analysis. Annika Bender conducted J774 assays and additional MM6 assays. The remaining authors contributed to the manuscript.

Paper III:

Cutaneous Innate Immune Sensing of Toll-like Receptor 2-6 Ligands Suppresses T Cell Immunity by Inducing Myeloid-Derived Suppressor Cells

I provided WT and mutant, as well as my ovalbumin-expressing *S. aureus* strains (ovalbumin data were unfortunately not included in the final manuscript) and participated in manuscript preparation.

Contributions to manuscripts

Minh-Thu Nguyen *et al.* (2014), in preparation

The vSA α specific lipoprotein like cluster (lpl) of S. aureus USA300 contributes to immune stimulation and invasion in human cells

I established the MM6 assay used for this publication, advised Minh-Thu Nguyen in cell culture and ELISA assays and contributed to the manuscript.

General introduction

1. Staphylococcaceae

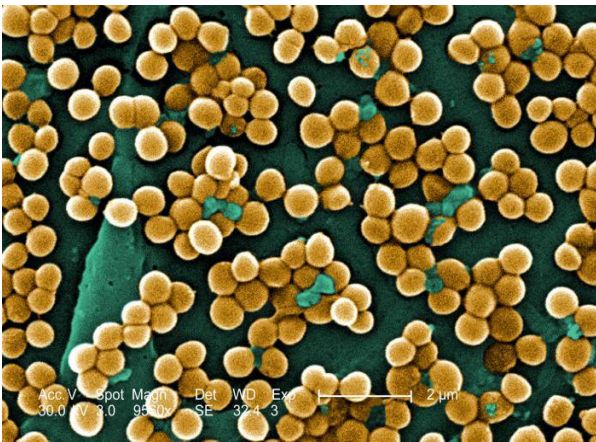


Fig. 1: Clusters of *S. aureus*, colored electron micrograph, Magnitude. ~ 5000x, (source: phil.cdc.gov)

Staphylococci (Greek: σταφυλή, *staphylē*, "bunch of grapes" and κόκκος, *kókkos*, "granule") are gram-positive, immotile, non-sporeforming, facultative anaerobic bacteria, and classified under phylum firmicutes (**Fig. 1**).

They are mostly catalase-positive and oxidase negative with a size between 0.5 to 1.5 μm .

As their name implies, staphylococci mostly

occur in "grape-like" clusters. Their genome size varies between 2 – 3 Mb with an average GC content between of 33 – 40 mol% (Götz *et al.*, 2006). *Staphylococcus aureus* (*S. aureus*) SA113 represents an intensively studied catalase-positive strain whose colonies are yellow due to the presence of staphyloxanthin. Together with *S. epidermidis*, it is found in normal human skin flora, mostly found in the nasal cavities, where it populates around 80 % of the human population (20% long-term and 60 % intermittent carriers) (Kluytmans *et al.*, 1997). In healthy adults, this colonization does not cause any problems. However, in some cases, such as in immunocompromised patients, *S. aureus* can cause severe infections e.g., osteomyelitis, endocarditis and sepsis. (Lowy, 1998).

S. aureus utilizes a vast range of molecular tools to colonize on different surfaces, to invade host cells and to evade the immune system. These tools include a variety of secreted toxins (e.g. enterotoxins, Panton-Valentine leukocidin, hemolysins, toxic shock syndrome toxin 1 and many more) and enzymes (e.g. proteases, nuclease and hyaluronidases) to lyse and disrupt host cells and tissues. Moreover, *S. aureus* expresses surface-bound adherence factors to facilitate extra- and intracellular movement and spreading, such as fibronectin-binding proteins A and B (FnbpA/B).

Furthermore, *S. aureus* is a highly adaptable bacterium, as it can change its physiology to survive under different unfavorable circumstances; this is achieved by the formation of biofilms or the induction of persister cells, so called small colony variants. (Götz, 2002; Fedtke *et al.*, 2004; Foster, 2005; Proctor *et al.*, 2006; Veldkamp and van Strijp, 2009).

In addition, the rise of hospital- or community-acquired Methicillin-resistant *Staphylococcus aureus* (HA/CA-MRSA) infections, caused by highly virulent and multi-resistant strains, is a serious, global threat for public health (Deurenberg and Stobberingh, 2009) and underlines the importance of intensive studies on staphylococci.

2. The innate immune system

The human immune system is a complex molecular and cellular defense machinery that protects our bodies from harmful agents, such as bacterial pathogens and it also maintains immune homeostasis. It is divided into two parts, the so called innate (nonspecific) and the adaptive (or acquired) immune system. The **innate immune** system acts as the body's first line defense, as it comprises a combination of different physical, chemical and biological barriers. It utilizes several specialized cells and mechanisms to attack invading and potential pathogenic microorganisms. Its function relies on germline-encoded pattern-recognition receptors (PRR), which sense highly conserved molecular patterns made by molecules present on the surface of bacteria, fungi or parasites (Medzhitov, 2001). These structures or molecules are called Pathogen-associated molecular patterns (PAMPs) or, to be more precise, Microbial-associated molecular patterns (MAMPs) (Ausubel, 2005; Didierlaurent *et al.*, 2005), which will be introduced in more detail in the next paragraph. The ingestion and following presentation of MAMPs by specialized immune cells leads to a subsequent expression and secretion of immune modulators, such as chemokines and cytokines (Jr. and Medzhitov, 2003), which in turn, orchestrate the adaptive immune system with the aim to clear an ongoing infection.

Part I: Innate immune sensing of staphylococcal peptidoglycan

Introduction

3. Toll-like receptors Microbial-associated molecular patterns (MAMPs) are very important and highly conserved molecules of microorganisms, and can be recognized by a variety of PRRs to trigger a subsequent immune response (Akira *et al.*, 2006). Therefore, they are considered to be potent inducers of an innate immune response. A very important class of PRRs are Toll-like receptors (TLRs), which are highly conserved, membrane-associated and non-catalytic proteins found ubiquitously in almost all cells from worms, such as *Caenorhabditis elegans*, up to humans (Janeway and Medzhitov, 2002).

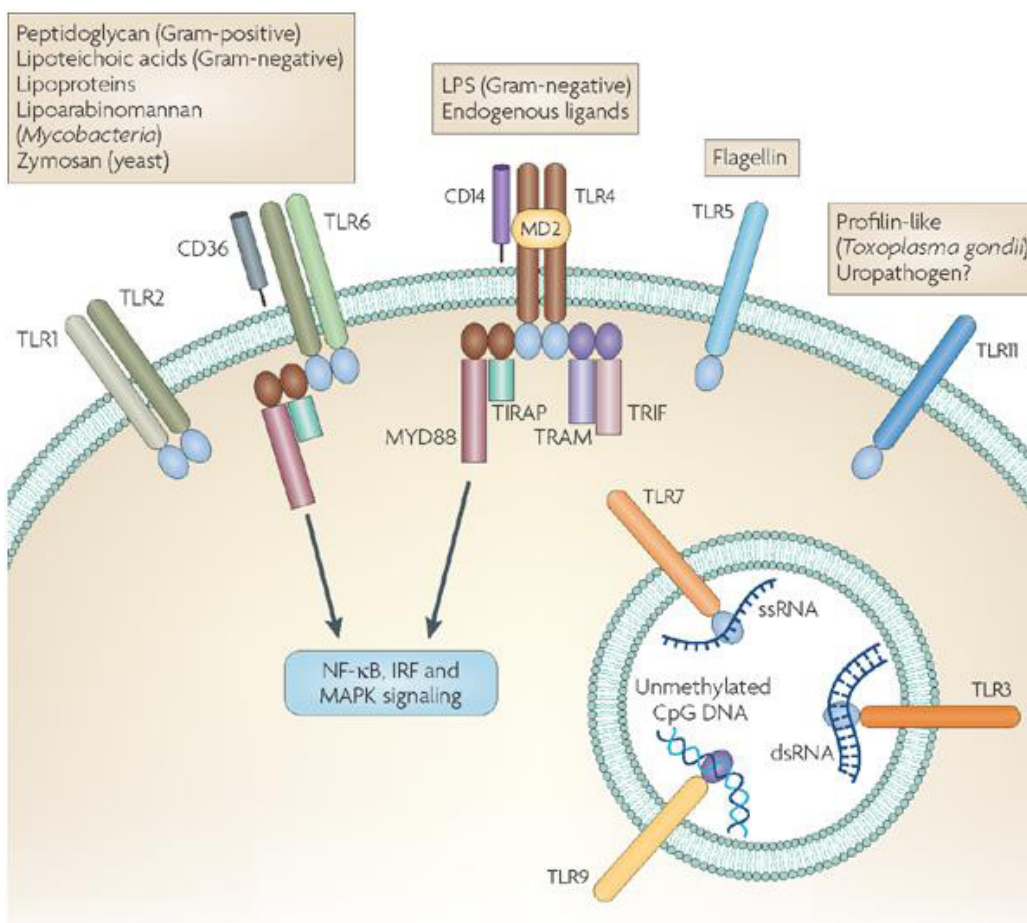


Fig. 2: Overview of human Toll-like receptors (Rakoff-Nahoum and Medzhitov, 2008)

At present, 12 different TLRs were identified, 10 of them in humans and 2 in mice (Akira *et al.*, 2006) and can be surface-bound (TLR1, 2, 4, 5 and 6) or found in intracellular compartments, such as endosomes (TLR3, 7, 8 and 9) (Matsumoto *et al.*, 2003; Akira and Takeda, 2004), or both. An overview of known TLRs in humans is shown in **Fig. 2**. TLRs consist of a characteristic cytoplasmic Toll-IL-1 receptor (TIR) domain, which is important for cell signaling and a cytoplasmic leucine-rich repeats (LRR) domain, responsible for ligand binding. Binding of a specific MAMP or ligand to its appropriate TLR binding domain initiates a signal cascade, leading to the induction of genes involved in innate immune response. These signal cascades involves two different adaptor molecules, called myeloid differentiation primary response protein 88 (MyD88) and TIR domain-containing adaptor protein inducing IFN β (TRIF) (Gay *et al.*, 2014). This leads to an upregulation of TLR genes, which induces the expression of TLR proteins within the infected cell, secretion of pro-inflammatory mediators, such as cytokines and chemokines, and antimicrobial peptides (Aderem and Underhill, 1999; Jr and Medzhitov, 2002). These molecules will in turn recruit more professional phagocytes and to the site of infection. Finally, this results in an inflammation with the five cardinal signs: calor (heat), rubor (redness), dolor (pain), tumor (swelling) and function laesa (limited function) (Lucignani, 2007). There are a multitude of known TLR ligands, such as the well-known lipopolysaccharide of Gram-negatives (Hoshino *et al.*, 1999) or flagellin (Gupta *et al.*, 2014), the main constituent of bacterial flagella, which is recognized by TLR5. Diacylated LPPs from *S. aureus* are recognized by a heterodimer of TLR2/6, whereas triacylated LPPs are recognized by TLR2/1 (Hirschfeld *et al.*, 2001; Akira, 2003). Other MAMPs are oligodeoxynucleotides (CpG DNA), single-stranded RNA (ssRNA), double-stranded RNA (ds RNA) and PGN. The latter is still subject to debate, because of its yet unknown minimal structure that binds to the LRR domain of TLR2 and recent papers, which could show that PGN is not sensed via TLR2 (Schäffler *et al.*, 2014).

In addition, it could be shown that small PGN fragments, such as muramyl dipeptide (MDP) are recognized by other intracellular PRRs, namely nucleotide-binding oligomerization domain-containing (NOD) proteins (Chamaillard *et al.*, 2003; Girardin *et al.*, 2003).

4. NOD-like receptors

Mammalian nucleotide-binding oligomerization domain-containing (NOD) proteins belong to the NOD-like receptor family of PRRs and function as cytosolic sensors for innate recognition of microorganisms and regulation of inflammatory responses, as well as the induction of apoptosis (Inohara and Nuñez, 2003). Therefore NOD ligands have to be internalized into the cells by processes like phagocytosis, in order for it to be accessible for recognition (Aderem and Underhill, 1999). Two well-known representatives of this protein family are NOD1 and NOD2. Both consist of an N-terminal caspase-recruitment domain (CARD), a central Nod domain and a C-terminal LRR domain, similar to TLRs. NOD1 and NOD2 recognize distinct PGN fragments. NOD1 senses D- γ -glutamyl-meso-DAP dipeptide (iE-DAP), which is a fragment of Gram-negative PGN (with some exceptions), whereas NOD2 recognizes muramyl dipeptide (MDP), a PGN fragment consisting of MurNAc with its lactic acid moiety linked to the N-terminus of an L-alanine-D-isoglutamine dipeptide. This structure can be found in almost all bacteria (Chamaillard *et al.*, 2003).

5. Dendritic cells, Monocytes and Macrophages

Professional antigen-presenting cells (APCs), like **dendritic cells** (DCs) play a crucial role in activating immune responses. DCs can be divided into two main subsets: cluster of differentiation (CD) 11c⁺ myeloid DCs (mDC) and CD11c⁻ plasmacytoid DCs (pDC) (McKenna *et al.*, 2004; Kadowaki, 2007). DCs are considered as so called sentinel cells, as their function mainly concerns scanning their environment for non-self antigens or possible threats.

When a DC detects such an antigen, it is internalized, processed and finally fragments of the initial antigen are presented on major histocompatibility complex II (MHC II) molecules to naïve CD4⁺ or CD8⁺ T cells within the peripheral lymph nodes. After recognition of the processed antigens, T cells start to mature and activate other immune cells (in the case of CD4⁺ cells) or kill infected cells (in the case of CD8⁺ cells) (Lipscomb and Masten, 2002; Shin *et al.*, 2006). Important cytokines, which are produced during this process, are interleukin 12 (IL-12) and type I interferons (IFN- α/β). IL-12 acts as a T cell stimulating factor that directs T helper cells (Th) towards a Th1 response (amplification of macrophage and CD8⁺ T cell activation) (Hsieh *et al.*, 1993). DCs are also capable of inducing a Th2, such as in the presence of thymic stromal lymphopoietin (TSLP) (Kadowaki, 2007). Therefore, DCs constitute a major link between innate and adaptive immunity. Another APC type is called **monocytes**, which express the typical marker cluster of differentiation (CD) 14 and potent producers of tumor necrosis factor alpha (TNF- α) (Ziegler-Heitbrock, 2007). They originate, like all cells of the immune system, from a pluripotent hematopoietic stem cell and more precisely, from a myeloid progenitor cell. Mature monocytes circulate in the blood and recent findings show that there is also a splenic reservoir of monocytes, where half of them are stored (Swirski *et al.*, 2009). They migrate to tissues, especially in the case of an inflammation, and differentiate into **macrophages**, as well as DCs, thus replenishing the tissue macrophage and DC populations (Gordon and Taylor, 2005). In our studies, we used a human monocytic cell line, called Mono-Mac-6 (MM6), which are clones of monocytes established from peripheral blood of a patient with monoblastic leukemia (Ziegler-Heitbrock *et al.*, 1988) and the J774 murine macrophage cell line (Ralph and Nakanishi, 1975).

6. Peptidoglycan

The cell wall of Gram-positive and Gram-negative bacteria differ in its structure and composition from one another. Gram-negative bacteria possess an inner and an additional outer membrane, which are separated by the so called periplasm and finally surrounded by a thin peptidoglycan (PGN) layer. This

layer consists usually of one - three molecules and has a thickness between 1.5 – 15 nm, whereas the cell wall of Gram-positive bacteria possess about 30 - 40 layers with an overall thickness of approximately 15 – 30 nm lacking a outer-membrane

(Vollmer *et al.*, 2007; Silhavy *et al.*, 2009). The PGN molecule is composed of a disaccharide backbone of alternating β -(1,4) linked N-acetylglucosamine (GlcNAc) and N-acetylmuramic acid (MurNAc), both

D-glucose derivatives. This glycan backbone is additionally cross-linked by a stem peptide that consists of five amino acids (aa), while it is synthesized. During the so-called transpeptidation reaction, which is catalyzed by penicillin-binding proteins (PBPs), the terminal D-alanine is separated to generate the energy needed to connect one stem-peptide to the other and hence also the glycan strands. This leads to the formation of a three dimensional network (Lovering *et al.*, 2012), which gives the cell its shape and protects it from the environment.

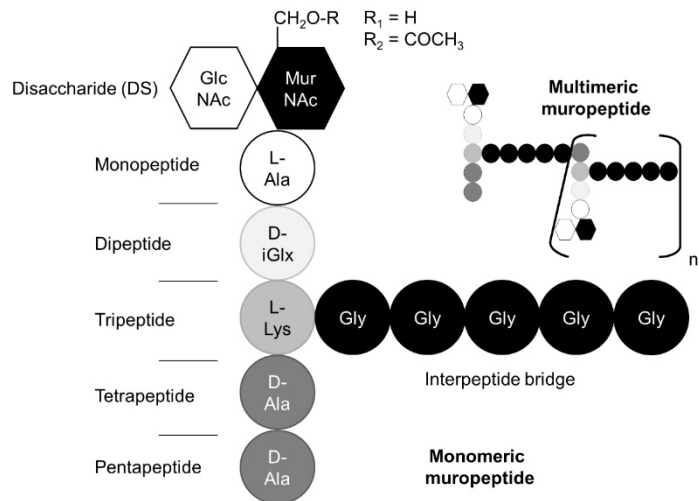


Fig. 3: Schematic structure of muropeptides of *S. aureus*

The minimal structure consists of the disaccharide (GlcNAc-MurNAc) with an adjacent stem peptide (L-Ala – D-iGlx – L-Lys/mDap – D-Ala – D-Ala) with Glx being either Gln or Glu. Our model organism *S. aureus* harbors also a pentaglycine interpeptide bridge branching from the L-Lys, which constitutes indirect cross-links between two adjacent stem peptides, as it is depicted in the multimeric muropeptide. (Kühner *et al.*, 2014, accepted in Scientific Reports)

In the case of *S. aureus*, these aa are L-alanine, D-glutamic acid, L-lysine and D-alanine (**Fig.3**). This tetrapeptide is amidated to the D-lactyl group of MurNAc and additionally cross-linked via a pentaglycine bridge to ensure stability (BERGERBACHI and TSCHERSKE, 1998; Barreteau *et al.*, 2007). Furthermore, *S. aureus* PGN is also modified at the C6 position of MurNAc is O-acetylated, which makes the PGN resistant to lysozyme (Bera *et al.*, 2005), an enzyme that hydrolyzes the β -(1,4) linkage between MurNAc and GlcNAc.

7. Inflammatory Bowel Diseases

Inflammatory bowel diseases (IBD) describe several idiopathic pathological conditions of the digestive tract, which belong to the class of autoimmune diseases. Some examples include ulcerative colitis (UC), an inflammation of the colon and rectum with an incidence of 24.3 per 100,000 person-years; another example would be a well-studied disease called Morbus Crohn (MD), which affects the whole gut, with an incidence of 12.7 per 100,000 person-years in Europe (Baumgart and Carding, 2007; Molodecky *et al.*, 2012). There are many possible factors, which can lead to a self-reacting gut associated lymphoid tissue (GALT) and thus IBD.

Main factors are most likely, alterations of the gut microbiome (Mukhopadhyia *et al.*, 2012) and genetic factors (Jostins *et al.*, 2012). For instance, insertion mutations of the PRR NOD2 do play an important role in the pathogenesis of Morbus Crohn (Hampe *et al.*, 2001). At present, there is no cure yet and therapy of IBD is based on immunosuppression to alleviate symptoms. Future therapies will utilize a method called fecal microbiota transplantation (FMT). In this approach, the microbiota isolated from the feces of healthy individuals is transferred to patients. Recent results were quite promising (Aroniadis and Brandt, 2013).

Aim of this study

The question, whether PGN is a TLR2 ligand or not, is still discussed. Many papers generated clear data strengthening the hypothesis that PGN, or fragments of this macromolecule, are not just sensed by NOD-like receptors, such as NOD1 and NOD2, but also via TLR2 (Girardin *et al.*, 2003; Chamailard *et al.*, 2003; Ajuwon *et al.*, 2009; *et al.*, 2009; Volz *et al.*, 2010; Müller-Anstett *et al.*, 2010). In contrast, Travassos *et al.* showed that sensing of PGN did not occur via TLR2.

Because of this ambiguity and the fact that most studies used PGN obtained from Sigma-Aldrich (which is known to be contaminated), we conducted our studies to elucidate, whether PGN is certainly sensed by TLR2 or whether the activation of immune cells originates from possible TLR2 activation by contaminants, such as LPPs. Therefore, we developed a new PGN isolation and analysis method to enable us to isolate sufficient amounts of PGN. We were also interested in the consequences concerning the interaction between NOD2 and TLR2 activation in the context of IBDs. Therefore, we studied the role of NOD2 mediated activation of DCs via natural *S. aureus* derived PGN and investigated the effect of combined NOD2 and TLR2 stimulation, compared to single stimulation of the NOD2 receptor alone. PGN fragments with a low degree of cross-linking, such as PGN monomers and MDP, have been shown to represent natural ligands for the NOD2 receptor (Volz *et al.*, 2010) and even cure mice from experimental colitis (Watanabe *et al.*, 2008), implicating an important role in the pathophysiology of IBDs. Therefore, we focused on the effect of polymeric staphylococcal PGN fragments (named PGNpol) in the activation of the innate immune system and additionally investigated the impact of PGNpol recognition in a DSS-colitis mouse model.

Results

Basically, there were just two methods so far, which have been used for PGN isolation ever since. The first method was developed for the analysis of PGN of Gram-negative bacteria (Glauner *et al.*, 1988) and the second method was transferred and adjusted to the thicker PGN of Gram-positives (de Jonge *et al.*, 1992). However, these two basic methods are very time consuming, utilizing dangerous chemicals (e.g. hydrofluoric acid (HF)) and yield very low amounts of PGN (ø 6 – 8 mg, depending on the volume of the culture). These sample limitations also complicated subsequent HPLC analysis of any possible alteration of the cell wall pattern during different physiological conditions. For our studies, there was an additional need for large amounts of highly pure PGN and its fragments, free of any possible contaminant, such as DNA, RNA, LPS and very important, lipoproteins, which are known to be TLR2 ligands. (Stoll *et al.*, 2005; Schmalzer *et al.*, 2009; Schmalzer, 2010). To overcome these experimental limitations, we developed a new method for fast isolation and high throughput analysis of highly pure PGN. Therefore, we modified the mentioned basic methods by omitting unnecessary boiling and centrifugation steps. We replaced ultra-centrifugation by normal centrifugation and finally, substituted the final 48 h of HF treatment for removing wall teichoic acids (WTA) by a simple 4 h hydrochloric acid (HCl) treatment, which in turn rendered many subsequent washing steps unnecessary (Paper I: Kühner *et al.*, 2014, accepted in Scientific Reports). The large number of omitted washing steps enabled us to increase the amount of isolated PGN up to 600 mg from a one liter *S. aureus* overnight culture. Moreover, the whole method was designed for performing in Eppendorf cups or even microtiter plates to analyze up to 96 samples in parallel. Next, we transferred the subsequent chromatographical procedure to an ultra-pressure liquid chromatography (UPLC) system, which firstly reduced the amount of samples and solvents

and secondly, the total time of analysis by the factor of 2,5 (70 minutes vs. 180 minutes). To prove our method, we isolated PGN of several species, e.g. *S. aureus* and *E. coli*, and digested it with mutanolysin or lysozyme, respectively. The muramidases mutanolysin and lysozyme are used to cleave the β -(1,4)-glycosidic bonds within the glycan backbone,

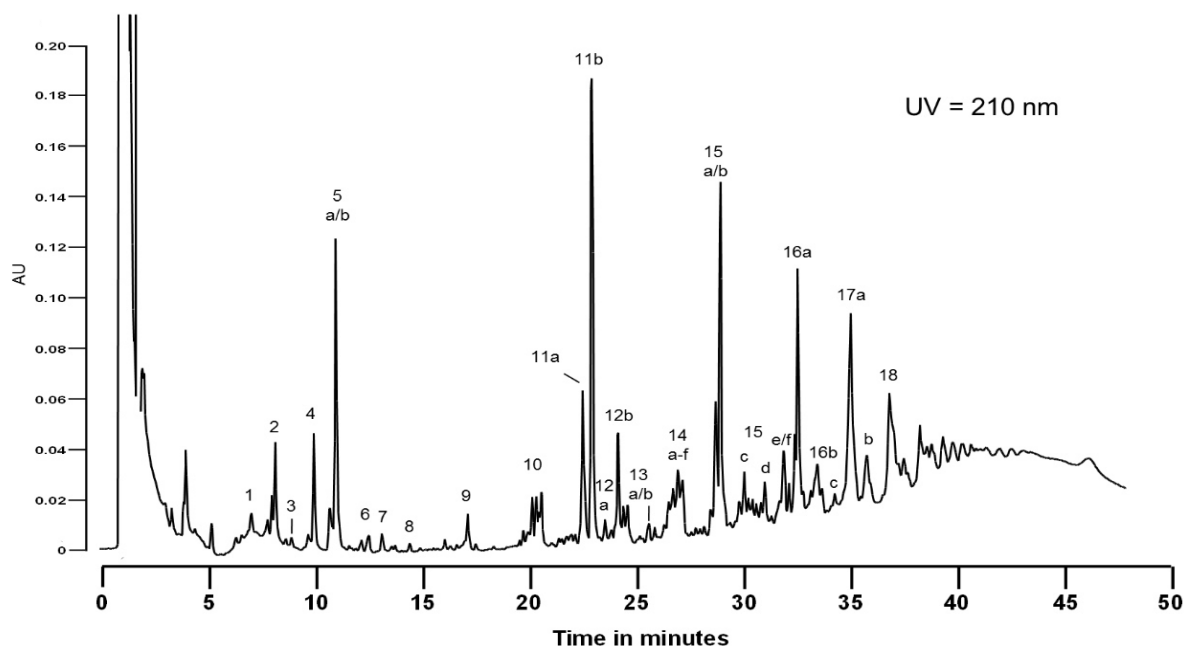


Fig. 4: Muropeptide profile of *S. aureus* SA1113 after mutanolysin digestion obtained by UPLC
Masses of indicated peaks are shown in table 1 (paper I, p. 52) including molecule composition and sum formula.

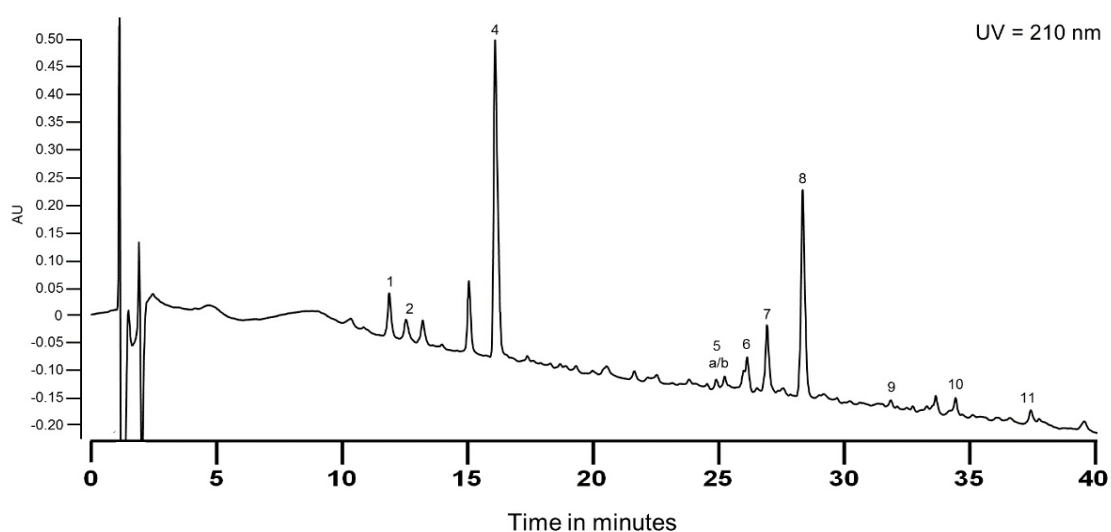


Fig. 5: Muropeptide profile of *E. coli* Nissle 1917 after lysozyme digestion obtained by UPLC
Masses of indicated peaks are shown in table 2 (paper I, p. 52) including molecule composition and sum formula.

resulting in the expected, species specific muropeptide pattern, as well as the appropriate molecular masses (**Fig.4 and 5**). O-acetylation, a modification of the C6 atom of MurNAc confers lysozyme resistance to pathogenic staphylococcal strains (Bera *et al.*, 2005; Bera *et al.*, 2006). This modification was thought to be removed during the final acidic treatment of PGN isolation. We analyzed HF treated PGN and compared it to HCl treated PGN and obtained the same muropeptide pattern. Strikingly, our data showed, for the first time, that most of the satellite peaks, as well as some of the peak shoulders, were in fact still O-acetylated (**Fig.6 and table S1 of paper I**).

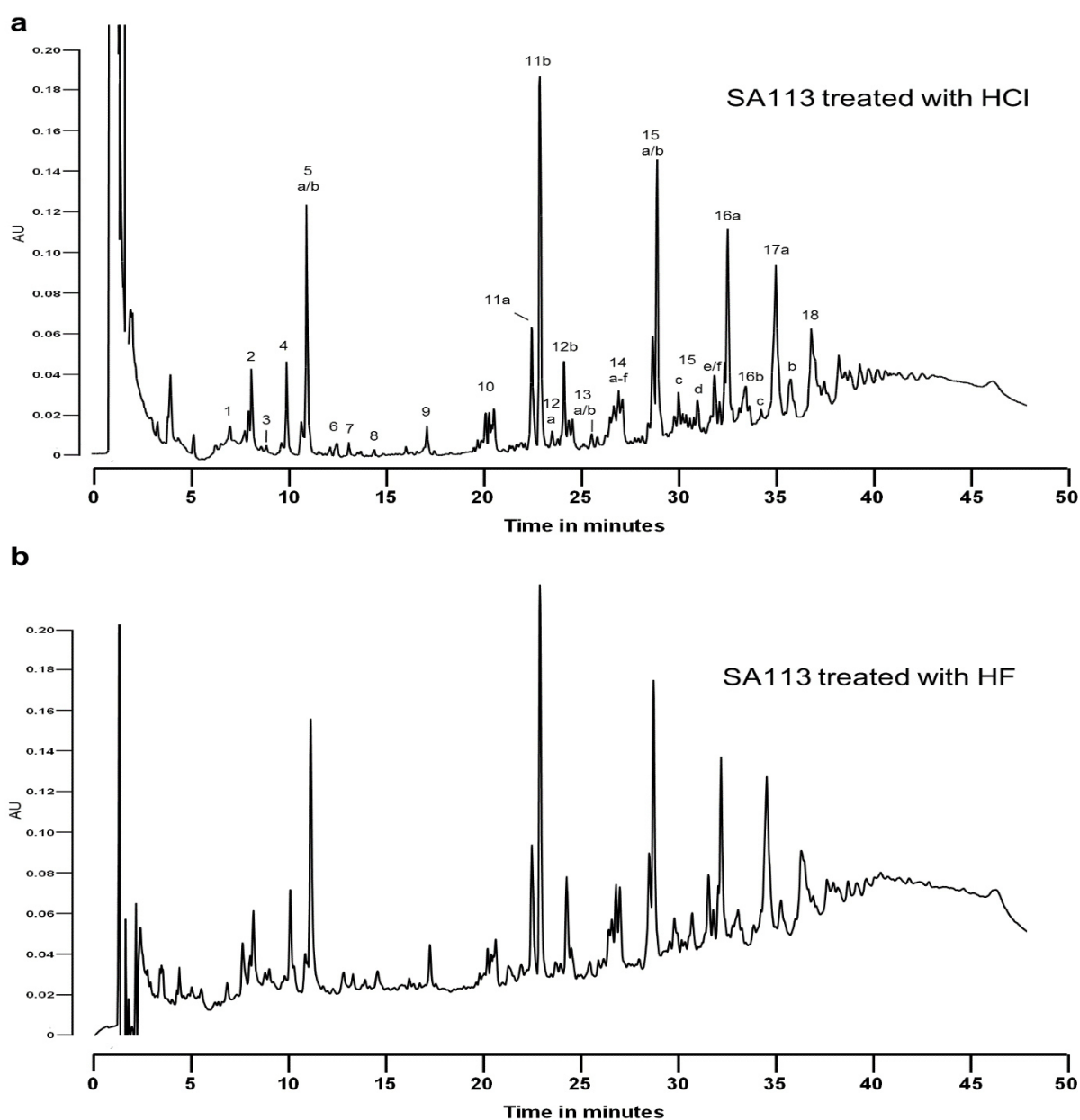


Fig. 6: Comparison of isolated peptidoglycan treated with HCL and HF

Muropeptide pattern of peptidoglycan of *S. aureus* SA113 treated with either HCl (a) or HF (b). The HF treated muropeptide pattern shows no differences compared to the HCl treated one. O-acetylated fragments listed in paper I, table S1, p. 62-65

Next, we upscaled our method from ultra-pressure liquid chromatographic (UPLC) to analytical and finally preparative HPLC dimensions. This upscaling procedure enabled us to isolate sufficient amounts of PGN fragments for further testing in *in-vitro* cell assays. We decided to investigate PGN of wildtype (WT) *S. aureus* SA113 and its available lipoprotein diacylglyceryl transferase (*lgt*) deletion mutant (*SA113Δlgt*). Monomeric (Fig. 7B) up to polymeric PGN (PGN_{pol}, Fig. 7A) fragments of both strains were collected and desalted, their molecular masses verified via MS and each sample was additionally tested prior and after lyophilization for LPS contamination, because LPS, as potent immunogenic molecule, might induce false positive results.

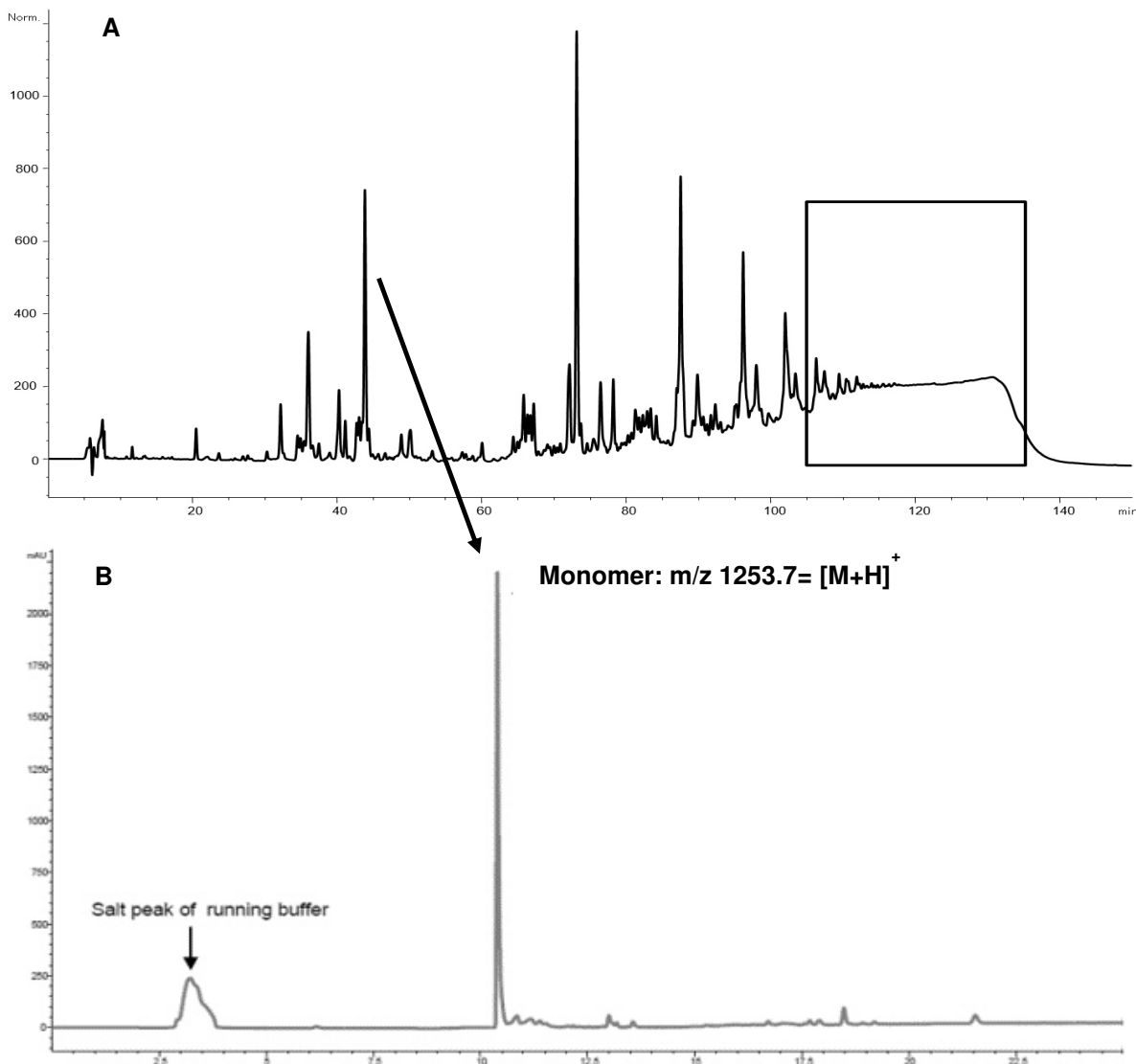


Fig. 7: Separation and analysis of PGN fragments of *S. aureus* SA113Δ*lgt* by HPLC. The box indicates collected PGN_{pol}, B The arrow indicates the desalted monomeric PGN fragment with appropriate molecular weight determined by MS.

To address the initial question, whether PGN is a TLR2 ligand or not, we stimulated 1×10^6 bone marrow-derived DCs (BMDCs) with different amounts of pure monomeric up to pentameric PGN fragments for their immunogenic capacity in DCs, MM6 and J774 cells and observed no induction of IL-6, IL-12p40, IL-8, and TNF- α , respectively (data not shown). The same was true for PGN_{pol} derived from *SA113 Δ lgt* (PGN_{pol Δ lgt}). In contrast, stimulation of DCs with PGN_{pol} derived from the wildtype strain induced a very high and significant signal for IL-6 and IL-12p40 (**Fig. 8**). We stimulated BMDCs with PGN_{pol} of both strains and analyzed maturation markers using flowcytometry (FACS) and indeed, we could observe,

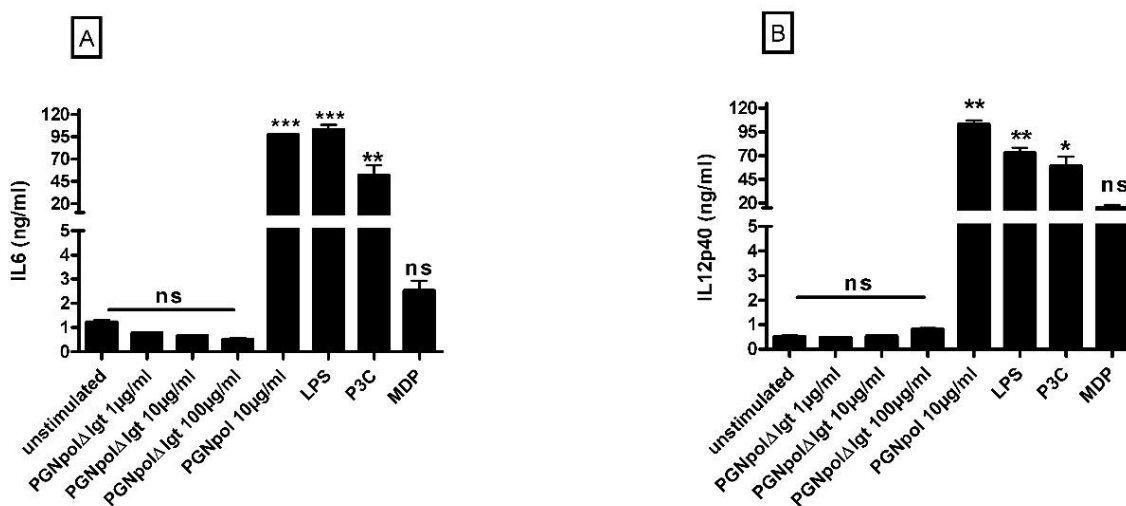


Figure 8: Stimulation with PGN_{pol}, but not with PGN_{pol Δ lgt}, leads to a significant secretion of IL-6 and IL-12p40 in DCs

Incubation of DCs with PGN_{pol} but not with PGN_{pol Δ lgt} stimulates IL-6 (A) and IL-12p40 (B) secretion, which is comparable to that induced by LPS or Pam3Cys. DCs are stimulated with PGN_{pol Δ lgt} up to a concentration of 100 μ g/ml. Stimulation with 10 μ g/ml PGN_{pol} leads to a high secretion of IL-6 and IL-12p40. Comparison was made between unstimulated cells and each stimulant using a nonparametric one-way ANOVA model for repeated measurements with a Bonferroni adjustment.

as expected, a significant increase in specific DC maturation markers, namely major histocompatibility complex II (MHCII) and the costimulatory protein CD40, in the case of stimulation with WT PGN_{pol}, but not with PGN_{pol Δ lgt}. (**Fig. 9**). Because of these findings, we decided to focus on PGN_{pol Δ lgt} for further experiments.

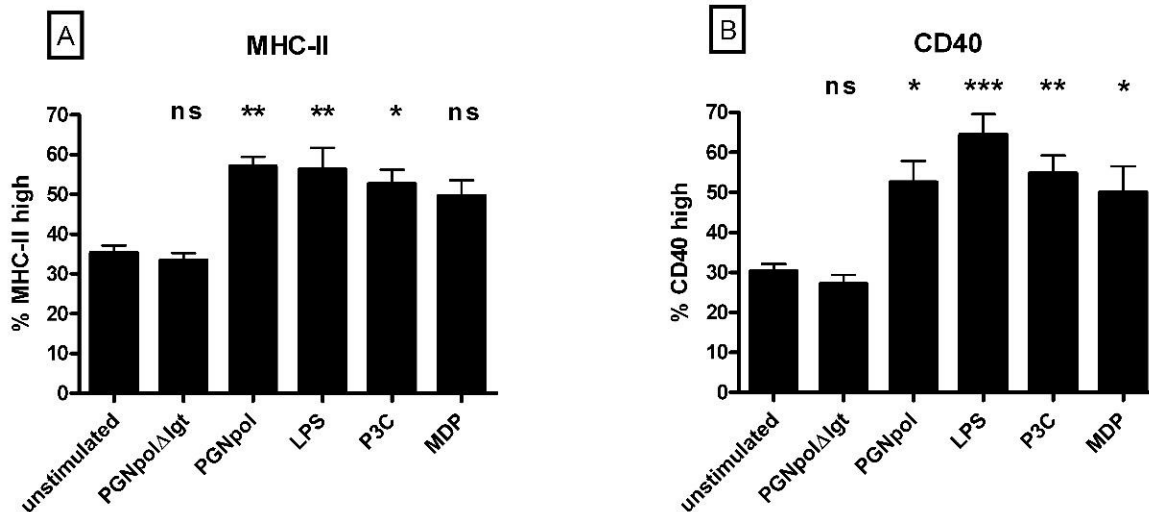


Figure 9: Stimulation with PGNpol, but not with PGNpolΔlgt, leads to an increased MHC class-II and CD40 expression in DCs

Immature BMDCs were activated with several NOD2 or TLR2 ligands. Maturation was quantified by FACS analysis assessing the levels of MHC class-II (A) and CD40 (B). The quantification was used based on isotype controls. Stimulation of DC with PGNpol 10 μg/ml leads to a strong signal of MHC class-II and CD40. In contrast, stimulation of DCs with PGNpolΔlgt 10 μg/ml does not lead to an increased expression of MHC class-II and CD40. Comparison was made between unstimulated cells and each stimulant using a nonparametric one-way ANOVA model for repeated measurements with a Bonferroni adjustment.

Interestingly, induction of IL-6 and IL-12p40 in BMDCs, as well as the induction of maturation markers, was abolished in BMDCs derived from NOD2-deficient mice, but only when stimulated with WT PGN_{pol}. This striking observation strongly indicates a clear synergistic effect of PGN_{pol} as NOD2 ligand and remaining LPPs within the polymeric PGN meshwork, acting as TLR2 ligand. The same pattern was observed for respective maturation markers (**Fig.10 and 11**).

To prove our hypothesis of a putative synergistic NOD2/TLR2 effect, we stimulated BMDCs either with PGNpolΔlgt, Pam3Cys, which resembles a triacylated LPP, or a combination of these two ligands. As expected, combinatorial stimulation of with PGN_{pol}Δlgt with Pam3Cys led to a significant increase in all tested cytokines (**Fig.12**). These experiments revealed synergistic effects on IL-12p40 and TNF-α secretion (an early response cytokine), but not on IL-6 secretion pattern.

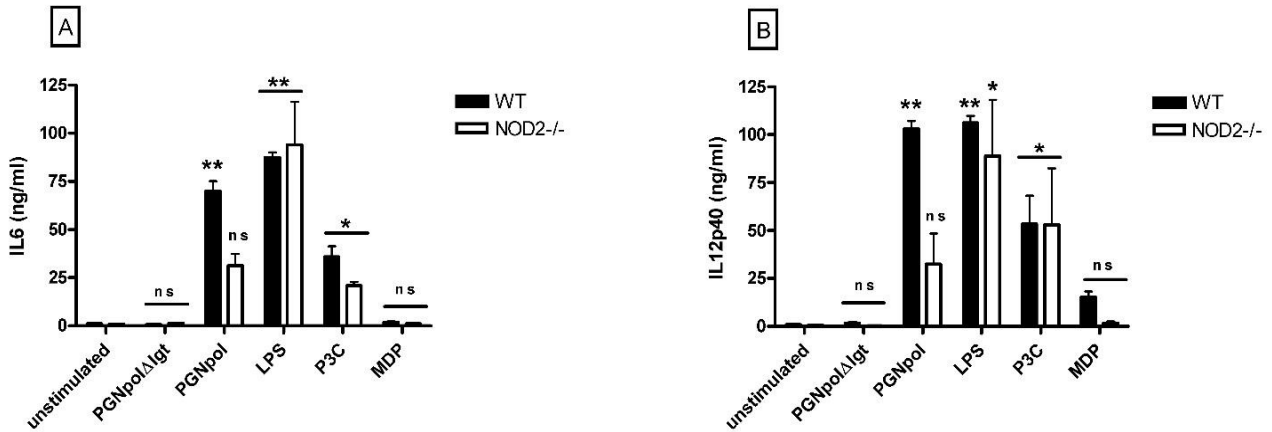


Figure 10: Stimulation with PGNpol in DCs is dependent on a NOD2 co-stimulus

Stimulation with PGNpol leads to a significant increased secretion of IL-6 (A) and IL-12p40 (B) in DCs from WT mice compared to unstimulated controls. In contrast, DCs derived from NOD2^{-/-} mice failed to induce IL-6 and IL-12p40 secretion upon stimulation with PGNpol. DCs from stimulated WT mice were compared to unstimulated DC's from WT mice. Respectively, DC's from stimulated NOD2^{-/-} mice were compared to unstimulated DC's from NOD2^{-/-} mice.

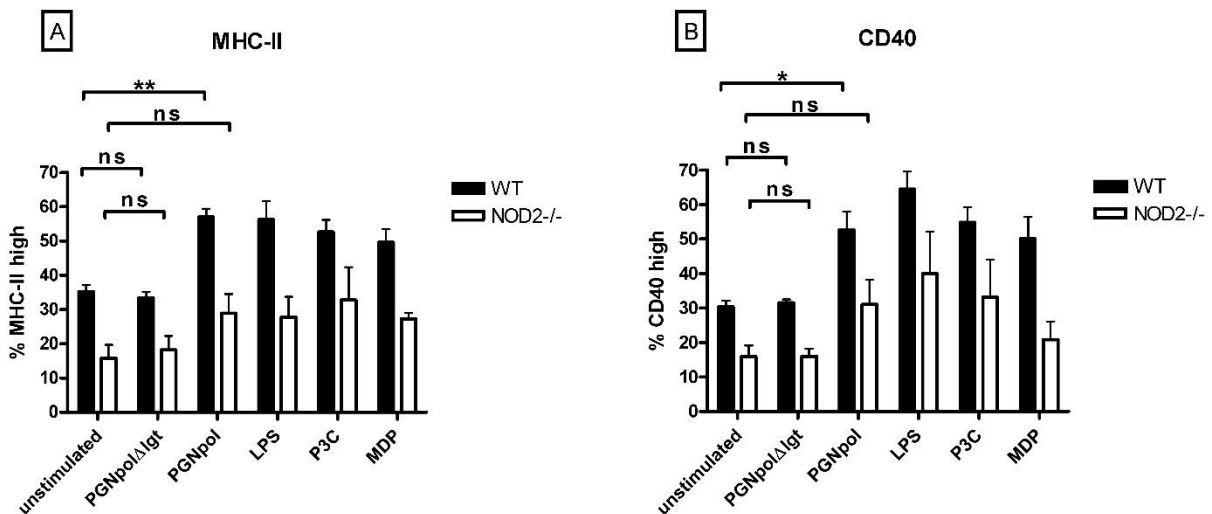


Figure 11: DC stimulation with PGNpol in WT mice leads to an increased expression of MHC class-II and CD40 compared to NOD2^{-/-} mice

Stimulation of DCs from NOD2^{-/-} mice with PGNpol 10 μg/ml did not lead to a significantly higher expression of MHC class-II (A) or CD40 (B), indicating that the co-stimulatory effect of NOD2 and TLR2 is necessary for effective maturation of DCs. Stimulated DCs from WT mice were compared to unstimulated DCs from WT mice, and unstimulated DCs from NOD2^{-/-} mice were compared to stimulated DCs from NOD^{-/-} mice. In addition, a comparison between DCs from WT and NOD2^{-/-} mice was made by using a nonparametric one-way ANOVA model for repeated measurements, with the Bonferroni adjustment.

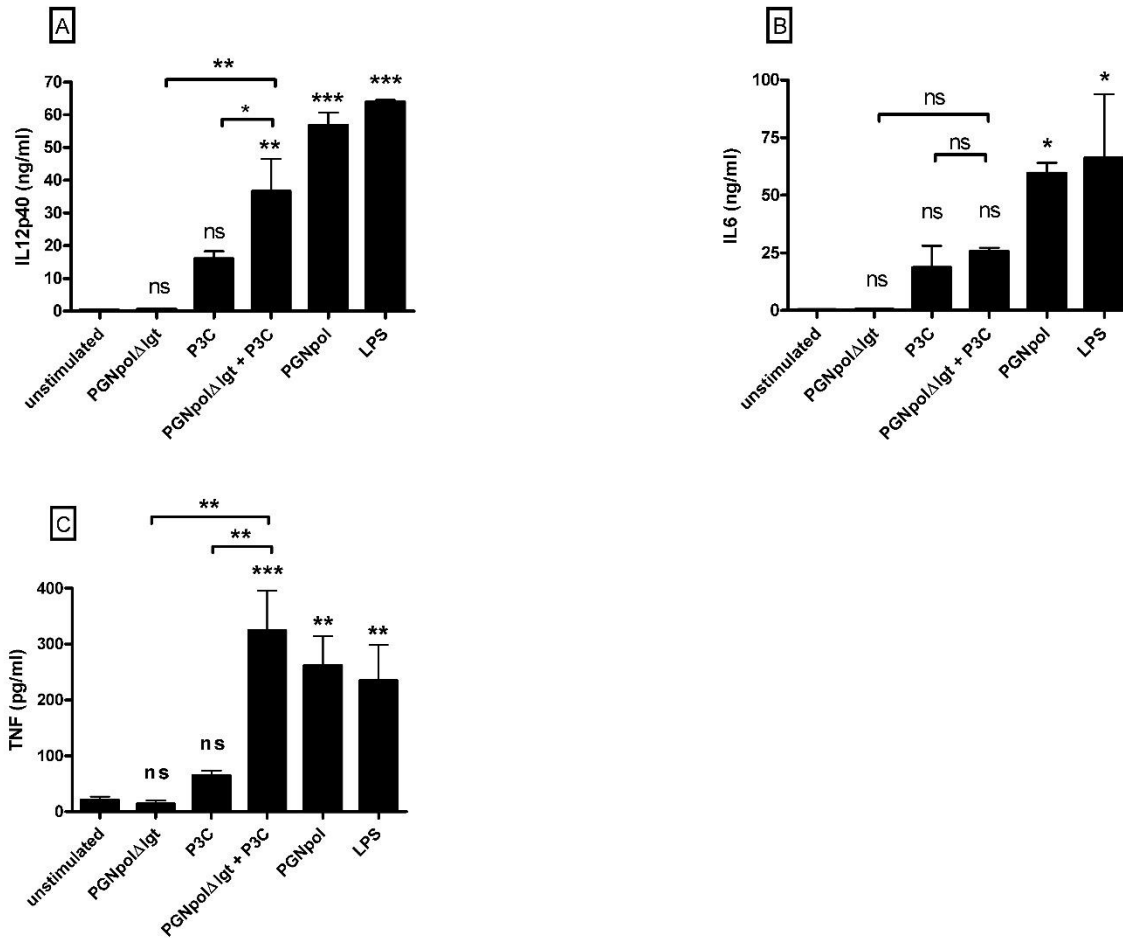


Figure 12: Combined stimulation of DCs with a NOD2 and TLR2 ligand leads to a stronger secretion of IL12p40 and TNF than stimulation with each of the stimuli alone

DCs were stimulated with PGNpolΔlgt 10 μg/ml, Pam3Cys 1 μg/ml and LPS 1 μg/ml. After stimulation with both ligands, PGNpolΔlgt and Pam3Cys, there was a significant higher signal of IL12p40 (A) and TNF (C) compared to stimulation with the single components alone. There was not a significantly higher signal of IL6 compared to stimulation with the single components (B). Unstimulated DCs from WT mice were compared to stimulated DCs from WT mice using a nonparametric one-way ANOVA model for repeated measurements with a Bonferroni adjustment.

To further substantiate these findings, we repeated our stimulation experiments with additional immune cells and could confirm our data in a human monocytic cell line (MM6, IL-8 secretion), as well as a murine macrophage cell line (J774, TNF-α secretion) (see Fig. 7 and 8, paper II).

Next, we were interested in how these signaling events could be interpreted within the context of IBD. Therefore, a possible protective effect, as described in Watanabe *et al.*, (2008) for MDP, of intraperitoneal PGN_{pol} administration was studied in a murine DSS colitis model. Acute colitis was induced by 3.5 % dextran sodium sulfate (DSS) in C57BL/6 (WT) and NOD2^{-/-} mice and 100 µg PGN_{pol} was administered intraperitoneally every third day. Mice were grouped in three categories:

1. WT or NOD2^{-/-} mice + PGN administration + DSS
2. WT or NOD2^{-/-} mice + PBS administration + DSS
3. WT or NOD2^{-/-} mice + PGN administration

After a seven-day treatment with 3.5 % DSS in the drinking water, C57BL/6 and NOD2^{-/-} mice showed signs of acute colitis with weight loss and bloody diarrhea. The two groups did not differ significantly between their colon weight and length and NOD2^{-/-} mice had a statistically significant trend towards less weight loss compared to C57BL/6 mice (Data not shown)

To further address the function of NOD2 activation, we studied the effect of intraperitoneal administration of either PGN_{pol} or PGN_{polΔIgt} in a murine colitis model. Unfortunately, both polymeric PGN types did not lead to a similar protective effect (**Fig. 13**), as it was shown for MDP. Because of a missing relevance, we did not add these results to our final publication.

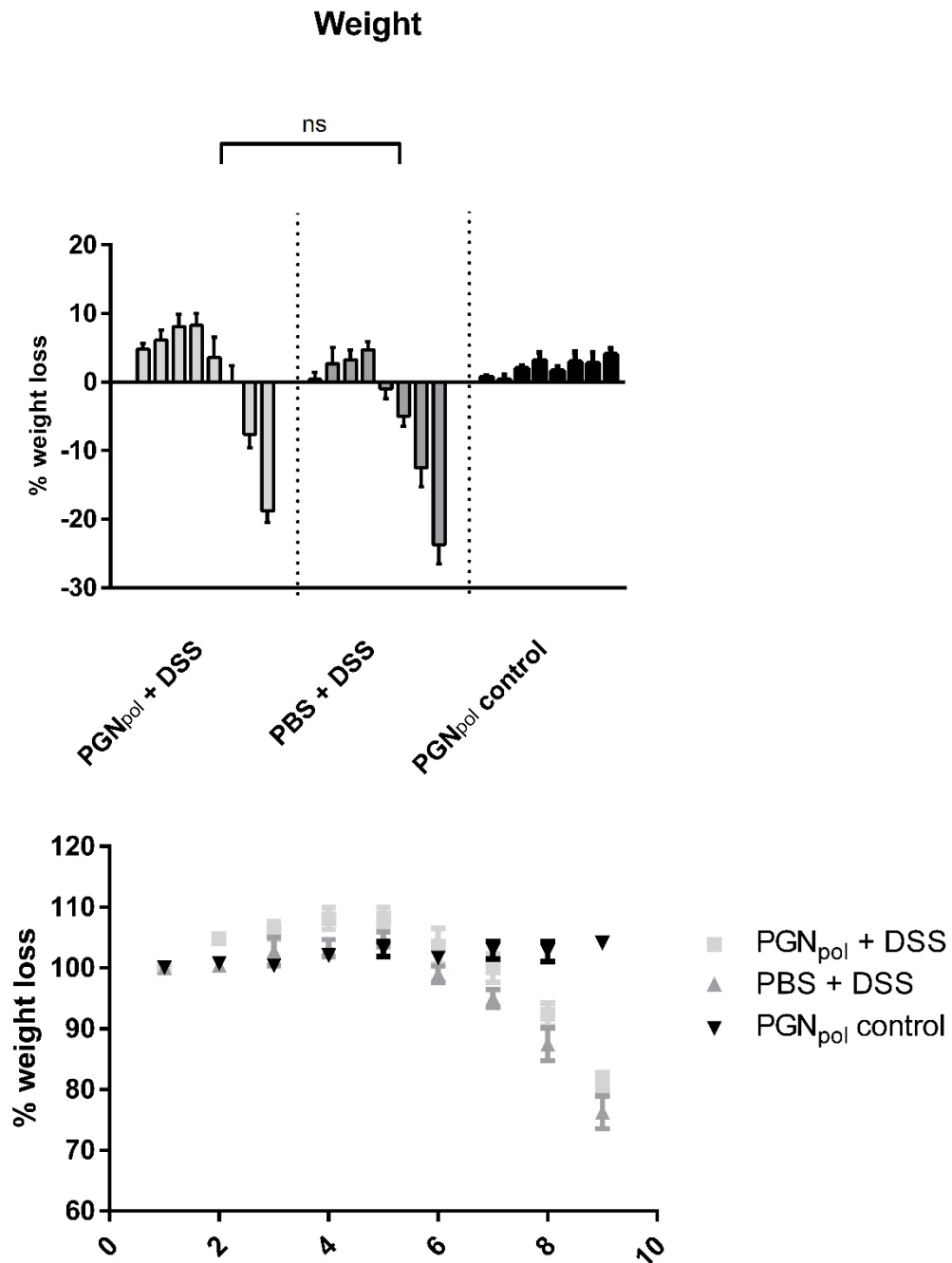


Figure 13: Effects of intraperitoneal PGN_{pol} administration in a DSS colitis mouse model

C57BL/6 (WT) and NOD2^{-/-} mice were treated with 100 µg solved PGN_{pol} every third day and sacrificed at day seven. Mice were analyzed for different disease symptoms. This figure shows and induced weight loss over time in DSS mice, but no protective effect.

Discussion

DCs are the most important immune cell type, linking innate immunity with downstream adaptive immunity and thereby taking over a very important role in the Mucosa-associated lymphoid tissue (MALT) (Cella *et al.*, 1997), intestinal homeostasis, and Morbus Crohn.

NOD2 is a well-studied PRR, sensing diverse PGN fragments, such as MDP, monomeric and polymeric PGN (Volz *et al.*, 2010; Iyer and Coggeshall, 2011) activating the transcription factor NF- κ B (Strober *et al.*, 2008). Insertion mutations within the caspase recruitment domain 15 (CARD15) of the NOD2 correlate with an increased susceptibility to Morbus Crohn (Hampe *et al.*, 2001), but it is still unclear, why this mutation may trigger chronic intestinal inflammations.

Until now, several publications addressed the complex interplay between NOD2 and TLR2 signaling events, which might have an influence on intestinal homeostasis. Synergistic effects of PRR sensing on the release of cytokines, such as IL6 and IL12p40 in stimulated BMDCs, being abolished in NOD2^{-/-} cells, were shown by a study of Magalhaes *et al.* in 2008. Other studies characterized anti-inflammatory effects of sensing PGN derived from specific lactobacilli species, being crucial for the probiotic effect of these strains (Macho Fernandez *et al.*, 2011), as well as protective effects of NOD2 activation by MDP in experimental colitis mice models (Watanabe *et al.*, 2008). These studies further support the hypothesis that activation of NOD2 seems to play a minor role in activating immune cells – in contrast to co-stimulation of NOD2 and TLR2 – but might lead to a downregulation of inflammatory pathways and thereby suppressing immune responses against harmless or even beneficial microbes. A “loss-of-function” in the NOD2 gene might therefore be an important part in the pathogenesis of Morbus Crohn.

In our study, stimulation of DCs, and other immune cells, with the sole NOD2 ligand PGN_{pol} Δ /*gt* does not lead to a significant NF- κ B-dependent immune response, but additional stimulation with a TLR2 ligand was needed to induce such a response, leading to the secretion of several distinct cytokines (IL-6, IL-8, IL-12p40, TNF- α).

In summary, we could show that the concept of synergistic amplification of PRR signaling, in our study activation of NOD2 and TLR2 PRRs and their respective signaling pathways, represent an important concept for modulating immune responses and the maintenance of immune homeostasis in the gut. According to our data, pure PGN molecules do not induce a significant immune response via TLR2 activation, unless a co-stimulation via NOD2 occurs, which subsequently result in a potent activation of DCs, macrophages, as well as monocytes. Our data are contrary to data obtained by Müller-Anstett *et al.* (2010), where a co-localization of pure and biotinylated PGN_{pol} led to IL-1 β , IL-6 and TNF- α secretion and NF- κ B activation. Our data are important for a better understanding of the complex interplay between these receptors in maintaining homeostasis of the intestinal immune system.

Part II: Adaptive immune response against staphylococcal lipoproteins in the context of atopic dermatitis

Introduction

8. Adaptive immunity

The second main part of our immune system is called the adaptive immune system, which has evolved in vertebrates to be activated by signals of the innate immune system. The adaptive immune system comprises of specialized immune cells, namely B and T cells, that specifically react against processed antigens. In contrast to the quite unspecific innate immune system, antigen specific receptors are deployed to recognize microbial antigens. These non-germline-encoded receptors, B cell receptors (BCR) and T cell receptors (TCR), are produced in a process called somatic or V(D)J recombination (Li *et al.*, 2004; Litman *et al.*, 2010). This genetic recombination process generates a vast repertoire of antigen specific BCR and TCR assuring the detection of almost every intruding antigen. According to their origin, B cells are named after the **b**one marrow and T cells after their place of maturation: the **t**hymus.

After recognizing an antigen presented by APCs via their B cell receptor (BCR), B cells secrete a soluble form of the same receptor, the so-called immunoglobulins or antibodies (Harwood and Batista, 2010). Antibodies in turn activate the complement system, a part of the innate immune system comprising of several serum proteins. These proteins, amongst others, opsonize pathogens by binding to their surface or deactivate toxins (Ravetch and Bolland, 2001). A striking feature of the adaptive immune system is its immunological memory, based on plasma B and memory T cells. This hallmark of the immune system provides a more rapid and more potent response to a second infection with the same pathogen (Kassiotis *et al.*, 2002; Zinkernagel *et al.*, 2003; Sallusto *et al.*, 2010).

Because of its importance, disorders in the normal and highly complex function of the immune system can lead to fatal diseases, like autoimmune disorders (e.g. inflammatory bowel diseases), cancer (O'Byrne and Dalglish, 2013) or allergies.

9. Lipoproteins

Lipoproteins (LPPs), as a part of the bacterial cell envelope, are proteins containing a lipid moiety, which are covalently linked to an N-terminal cysteine residue. This lipid moiety is anchored to the outer leaflet of the cell membrane. *S. aureus* expresses about 50 LPPs with mostly unknown functions. However, it has been established that they can act as ATP binding cluster (ABC) transport systems as demonstrated by SitC, as oligopeptide permease (OppA), peptidyl-prolyl cis/trans isomerase (PrsA) or a thiol-disulfide oxidoreductase activity (DsbA) (Schmaler *et al.*, 2010).

The biosynthesis of LPPs involves two steps: the first step is catalyzed by the phosphatidyl glycerol diacylglyceryl transferase (Lgt). This enzyme transfers a diacylglyceryl group from phosphatidylglycerol to a cysteine residue within a conserved sequence, called the lipobox, forming a thioether linkage. A specific signal peptide leads this pre-lipoprotein to the Sec machinery, where it gets cleaved by a lipoprotein-specific type II signalpeptidase (LspA) (Schmaler *et al.*, 2010). However, it is still debated, if *S. aureus* LPPs are di- or triacylated, as it is the case in *Escherichia coli*. In Gram-negatives, LPPs are mostly modified in a third step by an N-acyltransferase that transfers a third N-acyl group to the pre-mature lipoprotein (Kurokawa *et al.*, 2009). In addition, LPPs play a fundamental role in innate immune recognition processes. Diacylated LPPs are recognized by Toll-like receptors (TLRs) 2/6, whereas triacylated LPPs are recognized by TLR 2/1. This recognition induces a subsequent immune response and leads to the secretion of interleukin 6 (IL-6) and tumor necrosis factor alpha (TNF- α) (Stoll *et al.*, 2005).

Aim of this study

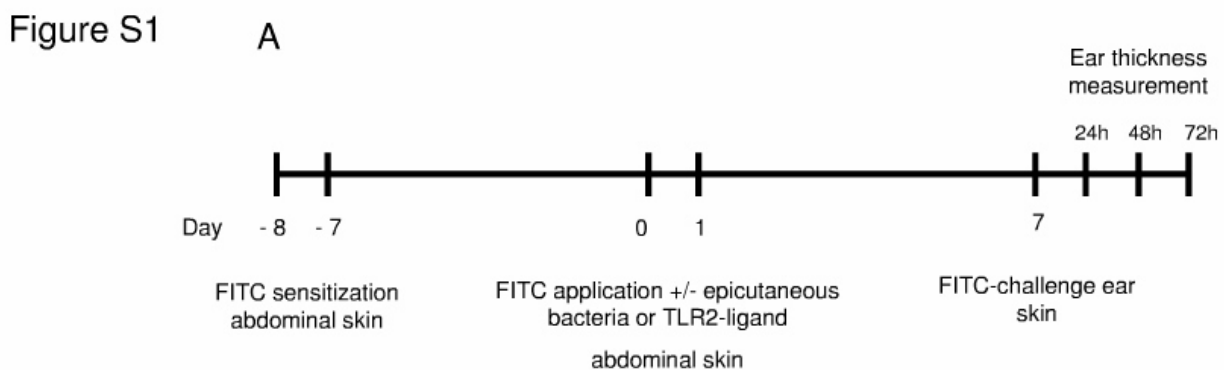
The human skin represents a very important organ with a large outer surface. It acts as a physical barrier and the site of first contact to a variety of microbes, thereby orchestrating innate, as well as consecutive adaptive immune responses. *S. aureus*, as described in the General Introduction section, is a natural commensal, but also one of the most potent skin pathogens. Because more than 90% of atopic dermatitis (AD) patients are colonized with *S. aureus*, there is a need to understand the skin-driven immunity better.

To elucidate the underlying molecular mechanisms of this phenomenon, we used different mice models (WT, TLR2^{-/-} and IL6^{-/-} BALB/c mice), combined with a murine T cell-mediated contact hypersensitivity (CHS) to fluorescein isothiocyanate (FITC), and infected these sensitized mice with *S. aureus* Newman and its lipoprotein-deficient Δlgt mutant. In addition, defined lipopeptides (synthetic fatty tails of lipoproteins) were applied cutaneously using the same mice models. We investigated ear swelling, activation of several immune cells, such as T cells and MDSCs, as well as IL-6 expression and secretion.

In the following section, the intriguing results of this study will be presented and discussed.

Results

To characterize skin-driven immunity, WT *S. aureus* Newman and its respective lipoprotein-deficient mutant Newman Δ lgt were applied cutaneously in order to mimick colonization or an infection of the skin with a Gram-positive bacterium. To investigate why and how this colonization or infection of the skin influences subsequent immune responses, mice pre-sensitized to FITC were infected with 3×10^8 cells at defined time points, as shown in **Fig. S1**.



Protocol of FITC-CHS with and without cutaneous exposure to *S. aureus* or TLR ligands.

Wild-type (WT) mice were sensitized by administration of FITC solution on the shaved abdomen on days -8 and -7. Together with the second application of FITC on days -1 and 0, some mice were epicutaneously exposed to living WT or lipoprotein deficient (Δ lgt) *S. aureus* or TLR ligands in addition. Control mice obtained phosphate-buffered saline (PBS). As read out for the cutaneous recall immune response, FITC was applied to the previously untreated ear skin on day 7 and the increase of ear thickness (ear swelling) was measured over a period of 3 days.

Infection with WT bacteria, in contrast to its isogenic Δ lgt mutant, significantly reduced ear swelling, the main symptom of induced dermatitis in mice (**Fig. 14 B** and **C**). This striking result can be explained with alterations in specific immune cell populations, such as a reduced FITC-specific T cell proliferation in skin-draining lymph nodes (**Fig. 14 D**), reduced numbers of CD4⁺ and CD8⁺ T cells in the spleen with a respective increase in Gr1⁺CD11b⁺ MDSCs (**Fig. 14 E**). These findings gain an additional clinical relevance in AD patients, where most patients carry staphylococci and exhibit an increase in MDSC numbers in PBMCs (**Fig. 14 F**).

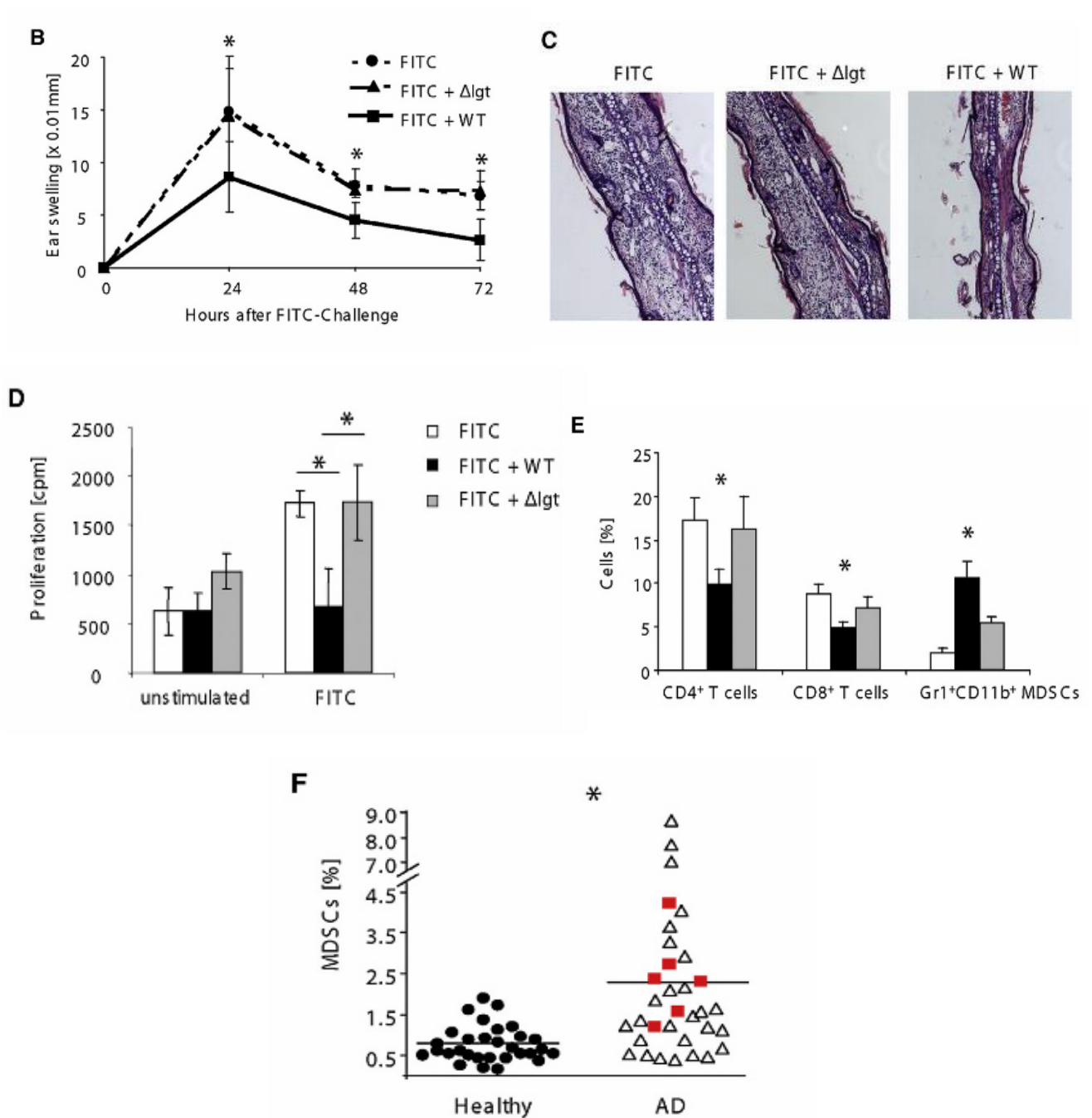


Figure 14: Cutaneous *Staphylococcus aureus* Induces Immune Suppression in mice and humans

FITC-sensitized WT BALB/c mice were treated either with living WT *S. aureus* Newman or its lipoprotein-deficient mutant (Δ lgt), ear swelling (mean \pm SD, n = 5) histology (H&E staining) (B), percentage of cell populations in the spleen (mean \pm SD, n = 5) (E) were investigated. *p < 0.05., (F) PBMCs from atopic dermatitis (AD) patients (n = 33) and healthy volunteers (n = 30) were analyzed for MDSCs, defined as CD11b⁺CD33⁺HLA-DR⁺CD14⁺ cells. The dots represent individual values, and the horizontal bar is the group mean. Red squares represent MDSCs of patients with severe AD and eczema herpeticum.

These data clearly indicate an immunosuppressive effect of cutaneous *S. aureus* application, which is triggered by the induction of MDSCs. The inability of SA113 Δlgt to induce immune suppression was a clear explanation for the induction of immune suppression by the recognition of LPPs. Together with the fact that LPPs are sensed differently via heterodimers of TLR2/1 (triacylated) or TLR2/6 (diacylated) (Henneke *et al.*, 2008), this led to our hypothesis that sensing of either diacylated or triacylated LPPs must be the cause of this immune reaction. To investigate this, we decided to repeat the same experiments and cutaneously applied synthetic molecules named FSL-1, Pam2Cys and Pam3Cys, resembling di- and triacylated fatty tails of LPPs.

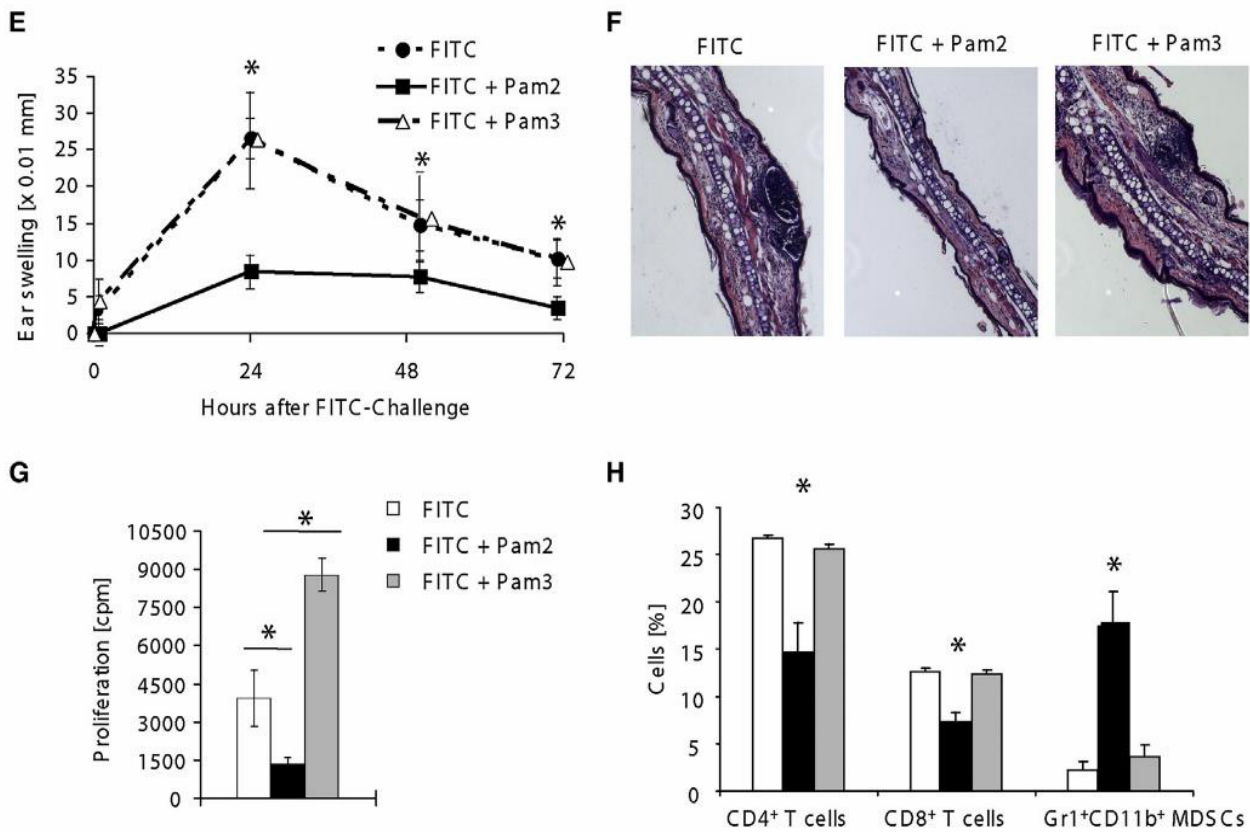


Figure 15: Cutaneous Exposure TLR2-6 but Not TLR2-1 Ligands Ameliorates T Cell-Mediated Recall Responses of the Skin

WT MBALB/c mice were cutaneously exposed to Pam2Cys or Pam3Cys. Ear swelling response (mean \pm SD, n = 5) (E), histology (H&E staining) (F), proliferation of skin-draining LN cells stimulated ex vivo with FITC (mean \pm SD of triplicates) (G), and the percentage of cell populations in the spleen (mean \pm SD, n = 5) (H) are shown. Data are representative of at least two independent experiments. Experiments shown in (A) were performed with FSL-1 from two different providers. *p < 0.05.

As shown in **Fig. 16 E and F**, cutaneous application of Pam2Cys (also FSL-1, **Fig. 2 A - D** of paper III), but not Pam3Cys, led to a decrease in ear swelling, a reduction in T cell proliferation (**Fig. 14 G**), as well as a significant increase in Gr1⁺CD11b⁺ MDSCs. Depletion of Gr1⁺ cells abolished immune suppression, which could be restored by adoptive transfer of MDSCs (previously exposed to Pam2Cys) (**Fig. 3 A** of paper III). Furthermore, treatment of Tlr2^{-/-} mice with Pam2Cys showed no decrease in ear swelling, T cell proliferation and no increase in Gr1⁺CD11b⁺ MDSCs (**Fig. 14 A - C**). These results indicate a clear TLR2-dependency of immune suppression by diacylated lipopeptides/LPPs, such as Pam2Cys.

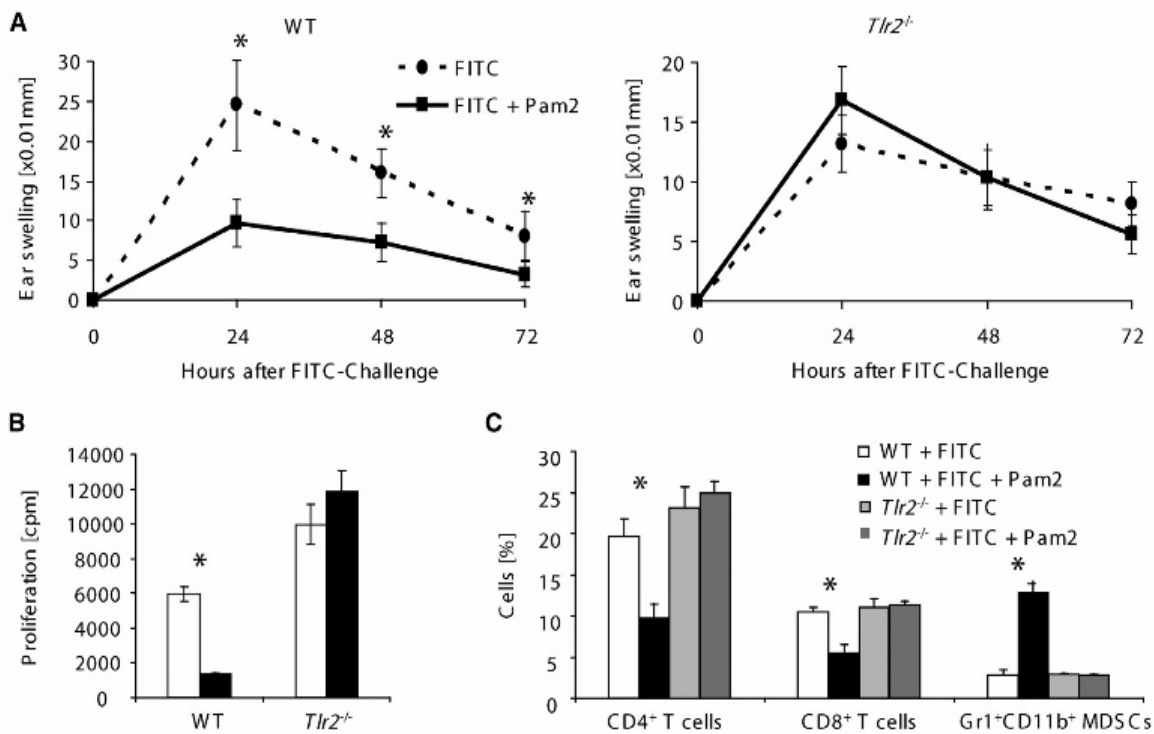


Figure 16: Pam2Cys-Induced Immune Suppression Is Dependent on TLR2

WT and Tlr2^{-/-} mice were treated following the protocol shown in Figure S1A and ear swelling (mean ± SD, n = 5) after FITC challenge (A), proliferation of lymph node cells after FITC stimulation ex vivo (mean ± SD of triplicates) (B), and the percentage of spleen cell populations (mean ± SD, n = 5) (C) were analyzed.

Discussion

Our skin, constantly exposed to and colonized by a vast number of bacteria, estimated as 10 times the amount of somatic cells (Costello *et al.*, 2009), Cutaneous innate immune sensing plays a key role in skin-related immune homeostasis and the control of subsequent adaptive immune responses in infections. In this study, cutaneous exposure to bacteria and bacterial MAMPs induced a strong immune suppression, which was mediated by MDSCs. These results highlight the ability of certain MAMPs to act as immunosuppressive agents, controlled by the activation of specific signaling pathways to evade the immune system.

We characterized these signaling properties and showed that cutaneous exposure to TLR2-TLR6, but not to TLR2-TLR1, ligands induced skin-resident MDSCs and consecutive cutaneous immune suppression. Bacterial LPPs differ in their acylation patterns, which in turn depend on environmental factors and growth phases. SitC, a well-known LPP from *S. aureus*, was shown to be triacylated, when the cells were in the exponential growth phase at neutral pH and diacylation occurring at acidic pH values. (Kurokawa *et al.*, 2012; Kurokawa *et al.*, 2012). With this knowledge, we could assume that LPPs might also differ in their TLR2 activation potential. As a result, acylation properties might characterize bacteria living on the skin, as pathogens or commensals. In addition, the pH of our skin is low and chronic *S. aureus* colonization is present in almost all AD patients, assuming *S. aureus* being in an exponential growth phase. Therefore, LPPs from *S. aureus* on the skin might be more diacylated. Together with our data and data published by Kaesler *et al.* (2014), which could identify TLR2 ligands as promoters for AD through IL4-mediated suppression of IL-10, we proposed following model, illustrated in **Fig. 17**.

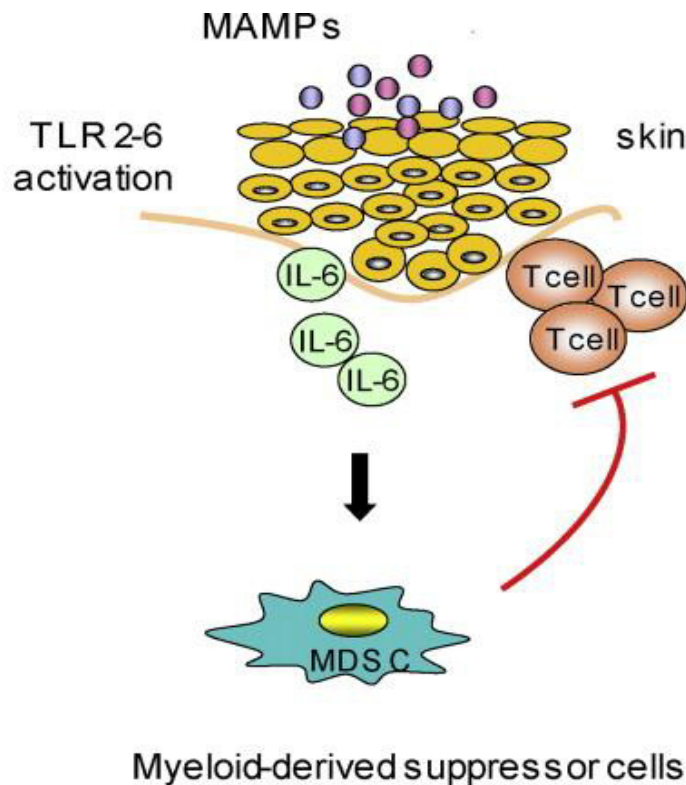


Figure 17: Model of skin-infecting *S. aureus* caused immune suppression

Diacylation of staphylococcal LPPs causes immune suppression by recruiting MDSCs via TLR2-dependent induction of IL-6

Diacylated lipopeptides present on the surface of *S. aureus*, activate TLR2-6 presented on skin resident cells, followed by increased IL-6 production leading to MDSC recruitment to the site of infection. This accumulation of MDSCs is a prerequisite of subsequent immune suppression and inhibition of a subsequent adaptive immune response.

In summary, we could identify an ingenious immune evasion mechanism triggered by *S. aureus*. These infections recruited MDSCs to the site of infection by modulating the acylation pattern of surface LPPs, which in fact led to immunosuppression. Our study nicely shows a direct link of cutaneous innate immune sensing with adaptive immune functions. The presence of bacteria on the skin with specifically acylated LPPs is able to counter-regulate inflammation and suppress immune responses.

Part III: The role of PGN in the development of food allergies in humans

Introduction

10. Allergies

In general, allergies are defined as hypersensitivity disorders, which are overreactions of our immune system against usually harmless antigens. This hypersensitivity leads to symptoms, such as eczema, itchiness, nausea, vomiting, but can also lead to a severe anaphylactic shock and death. Causes of allergies are very diverse and include, in particular, environmental factors, such as pollution and excessive usage of antibiotics or other chemicals in the food industry, a genetic predisposition and classical food-allergens, such as proteins derived from hen eggs, milk, fish and peanuts (Swert, 1999). The highest risk to develop an allergy is at young ages (Croner, 1992) and several studies showed a correlation between the antibiotic application in infants and an increasing incidence of allergic diseases (Droste *et al.*, 2000).

These disorders are divided mainly into four types (after Gell PGH, Coombs RRA, eds. Clinical Aspects of Immunology. 1st ed. Oxford, England: Blackwell; 1963):

1. Type I hypersensitivity (or immediate)
2. Type II hypersensitivity (or cytotoxic)
3. Type III hypersensitivity (immune complexes)
4. Type IV hypersensitivity (delayed type hypersensitivity)

Food allergies belong to type I hypersensitivities, representing classical IgE-mediated immune reactions and has to be distinguished from food intolerances based on their pathophysiology and cause. The initial recognition of an antigen or allergen,

such as ovalbumin (ova, the main protein found in egg white), results in the activation and maturation of naïve CD4⁺ T_h cells to T_h2 cells. This cell type produces IL-4 and interacts with B cells. This interaction acts in concert with IL-4 and results in production of IgE antibodies. This type of antibodies is able to binds its receptor FcεRI on basophilic granulocytes as well as mast cells. This first contact to an allergen is called acute response and results in sensitized, IgE-coated cells. During a later exposure, the same allergen, can bind to these sensitized cells, thereby cross-linking IgE antibodies and FcεRI receptors. This process leads to a degranulation and subsequent release of immune mediators, such as histamine and others, which in turn leads to classical allergic symptoms, as described before.

Aim of this study

There are several studies indicating the importance of the intestinal microbiota in preventing several diseases, amongst others food allergies. Furthermore, application of antibiotics, such as Penicillin (a β-lactam antibiotic, which inhibits PGN assembly) in early childhood alters the composition of this microbiota, which in turn may lead to an increased risk of asthma and allergies (Droste, Wieringa, Weyler, Nelen, *et al.*, 2000). Moreover, the occurrence of Staphylococci in infant gut microbiota correlates with an increased risk of developing atopic AD (Vael and Desager, 2009). Because of these findings, we hypothesized that inhibition of PGN assembly by β-lactam antibiotics, leading to cell lysis, could increase the number of available PGN fragments within the gut. This multitude of fragments, such as monomers, dimers, etc., could be easily uptaken through the infantile gut barrier, which is leakier than in adults (Järvinen *et al.*, 2013). These uptaken fragments are presented to intestinal DCs (Rescigno, 2014) with could finally lead to the subsequent development of a misguided immune reactions against these fragments and consequently to a food allergy.

To prove our hypothesis, we constructed two different avian ovalbumin (the major allergen of hen egg white) expressing staphylococcal vectors and transformed them into different staphylococcal strains: The first constructs encodes for ovalbumin, which is secreted to the culture supernatant, due to the presence of a signal peptide, whereas the second constructs facilitated the intracellular expression of ovalbumin. These constructs, bringing together a model allergen and a main bacterial constituent in a spatial and temporal manner, enables us to investigate the impact of PGN signaling via pathways of the innate immune system, on the pathophysiology of food allergies.

Results

A codon usage optimized, synthetic avian ovalbumin (*ova*) gene (SERPINB14, from *Gallus*

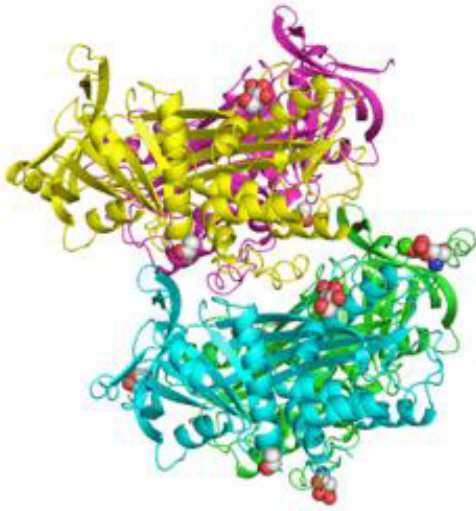


Figure 18: 3D model of avian ovalbumin

© RCSB Protein Data Bank

gallus, NCBI gene ID: 396058, size: 1161 bp) containing restriction sites for *Sall*, *XhoI* and *EcoRI*, was ordered from GeneArt (LifeTechnologies, Darmstadt). The carrier plasmid pMK was transformed into *E. coli* DH10B, which possesses particularly useful properties, such as a high transformation efficiency, the ability to take up and stably maintain large plasmids and the lack of methylation-dependent restriction systems (MDRS) (Durfee *et al.*, 2008). Isolated plasmid DNA was digested either with *XhoI/EcoRI* or *Sall/EcoRI* to generate compatible ends for ligation into plasmids pTX-*yfp-mreB* and pTX-*mch-cw*, respectively (pTX30 derivatives, containing fluorescent proteins Yfp and Mcherry, kindly provided by Wenqi Yu). Both constructs were ideal for achieving the mentioned goals of secreting vs. intracellular expression: pTX-*mch-cw* harbors sequences encoding a signal peptide (SP, containing an YSIRK motif) and a propeptide (PP, derived from a lipase of *S. hyicus*) upstream of a gene of interest. The SP facilitates secretion of proteins and the PP is thought to function as an intramolecular chaperone (Sturmfels *et al.*, 2001). Indeed, a first attempt to clone a construct for intracellular expression of ovalbumin failed due to the lack of this PP (see **Fig. 18**, construct (2)).

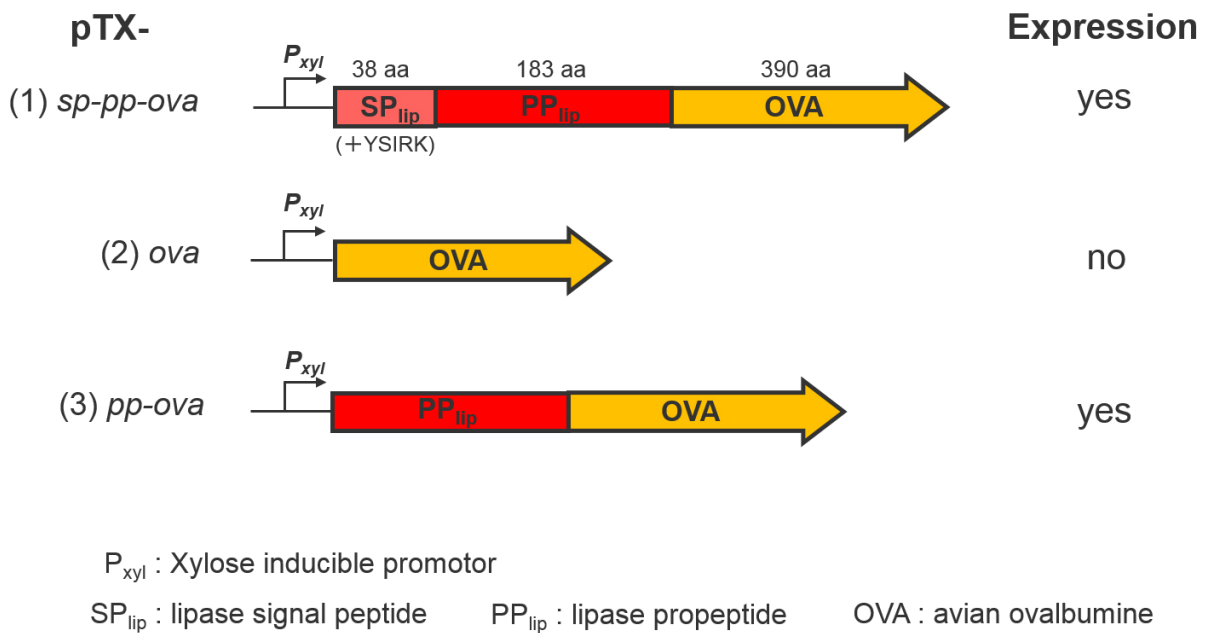


Figure 19: Overview of the assembled ovalbumin expression constructs

Peptides, their respective sizes and successful expression are indicated.

Cloning the ovalbumine gene downstream of these important genetic elements (see **Fig. 18**, construct (1 and 3)) was successful, verified by restriction analysis and sequence analysis of the resulting plasmids **pTX-*sp-pp-pva*** (for the secreted version) and **pTX-*pp-ova*** (intracellular version) by GATC (Konstanz), including its promotor. In contrast to construct 2, the other constructs led to a stable expression of ovalbumine, when transformed staphylococci were induced at an OD of 0,6 - =0,7 with 0.5 % xylose and subsequently grown for at least 16 - 24 h in Brain Heart Infusion (BHI) medium at 37°C under shaking conditions (160 rpm). Successful expression was verified after isolating whole protein fractions of lysed cells and their respective supernatants by semi-dry western blot analysis using monoclonal mice anti-ovalbumin antibodies (ab) (Abcam, Cambridge, UK). Representative western blots of a protein A-deficient SA113 strain (SA113 Δ *spa*), which lead to a decrease in background signals due to a lesser extent of unspecific binding of the ab to other remaining proteins on the blot, are shown in **Fig.19 A and B**.

Native ovalbumin has a molecular weight of approx. 45 kilodaltons (kDa) and always appeared as double band, which originates from a degradation during sodium dodecyl sulfate polyacrylamide gel electrophoresis (SDS-PAGE). The propeptide-ovalbumin fusion protein (named PP-OVA) has a size of 573 aa. Taken the average mass of an amino acid as 137 Da (calculated according to data from Promega (Mannheim)) PP-OVA should have a theoretical mass of 78,5 kDa.

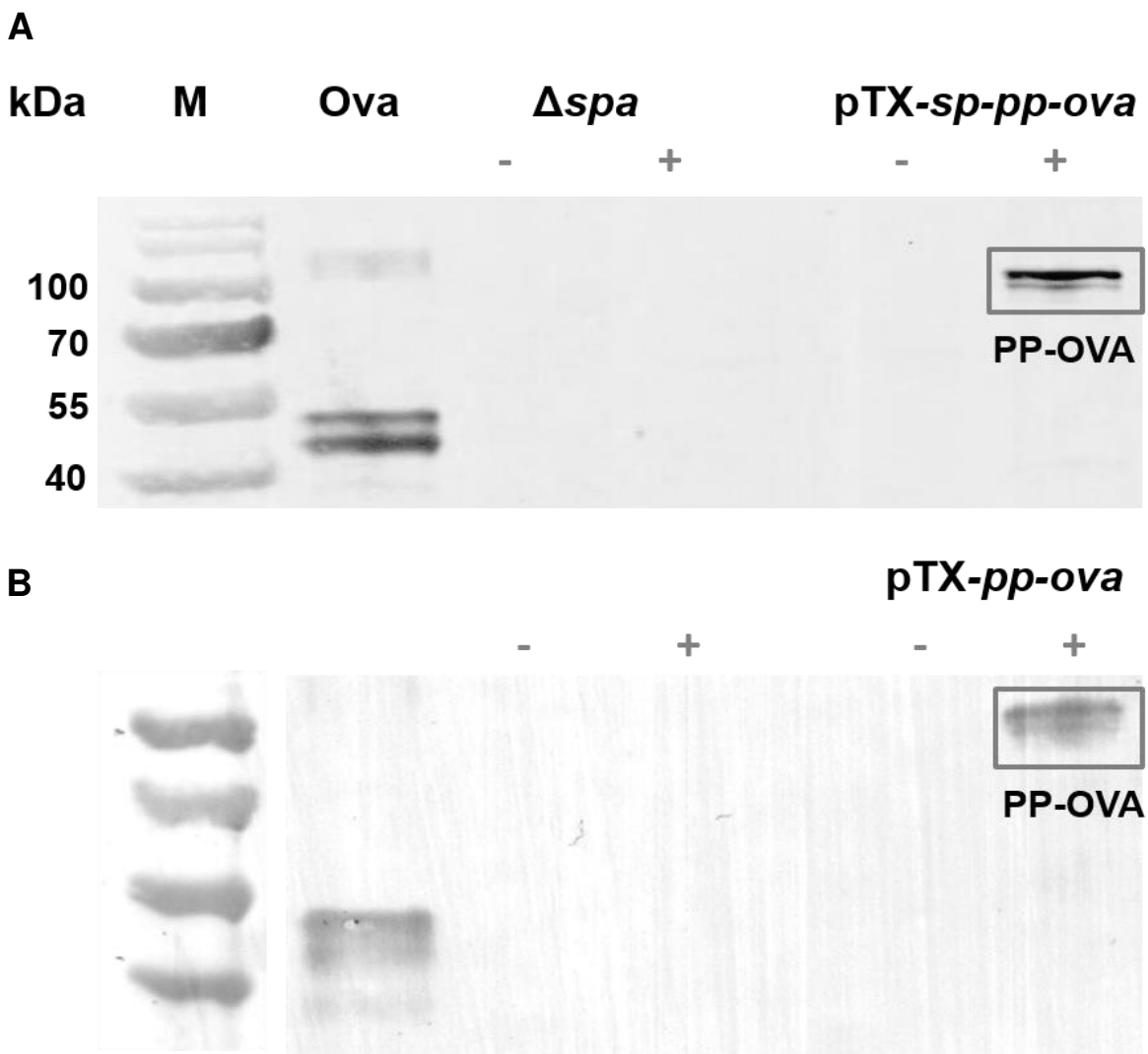


Figure 20: Ovalbumin expression in SA113 Δspa after 24 hours

Ovalbumin was isolated from the supernatant (A) of the same induced and lysed cells (B), respectively. For detection, a nitrocellulose membrane was incubated with a primary monoclonal mice anti-ovalbumin antibody. M: Marker; Ova: positive control with ovalbumin (Hyglos, Bernried); Δspa : negative control SA113 Δspa ; PP-OVA: propeptide-ovalbumin fusion protein; - and + indicates xylose induction

However, migration of isolated ovalbumin was observed at around 100 kDa. The reasons for such “gel shiftings” are still poorly understood. Potential protein glycosylation events, post-translational modifications or changes in detergent binding could explain this migration behavior, which was shown for transmembrane segments of membrane proteins, as well as cytosolic proteins (Rath *et al.*, 2009; Shi *et al.*, 2012).

Outlook

Currently, we are working on the additional validation of ovalbumin expression and secretion, utilizing a T cell proliferation assay based on bromodeoxyuridine (BrdU) incorporation during DNA synthesis in replicating cells. For our purposes, we are using an assay based on the proliferation of CD4⁺ T cells derived from transgenic mice, providing ova-specific T cell receptors. First results are quite promising, indicating a clear ovalbumin-specific proliferation, when xylose-induced (ovalbumin containing) supernatants of SA113Δ*spa* pTX-*sp-pp-ova* overnight cultures were applied onto a co-culture of 2 x 10⁵ CD4⁺ T cells with 3.8 x 10⁵ APCs in the presence of undiluted supernatants (**Fig. 21**). In contrast, stimulation with intracellular ovalbumin-expressing cultures (SA113Δ*spa* pTX-*pp-ova*) did not lead to a significant difference in T cell proliferation. A possible explanation is the fact that not all T cells derived from transgenic mice are in fact specific. The number of ova-specific T cells is estimated between 60 – 80 % of total T cells. This, together with other potentially APC-activating molecules, such as DNA, RNA, etc., lead to high proliferation rates in every samples, no matter, if xylose-induced or not (data not shown). Studies from Matsui *et al* (Matsui *et al.*, 2007; Matsui and Nishikawa, 2012) indicated an impact of PGN sensing on the development of allergies. Therefore, we will perform additional DC-T_h cell co-culture assays with subsequent analysis of the respective cytokine profiles with focus on IL-4 as major cytokine in T_h2 responses.

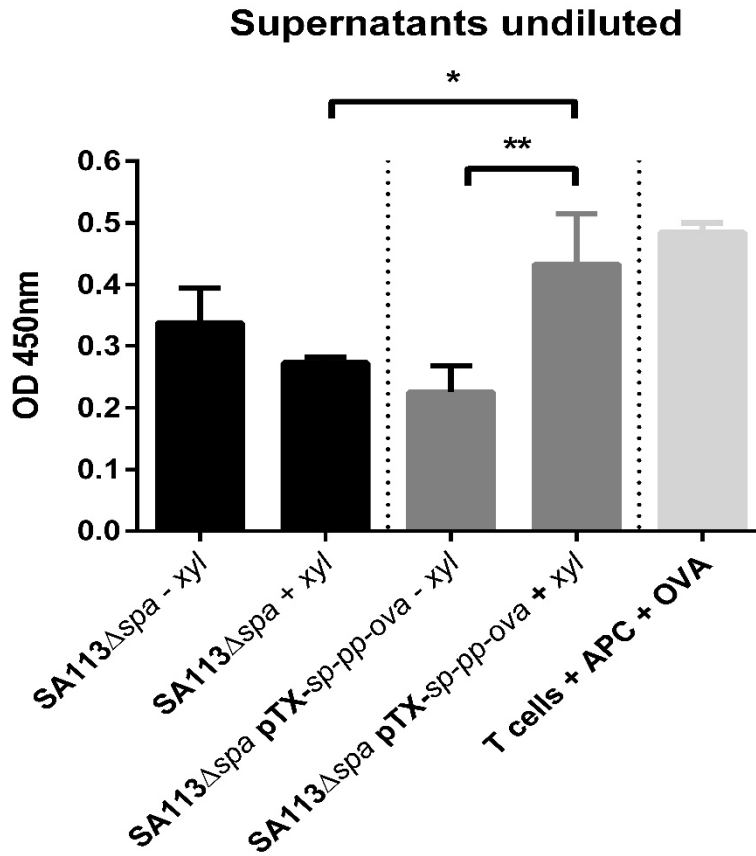


Figure 21: Proliferation of CD4⁺ T cells after stimulation of APCs with culture supernatants

Ovalbumin expression after induction with 0.5 % xylose of strain SA113 Δ spa pTX-sp-pp-ova led to a significant increase in proliferation of T cells, when compared to a non-ovalbumin producing strain and the same non-induced strain. Statistical analysis was done using a nonparametric one-way ANOVA model for repeated measurements with a Bonferroni adjustment.

References

- Aderem, A., and Underhill, D. (1999) Mechanisms of phagocytosis in macrophages.
- Ajuwon, K., Banz, W., and Winters, T. (2009) Stimulation with Peptidoglycan induces interleukin 6 and TLR2 expression and a concomitant downregulation of expression of adiponectin receptors 1 and 2 in 3T3-L1 adipocytes. *Journal of Inflammation* **6**: 8.
- Akira, S. (2003) Mammalian Toll-like receptors. *Current Opinion in Immunology* **15**: 511.
- Akira, S., and Takeda, K. (2004) Toll-like receptor signalling. *Nat Rev Immunol* **4**: 499–511 <http://dx.doi.org/10.1038/nri1391>.
- Akira, S., Uematsu, S., and Takeuchi, O. (2006) Pathogen recognition and innate immunity. *Cell* **124**: 783–801.
- Aroniadis, O.C., and Brandt, L.J. (2013) Fecal microbiota transplantation: past, present and future. *Curr Opin Gastroenterol* **29**: 79–84 <http://meta.wkhealth.com/pt/pt-core/template-journal/lwwgateway/media/landingpage.htm?issn=0267-1379&volume=29&issue=1&spage=79>.
- Ausubel, F. (2005) Are innate immune signaling pathways in plants and animals conserved? *Nature Immunology* **6**: 973–979.
- Barreteau, H., Kovac, A., Boniface, A., Sova, M., Gobec, S., and Blanot, D. (2008) Cytoplasmic steps of peptidoglycan biosynthesis. *FEMS Microbiol Rev* **32**: 168–207.
- Baumgart, D.C., and Carding, S.R. (2007) Inflammatory bowel disease: cause and immunobiology. *Lancet* **369**: 1627–40 [http://linkinghub.elsevier.com/retrieve/pii/S0140-6736\(07\)60750-8](http://linkinghub.elsevier.com/retrieve/pii/S0140-6736(07)60750-8).
- Bera, A., Biswas, R., Herbert, S., and Gotz, F. (2006) The Presence of Peptidoglycan O-Acetyltransferase in Various Staphylococcal Species Correlates with Lysozyme Resistance and Pathogenicity. *Infection and Immunity* **74**: 45984604.

- Bera, A., Herbert, S., Jakob, A., Vollmer, W., and Götz, F. (2005) Why are pathogenic staphylococci so lysozyme resistant? The peptidoglycan O- acetyltransferase OatA is the major determinant for lysozyme resistance of *Staphylococcus aureus*. *Molecular Microbiology* **55**: 778–787.
- BERGERBACHI, B., and TSCHIRSKE, M. (1998) Role of fem factors in methicillin resistance. *Drug Resistance Updates* **1**: 325335.
- Cella, M., Sallusto, F., and Lanzavecchia, A. (1997) Origin, maturation and antigen presenting function of dendritic cells. *Current opinion in immunology* **9**: 10–16 <http://www.sciencedirect.com/science/article/pii/S0952791597801537>.
- Chamaillard, M., Hashimoto, M., Horie, Y., Masumoto, J., Qiu, S., Saab, L., *et al.* (2003) An essential role for NOD1 in host recognition of bacterial peptidoglycan containing diaminopimelic acid. *Nat Immunol* **4**: 702–7.
- Chiu, Y.-C.C., Lin, C.-Y.Y., Chen, C.-P.P., Huang, K.-C.C., Tong, K.-M.M., Tzeng, C.-Y.Y., *et al.* (2009) Peptidoglycan enhances IL-6 production in human synovial fibroblasts via TLR2 receptor, focal adhesion kinase, Akt, and AP-1- dependent pathway. *J Immunol* **183**: 2785–92 <http://www.jimmunol.org/cgi/pmidlookup?view=long&pmid=19635908>.
- Costello, E.K., Lauber, C.L., Hamady, M., Fierer, N., Gordon, J.I., and Knight, R. (2009) Bacterial community variation in human body habitats across space and time. *Science* **326**: 1694–7 <http://www.sciencemag.org/cgi/pmidlookup?view=long&pmid=19892944>.
- Croner, S. (1992) Prediction and detection of allergy development: Influence of genetic and environmental factors. *The Journal of Pediatrics* **121**.
- Deurenberg, R.H., and Stobberingh, E.E. (2009) The molecular evolution of hospital- and community-associated methicillin-resistant *Staphylococcus aureus*. *Curr Mol Med* **9**: 100–15 <http://www.eurekaselect.com/68849/article>.
- Didierlaurent, A., Simonet, M., and Sirard, J. (2005) Intestinal epithelial barrier and mucosal immunity. *Cellular and Molecular Life Sciences* **62**: 12851287.

- Droste, J.H., Wieringa, M.H., Weyler, J.J., Nelen, V.J., Vermeire, P.A., and Bever, H.P. Van (2000) Does the use of antibiotics in early childhood increase the risk of asthma and allergic disease? *Clin Exp Allergy* **30**: 1547–53
<http://onlinelibrary.wiley.com/resolve/openurl?genre=article&sid=nlm:pubmed&issn=0954-7894&date=2000&volume=30&issue=11&spage=1547>.
- Durfee, T., Nelson, R., Baldwin, S., Plunkett, G., Burland, V., Mau, B., *et al.* (2008) The complete genome sequence of *Escherichia coli* DH10B: insights into the biology of a laboratory workhorse. *J Bacteriol* **190**: 2597–606.
- Fedtke, I., Götz, F., and Peschel, A. (2004) Bacterial evasion of innate host defenses--the *Staphylococcus aureus* lesson. *Int J Med Microbiol* **294**: 189–94.
- Foster, T.J. (2005) Immune evasion by staphylococci. *Nat Rev Microbiol* **3**: 948–58.
- Gay, N.J., Symmons, M.F., Gangloff, M., and Bryant, C.E. (2014) Assembly and localization of Toll-like receptor signalling complexes. *Nat Rev Immunol* **14**: 546–58.
- Giesbrecht, P., Kersten, T., Maidhof, H., and Wecke, J. (1998) Staphylococcal cell wall: morphogenesis and fatal variations in the presence of penicillin. *Microbiol Mol Biol Rev* **62**: 1371–414 <http://mmbbr.asm.org/cgi/pmidlookup?view=long&pmid=9841676>.
- Girardin, S.E., Boneca, I.G., Viala, J., Chamaillard, M., Labigne, A., Thomas, G., *et al.* (2003) Nod2 is a general sensor of peptidoglycan through muramyl dipeptide (MDP) detection. *J Biol Chem* **278**: 8869–72.
- Glauner, B., Höltje, J.V., and Schwarz, U. (1988) The composition of the murein of *Escherichia coli*. *J Biol Chem* **263**: 10088–95
<http://www.jbc.org/cgi/pmidlookup?view=long&pmid=3292521>.
- Gordon, S., and Taylor, P. (2005) Monocyte and macrophage heterogeneity. *Nature Reviews Immunology* **5**: 953–964.
- Gupta, S.K., Bajwa, P., Deb, R., Chellappa, M.M., and Dey, S. (2014) Flagellin a toll-like receptor 5 agonist as an adjuvant in chicken vaccines. *Clin Vaccine Immunol* **21**: 261–70.

- Götz, F, Bannerman, T, and Schleifer, KH (2006) The genera *Staphylococcus* and *Micrococcus*. *The prokaryotes* http://link.springer.com/10.1007/0-387-30744-3_1.
- Götz, F. (2002) *Staphylococcus* and biofilms. *Molecular Microbiology* **43**: 1367–1378.
- Hampe, J., Cuthbert, A., Croucher, P., Mirza, M., Mascheretti, S., Fisher, S., *et al.* (2001) Association between insertion mutation in NOD2 gene and Crohn's disease in German and British populations. *The Lancet* .
- Harwood, N., and Batista, F. (2010) Early Events in B Cell Activation. *Immunology* **28**: 185–210.
- Henneke, P., Dramsi, S., Mancuso, G., Chraibi, K., Pellegrini, E., Theilacker, C., *et al.* (2008) Lipoproteins are critical TLR2 activating toxins in group B streptococcal sepsis. *J Immunol* **180**: 6149–58 <http://www.jimmunol.org/cgi/pmidlookup?view=long&pmid=18424736>.
- Hirschfeld, M., Weis, J.J., Toshchakov, V., Salkowski, C.A., Cody, M.J., Ward, D.C., *et al.* (2001) Signaling by toll-like receptor 2 and 4 agonists results in differential gene expression in murine macrophages. *Infect Immun* **69**: 1477–82.
- Hoshino, K., Takeuchi, O., Kawai, T., Sanjo, H., Ogawa, T., Takeda, Y., *et al.* (1999) Cutting edge: Toll-like receptor 4 (TLR4)-deficient mice are hyporesponsive to lipopolysaccharide: evidence for TLR4 as the Lps gene product. *J Immunol* **162**: 3749–52.
- Hsieh, C.S., Macatonia, S.E., Tripp, C.S., Wolf, S.F., O'Garra, A., and Murphy, K.M. (1993) Development of TH1 CD4+ T cells through IL-12 produced by *Listeria*-induced macrophages. *Science* **260**: 547–9 <http://www.sciencemag.org/cgi/pmidlookup?view=long&pmid=8097338>.
- Inohara, N., and Nuñez, G. (2003) NODs: intracellular proteins involved in inflammation and apoptosis. *Nat Rev Immunol* **3**: 371–82 <http://dx.doi.org/10.1038/nri1086>.
- Iyer, J., and Coggeshall, K. (2011) Cutting edge: primary innate immune cells respond efficiently to polymeric peptidoglycan, but not to peptidoglycan monomers. *Journal of immunology (Baltimore, Md : 1950)* **186**: 3841–5.

- Janeway, C.A., and Medzhitov, R. (2002) Innate immune recognition. *Annu Rev Immunol* **20**: 197–216
http://arjournals.annualreviews.org/doi/full/10.1146/annurev.immunol.20.083001.084359?url_ver=Z39.88-2003&rfr_id=ori:rid:crossref.org&rfr_dat=cr_pub%3dpubmed.
- Jonge, B.L. de, Chang, Y.S., Gage, D., and Tomasz, A. (1992) Peptidoglycan composition of a highly methicillin-resistant *Staphylococcus aureus* strain. The role of penicillin binding protein 2A. *J Biol Chem* **267**: 11248–54
<http://www.jbc.org/cgi/pmidlookup?view=long&pmid=1597460>.
- Jostins, L., Ripke, S., Weersma, R.K., Duerr, R.H., McGovern, D.P., Hui, K.Y., *et al.* (2012) Host-microbe interactions have shaped the genetic architecture of inflammatory bowel disease. *Nature* **491**: 119–24 <http://dx.doi.org/10.1038/nature11582>.
- Jr, J., and Medzhitov, R. (2002) Innate immune recognition. .
- Järvinen, K.M., Konstantinou, G.N., Pilapil, M., Arrieta, M.-C.C., Noone, S., Sampson, H.A., *et al.* (2013) Intestinal permeability in children with food allergy on specific elimination diets. *Pediatr Allergy Immunol* **24**: 589–95.
- Kadowaki, N. (2007) Dendritic Cells—A Conductor of T Cell Differentiation—. *Allergology International* **56**: 193–199.
- Kaesler, S., Volz, T., Skabytska, Y., Köberle, M., Hein, U., Chen, K.-M.M., *et al.* (2014) Toll-like receptor 2 ligands promote chronic atopic dermatitis through IL-4-mediated suppression of IL-10. *J Allergy Clin Immunol* **134**: 92–9.
- Kassiotis, G., Garcia, S., Simpson, E., and Stockinger, B. (2002) Impairment of immunological memory in the absence of MHC despite survival of memory T cells. *Nat Immunol* **3**: 244–50 <http://dx.doi.org/10.1038/ni766>.
- Kluytmans, J., Belkum, A., and Verbrugh, H. (1997) Nasal carriage of *Staphylococcus aureus*: epidemiology, underlying mechanisms, and associated risks. *Clinical microbiology reviews* **10**: 505–20.

- Kurokawa, K., Kim, M.-S.S., Ichikawa, R., Ryu, K.-H.H., Dohmae, N., Nakayama, H., and Lee, B.L. (2012) Environment-mediated accumulation of diacyl lipoproteins over their triacyl counterparts in *Staphylococcus aureus*. *J Bacteriol* **194**: 3299–306.
- Kurokawa, K., Lee, H., Roh, K.-B.B., Asanuma, M., Kim, Y.S., Nakayama, H., *et al.* (2009) The Triacylated ATP Binding Cluster Transporter Substrate-binding Lipoprotein of *Staphylococcus aureus* Functions as a Native Ligand for Toll-like Receptor 2. *J Biol Chem* **284**: 8406–11 <http://www.jbc.org/cgi/pmidlookup?view=long&pmid=19139093>.
- Kurokawa, K., Ryu, K.-H.H., Ichikawa, R., Masuda, A., Kim, M.-S.S., Lee, H., *et al.* (2012) Novel bacterial lipoprotein structures conserved in low-GC content gram-positive bacteria are recognized by Toll-like receptor 2. *J Biol Chem* **287**: 13170–81.
- Li, A., Rue, M., Zhou, J., Wang, H., Goldwasser, M.A., Neubergh, D., *et al.* (2004) Utilization of Ig heavy chain variable, diversity, and joining gene segments in children with B-lineage acute lymphoblastic leukemia: implications for the mechanisms of VDJ recombination and for pathogenesis. *Blood* **103**: 4602–9.
- Lipscomb, M., and Masten, B. (2002) Dendritic cells: immune regulators in health and disease. *Physiological reviews* **82**: 97–130.
- Litman, G., Rast, J., and Fugmann, S. (2010) The origins of vertebrate adaptive immunity. *Nature Reviews Immunology* **10**: 543–553.
- Lovering, A.L., Safadi, S.S., and Strynadka, N.C. (2012) Structural perspective of peptidoglycan biosynthesis and assembly. *Annu Rev Biochem* **81**: 451–78 http://arjournals.annualreviews.org/doi/full/10.1146/annurev-biochem-061809-112742?url_ver=Z39.88-2003&rfr_id=ori:rid:crossref.org&rfr_dat=cr_pub%3dpubmed.
- Lowy, F.D. (1998) *Staphylococcus aureus* infections. *N Engl J Med* **339**: 520–32 http://www.nejm.org/doi/abs/10.1056/NEJM199808203390806?url_ver=Z39.88-2003&rfr_id=ori:rid:crossref.org&rfr_dat=cr_pub%3dpubmed.

- Lucignani, G. (2007) Rubor, calor, tumor, dolor, functio laesa... or molecular imaging. *Eur J Nucl Med Mol Imaging* **34**: 2135–41 <http://dx.doi.org/10.1007/s00259-007-0617-9>.
- Macho Fernandez, E., Fernandez, E.M., Valenti, V., Rockel, C., Hermann, C., Pot, B., *et al.* (2011) Anti-inflammatory capacity of selected lactobacilli in experimental colitis is driven by NOD2-mediated recognition of a specific peptidoglycan-derived muropeptide. *Gut* **60**: 1050–9 <http://gut.bmj.com/cgi/pmidlookup?view=long&pmid=21471573>.
- Magalhaes, J.G., Fritz, J.H., Bourhis, L. Le, Sellge, G., Travassos, L.H., Selvanantham, T., *et al.* (2008) Nod2-dependent Th2 polarization of antigen-specific immunity. *J Immunol* **181**: 7925–35.
- Matsui, K, and Nishikawa, A (2012) Peptidoglycan From Staphylococcus aureus Induces TH 2 Immune Response in Mice. *Journal of Investigational Allergology and Clinical ...* <http://www.jiaci.org/issues/vol22issue2/1.pdf>.
- Matsui, K., Wirotsangthong, M., and Nishikawa, A. (2007) Percutaneous application of peptidoglycan from Staphylococcus aureus induces eosinophil infiltration in mouse skin. *Clin Exp Allergy* **37**: 615–22 <http://onlinelibrary.wiley.com/resolve/openurl?genre=article&sid=nlm:pubmed&issn=0954-7894&date=2007&volume=37&issue=4&spage=615>.
- Matsumoto, M., Funami, K., Tanabe, M., Oshiumi, H., Shingai, M., Seto, Y., *et al.* (2003) Subcellular localization of Toll-like receptor 3 in human dendritic cells. *J Immunol* **171**: 3154–62.
- McKenna, K., Beignon, A.-S.S., and Bhardwaj, N. (2005) Plasmacytoid dendritic cells: linking innate and adaptive immunity. *J Virol* **79**: 17–27 <http://jvi.asm.org/cgi/pmidlookup?view=long&pmid=15596797>.
- Medzhitov, R. (2001) Toll-like receptors and innate immunity. *Nature Reviews Immunology* **1**: 135–145.

- Molodecky, N.A., Soon, I.S., Rabi, D.M., Ghali, W.A., Ferris, M., Chernoff, G., *et al.* (2012) Increasing incidence and prevalence of the inflammatory bowel diseases with time, based on systematic review. *Gastroenterology* **142**: 46–54.e42; quiz e30.
- Mukhopadhyaya, I., Hansen, R., El-Omar, E.M., and Hold, G.L. (2012) IBD-what role do Proteobacteria play? *Nat Rev Gastroenterol Hepatol* **9**: 219–30.
- Müller-Anstett, M.A., Müller, P., Albrecht, T., Nega, M., Wagener, J., Gao, Q., *et al.* (2010) Staphylococcal peptidoglycan co-localizes with Nod2 and TLR2 and activates innate immune response via both receptors in primary murine keratinocytes. *PLoS ONE* **5**: e13153 <http://dx.plos.org/10.1371/journal.pone.0013153>.
- O’Byrne, K., and Dalglish, A. (2013) Chronic immune activation and inflammation as the cause of malignancy. *British Journal of Cancer* **85**.
- Proctor, R.A., Eiff, C. von, Kahl, B.C., Becker, K., McNamara, P., Herrmann, M., and Peters, G. (2006) Small colony variants: a pathogenic form of bacteria that facilitates persistent and recurrent infections. *Nat Rev Microbiol* **4**: 295–305.
- Rakoff-Nahoum, S., and Medzhitov, R. (2008) Toll-like receptors and cancer. *Nature Reviews Cancer* .
- Ralph, P., and Nakoinz, I. (1975) Phagocytosis and cytolysis by a macrophage tumour and its cloned cell line. *Nature* **257**: 393–4.
- Rath, A., Glibowicka, M., Nadeau, V.G., Chen, G., and Deber, C.M. (2009) Detergent binding explains anomalous SDS-PAGE migration of membrane proteins. *Proc Natl Acad Sci USA* **106**: 1760–5.
- Ravetch, J.V., and Bolland, S. (2001) IgG Fc receptors. *Annu Rev Immunol* **19**: 275–90.
- Rescigno, M. (2014) Dendritic cell-epithelial cell crosstalk in the gut. *Immunol Rev* **260**: 118–28.
- Sallusto, F., Lanzavecchia, A., Araki, K., and Ahmed, R. (2010) From Vaccines to Memory and Back. *Immunity* **33**.

- Schaffler, H., Demircioglu, D., Kuhner, D., Menz, S., Bender, A., Autenrieth, I., *et al.* (2014) NOD2 Stimulation by Staphylococcus aureus-Derived Peptidoglycan Is Boosted by Toll-Like Receptor 2 Costimulation with Lipoproteins in Dendritic Cells. *Infection and Immunity* **82**: 46814688.
- Schmaler, M. (2010) Staphylococcus aureus lipoproteins-TLR2-mediated activation of innate and adaptive immunity. <http://edoc.unibas.ch/1098/>.
- Schmaler, M., Jann, N., Ferracin, F., Landolt, L., Biswas, L., Götz, F., and Landmann, R. (2009) Lipoproteins in Staphylococcus aureus mediate inflammation by TLR2 and iron-dependent growth in vivo. *Journal of immunology (Baltimore, Md : 1950)* **182**: 7110–8.
- Schmaler, M., Jann, N., Götz, F., and Landmann, R. (2010) Staphylococcal lipoproteins and their role in bacterial survival in mice. *International journal of medical microbiology : IJMM* **300**: 155–60.
- Shi, Y., Mowery, R.A., Ashley, J., Hentz, M., Ramirez, A.J., Bilgicer, B., *et al.* (2012) Abnormal SDS-PAGE migration of cytosolic proteins can identify domains and mechanisms that control surfactant binding. *Protein Sci* **21**: 1197–209 <http://dx.doi.org/10.1002/pro.2107>.
- Shin, J.-S.S., Ebersold, M., Pypaert, M., Delamarre, L., Hartley, A., and Mellman, I. (2006) Surface expression of MHC class II in dendritic cells is controlled by regulated ubiquitination. *Nature* **444**: 115–8.
- Silhavy, T.J., Kahne, D., and Walker, S. (2010) The bacterial cell envelope. *Cold Spring Harb Perspect Biol* **2**: a000414
<http://cshperspectives.cshlp.org/cgi/pmidlookup?view=long&pmid=20452953>.
- Stoll, H., Dengjel, J., Nerz, C., and Gotz, F. (2005) Staphylococcus aureus Deficient in Lipidation of Prelipoproteins Is Attenuated in Growth and Immune Activation. *Infection and Immunity* **73**: 24112423.
- Strober, W., Kitani, A., Fuss, I., Asano, N., and Watanabe, T. (2008) The molecular basis of NOD2 susceptibility mutations in Crohn's disease. *Mucosal Immunology* .

- Sturmfels, A., Götz, F., and Peschel, A. (2001) Secretion of human growth hormone by the food-grade bacterium *Staphylococcus carnosus* requires a propeptide irrespective of the signal peptide used. *Archives of Microbiology* **175**: 295–300.
- Swert, L. (1999) Risk factors for allergy. *European Journal of Pediatrics* **158**.
- Swirski, F., Nahrendorf, M., Etzrodt, M., Wildgruber, M., Cortez-Retamozo, V., Panizzi, P., *et al.* (2009) Identification of splenic reservoir monocytes and their deployment to inflammatory sites. *Science (New York, NY)* **325**: 612–6.
- Travassos, L., Girardin, S., Philpott, D., Blanot, D., Nahori, M., Werts, C., and Boneca, I. (2004) Toll- like receptor 2- dependent bacterial sensing does not occur via peptidoglycan recognition. *EMBO reports* **5**: 1000–1006.
- Vael, C., and Desager, K. (2009) The importance of the development of the intestinal microbiota in infancy. *Curr Opin Pediatr* **21**: 794–800.
- Veldkamp, K.E., and Strijp, J.A. van (2009) Innate immune evasion by staphylococci. *Adv Exp Med Biol* **666**: 19–31.
- Vollmer, W., Blanot, D., and Pedro, M.A. de (2008) Peptidoglycan structure and architecture. *FEMS Microbiol Rev* **32**: 149–67.
- Volz, T., Nega, M., Buschmann, J., Kaesler, S., Guenova, E., Peschel, A., *et al.* (2010) Natural *Staphylococcus aureus*-derived peptidoglycan fragments activate NOD2 and act as potent costimulators of the innate immune system exclusively in the presence of TLR signals. *The FASEB Journal* **24**: 4089–4102.
- Watanabe, T., Asano, N., Murray, P.J., Ozato, K., Taylor, P., Fuss, I.J., *et al.* (2008) Muramyl dipeptide activation of nucleotide-binding oligomerization domain 2 protects mice from experimental colitis. *J Clin Invest* **118**: 545–59 <http://dx.doi.org/10.1172/JCI33145>.
- Ziegler-Heitbrock, H.W., Thiel, E., Fütterer, A., Herzog, V., Wirtz, A., and Riethmüller, G. (1988) Establishment of a human cell line (Mono Mac 6) with characteristics of mature monocytes. *Int J Cancer* **41**: 456–61.

Ziegler-Heitbrock, L. (2007) The CD14+ CD16+ blood monocytes: their role in infection and inflammation. *Journal of Leukocyte Biology* **81**: 584–592.

Zinkernagel, R., Bachmann, M., Kündig, T., Oehen, S., Pirchet, H., and Hengartner, H. (2003) ON IMMUNOLOGICAL MEMORY. *Immunology* **14**: 333–367.

Curriculum vitae

Name: Doğan Doruk Demircioğlu

Geburtstag: 07.05.1982

Geburtsort: Reutlingen

Schul- und Universitätsausbildung:

1988 bis 1992 Freie Evangelische Grundschule Reutlingen (FES)

1992 bis 1999 Johannes-Kepler-Gymnasium Reutlingen (JKG)

1999 bis 2003 Isolde-Kurz-Gymnasium Reutlingen (IKG)

2004 bis 2005 Studium der Bioinformatik
Eberhard-Karls-Universität Tübingen

2005 bis 2011 Studium der Biologie
Eberhard-Karls-Universität Tübingen
Hauptfach: Mikrobiologie
Biologisches Nebenfach: Immunologie
Nichtbiologisches Nebenfach: Virologie

04/2010 bis 04/2011 Diplomarbeit am Lehrstuhl Mikrobielle Genetik (AG Götz)
Eberhard-Karls-Universität Tübingen

10/2011 bis 10/2014 Dissertation am Lehrstuhl Mikrobielle Genetik (AG Götz)
Eberhard-Karls-Universität Tübingen

Acknowledgements

Coming to the end of my doctoral thesis, I would like to thank several people, who were always there for me during my journey through the hell.

First, I would like to thank my parents: my lovely mother Şükran Demircioğlu and my lovely father Güner Zafer Demircioğlu. They encouraged and supported me through all the years I've been studying and suffering. When times were hard, I could always lean back and fill up my empty batteries in a wonderful home.

I would also like to thank my supervisor Prof. Dr. Friedrich Götz, who has offered me the opportunity to work on an interesting topic. I thank my collaborators Prof. Dr. med. Tilo Biedermann, Dr. med. Thomas Volz and Dr. rer. nat. Yuliya Skabytska for a fruitful cooperation.

Special thanks to Daniel Kühner, who always supported me, whenever I was facing a problem and taught me how to use an HPLC, which is a technique I totally love. Special thanks are also to my countryman Ali Coşkun, who brought a little peace of my home to my lab and with whom I could always talk about my sorrows, no matter if scientific or personal. A third special thank you to my vietnamese friend Minh-Thu Nguyen, with whom I also worked together on fatty acids and lipoproteins. We had really funny discussions and shared our sorrows. And there were quite much of them during all the years.

I am also very grateful to all the other lab members, which helped me, whenever they could: Ya-Yun Chu (aka YY), Linda Dube (especially for teaching me Westernblots), Sophia Krauß, Martin Schlag, Ute Bertsche, Ralph Bertram, Martina Leibig, Ralf Rosenstein, Regine Stemmler (the best TA on this planet), Silvana Perconti, Peter Popella and Patrick Ebner.

List of publications

Paper I:

Daniel Kühner, Mark Stahl, **Doğan D. Demircioğlu**, Ute Bertsche

From cells to muropeptide structures in 24 h: Peptidoglycan mapping by ULPC-MS

Sci Rep. 2014 Dec 16;4:7494. doi: 10.1038/srep07494

Paper II:

Holger Schäffler*; **Doğan D. Demircioğlu***; Daniel Kühner; Sarah Menz; Annika Bender; Ingo B Autenrieth; Peggy Bodammer; Georg Lamprecht; Friedrich Götz; Julia-Stefanie S. Frick

NOD2 Stimulation by Staphylococcus aureus-Derived Peptidoglycan Is Boosted by Toll-Like Receptor 2 Costimulation with Lipoproteins in Dendritic Cells.

Infect. Immun. November 2014 vol. 82 no. 11 4681-4688

*H.S. and D.D.D. contributed equally to this article.

Paper III:

Yuliya Skabytska, Florian Wölbing, Claudia Günther, Martin Köberle, Susanne Kaesler, Ko-Ming Chen, Emmanuella Guenova, **Doruk Demircioğlu**, Wolfgang E. Kempf, Thomas Volz, Hans-Georg Rammensee, Martin Schaller, Martin Röcken, Friedrich Götz and Tilo Biedermann

Cutaneous Innate Immune Sensing of Toll-like Receptor 2-6 Ligands Suppresses T Cell Immunity by Inducing Myeloid-Derived Suppressor Cells

Immunity Volume 41, Issue 5, p762–775, 20 November 2014,

<http://dx.doi.org/10.1016/j.immuni.2014.10.009>



OPEN

SUBJECT AREAS:

CELLULAR
MICROBIOLOGY

PATHOGENS

HIGH-THROUGHPUT SCREENING

CHROMATOGRAPHY

Received

11 September 2014

Accepted

19 November 2014

Published

16 December 2014

Correspondence and requests for materials should be addressed to U.B. (ute.bertsche@uni-tuebingen.de)

From cells to muropeptide structures in 24 h: Peptidoglycan mapping by UPLC-MS

Daniel Kühner¹, Mark Stahl², Dogan D. Demircioglu³ & Ute Bertsche¹

¹Eberhard Karls University Tuebingen, IMIT - Microbial Genetics, Waldhaeuser Str. 70/8, 72076 Tuebingen, Germany, ²Eberhard Karls University Tuebingen, Center for Plant Molecular Biology, Central Facilities, Auf der Morgenstelle 32, 72076 Tuebingen, Germany, ³Eberhard Karls University Tuebingen, IMIT - Microbial Genetics, Auf der Morgenstelle 28, 72076 Tuebingen, Germany.

Peptidoglycan (PGN) is ubiquitous in nearly all bacterial species. The PGN sacculus protects the cells against their own internal turgor making PGN one of the most important targets for antibacterial treatment. Within the last sixty years PGN composition has been intensively studied by various methods. The breakthrough was the application of HPLC technology on the analysis of muropeptides. However, preparation of pure PGN relied on a very time consuming method of about one week. We established a purification protocol for both Gram-positive and Gram-negative bacteria which can be completely performed in plastic reaction tubes yielding pure muropeptides within 24 hours. The muropeptides can be analyzed by UPLC-MS, allowing their immediate determination. This new rapid method provides the feasibility to screen PGN composition even in high throughput, making it a highly useful tool for basic research as well as for the pharmaceutical industry.

The bacterial cell wall is mainly composed of peptidoglycan (PGN) with attached proteins and modifications like wall teichoic acids (WTAs). PGN is a rigid structure of alternating N-Acetylglucosamine-N-Acetylmuramic acid (GlcNAc-MurNAc) glycan chains cross-linked by peptides. The peptide moiety consists of a stem peptide (L-Alanine – D-iGlutamate/iGlutamine – L-Lysin/meso-Diaminopimelic acid – D-Alanine – D-Alanine). L-Lysin (L-Lys) is mainly a feature of Gram-positives, while meso-Diaminopimelic acid (mDAP) is typical for Gram-negatives as well as for *Bacillus subtilis*. We will abbreviate the second amino acid of the stem peptide by Glx which is either glutamine (Gln) or glutamate (Glu). Our model organism *S. aureus* harbors also a five-glycine (Gly₅) interpeptide bridge branching from the L-lysine (Lys), which constitutes indirect cross-links between two adjacent stem peptides¹. The resulting macromolecule forms a bag shaped sacculus covering the whole bacterial cell. It is unique to bacteria ensuring their shape and protecting them against their own internal turgor. Loss of its integrity results in cell lysis, making PGN one of the most important targets for antibacterial treatment. Indeed, it is the target for well-known therapeutic drugs such as β -lactams or vancomycin, which all inhibit the late steps of glycan chain polymerization and/or cross-linking, both occurring outside the cytoplasmic membrane. With the emergence of new and highly multi-resistant bacterial strains, we are in an urgent need of new anti-microbial drugs. Therefore, it is, amongst others, important to understand the complex interplay between the PGN structure, (changes in) its chemical composition and also subsequent immune responses.

Since its first isolation in 1951 by Salton and Horne² PGN composition has been intensively studied with various methods. The original determination of the glycan and peptide composition was performed by paper chromatography¹. The breakthrough was by Glauner in 1988³, who for the first time applied high pressure liquid chromatography (HPLC) technology on the analysis of muropeptides. Muropeptides result from enzymatic digestion of the glycan strands into disaccharides, with part of them still being cross-linked by peptides to various extensions. Glauner extensively studied the effects of pH, buffer concentrations, and temperature on HPLC separation of muropeptides of the Gram-negative bacterium *E. coli*. Later, a protocol for PGN isolation and HPLC analysis of the Gram-positive *Staphylococcus aureus* was established by deJonge *et al.*⁴. Basically, these two protocols have been used ever since. However, both of them are very time consuming taking about a week to obtain pure PGN. Both protocols rely on multiple boiling steps with sodiumdodecylsulfate (SDS), which has to be washed out by extensive ultracentrifugation steps for about an hour each. Last year a protocol for isolation of *E. coli* PGN for ultra-performance liquid chromatography (UPLC) analysis was reported, that is substantially



shorter⁵. However, it still relies on washing in an ultracentrifuge thereby limiting the amounts of samples that can be prepared in parallel.

PGN research has experienced a revival within the last decade. Even PGN from bacteria like *Chlamydiae*, which had long been thought to not contain a PGN sacculus, was now successfully isolated and analyzed⁶. In addition, it had been shown, that growth conditions^{7,8} as well as various antibiotics as β -lactams and daptomycin affect PGN composition^{9–11}. To test PGN composition of different bacteria and under various conditions, a faster analysis method was needed. One which allows to test several conditions in parallel and which can also be applied to bacteria that are not easily grown in high amounts.

We established a purification protocol which can be completely performed in 2 ml reaction tubes, allowing the isolation of up to 48 samples in parallel or even in 96 well plates, yielding pure muropeptides in 24 hours. The muropeptides can be subsequently analyzed by UPLC. This reduces the amount of sample needed and the analysis time from about three hours (HPLC) to 70 min per sample. In addition, the LC conditions were adapted to mass spectrometry (MS) with suitable solvents so that the whole PGN can be directly analyzed by UPLC-MS. This allows for muropeptide determination without first collecting and desalting LC peaks and results in a complete PGN mapping. Taken together, the whole procedure is reduced from about two weeks to 24 hours. Furthermore, this fast isolation method also makes it much easier to obtain larger amounts of PGN which can be used to collect special muropeptides that can then be tested for their ability to stimulate the immune system¹².

Results and Discussion

Peptidoglycan isolation. All steps are performed in 2 ml reaction tubes with a U-shaped bottom. A detailed step-to-step protocol is given in the online method. The method is based on the isolation of PGN by boiling in 1 M NaCl. In the case of some Gram-positive strains we experienced that NaCl treatment is not sufficient. A 0.25% sodium dodecylsulfate (SDS) solution in 0.1 M Tris/HCl (pH 6.8) was then used instead. The SDS has to be washed out again thoroughly. A test for residual SDS is available and should be performed¹³. The resulting cell walls are washed with water and broken into smaller fragments by sonication. DNase, RNase, and trypsin are used to digest residual nucleic acids as well as cell wall bound proteins. The enzymes are inactivated by boiling and the cell walls are washed again with water. Treatment with 1 N HCl releases bound wall teichoic acids (WTA) or other glycoposphates. Higher concentrations of HCl must be avoided, as they result in clumping of the sample. In former protocols⁴, 48% HF was used to release WTA, but comparison of PGN treated with HCl or with HF showed no significant differences (see Fig. S1). Washing the pellet until the pH is neutral results in pure PGN that can be digested by cell wall hydrolases. In our case the PGN was digested with mutanolysin for 16 hours at 37°C shaking.

Peptidoglycan analysis by UPLC. Prior to UPLC analysis the MurNac residues of the muropeptides are reduced into Nac-muraminitol by sodium borohydrate (NaBH₄). Otherwise, mutarotation of the non-reduced glycan end would result in double peaks. Analysis is performed by UPLC (or HPLC) using trifluoroacetic acid (TFA) and a methanol gradient from 5 to 30% (for Gram-positives) or from 0 to 30% (for Gram-negatives) in 70 min. TFA is an ion pairing agent that forms an ion bond with the muropeptides resulting in a good separation of mixed analytes. As TFA is volatile it can also be used for MS analysis. However, it reduces the sensitivity of the mass spectrometer which might require extra washing after use. After testing several different

columns, the reversed phase UPLC column CSH C18, 130Å, 1.7 μ m, 2.1 mm \times 100 mm of Waters was best suited for our needs.

Peptidoglycan mapping by UPLC-MS. The samples can also be directly analyzed by UPLC-MS. We used a Synapt G2 mass spectrometer coupled to a Waters Acquity H-class and operated in positive ESI mode with a scan range from 50–2,000. The data was analyzed by MassLynx. As an example for PGN isolation by this new method, UPLC analysis and MS-mapping are presented in Fig. 1 and Fig. 2. For Gram-positives we used *Staphylococcus aureus* (*S. aureus*) SA113¹⁴ and for Gram-negatives *Escherichia coli* (*E. coli*) Nissle 1917¹⁵.

Exemplary analysis of *S. aureus* SA113 by UPLC and UPLC-MS.

The methicillin sensitive *S. aureus* strain SA113 was grown over night in BM medium. We isolated its PGN and analyzed it by UPLC as well as by UPLC-MS. This enabled us to directly determine the masses of all muropeptide peaks we got by UPLC separation. The total ion current (TIC) chromatogram obtained by UPLC-MS was almost identical to the UV pattern of UPLC alone with two exceptions: 1) Retention time of the peaks in the quaternary UPLC was about 1 min longer than in the binary UPLC-MS system. Therefore, in tables 1 and S1 only the TIC retention times are given. 2) The signal of some muropeptides, that turned out to be O-acetylated, were stronger in the TIC than in the UV (e.g. peaks 9 in Fig. 1a and b).

The UV chromatogram of the UPLC as well as the TIC chromatogram of the MS show the expected pattern as it had been published before for the methicillin resistant *S. aureus* COL by de Jonge *et al.* in 1992^{4,16}. By coupling UPLC to MS we could directly determine the masses and subsequently the potential structures of almost all peaks. The obtained masses verified that the main peaks contained the expected muropeptides starting with the monomeric peak 5 (Penta(Gln)Gly₅) which is the basic structure of all muropeptides. Peaks 11, 15, 16, 17 and 18 were composed of this basic structure cross-linked by the Gly₅ interpeptide bridge into dimers, trimers, tetramers, pentamers, and hexamers, respectively (for general structures see Fig. 3). This proved that our substantially shortened purification method as well as the adaption of UPLC-MS is working properly. Tab. 1 gives an overview on the muropeptides of the main peaks that we detected in our analysis which had already been determined before^{4,17}. The complete results of our PGN mapping of *S. aureus* SA113 is given in Tab. S1. All structures were drawn by ChemDrawUltra 13.0 (PerkinElmer), which automatically calculated the mass of the molecule and the proposed sum formula. The latter is given. As can be judged by the peak forms in the UPLC chromatogram, most peaks are composed of several muropeptides. While all of them have the same basic structure (MurNac-GlcNac with stem peptide and Gly₅ interpeptide bridge), several modifications occur, which will be discussed in detail:

The lengths of the stem peptides are variable. Monomeric stem peptides of *S. aureus* are mostly composed of the following five amino acids (L-Ala – D-iGln – L-Lys – D-Ala – D-Ala) with the D-iGln resulting from the amidation of the original D-iGlu^{18,19}. These structures are called “Pentas”. Cross-linking of several muropeptides by their interpeptide bridges forms multimeric muropeptides with normally one Penta and several Tetras, as the last D-Ala is cleaved off during the transpeptidation reaction. The resulting muropeptides are called “Penta-Tetra_n”. However, several of the higher cross-linked muropeptides had lost the last D-Ala on the Penta stem peptide shortening it to a Tetra, forming “Tetra_n” muropeptides. No further degradation into tripeptides was observed suggesting that *S. aureus* does not possess an L,D-carboxypeptidase activity.

In *S. aureus*, the D-iGlu at position two of the stem peptide is almost quantitatively amidated resulting in D-iGln^{18,19}. However, some muropeptides still harbor the original D-iGlu. While these non-amidated forms have been published to have a shorter retention time than their amidated counterparts¹⁸, in our system they had

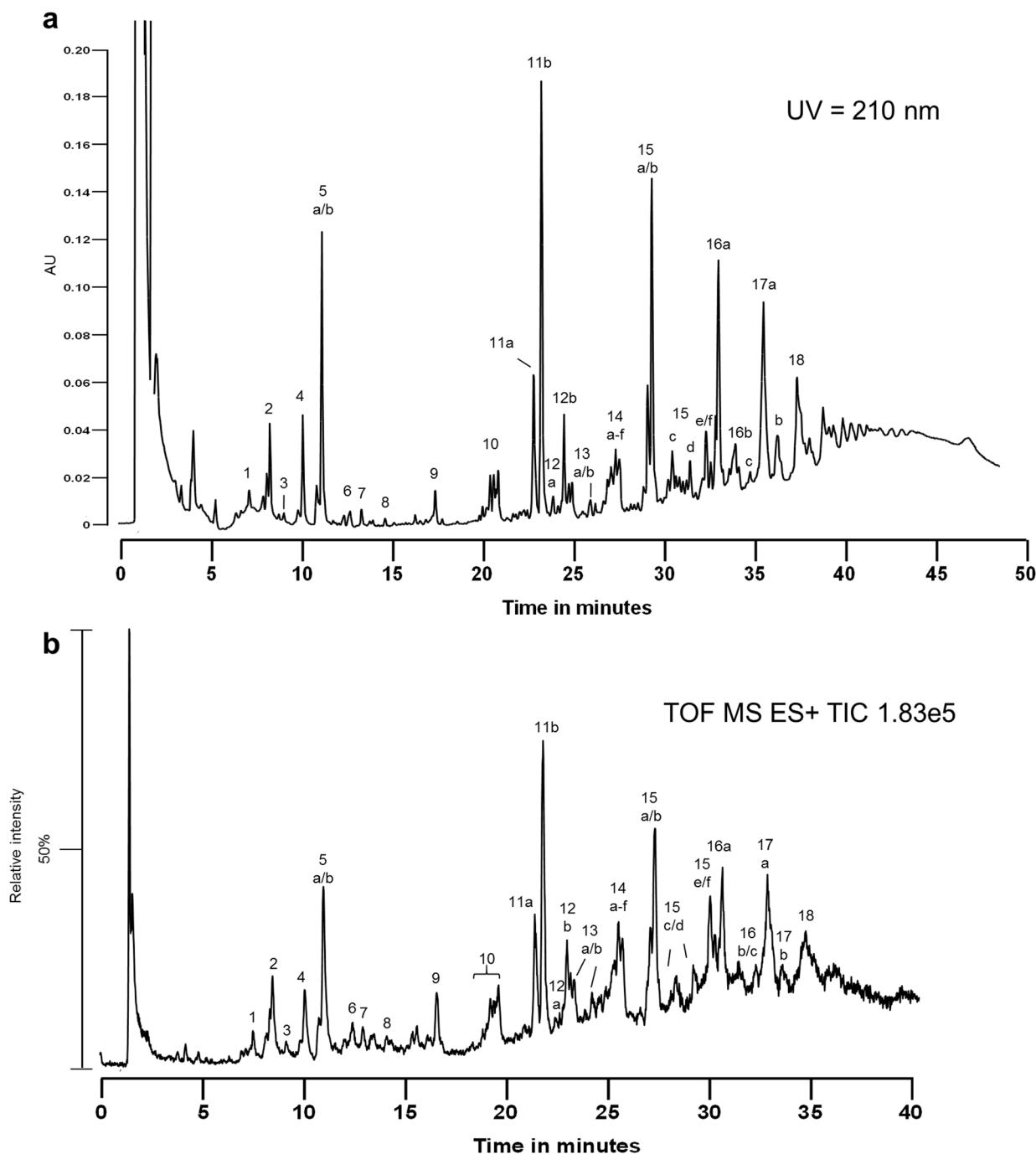


Figure 1 | Muropeptide profile of *S. aureus* SA113 obtained by UPLC and UPLC/MS. (a) Muropeptide profile of *S. aureus* SA113 obtained by reversed phase UPLC. (b) TIC of UPLC/MS analysis of *S. aureus* SA113 obtained by reversed-phase UPLC coupled to MS. Masses of indicated peaks are shown in table 1 and table S1 including molecule composition and proposed sum formula.

longer retention times. This might be due to the different column used for analysis.

The length and the composition of the interpeptide bridge varies. Gly numbers that are not a multiple of 5 indicate that this very muropeptide was originally part of a bigger molecule but had been reorganized within the PGN sacculus. For example we found monomeric muropeptides with 6, 7, 8 or 9 Gly residues instead of 5, and dimeric muropeptides with 6, 7, 8 or 9 Gly residues instead of 10. In Tab. 1 and Tab. S1 the sum of all Gly residues of each muropeptide is given. In addition, two muropeptides contained Ala in exchange for one Gly in the interpeptide bridge. Muropeptides harboring various numbers of Gly residues or Ala in their interpeptide bridge have been published before⁴.

There also occur changes in the saccharide moiety. Several muropeptides had lost one GlcNAc residue. In rare cases we also found an additional GlcNAc residue, which resulted in a muropeptide with a trisaccharide, but we did not observe the addition of an extra MurNac. In table S1 the addition or loss of a GlcNAc residue is given as +1 or -1 respectively.

Even though O-acetylation had been thought to be lost during acidic treatment, we detected that most of the small peak groups, as well as some of the peak shoulders, both of which had not been analyzed so far, were composed of acetylated muropeptides. Even treatment with HF did not result in a loss of the O-acetylated muropeptides (see Fig. S1). As an example, peak 9 contained only the O-

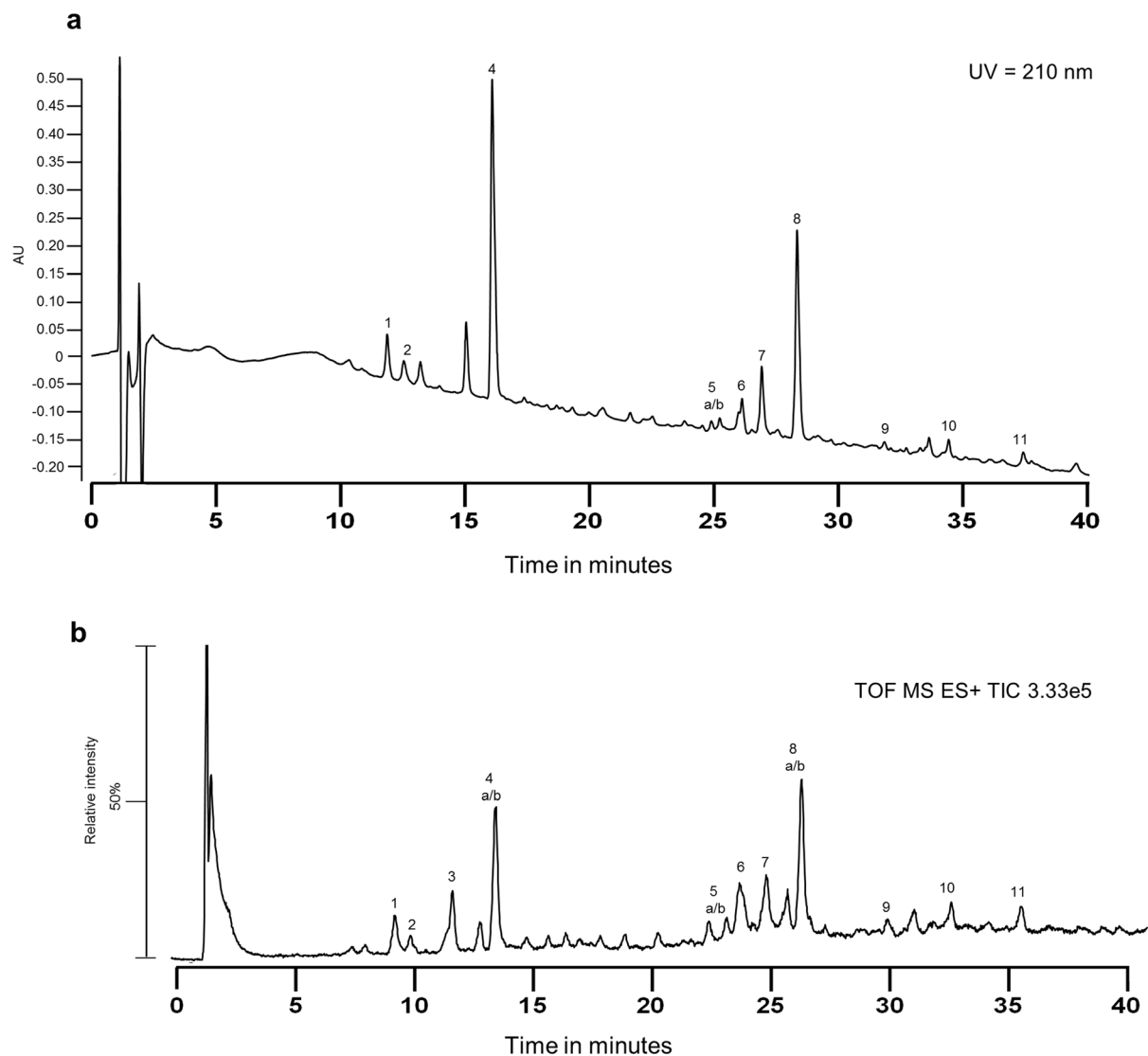


Figure 2 | Muropeptide profile of *E. coli* Nissle 1917 obtained by UPLC and UPLC/MS. (a) Muropeptide profile of *E. coli* Nissle 1917 obtained by reversed phase UPLC. (b) TIC of UPLC/MS analysis of *E. coli* Nissle 1917 obtained by reversed-phase UPLC coupled to MS. Masses of indicated peaks are shown in table 2 and table S2 including molecule composition and proposed sum formula.

acetylated monomer Penta-Gly₅. If HF caused de-O-acetylation, this peak should be missing in Fig. S1B, but it is not. The PGN of pathogenic staphylococcal strains is highly O-acetylated on the 6th C-atom

of the MurNAc, which renders the bacterium resistant against lysozyme²⁰. Lysozyme is an enzyme produced by humans and animals as a defense mechanism. It hydrolyzes PGN and therefore kills bacteria.

Table 1 | Muropeptides of *S. aureus* SA113 analyzed by UPLC-MS

Peak	Reten-tion time in TIC [min]	M+H ⁺		Lengths of the stem peptides	Inter-peptide bridges		
		Measured	Proposed sum formula		Gly	Ala	Prev. pub.
2	8.56	1239.5792	C48H83N14O24+	Tetra	6		4
4	10.17	1025.5032	C41H73N10O20+	Penta	1		4
5b	11.08	1253.5861	C49H85N14O24+	Penta	5		4
8	14.20	1267.6096	C50H87N14O24+	Penta	4	1	4
11b	21.93	2417.1181	C95H162N27O46+	Penta-Tetra	10		4
12b	23.12	2328.0745	C92H155N26O44+	Tetra ₂ (cyclic)	10		17
15b	27.45	3580.6630	C141H239N40O68+	Penta-Tetra ₂	15		4
16a	30.80	4744.1962	C187H316N53O90+	Penta-Tetra ₃	20		4
17a	33.01	5907.7014	C233H393N66O112+	Penta-Tetra ₄	25		
18	34.90	7071.2313	C279H470N79O134+	Penta-Tetra ₅	30		

Each muropeptide contains one to six stem-peptides, each consisting of L-Ala – D-Gln – L-Lys – D-Ala (– D-Ala). The amount of Gly molecules building the interpeptide bridges is given as the sum of all Gly residues present in each muropeptide. In rare cases one Gly is replaced by an Ala. The last column refers to the original reference of the respective muropeptide.

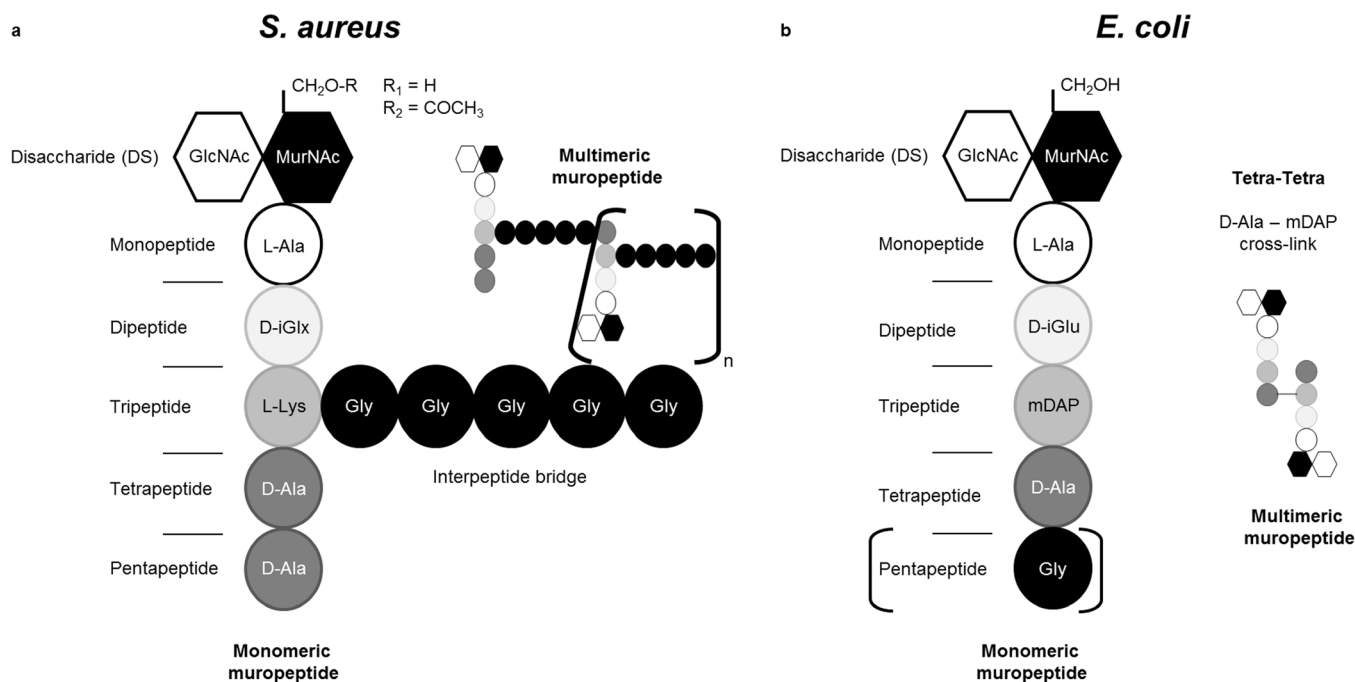


Figure 3 | Schematic structure of mucopeptides of *S. aureus* and *E. coli*. The basic structure consists of the disaccharide (GlcNAc-MurNAc) with an adjacent stem peptide (L-Ala – D-iGlx – L-Lys – D-Ala – D-Ala) with Glx being either Gln or Glu. Our model organism *S. aureus*, harbors also a five-glycine interpeptide bridge branching from the L-Lys, which constitutes indirect cross-links between two adjacent stem peptides, as it is depicted in the multimeric mucopeptide. The C at position 6 of the MurNAc can be O-acetylated.

Even though we cannot exclude that part of the O-acetylation is lost during isolation, a change of the respective peaks would be an indication for changes in the O-acetylation grade and could be useful to screen for possible mutants or for drugs affecting O-acetylation.

A very small amount of MurNAc residues seemed not to be completely reduced to NAc-muraminitol. This also resulted in longer retention times compared to the reduced counterparts.

Exemplary analysis of *E. coli* Nissle 1917 by UPLC and UPLC-MS.

As an example for Gram-negative bacteria we grew *E. coli* Nissle 1917 overnight in LB medium and isolated its PGN. The PGN was digested by mutanolysin and analyzed by UPLC and UPLC-MS (Fig. 2). Again, the UV pattern was very similar to the TIC chromatogram

and we could determine the masses of most mucopeptide peaks. The masses we found resulted in proposed mucopeptide structures that are in accordance with the ones previously published by Glauner³ (Tab. 2). The complete analysis is given in Tab. S2.

We found the expected monomeric mucopeptides with the Tri and the Tetra stem-peptide (peak 1 and 4, respectively), the dimeric mucopeptides Tetra-Tri and Tetra-Tetra (peaks 7 and 8, respectively) as well as in small amounts the trimeric mucopeptide Tetra-Tetra-Tetra (peak 10). (For a schematic drawing of the Gram-negative mucopeptides see Fig. 3b). Interestingly, for the Tetra, the Tetra-Tri and the Tetra-Tetra, we always got two peaks in the TIC chromatogram but only one in the UV chromatogram. We fragmented the respective peaks and they seem to be stereo-isomers as in all

Table 2 | Mucopeptides of *E. coli* Nissle 1917 analyzed by UPLC-MS

Peak	Retention time in TIC [min]	M+H ⁺		Proposed sum formula	Length of the stem peptides	Prev. pub.
		Measured				
1	9.27	871.3793		C34H59N6O20+	Tri	3
2	9.95	928.3986		C36H62N7O21+	Tetra-Gly(4)	3
3	11.69	699.2936		C27H47N4O17+	Di	3
		999.4775		C39H67N8O22+	Penta-Gly(5)	3
4a	12.81	942.4180		C37H64N7O21+	Tetra	
4b	13.50	942.4177		C37H64N7O21+	Tetra	3
5a	22.40	1851.8278		C73H123N14O41+	Tetra-Tetra-Gly(4)	
5b	23.10	1851.7966		C73H123N14O41+	Tetra-Tetra-Gly(4)	3
6	23.60	1922.8710		C76H128N15O42+	Tetra-Penta-Gly(5)	3
		1794.7766		C71H120N13O40+	Tetra-Tri	3
7	24.70	1794.7758		C71H120N13O40+	Tetra-Tri	3
8a	25.59	1865.8140		C74H125N14O41+	Tetra-Tetra	
8b	26.18	1865.8140		C74H125N14O41+	Tetra-Tetra	3
9	29.75	2846.2697		C113H189N22O62+	Penta-Gly(5)-Tetra-Tetra	
10	32.40	2789.2146		C111H186N21O61+	Tetra-Tetra-Tetra	3
11	35.30	1845.7744		C74H121N14O40+	anhydro Tetra-Tetra	3

Each mucopeptide contains one to three stem-peptides, each consisting of L-Ala – D-Glu – mDAP – D-Ala. In some cases the D-Ala on position four is replaced by a Gly. Some mucopeptides contain Penta stem-peptides with Gly on position five. The last column refers to the original reference of the respective mucopeptide.



three cases closely related fragmentation spectra with different relative fragment peak intensities were obtained. Fig. S2 gives the exemplary fragmentation of peaks 8a and 8b, both being the Tetra-Tetra muropeptide. We did not get any hints for mDap-mDap-crosslinking, as it had been seen in strain *E. coli* W7³.

The monomeric peak 3 in the TIC chromatogram is not in correlation with any peak of the UV chromatogram. Vice versa, the UV chromatogram has two unlabeled peaks, for which we cannot assign a muropeptide. Peak 3 of the TIC chromatogram contains 4 muropeptides (Tab. S2) with two of them being already known from the Glauner analysis³, the Di and the Penta-Gly(5) monomer. While these two peaks in the Glauner analysis have a higher retention time than the Tetra, they have a shorter retention time when analyzed with our conditions. The same is seen for Tetra-Penta-Gly(5) (peak 6) which in our system elutes before the Tetra-Tri and not after it.

With these few exceptions the elution profile of the *E. coli* muropeptides under our conditions is the same as already known. We also found one anhydro Tetra-Tetra muropeptide (peak 11), but we did not find any structures still containing lysine and arginine, which would be remnants from Braun's Lipoprotein²¹. Instead we found masses corresponding to muropeptides which had lost the GlcNAc moiety (Tab. S2). These are probably features of the strain we used. As expected, in all muropeptides with a Penta stem-peptide, the amino acid in position five is a Gly, as the last D-Ala is cleaved off by the D,D-carboxypeptidase penicillin-binding protein (PBP) 5²². We did obtain masses for the peaks between minutes 14 and 21, but they did not fit any muropeptide structures and are therefore not given.

Conclusion

We have presented here a very quick method for PGN isolation with additional analysis on UPLC-MS all within 24 hours. This method is suitable for high throughput screening of various bacterial strains or growth conditions, as it is performed in either 2 ml plastic reaction tubes or even in microtiter plates. With this new procedure we mapped the whole PGN of *S. aureus* SA113 up to the hexameric cross-linked muropeptide. In addition to the already known muropeptide structures of the prevalent peaks we have also presented masses and structures for the so far unidentified smaller peak groups in between. As an example for Gram-negatives we analyzed the PGN of *E. coli* Nissle 1917 and corroborated former publications.

Methods

The protocols will also be provided at www.nature.com/protocolexchange.

Bacterial strains. *S. aureus* SA113¹⁴ and *E. coli* Nissle 1917¹⁵.

Cell growth. The cells were grown in their respective medium to the needed OD. Basic medium (BM) for *S. aureus* consisted of Soy Peptone (10 g; Plato), Yeast Extract (5 g; Deutsche Hefewerke), NaCl (5 g; Carl-Roth), Glucose (1 g; Carl Roth) and K₂HPO₄ (1 g; Applichem). Deionized water was added to a final volume of 1 liter and pH was adjusted to 7.2. LB medium for *E. coli* consisted of Peptone (10 g; Plato), Yeast Extract (5 g; Deutsche Hefewerke) and NaCl (5 g; Carl Roth). Deionized water was added to a final volume of 1 liter and pH was adjusted to 7.2.

Reagents. Unless otherwise stated, all reagents were bought from Sigma-Aldrich.

Midpreparation for UPLC/MS or HPLC/MS analysis. This protocol results in sample amounts suitable for several analyses. From 2 ml of culture of OD₅₇₈ ≈ 10 about 300 μl purified PGN are gained. Spin down 2 ml of an overnight culture in a 2 ml microcentrifuge tube (Eppendorf) for 5 min at 10,000 rpm. Alternatively: Spin down 2 × 2 ml of a culture with a lower OD. Resuspend the pellet in 1 ml solution A (1 M sodium chloride) and boil the suspension for 20 minutes at 100 °C in a heating block. [Δ CRITICAL STEP 1: Sometimes, NaCl treatment is not sufficient for peptidoglycan isolation from the cells. Use 0.25% SDS solution in 0.1 M Tris/HCl (pH 6.8) instead. SDS has to be washed out thoroughly after boiling. Make sure the samples are boiling at 100 °C. Bad isolation results are mostly caused by too low heat.] Spin down the suspension (5 min at 10,000 rpm), wash it at least twice with 1.5 ml ddH₂O and resuspend the pellet in 1 ml ddH₂O. Put the sample to a sonifier waterbath for 30 minutes. Add 500 μl of solution B (15 μg/ml DNase and 60 μg/ml RNase in 0.1 M TRIS/HCl, pH 6.8) and incubate for 60 minutes at 37 °C in a shaker. Add 500 μl of solution C (50 μg/ml trypsin in ddH₂O) and incubate for additional 60

minutes at the same conditions. To inactivate the enzymes boil the suspension for 3 minutes at 100 °C in a heating block, then spin the sample down (5 min at 10,000 rpm) and wash it once with 1 ml ddH₂O. To release WTA resuspend the pellet in 500 μl of 1 M HCl (ready-to-use solution from Applichem) and incubate for 4 h at 37 °C in a shaker. Spin down the suspension (5 min at 10,000 rpm) and wash with ddH₂O until the pH is 5–6. Afterwards, resuspend the pellet in 100–250 μl digestion buffer (12.5 mM sodium dihydrogen-phosphate, pH 5.5) to an OD₅₇₈ of 3.0 and add 1/10 volume of mutanolysin solution (5,000 U/ml of mutanolysin in ddH₂O). [Δ CRITICAL STEP 2: If OD₅₇₈ is too high the sample is too concentrated. Therefore, the digestion with mutanolysin might be disturbed. Measurement of OD is tricky, because peptidoglycan sinks to the bottom. Mix the suspension carefully with a pipette and measure OD rapidly.] Then incubate the sample for 16 h at 37 °C (150 rpm shaking). Inactivate mutanolysin by boiling (100 °C) for 3 min. Spin the sample down (5 min at 10,000 rpm) and use the supernatant. Before applying the sample to the UPLC system, MurNAc has to be reduced to NAc-muraminitol. Therefore, add 50 μl of reduction solution (10 mg/ml sodium borohydrate in 0.5 M borax in ddH₂O at pH 9.0; both reagents were purchased from Merck) and incubate the sample for 20 minutes at room temperature. Stop the reaction with 10 μl phosphoric acid (98%). The resulting pH must be between 2 and 3. Then analyze the sample by UPLC/MS or HPLC/MS.

Minipreparation in 96 well plate for UPLC/MS analysis. This protocol gives just enough material for one sample for UPLC/MS analysis. For different growth parameters, use a divisible 96 well plate. Use a multichannel pipette for all resuspension steps. Always cover the samples properly with a foil (Greiner) or lid to avoid evaporation or mixing of samples!

Always use a 96 well-plate with U-shaped bottom (Greiner). Spin down 200 μl of the culture for 10 min at 4,700 rpm in a plate centrifuge. Resuspend each pellet in 200 μl solution A (1 M sodium chloride) and boil the suspension for 30 minutes at 100 °C in a heating block. [Δ CRITICAL STEP 1: Sometimes, NaCl treatment is not sufficient for peptidoglycan isolation from the cells. Use 0.25% SDS solution in 0.1 M Tris/HCl (pH 6.8) instead. SDS has to be washed out thoroughly after boiling.] The plate must be covered with foil. Make sure the samples are boiling at 100 °C. Bad isolation results are mostly caused by too low heat. Spin down the suspension (10 min at 4,700 rpm with foil coverage or lid) and wash at least twice with 200 μl ddH₂O. Afterwards, resuspend each pellet in 150 μl ddH₂O. Close the wells carefully with a foil coverage (NOT lid), so that no water can ingress to the sample. Place the plate to a sonifier waterbath for 30 minutes (plate floats). Spin down the suspension (10 min at 4,700 rpm) and resuspend each pellet in 100 μl of solution B (15 μg/ml DNase and 60 μg/ml RNase in 0.1 M TRIS/HCl, pH 6.8). Properly close plate with foil coverage and incubate for 60 minutes at 37 °C in a shaker at 150 rpm. It is better to place samples at the edge of the shaker than in the middle. Add 100 μl of solution C (50 μg/ml trypsin in ddH₂O), properly close plate with foil coverage and incubate for another 60 minutes at 37 °C in a shaker at 150 rpm. To inactivate the enzymes boil the suspension for 5 minutes at 100 °C. Spin down the suspension (10 min at 4,700 rpm) and wash each pellet once with 200 μl ddH₂O. To release WTA resuspend each pellet in 200 μl of 1 M HCl (ready-to-use solution from Applichem) and incubate for 4 h at 37 °C in a shaker (150 rpm, with foil coverage). Spin down the suspension (10 min at 4,700 rpm) and wash pellets with ddH₂O until the pH is 5–6. Resuspend each pellet in 50 μl digestion buffer (12.5 mM sodium dihydrogen-phosphate, pH 5.5) and add 5 μl mutanolysin solution (5,000 U/ml of mutanolysin in ddH₂O). Incubate the well plate for 16 h at 37 °C (at 150 rpm, with foil coverage). Boil the samples on the heating block (100 °C) for 5 minutes to inactivate mutanolysin. Afterwards spin the plate down (10 min at 4,700 rpm) and use the supernatant. Before applying the samples to the UPLC system, MurNAc has to be reduced to NAc-muraminitol. Add 10 μl of the reduction solution (10 mg/ml sodium borohydrate in 0.5 M borax in ddH₂O at pH 9.0; both reagents were purchased from Merck) to each sample and incubate for 20 min at room temperature. [Δ CRITICAL STEP 2: The reduction solution contains a lot of bubbles. Transfer of the exact volume of 10 μl reduction solution is not possible. Set your pipette to a volume of 100 μl and add 1 drop to each sample. This accords to the needed volume.] Stop the reaction with 5 μl phosphoric acid (50%). The pH must be between 2 and 3 (add phosphoric acid very slow and carefully!). Then analyze the samples by UPLC or UPLC/MS.

UPLC/MS ANALYSIS. An Acquity UPLC was coupled to a SynaptG2 mass spectrometer (both Waters). We used a C18 CSH 130Å, 1.7 μm, 2.1 mm × 100 mm column with the respective guard column (C18 CSH 130Å, 1.7 μm, 2.1 mm × 5 mm) available at Waters. As MS standard L-Enk was used.

The column temperature was 52 °C and the injection volume was 10 μl with no loop overflow. Muropeptides were detected at 210 nm (DAD) or by MS. The MS was set to positive ESI mode with a scan range from 50–2,000. The capillary voltage was 3 kV. The sampling cone was set to 30 and the extraction cone to 3.0. Source temperature was set to 120 °C and desolvation temperature to 450 °C. The flow of the cone gas was 10 l/h and of the desolvation gas 800 l/h.

For muropeptide separation by UPLC/MS we used solvent A (0.1% TFA in 5% methanol); for Gram-negatives omit methanol) and solvent B (0.1% TFA in 30% methanol). TFA (trifluoroacetic acid) was bought from Carl Roth, methanol (UV grade) from Sigma-Aldrich. We applied a flow rate of 0.176 ml/min starting with 100% solvent A for 1 min. Afterwards, a linear gradient was run in 59 min to 100% solvent B. The post run was 5 min with 100% solvent B and additional 10 min with 100% solvent A for re-equilibration. [Δ CRITICAL STEP: A long and intensive equilibration of the column and an exact column temperature is very important.



Wash the column 30 min with methanol, 30 min with ddH₂O water, 30 min with solvent B, and 30 min with solvent A to a steady baseline. Degassed solvents should be self-evident.]

- Schleifer, K. H. & Kandler, O. Peptidoglycan types of bacterial cell walls and their taxonomic implications. *Bacteriol Rev* **36**, 407–477 (1972).
- Salton, M. R. J. & Horne, R. W. Studies of the bacterial cell wall. 2. Methods of preparation and some properties of cell walls. *Biochimica et Biophysica Acta* **7**, 177–197 (1951).
- Glauner, B. Separation and quantification of muropeptides with high-performance liquid chromatography. *Anal Biochem* **172**, 451–464 (1988).
- de Jonge, B. L., Chang, Y. S., Gage, D. & Tomasz, A. Peptidoglycan composition of a highly methicillin-resistant *Staphylococcus aureus* strain. The role of penicillin binding protein 2A. *J Biol Chem* **267**, 11248–11254 (1992).
- Desmarais, S. M., Cava, F., de Pedro, M. A. & Huang, K. C. Isolation and Preparation of Bacterial Cell Walls for Compositional Analysis by Ultra Performance Liquid Chromatography. *JoVE* e51183, doi:doi:10.3791/51183 (2014).
- Pilhofer, M. *et al.* Discovery of chlamydial peptidoglycan reveals bacteria with murein sacculi but without FtsZ. *Nat Commun* **4**, 2856, doi:10.1038/ncomms3856 (2013).
- Takacs, C. N. *et al.* Growth medium-dependent glycine incorporation into the peptidoglycan of *Caulobacter crescentus*. *PLoS One* **8**, e57579, doi:10.1371/journal.pone.0057579 (2013).
- Zhou, X. & Cegelski, L. Nutrient-dependent structural changes in *S. aureus* peptidoglycan revealed by solid-state NMR spectroscopy. *Biochemistry* **51**, 8143–8153, doi:10.1021/bi3012115 (2012).
- Bertsche, U. *et al.* Increased cell wall teichoic acid production and D-alanylation are common phenotypes among daptomycin-resistant methicillin-resistant *Staphylococcus aureus* (MRSA) clinical isolates. *PLoS One* **8**, e67398, doi:10.1371/journal.pone.0067398 (2013).
- Bertsche, U. *et al.* Correlation of daptomycin resistance in a clinical *Staphylococcus aureus* strain with increased cell wall teichoic acid production and D-alanylation. *Antimicrob Agents Chemother* **55**, 3922–3928, doi:10.1128/AAC.01226-10 (2011).
- Baek, K. T. *et al.* beta-Lactam Resistance in Methicillin-Resistant *Staphylococcus aureus* USA300 Is Increased by Inactivation of the ClpXP Protease. *Antimicrob Agents Chemother* **58**, 4593–4603, doi:10.1128/AAC.02802-14 (2014).
- Müller-Anstett, M. A. *et al.* Staphylococcal peptidoglycan co-localizes with Nod2 and TLR2 and activates innate immune response via both receptors in primary murine keratinocytes. *PLoS One* **5**, e13153, doi:10.1371/journal.pone.0013153 (2010).
- Hayashi, K. A rapid determination of sodium dodecyl sulfate with methylene blue. *Anal Biochem* **67**, 503–506 (1975).
- Iordanescu, S. Host controlled restriction mutants of *Staphylococcus aureus*. *Archives roumaines de pathologie experimentales et de microbiologie* **34**, 55–58 (1975).
- Jacobi, C. A. & Malfertheiner, P. *Escherichia coli* Nissle 1917 (Mutaflor): new insights into an old probiotic bacterium. *Digestive diseases (Basel, Switzerland)* **29**, 600–607, doi:10.1159/000333307 (2011).
- de Jonge, B. L., Chang, Y. S., Gage, D. & Tomasz, A. Peptidoglycan composition in heterogeneous Tn551 mutants of a methicillin-resistant *Staphylococcus aureus* strain. *J Biol Chem* **267**, 11255–11259 (1992).
- Boneca, I. G., Xu, N., Gage, D. A., de Jonge, B. L. & Tomasz, A. Structural characterization of an abnormally cross-linked muropeptide dimer that is accumulated in the peptidoglycan of methicillin- and cefotaxime-resistant mutants of *Staphylococcus aureus*. *J Biol Chem* **272**, 29053–29059 (1997).
- Figueiredo, T. A. *et al.* Identification of genetic determinants and enzymes involved with the amidation of glutamic acid residues in the peptidoglycan of *Staphylococcus aureus*. *PLoS Pathog* **8**, e1002508, doi:10.1371/journal.ppat.1002508 (2012).
- Münch, D. *et al.* Identification and *in vitro* analysis of the GatD/MurT enzyme-complex catalyzing lipid II amidation in *Staphylococcus aureus*. *PLoS Pathog* **8**, e1002509, doi:10.1371/journal.ppat.1002509 (2012).
- Bera, A., Biswas, R., Herbert, S. & Götz, F. The presence of peptidoglycan O-acetyltransferase in various staphylococcal species correlates with lysozyme resistance and pathogenicity. *Infect. Immun.* **74**, 4598–4604 (2006).
- Braun, V. & Wolff, H. The murein-lipoprotein linkage in the cell wall of *Escherichia coli*. *Eur J Biochem* **14**, 387–391 (1970).
- Potluri, L. *et al.* Septal and lateral wall localization of PBP5, the major D,D-carboxypeptidase of *Escherichia coli*, requires substrate recognition and membrane attachment. *Molecular Microbiology* **77**, 300–323, doi:10.1111/j.1365-2958.2010.07205.x (2010).

Acknowledgments

This work was funded by the Deutsche Forschungsgemeinschaft (SFB766 to UB) and Baden-Württemberg Stiftung (P-BWS-Glyko/21-Götz) to DDD. We thank F. Götz for helpful discussions and F. Götz and P. Schwartz for critical reading of the manuscript.

Author contributions

D.K., M.S., D.D.D., Conception and design, Acquisition of data, Analysis and interpretation of data; U.B., Conception and design, Interpretation of data, Writing the article.

Additional information

Supplementary information accompanies this paper at <http://www.nature.com/scientificreports>

Competing financial interests: The authors declare no competing financial interests.

How to cite this article: Kühner, D., Stahl, M., Demircioglu, D.D. & Bertsche, U. From cells to muropeptide structures in 24 h: Peptidoglycan mapping by UPLC-MS. *Sci. Rep.* **4**, 7494; DOI:10.1038/srep07494 (2014).



This work is licensed under a Creative Commons Attribution-NonCommercial-ShareAlike 4.0 International License. The images or other third party material in this article are included in the article's Creative Commons license, unless indicated otherwise in the credit line; if the material is not included under the Creative Commons license, users will need to obtain permission from the license holder in order to reproduce the material. To view a copy of this license, visit <http://creativecommons.org/licenses/by-nc-sa/4.0/>

Supplementary Information

From cells to muropeptide structures in 24 h: Peptidoglycan mapping by UPLC-MS

Daniel Kühner¹, Mark Stahl², Dogan D. Demircioglu³, and Ute Bertsche^{1*}

*Corresponding author: ute.bertsche@uni-tuebingen.de

Table S1: Muropeptides of *S. aureus* SA113 analyzed by UPLC-MS

This table gives a summary of all muropeptides of *S. aureus* SA113 that could be detected by UPLC-MS. All structures were drawn by ChemDrawUltra (PerkinElmer) which automatically calculates the mass of the molecule and the sum formula. The latter is given. Each muropeptide contains one to six stem-peptides, each consisting of L-Ala – D-Glx – L-Lys – D-Ala (– D-Ala). In general, Glx is Gln. Non-amidated Glu is indicated separately. The length of each of the stem peptides is stated. The amount of Gly residues building the interpeptide bridges is given as the sum of all Gly residues present in each muropeptide. In rare cases one Gly is replaced by one Ala. Changes on the saccharide moiety (loss or addition of GlcNAc; O-Acetylation; rare non-reduced MurNAc) are shown. The muropeptides of the main peaks, which are also given in Tab. 1, are highlighted in bold. In Tab. 1 also the original references for these peaks are given. n.d. ... not determined

Table S1: Muropeptides of *S. aureus* SA113 analyzed by UPLC-MS

0

Peak	Retention time in TIC [min]	M+H ⁺	Proposed sum formula	Lengths of the stem peptides	Non-amidated Glu	Interpeptide bridges		Changes in the saccharide moiety		
		Measured				Gly	Ala	GlcNAc	O-Acetyl	non-red.
1	7.61	979.4799	n.d.							
2	8.56 shoulder	1036.4937	C40H70N13O19+	Tetra		6		-1		
		1093.5164	C42H73N14O20+	Tetra		7		-1		
		1150.5417	C44H76N15O21+	Tetra		8		-1		
		1207.5699	C46H79N16O22+	Tetra		9		-1		
	8.56	1239.5699	C48H83N14O24+	Tetra		6				
		1296.5939	C50H86N15O25+	Tetra		7				
		1353.6135	C52H89N16O26+	Tetra		8				
		1410.6370	C54H92N17O27+	Tetra		9				
3	9.24	954.4640	C38H68N9O19+	Tetra	1	1				
4	10.17	1025.5032	C41H73N10O20+	Penta		1				
		1182.5502	C46H80N13O23+	Tetra		5				
5a	10.86	879.4431	C35H63N10O16+	Penta		2		-1		
		936.4638	C37H66N11O17+	Penta		3		-1		
		1082.5231	C43H76N11O21+	Penta		2				
		1139.5428	C45H79N12O22+	Penta		3				
5b	11.08	1050.5082	C41H72N13O19+	Penta		5		-1		
		1253.5861	C49H85N14O24+	Penta		5				
6	12.52	1224.5674	C48H82N13O24+	Tetra		5			1	
7	13.02	1254.5664	C49H84N13O25+	Penta	1	5				1
8	14.20	1267.6096	C50H87N14O24+	Penta		4	1			
9	16.68	1295.5968	C51H87N14O25+	Penta		5			1	

Peak	Retention time in TIC [min]	M+H ⁺	Proposed sum formula	Lengths of the stem peptides	Non-amidated Glu	Interpeptide bridges		Changes in the saccharide moiety		
		Measured				Gly	Ala	GlcNAc	O-Acetyl	non-red.
10	19.00 to 19.70	1296.5902	C51H86N13O26+	Penta	1	5			1	
		2143.0192	C85H144N23O41+	Penta-Tetra	2	8		-1	1	
		2574.1760	C101H169N28O50+	Tetra ₂	1	13			1	
		2199.9962	C87H147N24O42+	Penta-Tetra	1	9		-1	1	
		2257.0518	C89H150N25O43+	Penta-Tetra	1	10		-1	1	
		2289.0616	C91H154N23O45+	Penta-Tetra		7			1	
		2346.0781	C93H157N24O46+	Penta-Tetra		8			1	
		2403.0937	C95H160N25O47+	Penta-Tetra		9			1	
		2460.1237	C97H163N26O48+	Penta-Tetra		10			1	
11a	21.52	2189.0486	C87H150N23O42+	Penta-Tetra		6				
		2346.0766	C93H157N24O46+	Penta-Tetra	1	8			1	
11b	21.93	2417.1181	C95H162N27O46+	Penta-Tetra		10				
12a	22.52	2124.9932	C84H142N25O39+	Tetra ₂ (cyclic)		10		-1		
12b	23.12	2328.0745	C92H155N26O44+	Tetra₂ (cyclic)		10				
13a	23.47	2418.1006	C95H161N26O47+	Penta-Tetra	1	10				
13b	24.34	2431.1341	C96H164N27O46+	Penta-Tetra		9	1			
14a	24.81	2329.0461	C92H154N25O45+	Tetra ₂ (cyclic)	1	10				
		2415.1060	C95H160N27O46+	Penta-Tetra		10				1
14b	25.04	2388.1040	C94H159N26O46+	Tetra-Tetra		10			1	
		2415.1072	C95H160N27O46+	Penta-Tetra		10				1
		3509.6299	C139H234N37O68+	Penta-Tetra ₂		13			1	

2

Peak	Retention time in TIC [min]	M+H ⁺	Proposed sum formula	Lengths of the stem peptides	Non-amidated Glu	Interpeptide bridges		Changes in the saccharide moiety		
		Measured				Gly	Ala	GlcNAc	O-Acetyl	non-red.
14c	25.47	2185.0298	C87H146N23O42+	Penta-Tetra		6				2
		2388.1040	C94H159N26O46+	Tetra-Tetra		10			1	
14d	25.67	2256.0534	C89H151N26O42+	Penta-Tetra		10		-1	1	
14e	25.85	3566.7134	C140H237N40O68+	Penta-Tetra ₂		16			1	
		2459.1380	C97H164N27O47+	Penta-Tetra		10			1	
14f	26.74	3567.6179	C141H236N37O70+	Penta-Tetra ₂	2	14			1	
15a	27.23	2460.1220	C97H163N26O48+	Penta-Tetra	1	10			1	
		3281.5076	C130H222N35O63+	Tetra ₃		11				
		3377.5886	C133H226N39O63+	Penta-Tetra ₂		15		-1		
		3509.6465	C138H234N39O67+	Tetra ₃		15				
15b	27.45	3352.5787	C133H227N36O64+	Penta-Tetra ₂		11				
		3377.5886	C133H226N39O63+	Penta-Tetra ₂		15		-1		
		3580.6630	C141H239N40O68+	Penta-Tetra₂		15				
15c	28.50	3581.6525	C141H238N39O69+	Penta-Tetra ₂	1	15				
15d	29.35	3507.6278	C138H232N39O67+	Tetra ₃		15				1
		3547.8803	C140H232N39O68+	Tetra ₃		15			1	2
		3578.6621	C141H237N40O68+	Penta-Tetra ₂		15				1
		4730.1515	C187H314N51O91+	Penta-Tetra ₂	1	15			1	
15e	30.19	3394.5530	C134H228N37O65+	Tetra ₃	1	13				1
		3419.6141	C135H228N39O64+	Penta-Tetra ₂		15		-1	1	
		3551.6252	C140H236N39O68+	Tetra ₃		15			1	
		3622.6978	C143H241N40O69+	Penta-Tetra ₂		15			1	

3

Peak	Retention time in TIC [min]	M+H ⁺	Proposed sum formula	Lengths of the stem peptides	Non-amidated Glu	Interpeptide bridges		Changes in the saccharide moiety		
		Measured				Gly	Ala	GlcNAc	O-Acetyl	non-red.
15e	30.19	3622.6978	C143H241N40O69+	Penta-Tetra ₂		15			1	
15f	30.40	3622.6910	C143H241N40O69+	Penta-Tetra ₂		15			1	
16a	30.80	4541.1010	C179H303N52O85+	Penta-Tetra ₃		20		-1		
		4673.1534	C184H311N52O89+	Tetra ₄		20				
		4744.1962	C187H316N53O90+	Penta-Tetra₃		20				
16b	31.60	4742.0843	C187H314N53O90+	Penta-Tetra ₃		20				1
		4745.1578	C187H315N52O91+	Penta-Tetra ₃	1	20				
16c	32.44	4742.2070	C187H314N53O90+	Penta-Tetra ₃		20				1
		3620.6402	C143H239N40O69+	Penta-Tetra ₂		20			1	1
		4539.0782	C179H301N52O85+	Penta-Tetra ₃		20		-1		
		4671.1277	C184H309N52O89+	Tetra ₄		20				
17a	33.01	4786.2042	C189H318N53O91+	Penta-Tetra ₃		20			1	
		3664.6502	C145H243N40O70+	Penta-Tetra ₂		15			2	
		5836.6706	C230H388N65O111+	Tetra ₅		25				
		5907.7014	C233H393N66O112+	Penta-Tetra₄		25				
17b	33.77	5907.6914	C233H393N66O112+	Penta-Tetra ₄		25				
		4787.1722	C189H318N53O91+	Penta-Tetra ₃	1	20			1	
18	34.90	4784.1642	C189H316N53O91+	Penta-Tetra ₃		20			1	1
		4828.2174	C191H320N53O92+	Penta-Tetra ₃		20			2	
		5746.6426	C227H382N65O108+	Penta-Tetra ₄		25		-1	1	
		5878.6954	C232H390N65O112+	Tetra ₅		25			1	
		5949.7002	C235H395N66O113+	Penta-Tetra ₄		25			1	
		7071.2313	C279H470N79O134+	Penta-Tetra₅		30				

5 **Table S2: Muropeptides of *E. coli* Nissle 1917 analyzed by UPLC-MS**

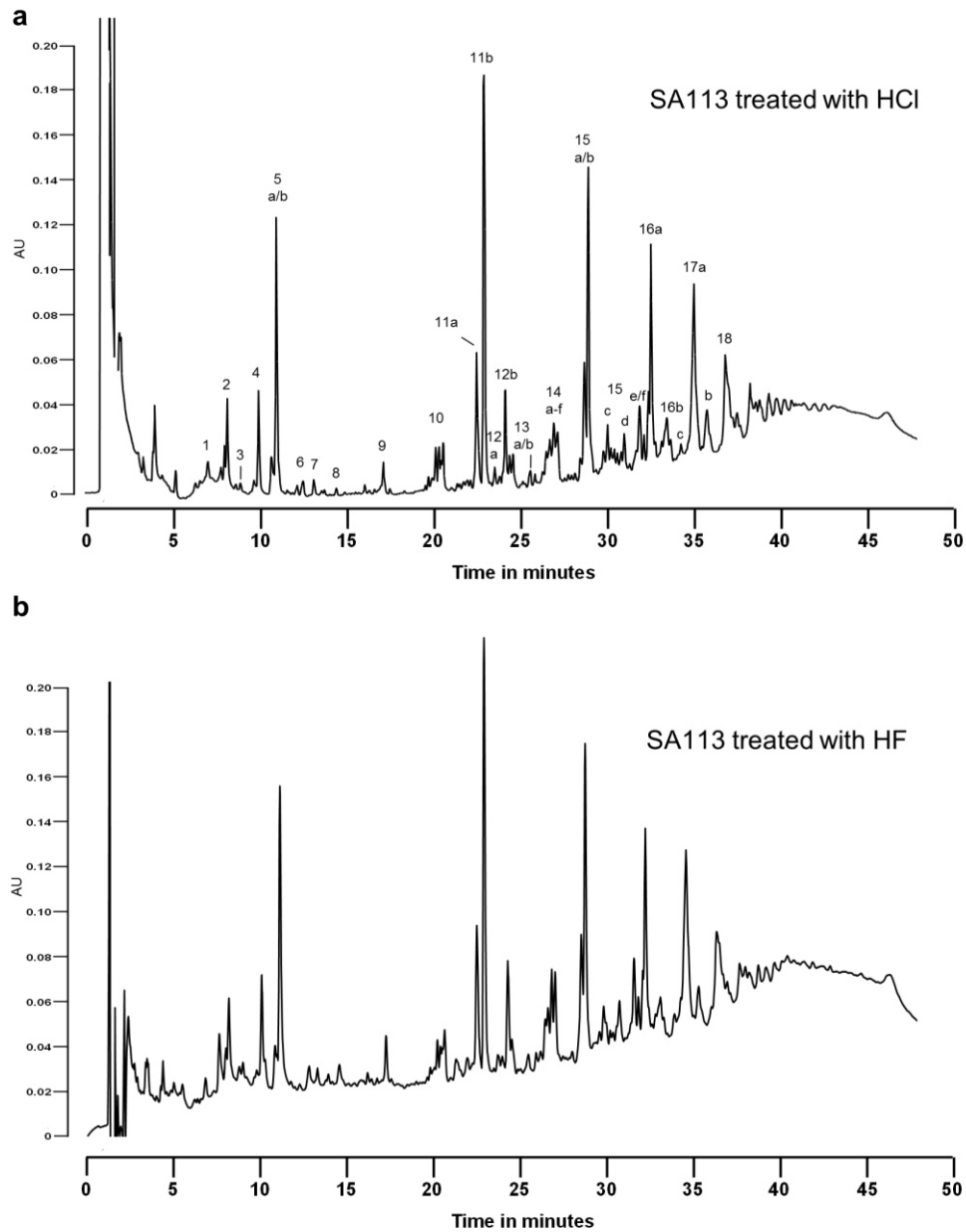
6 This table summarizes the muropeptides of *E. coli* Nissle 1917 that could be detected by
 7 UPLC-MS. The sum formula to each mass is given. Each muropeptide contains one to three
 8 stem-peptides, each consisting of L-Ala – D-Glu – mDAP – D-Ala (– Gly). The length of each
 9 of the stem peptides is stated. In some cases Penta stem-peptides with Gly on position 5 are
 10 present. Loss of GlcNAc or acetyl is shown as -GlcNAc and -Acetyl. The muropeptides of the
 11 main peaks, which are also given in Tab. 2, are highlighted in bold.

12

Peak	Retention time in TIC [min]	M+H ⁺	Proposed sum formular	Length of the stem peptides
		Measured		
1	9.27	871.3793	C34H59N6O20+	Tri
		668.2999	C26H46N5O15+	Tri (-GlcNAc)
2	9.95	928.3986	C36H62N7O21+	Tetra-Gly(4)
		725.3201	C28H49N6O16+	Tetra-Gly(4) (-GlcNAc)
		999.4708	C39H67N8O22+	Penta-Gly(5)
3	11.69	699.2936	C27H47N4O17+	Di
		999.4775	C39H67N8O22+	Penta-Gly(5)
		900.4092	C35H62N7O20+	Tetra (-Acetyl)
		796.3969	C31H54N7O17+	Penta-Gly(5) (-GlcNAc)
4a	12.81	942.4180	C37H64N7O21+	Tetra
4b	13.50	942.4177	C37H64N7O21+	Tetra
		739.3378	C29H51N6O16+	Tetra (-GlcNAc)
5a	22.40	1851.8278	C73H123N14O41+	Tetra-Tetra-Gly(4)
5b	23.10	1851.7966	C73H123N14O41+	Tetra-Tetra-Gly(4)
6	23.60	1922.8710	C76H128N15O42+	Tetra-Penta-Gly(5)
		1794.7766	C71H120N13O40+	Tetra-Tri
7	24.70	1794.7758	C71H120N13O40+	Tetra-Tri
8a	25.59	1865.8140	C74H125N14O41+	Tetra-Tetra
8b	26.18	1865.8140	C74H125N14O41+	Tetra-Tetra
9	29.75	2846.2697	C113H189N22O62+	Penta (Gly5)-Tetra-Tetra
10	32.40	2789.2146	C111H186N21O61+	Tetra-Tetra-Tetra
11	35.30	1845.7744	C74H121N14O40+	anhydro Tetra-Tetra

13

14



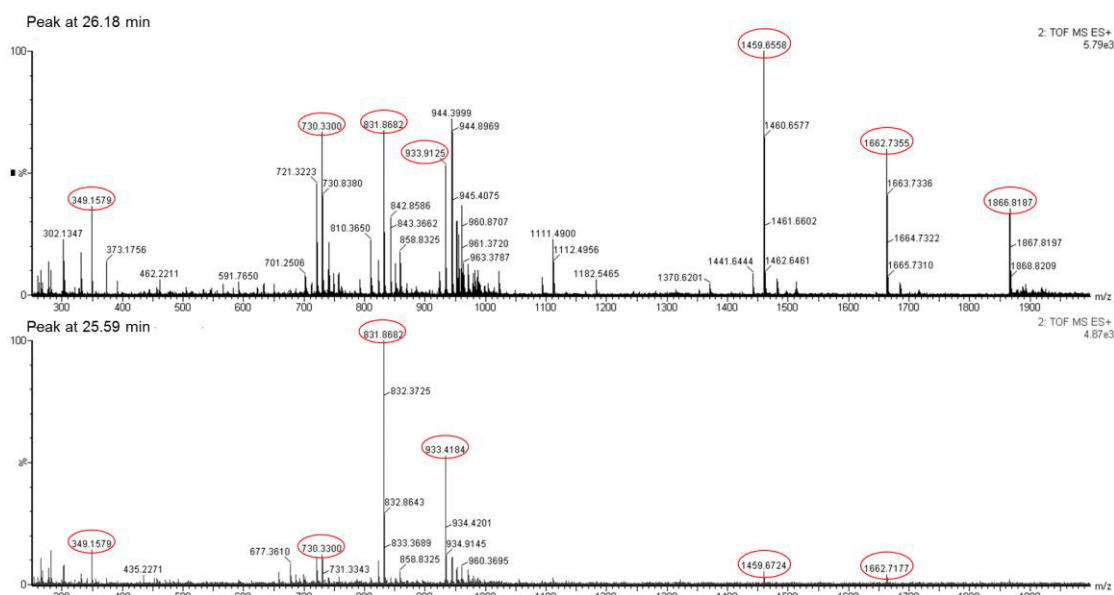
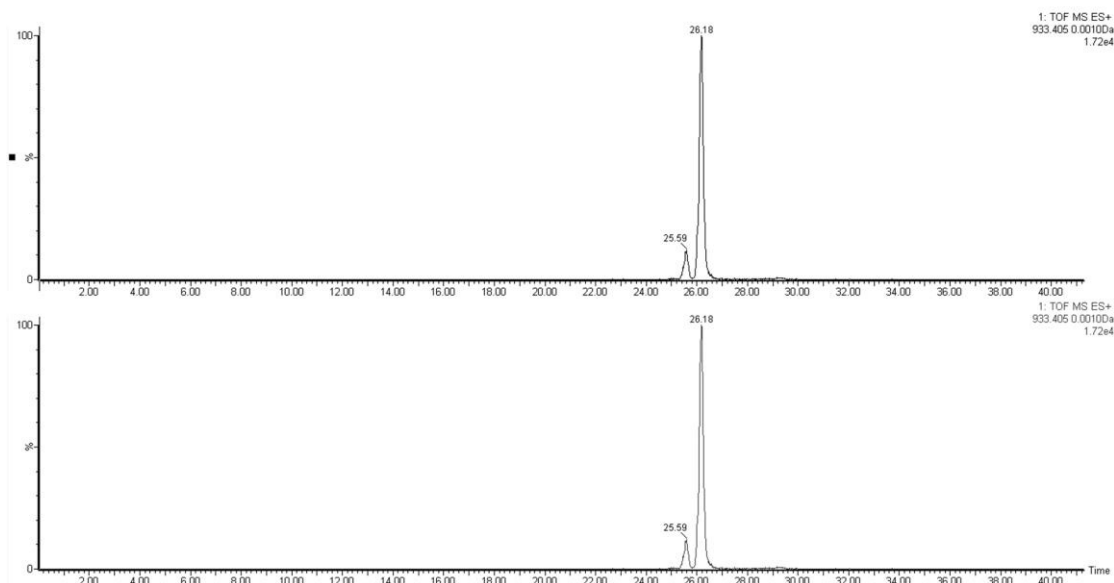
15

16

17 **Fig. S1: Comparison of isolated peptidoglycan treated with HCl and HF**

18 We compared the mucopeptide pattern of peptidoglycan of *S. aureus* SA113 treated with
 19 either HCl (a) or HF (b). The HF treated mucopeptide pattern shows no differences compared
 20 to the HCl treated one.

21



22

23

24 **Fig. S2: Fragmentation of *E. coli* Nissle 1917 Peaks 8a and 8b**

25 The peaks 8a and 8b were fragmented (MS^E all ion fragmentation, bottom panel). The
 26 resulting fragment patterns are closely related, but the relative fragment peak intensities
 27 vary. This, in combination with the close but different chromatographic retention times, is
 28 typically caused by two stereoisomers. This is also seen in the top panel, where the search
 29 for the respective mass resulted in two peaks.

NOD2 Stimulation by *Staphylococcus aureus*-Derived Peptidoglycan Is Boosted by Toll-Like Receptor 2 Costimulation with Lipoproteins in Dendritic Cells

Holger Schäffler,^a Dogan Doruk Demircioglu,^b Daniel Kühner,^b Sarah Menz,^{c,d} Annika Bender,^{c,d} Ingo B. Autenrieth,^{c,d} Peggy Bodammer,^a Georg Lamprecht,^a Friedrich Götz,^b Julia-Stefanie Frick^{c,d}

Division of Gastroenterology, Department of Medicine II, University of Rostock, Rostock, Germany^a; Microbial Genetics, University of Tübingen, Tübingen, Germany^b; Institute of Medical Microbiology and Hygiene, University of Tübingen, Tübingen, Germany^c; Deutsches Zentrum für Infektionsforschung (DZIF), Partner Site Tübingen, Tübingen, Germany^d

Mutations in the nucleotide-binding oligomerization domain-containing protein 2 (NOD2) play an important role in the pathogenesis of Crohn's disease. NOD2 is an intracellular pattern recognition receptor (PRR) that senses bacterial peptidoglycan (PGN) structures, e.g., muramyl dipeptide (MDP). Here we focused on the effect of more-cross-linked, polymeric PGN fragments (PGNpol) in the activation of the innate immune system. In this study, the effect of combined NOD2 and Toll-like receptor 2 (TLR2) stimulation was examined compared to single stimulation of the NOD2 receptor alone. PGNpol species derived from a lipoprotein-containing *Staphylococcus aureus* strain (SA113) and a lipoprotein-deficient strain (SA113 Δ Igt) were isolated. While PGNpol constitutes a combined NOD2 and TLR2 ligand, lipoprotein-deficient PGNpol Δ Igt leads to activation of the immune system only via the NOD2 receptor. Murine bone marrow-derived dendritic cells (BMDCs), J774 cells, and Mono Mac 6 (MM6) cells were stimulated with these ligands. Cytokines (interleukin-6 [IL-6], IL-12p40, and tumor necrosis factor alpha [TNF- α]) as well as DC activation and maturation parameters were measured. Stimulation with PGNpol Δ Igt did not lead to enhanced cytokine secretion or DC activation and maturation. However, stimulation with PGNpol led to strong cytokine secretion and subsequent DC maturation. These results were confirmed in MM6 and J774 cells. We showed that the NOD2-mediated activation of DCs with PGNpol was dependent on TLR2 costimulation. Therefore, signaling via both receptors leads to a more potent activation of the immune system than that with stimulation via each receptor alone.

Crohn's disease is a systemic inflammatory disease, and together with ulcerative colitis, it forms the complex of inflammatory bowel diseases (IBD). Mutations within the NOD2 gene, encoding nucleotide-binding oligomerization domain-containing protein 2 (NOD2), have been identified as risk factors for the development of Crohn's disease (1–3). NOD2 is an intracellular pattern recognition receptor that senses peptidoglycan (PGN) fragments, such as muramyl dipeptide (MDP), derived from Gram-positive bacteria, to activate a cascade of reactions which consecutively lead to the activation of the transcription factor NF- κ B (4).

Dendritic cells (DCs) are important professional antigen-presenting cells (APCs) in the intestine (5, 6) and are crucial for T cell activation and polarization (7, 8). Depending on the antigen, DCs can promote either inflammation or tolerance (9). DCs are thought to contribute to the pathogenesis of Crohn's disease (10, 11) by inducing T cell activation via antigen presentation. As an example, colonic CD11c⁺ DCs isolated from inflamed parts of the gut from IBD patients showed an increased expression of Toll-like receptor 2 (TLR2), TLR4, and the costimulatory molecule CD40 compared to DCs from noninflamed areas or DCs from healthy controls (12). Also, the ability of DCs to induce tolerogenic regulatory T cells might be lost in Crohn's disease patients (13).

PGN fragments with a low degree of cross-linking, such as PGN monomers, have been shown to be natural ligands for the NOD2 receptor (14). However, the role of more-cross-linked PGN fragments, so called polymeric PGN (PGNpol), and their effect in stimulating immune cells are still unclear, as even highly purified PGNpol might be contaminated with potent immune-

stimulating lipoproteins (15). Using *Bacillus anthracis* peptidoglycan, it has been shown that polymeric PGN is a more potent activator of innate immune cells than MDP or monomeric PGN (16).

The importance of PGN in inflammation was recently demonstrated in mice infected with wild-type (WT) *Staphylococcus aureus* and corresponding O-acetyltransferase A (OatA) mutants. In *S. aureus*, PGN is modified by an O-acetyltransferase at the C-6 OH position of N-acetylmuramic acid (17). This modification, which occurs only in pathogenic staphylococcal strains (18), confers complete resistance of PGN to lysozyme, while mutations of the *oatA* gene result in a PGN that is sensitive to lysozyme (17, 19). In comparing PGNpol from WT *S. aureus* with PGN from the *oatA*-deficient mutant (*S. aureus* Δ *oatA*), it turned out that WT PGNpol strongly suppressed interleukin-1 β (IL-1 β) secretion and inflammasome activation, while the PGNpol of the *S. aureus* Δ *oatA* strain strongly increased IL-1 β secretion and inflammasome activation (20). In the absence of *oatA*, PGN is degraded

Received 24 May 2014 Returned for modification 14 June 2014

Accepted 12 August 2014

Published ahead of print 25 August 2014

Editor: A. J. Bäuml

Address correspondence to Holger Schäffler, holger.schaeffler@med.uni-rostock.de.

H.S. and D.D.D. contributed equally to this article.

Copyright © 2014, American Society for Microbiology. All Rights Reserved.

doi:10.1128/IAI.02043-14

by lysozyme, resulting in a number of PGN breakdown products which boost inflammation. Thus, modification of PGN by *O*-acetylation in *S. aureus* is an efficient immune escape mechanism.

The interplay between the NOD2 and TLR2 pathways is complex, and interactions between both receptors seem to contribute to activation or inhibition of the immune system (21). NOD2 was shown to be part of an inhibitory system which blocks TLR2-mediated inflammation, resulting in less Th1 cytokine production after stimulation (22). Additionally, activation of mouse peritoneal macrophages with the NOD2 ligand MDP resulted in downregulation of TLR2/1 signaling-mediated IL-1 β expression (23). However, different studies suggest a synergistic role for NOD2 and TLR2 (24).

Additionally, it is still controversially discussed whether PGN interacts with TLR2. PGN isolated from either Gram-negative or Gram-positive bacteria is reported not to be sensed by TLR2 (25). However, stimulation of primary mouse keratinocytes (MKs) with PGNpol from *S. aureus* SA113 resulted in internalization of the molecule and colocalization with NOD2 and TLR2 receptors and induced subsequent host immune responses (26). Additionally, lipoproteins of *S. aureus* have been shown to activate TLR2 (26–29).

To further elucidate the interaction between the NOD2 and TLR2 pathways, we investigated the innate immune sensing of two different types of naturally occurring *S. aureus*-derived PGN polymers. PGN of *S. aureus* SA113 contains traces of lipoproteins. This PGN is referred to as the wild-type PGN. The other PGNpol fraction was derived from the *S. aureus* SA113 Δ lgt mutant, which is unable to lipidate prolipoproteins and whose PGNpol therefore does not contain lipoproteins (30).

By studying the effects of PGNpol from the wild type and that from the Δ lgt mutant (PGNpol Δ lgt) on DC maturation and activation as well as cytokine secretion, we showed that PGNpol is a potent stimulator of the immune system, through both NOD2 and TLR2, while PGNpol Δ lgt, as a selective NOD2 ligand, does not induce host immune responses. However, the addition of the synthetic TLR2 ligand Pam3Cys (P3C) to PGNpol Δ lgt resulted in activation of the host immune response. Costimulation with the NOD2 ligand PGNpol Δ lgt and the TLR2 ligand P3C had a synergistic effect on cytokine production, suggesting that NOD2-dependent activation of DCs with PGN requires TLR2 costimulation by lipoproteins.

MATERIALS AND METHODS

Animals. C57BL/6 mice were purchased from Charles River (Sulzfeld, Germany). NOD2^{-/-} mice were a kind gift from Tilo Biedermann (Department of Dermatology, Eberhard Karls University, Tübingen, Germany). All mice were housed under specific-pathogen-free conditions at the animal facilities of the University of Tübingen according to German law and European guidelines. All experiments were approved by the local authorities (Regierungspräsidium Tübingen; Anzeigenummer 1.12.11).

Isolation of BMDCs. Bone marrow-derived dendritic cells (BMDCs) were isolated by flushing the bone marrow from the femurs and tibias of 8- to 14-week-old WT and NOD2^{-/-} mice according to a previously described method (31), with minor modifications.

Cells were harvested at day 8 and used to evaluate the effects of stimulation with different bacterial PGN products on cytokine release and expression of surface markers, as described below.

Stimulation of BMDCs. DCs were stimulated with different ligands, e.g., P3C for TLR2, lipopolysaccharide (LPS) for TLR4, or MDP and PGNpol Δ lgt for NOD2, or stimulated with the combined NOD2 and

TLR2 ligand PGNpol, at a dose of 1 μ g/ml if not otherwise mentioned. The different PGN types were used at a concentration of 10 μ g/ml if not otherwise mentioned. After 24 h, supernatants were harvested and analyzed for tumor necrosis factor alpha (TNF- α), IL-6, and IL-12p40 cytokine concentrations. Additionally, the expression of DC activation and maturation surface markers major histocompatibility complex class II (MHC-II) and CD40 was determined by flow cytometry.

Cytokine analysis by ELISA. Concentrations of murine IL-6, IL-8, IL-12p40, and TNF- α in cell culture supernatants were measured by enzyme-linked immunosorbent assay (ELISA) according to the manufacturer's protocol (BD Bioscience, Heidelberg, Germany).

Fluorescence-activated cell sorter (FACS) analysis. Immature DCs were harvested and stimulated for 24 h with different NOD2 or TLR ligands. Cells were washed with phosphate-buffered saline (PBS) and 1% fetal calf serum (FCS). Fc-Block was used to prevent nonspecific binding of antibodies. DCs were incubated for 30 min at 4°C with a fluorochrome-conjugated antibody. The following antibodies were used for staining: allophycocyanin-conjugated anti-mouse CD11c, fluorescein isothiocyanate (FITC)-conjugated anti-mouse CD40, CD80, and CD86, phycoerythrin (PE)-conjugated anti-mouse TLR2 and TLR4 (all antibodies from BD Pharmingen), and appropriate isotype controls. After another washing step (twice), the cells were fixed with 4% paraformaldehyde (PFA). A total of 5×10^4 cells were analyzed using a FACS LSR Fortessa flow cytometer (BD Bioscience, Heidelberg, Germany). Data were analyzed with FlowJo 7.6.4 (TreeStar Inc.).

Culture and stimulation of J774 cells and MM6 cells. J774 cells were grown in VLE-RPMI 1640 medium with stable glutamine (Biochrom, Berlin, Germany), 10% FCS, 1% nonessential amino acids, 1% sodium pyruvate, and 0.5% mercaptoethanol. A total of 1×10^6 cells were seeded per well and incubated for 1 h. J774 cells were stimulated with Pam3Cys or PGNpol Δ lgt for 48 h. After stimulation, supernatants were collected, and cytokine (TNF- α) concentrations were determined by ELISA (BD Bioscience, Heidelberg, Germany). Mono Mac 6 (MM6) cells were cultured in VLE-RPMI 1640 medium with stable glutamine (Biochrom, Berlin, Germany), 10% FCS, 1% nonessential amino acids, and 1% penicillin-streptomycin. After stimulation of the Mono Mac 6 cells with Pam3Cys and PGNpol Δ lgt for 48 h, the supernatants were collected, and the concentration of IL-8 was analyzed by use of an ELISA kit (BD Biosciences) according to the manufacturer's instructions.

Strains and growth conditions. *Staphylococcus aureus* SA113 (wild type) and the Δ lgt mutant (no expression of mature lipoproteins) were grown in tryptic soy broth (Sigma, Steinheim, Germany) at 37°C with aeration for 16 h. The optical density at 578 nm was 12 (Helios α spectrophotometer; Thermo Scientific).

Isolation of polymeric peptidoglycan (PGNpol). The isolation of ultrapurified PGN, free of DNA, RNA, proteins, wall teichoic acids, lipoteichoic acids, and salts, was done according to the method of de Jonge et al. (32), with some modifications. These modifications included the usage of three different buffers (buffers A to C). The pellet of a 50-ml overnight culture was boiled in 10 ml buffer A (2.5% SDS in 0.1 M Tris-HCl, pH 6.8) for 20 min at 100°C. The SDS was removed by several washing steps with double-distilled water at 4,700 rpm at room temperature. The pellet was resuspended with 20 ml 0.1 M Tris-HCl, pH 6.8. Cells were disrupted by vortexing with glass beads (150 to 212 μ m). The supernatant was subsequently incubated with buffer B for 1 h (10 μ g/ml DNase and 50 μ g/ml RNase in 0.1 M Tris-HCl, pH 6.8), with buffer C overnight (50 μ g/ml trypsin in double-distilled water), and, finally, with hydrofluoric acid (HF) for 4 h. HF was washed out with double-distilled water, and the PGN was lyophilized overnight.

Lyophilized PGN (10 mg/ml) was digested with 500 U mutanolysin of *Streptomyces globosporus* ATCC 21553 (Sigma) in a 12.5 mM phosphate buffer (pH 5.5) at 37°C for 16 h. The sample was boiled for 3 min and centrifuged for 5 min at 10,000 rpm. The supernatant was reduced with sodium borohydride in 0.5 M borate buffer (pH 9) for 20 min at room

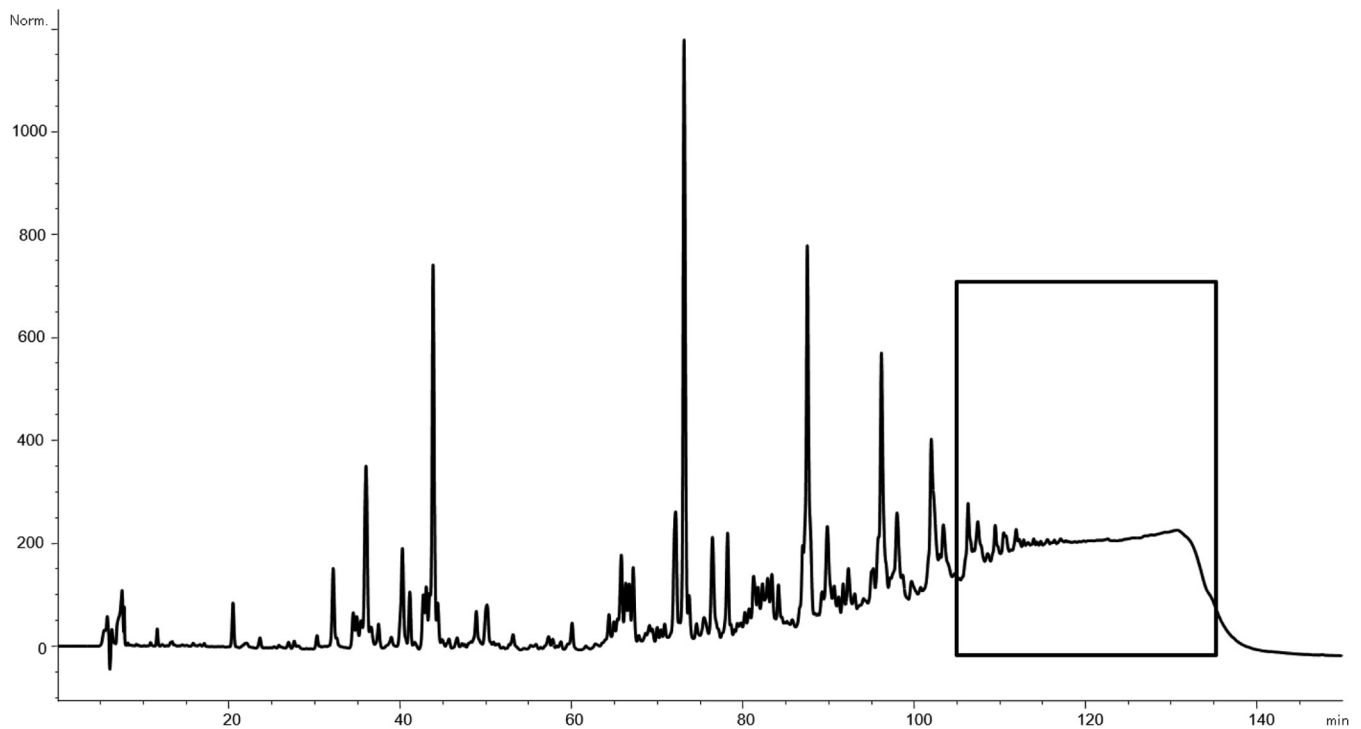


FIG 1 Separation and analysis of polymeric PGN. Separation and analysis of the peptidoglycan polymer were performed using an Agilent 1200 analytical HPLC system. The corresponding polymer peak ($r_t = 105$ to 135 min) was collected and desalted. Remaining LPS impurities were removed. Shown is the pattern for muramidase-digested PGN from an *S. aureus* SA113 wild-type overnight culture. The boxed sequence indicates the collected polymeric PGN fragments.

temperature. The pH was subsequently adjusted to 2 with orthophosphoric acid. Samples were further processed or stored at -20°C .

The separation and analysis of the peptidoglycan polymer were performed by high-pressure liquid chromatography (HPLC), based on the method of Glauner (33), using an Agilent 1200 analytical HPLC system. A 250- by 4.6-mm reversed-phase column (Prontosil 120-3-C18 AQ; Bischoff) guarded by a 20- by 4.6-mm precolumn was used. The samples were eluted at a flow rate of 0.5 ml/min, using a linear gradient starting from 100% buffer A (100 mM NaH_2PO_4 , 5% [vol/vol] methanol, pH 2.5) to 100% buffer B (100 mM NaH_2PO_4 , 30% [vol/vol] methanol, pH 2.8) within 155 min. The column temperature was set to 52°C . The eluted muropeptides were detected by UV absorption at 205 nm. The corresponding polymer peak ($r_t = 105$ to 135 min) (Fig. 1) was collected and desalted on the same column, using a water-acetonitrile gradient.

LPS contamination was checked using an Endosafe-PTS system (Charles River, Sulzfeld, Germany). Remaining LPS impurities were removed using an Endo Trap Red endotoxin removal kit (Hyglos). Very low LPS contents could be detected (<0.005 endotoxin unit [EU]/mg).

Statistical analysis. Statistical analysis was performed using GraphPad Prism software (GraphPad, La Jolla, CA). Parameters were analyzed by a nonparametric one-way analysis of variance (ANOVA) model for repeated measurements, with the Bonferroni adjustment (*, $P < 0.05$; **, $P < 0.01$; and ***, $P < 0.001$). P values of <0.05 were considered significant. Error bars represent standard errors of the means (SEM). If not otherwise mentioned, figures show means \pm SEM of values from three experiments per group. Stimulated DCs from WT mice were compared to unstimulated DCs from WT mice, and stimulated DCs from $\text{NOD2}^{-/-}$ mice were compared to unstimulated DCs from $\text{NOD2}^{-/-}$ mice.

RESULTS

Purification of polymeric peptidoglycan (PGNpol) from *S. aureus* and its Δlgt mutant. To address the importance of lipopeptide impurities within the PGN fractions in signaling, we isolated

polymeric PGN from two *S. aureus* SA113 strains. On the one hand, we isolated PGN from wild-type SA113, containing residual mature lipoproteins within the polymeric PGN meshwork. On the other hand, we isolated PGN from SA113 Δlgt , which is considered lipoprotein free because of its inability to produce mature lipoproteins. A typical pattern for PGN from WT SA113 after muramidase digestion is shown in Fig. 1. The pattern for PGN from SA113 Δlgt was identical to the WT pattern and is therefore not shown.

Activation and maturation of DCs by PGNpol are due to residual lipoproteins. In order to elucidate the role of *S. aureus*-derived polymeric PGN in the NOD2-mediated activation of BMDCs, these cells were stimulated with PGN isolated from either WT *S. aureus* SA113 (PGNpol) or SA113 Δlgt (PGNpol Δlgt). PGNpol is a ligand of NOD2, but while PGNpol Δlgt is lipoprotein free, the PGNpol preparation contains lipoproteins of *S. aureus*, which are known to be ligands of TLR2 (30).

For control purposes, Pam3Cys (a synthetic triacylated lipopeptide), LPS, and MDP were used as specific ligands for TLR2, TLR4, and NOD2, respectively. Incubation of DCs with increasing concentrations of PGNpol Δlgt (up to 100 $\mu\text{g}/\text{ml}$) did not stimulate secretion of IL-6, as indicated in Fig. 2A. In contrast, PGNpol (10 $\mu\text{g}/\text{ml}$) strongly stimulated IL-6 secretion, to a degree that was comparable with that induced by LPS or Pam3Cys. Furthermore, incubation with PGNpol Δlgt (up to 100 $\mu\text{g}/\text{ml}$) did not induce secretion of IL-12p40 (Fig. 2B), while PGNpol (10 $\mu\text{g}/\text{ml}$) strongly stimulated IL-12p40 secretion.

In order to find out whether PGNpol and PGNpol Δlgt lead to DC maturation, DCs were stimulated with PGNpol Δlgt or PGNpol and afterwards analyzed for MHC-II and CD40

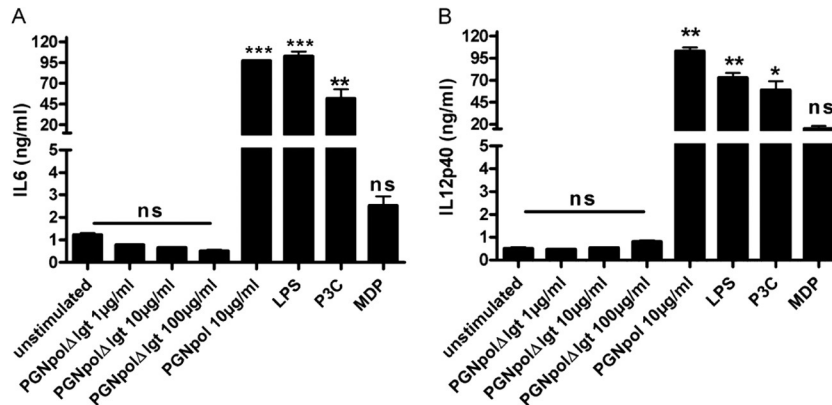


FIG 2 Stimulation with PGNpol, but not PGNpolΔlgt, leads to significant secretion of IL-6 and IL-12p40 in DCs. Incubation of DCs with PGNpol, but not PGNpolΔlgt, stimulated IL-6 (A) and IL-12p40 (B) secretion, which was comparable to that induced by LPS or Pam3Cys. DCs were stimulated with PGNpolΔlgt at concentrations of up to 100 μg/ml. Stimulation with 10 μg/ml PGNpol led to high levels of secretion of IL-6 and IL-12p40. A comparison was made between unstimulated cells and each stimulant by using a nonparametric one-way ANOVA model for repeated measurements, with the Bonferroni adjustment. ns, not significant.

surface expression by flow cytometry. DCs stimulated with PGNpol expressed high levels of MHC-II and CD40, resulting in highly activated and mature DCs. In contrast, expression of these surface molecules was nearly unaffected in DCs exposed to PGNpolΔlgt, suggesting a reduced ability of PGNpolΔlgt to activate and mature DCs (Fig. 3).

Stimulation with PGNpol leads to increased activation and maturation of DCs compared to the case with PGNpolΔlgt. To further elucidate the effect of a bacterial NOD2 ligand and the potentially costimulatory effect of a TLR2 ligand, DCs from NOD2^{-/-} mice were compared to DCs from WT mice.

First, secretion of IL-12p40 was tested after stimulation with PGNpolΔlgt and PGNpol. Consistent with the data shown in Fig. 2A, there was no detectable secretion of IL-12p40 after stimulation with PGNpolΔlgt in DCs from either WT mice or NOD2^{-/-} mice.

In contrast, stimulation with PGNpol induced a significantly smaller IL-12p40 signal in DCs from NOD2^{-/-} mice than in DCs from WT mice (Fig. 4). These data strongly suggest that a combined NOD2 and TLR2 signal is necessary to induce a strong se-

cretion of IL-12p40 and that the smaller signal in the DCs from NOD2^{-/-} mice was the result of the sole activation of TLR2. Similar results were obtained with IL-6 after stimulation of DCs from NOD2^{-/-} mice with PGNpolΔlgt and PGNpol (data not shown).

To further test the effect of combined TLR2 and NOD2 stimulation on DC activation and maturation, we analyzed the expression of the DC surface markers MHC-II and CD40 by flow cytometry. In NOD2^{-/-} DCs, incubation with PGNpol led to a significantly smaller proportion of MHC-II^{high} cells than the case in stimulated WT DCs (Fig. 5A). Furthermore, there was an increased expression of CD40 in DCs after stimulation with PGNpol compared to PGNpolΔlgt (Fig. 5B). Taken together, our data strongly suggest that a combined stimulation of the TLR2 and NOD2 pathways by PGNpol is important for the activation and maturation of DCs.

Combined stimulation of DCs with PGNpolΔlgt and Pam3Cys reveals synergistic effects on TNF-α secretion pattern. TNF-α is a key cytokine in IBD and is well known for its role in mediating innate immune responses (34). To confirm our hypothesis that combined stimulation with TLR2 and NOD2 ligands

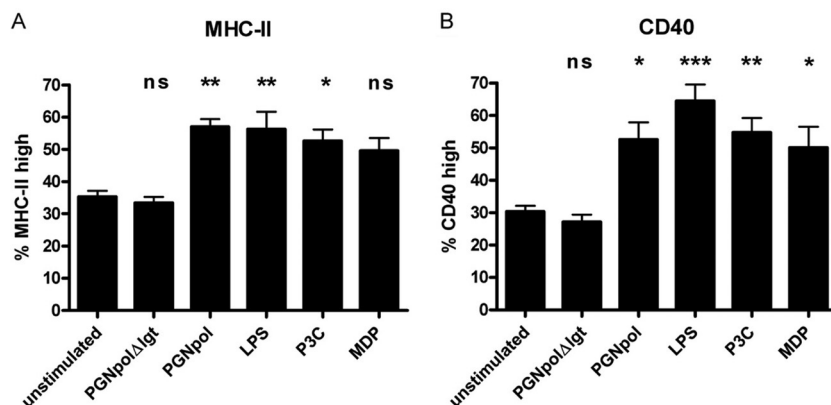


FIG 3 Stimulation with PGNpol, but not PGNpolΔlgt, leads to increased MHC-II and CD40 expression in DCs. Immature BMDCs were activated with several NOD2 or TLR2 ligands. Maturation was quantified by FACS analysis to assess the levels of MHC-II (A) and CD40 (B). The quantification was based on isotype controls. Stimulation of DCs with PGNpol (10 μg/ml) led to strong MHC-II and CD40 signals. In contrast, stimulation of DCs with PGNpolΔlgt (10 μg/ml) did not lead to increased expression of MHC-II and CD40. A comparison was made between unstimulated cells and each stimulant by using a nonparametric one-way ANOVA model for repeated measurements, with the Bonferroni adjustment.

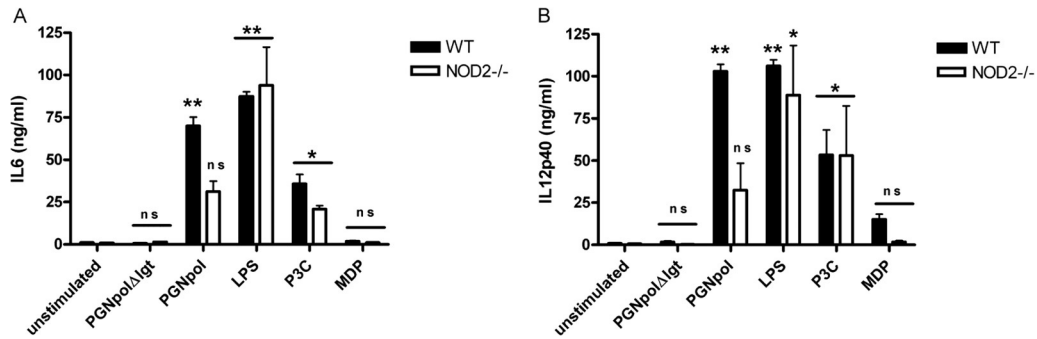


FIG 4 Stimulation with PGNpol in DCs is dependent on a NOD2 costimulus. Stimulation with PGNpol led to significantly increased secretion of IL-6 (A) and IL-12p40 (B) in DCs from WT mice compared to unstimulated controls. In contrast, DCs derived from NOD2^{-/-} mice failed to show increased IL-6 and IL-12p40 secretion upon stimulation with PGNpol. Stimulated DCs from WT mice were compared to unstimulated DCs from WT mice, and stimulated DCs from NOD2^{-/-} mice were compared to unstimulated DCs from NOD2^{-/-} mice.

acts synergistically on DC cytokine secretion, we costimulated DCs with the NOD2 ligand PGNpolΔIgt and the TLR2 ligand Pam3Cys and determined the secretion of TNF-α. In line with our hypothesis, the costimulation induced a significantly enhanced expression of TNF-α in DCs compared to the case in PGNpolΔIgt- or P3C-monostimulated DCs (Fig. 6).

To further confirm these findings, the experiments were extended to additional immune cells, i.e., a murine macrophage cell line (J774 cells) (Fig. 7) and a human monocyte cell line (MM6 cells) (Fig. 8). In both cell lines, the synergistic costimulation with PGNpolΔIgt and P3C resulted in an increased expression of pro-inflammatory cytokines, indicating that the observed effect is not restricted to mouse DCs but seems to be relevant for the activation of different types of innate immune cells.

DISCUSSION

NOD2 mutations play an important role in Crohn's disease (1, 2). However, how exactly these mutations contribute to this specific disease still remains uncovered. NOD2, as an important intracellular receptor of the innate immune system, senses bacterial cell wall products, such as MDP, and activates NF-κB (35). While

MDP was the first NOD2 ligand described (36, 37), it later became clear that polymeric (16, 38) as well as monomeric (14) PGN also activates NOD2. DCs are the most potent APCs in the intestinal mucosa and have important functions in the mucosa-associated immune system (39). Because of their important role in activating and also regulating the immune system, they also seem to play an important role in Crohn's disease (11). Therefore, we studied the role of NOD2-mediated activation of DCs via natural *S. aureus*-derived PGN. In the present study, we focused on the role of polymeric PGN, which is an important part of the bacterial cell wall. Defined isogenic *S. aureus* mutant strains were used to elucidate the effect of NOD2 ligand (PGNpolΔIgt) monostimulation or the synergistic effect of NOD2 and TLR2 ligand (PGNpol) costimulation. While monostimulation with a natural NOD2 ligand (PGNpolΔIgt) did not lead to activation and maturation of DCs, costimulation with a NOD2 and TLR2 ligand (PGNpol) led to strong activation and increased cytokine secretion (IL-6 and IL-12p40) of DCs *in vivo*. This effect was seen not only in isolated DCs but also in J774 cells (macrophages) and MM6 cells (monocytes). In addition to already published work by Müller-Anstett et al. (26), our data indicate that singular NOD2 activation seems to

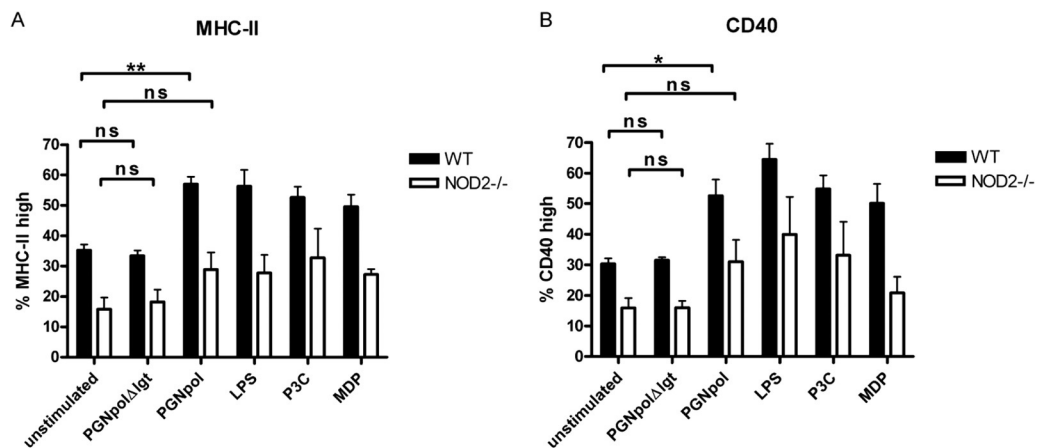


FIG 5 DC stimulation with PGNpol in WT mice leads to increased expression of MHC-II and CD40 compared to that in NOD2^{-/-} mice. Stimulation of DCs from NOD2^{-/-} mice with PGNpol (10 μg/ml) did not lead to significantly more expression of MHC-II (A) or CD40 (B), indicating that the costimulatory effect of NOD2 and TLR2 is necessary for effective maturation of DCs. Stimulated DCs from WT mice were compared to unstimulated DCs from WT mice, and unstimulated DCs from NOD2^{-/-} mice were compared to stimulated DCs from NOD2^{-/-} mice. In addition, a comparison between DCs from WT and NOD2^{-/-} mice was made by using a nonparametric one-way ANOVA model for repeated measurements, with the Bonferroni adjustment.

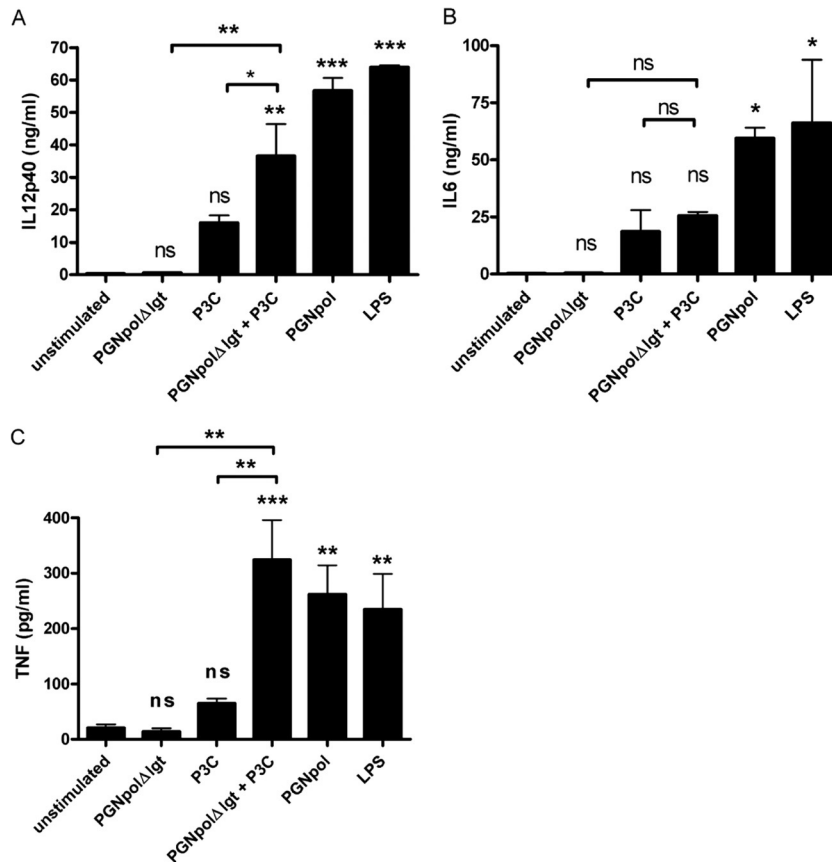


FIG 6 Combined stimulation of DCs with NOD2 and TLR2 ligands leads to stronger secretion of IL-12p40 and TNF than stimulation with each of the stimuli alone. DCs were stimulated with PGNpolΔlgt (10 μg/ml), Pam3Cys (1 μg/ml), and LPS (1 μg/ml). After stimulation with both PGNpolΔlgt and Pam3Cys, there were significantly higher signals for IL-12p40 (A) and TNF (C) than the case for stimulation with the single components alone. (B) There was not a significantly higher signal of IL-6 than that for stimulation with the single components. Unstimulated DCs from WT mice were compared to stimulated DCs from WT mice by using a nonparametric one-way ANOVA model for repeated measurements, with the Bonferroni adjustment.

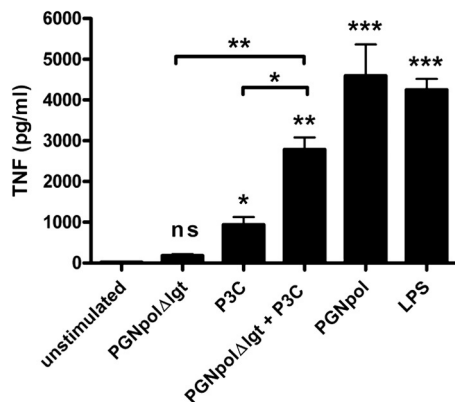


FIG 7 Combined stimulation of J774 cells with NOD2 and TLR2 ligands leads to significant TNF-α secretion. J774 cells were stimulated with Pam3Cys (1 ng/ml), PGNpolΔlgt (10 μg/ml), PGNpol (10 μg/ml), and LPS (1 μg/ml) for 48 h. After stimulation with both PGNpolΔlgt and Pam3Cys, there was a significant increase of TNF-α, which seemed to be higher than stimulation with the single components. Unstimulated DCs from WT mice were compared to stimulated DCs from WT mice by using a nonparametric one-way ANOVA model for repeated measurements, with the Bonferroni adjustment.

play a minor role in activating immune cells. However, synergistic costimulation of the NOD2 and TLR2 pathways results in potent activation of DCs, macrophages, and monocytes.

In patients with Crohn's disease, an exaggerated Th1-mediated immune response may contribute to mucosal inflammation (40). *In vivo*, MDP itself is not able to induce a Th1 cytokine profile but rather invokes a Th2 immune response (41). Additionally, in support of our results, it has been demonstrated that combined stimulation with MDP plus a TLR2 or TLR4 ligand leads to a synergistic release of IL-6 and IL-12p40 in BMDCs, which is abolished in NOD2^{-/-} DCs (41). While stimulation of the innate immune system with a sole NOD2 ligand, in our case *S. aureus*-derived polymeric PGNpolΔlgt, does not lead to an immune response, such a response is markedly enhanced after dual stimulation via the NOD2 and TLR2 pathways. The complex interplay between NOD2 and TLR2 signaling might have an influence on intestinal homeostasis.

However, how can these results be translated into the clinical entity of Crohn's disease? Activation of NOD2 by MDP protects mice from experimental colitis (42), thus promoting intestinal homeostasis. Additionally, PGN from specific lactobacilli features anti-inflammatory effects and thus seems to be crucial for the probiotic action of these specific strains (43). These studies further support the hypothesis that stimulation of NOD2 alone—as op-

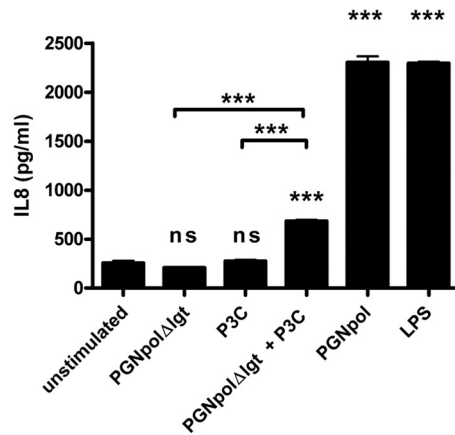


FIG 8 Combined but not single stimulation of MM6 cells with NOD2 and TLR2 ligands leads to a significant increase of IL-8. MM6 cells were stimulated with Pam3Cys (10 ng/ml), PGNpolΔlgt (10 μg/ml), PGNpol (10 μg/ml), and LPS (1 μg/ml) for 48 h. After stimulation with both PGNpolΔlgt and Pam3Cys, there was a significant increase of IL-8, whereas stimulation with single components did not lead to IL-8 secretion. Stimulated DCs from WT mice were compared to unstimulated DCs from WT mice. Unstimulated DCs from WT mice were compared to stimulated DCs from WT mice by using a nonparametric one-way ANOVA model for repeated measurements, with the Bonferroni adjustment.

posed to costimulation of NOD2 and TLR2—can possibly lead to downregulation of inflammatory pathways. A “loss of function” in the NOD2 gene might therefore be an important part of the pathogenesis of Crohn’s disease.

In summary, we showed that in DCs, synergistic costimulation of the NOD2 and TLR2 signaling cascades leads to an increased activation and maturation of DCs, and also to increased cytokine secretion, compared to the case with monostimulation. These results might be important for a better understanding of the complex interplay between these receptors in maintaining homeostasis in the intestinal immune system.

ACKNOWLEDGMENTS

This work was supported by Glykobiologie/Glykomik contract research of the Baden-Württemberg Stiftung, by DFG grants SFB 685 and SPP1656, and by the BMBF.

REFERENCES

- Hampe J, Cuthbert A, Croucher PJ, Mirza MM, Mascheretti S, Fisher S, Frenzel H, King K, Hasselmeyer A, MacPherson AJ, Bridger S, van Deventer S, Forbes A, Nikolaus S, Lennard-Jones JE, Foelsch UR, Krawczak M, Lewis C, Schreiber S, Mathew CG. 2001. Association between insertion mutation in NOD2 gene and Crohn’s disease in German and British populations. *Lancet* 357:1925–1928. [http://dx.doi.org/10.1016/S0140-6736\(00\)05063-7](http://dx.doi.org/10.1016/S0140-6736(00)05063-7).
- Hugot JP, Chamaillard M, Zouali H, Lesage S, Cezard JP, Belaiche J, Almer S, Tysk C, O’Morain CA, Gassull M, Binder V, Finkel Y, Cortot A, Modigliani R, Laurent-Puig P, Gower-Rousseau C, Macry J, Colombel JF, Sahbatou M, Thomas G. 2001. Association of NOD2 leucine-rich repeat variants with susceptibility to Crohn’s disease. *Nature* 411:599–603. <http://dx.doi.org/10.1038/35079107>.
- Ogura Y, Bonen DK, Inohara N, Nicolae DL, Chen FF, Ramos R, Britton H, Moran T, Karaliuskas R, Duerr RH, Achkar JP, Brant SR, Bayless TM, Kirschner BS, Hanauer SB, Nunez G, Cho JH. 2001. A frameshift mutation in NOD2 associated with susceptibility to Crohn’s disease. *Nature* 411:603–606. <http://dx.doi.org/10.1038/35079114>.
- Strober W, Murray PJ, Kitani A, Watanabe T. 2006. Signalling pathways and molecular interactions of NOD1 and NOD2. *Nat. Rev. Immunol.* 6:9–20. <http://dx.doi.org/10.1038/nri1747>.

- Ng SC, Kamm MA, Stagg AJ, Knight SC. 2010. Intestinal dendritic cells: their role in bacterial recognition, lymphocyte homing, and intestinal inflammation. *Inflamm. Bowel Dis.* 16:1787–1807. <http://dx.doi.org/10.1002/ibd.21247>.
- Niess JH, Brand S, Gu X, Landsman L, Jung S, McCormick BA, Vyas JM, Boes M, Ploegh HL, Fox JG, Littman DR, Reinecker HC. 2005. CX3CR1-mediated dendritic cell access to the intestinal lumen and bacterial clearance. *Science* 307:254–258. <http://dx.doi.org/10.1126/science.11102901>.
- Coomes JL, Powrie F. 2008. Dendritic cells in intestinal immune regulation. *Nat. Rev. Immunol.* 8:435–446. <http://dx.doi.org/10.1038/nri2335>.
- Strober W. 2009. The multifaceted influence of the mucosal microflora on mucosal dendritic cell responses. *Immunity* 31:377–388. <http://dx.doi.org/10.1016/j.immuni.2009.09.001>.
- Iwasaki A, Medzhitov R. 2004. Toll-like receptor control of the adaptive immune responses. *Nat. Immunol.* 5:987–995. <http://dx.doi.org/10.1038/ni1112>.
- Baumgart DC, Sandborn WJ. 2012. Crohn’s disease. *Lancet* 380:1590–1605. [http://dx.doi.org/10.1016/S0140-6736\(12\)60026-9](http://dx.doi.org/10.1016/S0140-6736(12)60026-9).
- Niess JH. 2008. Role of mucosal dendritic cells in inflammatory bowel disease. *World J. Gastroenterol.* 14:5138–5148. <http://dx.doi.org/10.3748/wjg.14.5138>.
- Hart AL, Al-Hassi HO, Rigby RJ, Bell SJ, Emmanuel AV, Knight SC, Kamm MA, Stagg AJ. 2005. Characteristics of intestinal dendritic cells in inflammatory bowel diseases. *Gastroenterology* 129:50–65. <http://dx.doi.org/10.1053/j.gastro.2005.05.013>.
- Iliev ID, Spadoni I, Mileti E, Matteoli G, Sonzogni A, Sampietro GM, Foschi D, Caprioli F, Viale G, Rescigno M. 2009. Human intestinal epithelial cells promote the differentiation of tolerogenic dendritic cells. *Gut* 58:1481–1489. <http://dx.doi.org/10.1136/gut.2008.175166>.
- Volz T, Nega M, Buschmann J, Kaesler S, Guenova E, Peschel A, Rocken M, Götz F, Biedermann T. 2010. Natural Staphylococcus aureus-derived peptidoglycan fragments activate NOD2 and act as potent costimulators of the innate immune system exclusively in the presence of TLR signals. *FASEB J.* 24:4089–4102. <http://dx.doi.org/10.1096/fj.09-151001>.
- Hashimoto M, Tawaratsumida K, Kariya H, Kiyohara A, Suda Y, Krikae F, Kirikae T, Götz F. 2006. Not lipoteichoic acid but lipoproteins appear to be the dominant immunobiologically active compounds in Staphylococcus aureus. *J. Immunol.* 177:3162–3169. <http://dx.doi.org/10.4049/jimmunol.177.5.3162>.
- Iyer JK, Coggeshall KM. 2011. Cutting edge: primary innate immune cells respond efficiently to polymeric peptidoglycan, but not to peptidoglycan monomers. *J. Immunol.* 186:3841–3845. <http://dx.doi.org/10.4049/jimmunol.1004058>.
- Bera A, Herbert S, Jakob A, Vollmer W, Götz F. 2005. Why are pathogenic staphylococci so lysozyme resistant? The peptidoglycan O-acetyltransferase OatA is the major determinant for lysozyme resistance of Staphylococcus aureus. *Mol. Microbiol.* 55:778–787. <http://dx.doi.org/10.1111/j.1365-2958.2004.04446.x>.
- Bera A, Biswas R, Herbert S, Götz F. 2006. The presence of peptidoglycan O-acetyltransferase in various staphylococcal species correlates with lysozyme resistance and pathogenicity. *Infect. Immun.* 74:4598–4604. <http://dx.doi.org/10.1128/IAI.00301-06>.
- Herbert S, Bera A, Nerz C, Kraus D, Peschel A, Goerke C, Meehl M, Cheung A, Götz F. 2007. Molecular basis of resistance to muramidase and cationic antimicrobial peptide activity of lysozyme in staphylococci. *PLoS Pathog.* 3:e102. <http://dx.doi.org/10.1371/journal.ppat.0030102>.
- Shimada T, Park BG, Wolf AJ, Brikos C, Goodridge HS, Becker CA, Reyes CN, Miao EA, Aderem A, Götz F, Liu GY, Underhill DM. 2010. Staphylococcus aureus evades lysozyme-based peptidoglycan digestion that links phagocytosis, inflammasome activation, and IL-1β secretion. *Cell Host Microbe* 7:38–49. <http://dx.doi.org/10.1016/j.chom.2009.12.008>.
- Netea MG, Kullberg BJ, de Jong DJ, Franke B, Sprong T, Naber TH, Drenth JP, Van der Meer JW. 2004. NOD2 mediates anti-inflammatory signals induced by TLR2 ligands: implications for Crohn’s disease. *Eur. J. Immunol.* 34:2052–2059. <http://dx.doi.org/10.1002/eji.200425229>.
- Watanabe T, Kitani A, Murray PJ, Strober W. 2004. NOD2 is a negative regulator of Toll-like receptor 2-mediated T helper type 1 responses. *Nat. Immunol.* 5:800–808. <http://dx.doi.org/10.1038/ni1092>.
- Dahiya Y, Pandey RK, Sodhi A. 2011. Nod2 downregulates TLR2/1

- mediated IL1beta gene expression in mouse peritoneal macrophages. *PLoS One* 6:e27828. <http://dx.doi.org/10.1371/journal.pone.0027828>.
24. Kobayashi KS, Chamaillard M, Ogura Y, Henegariu O, Inohara N, Nunez G, Flavell RA. 2005. Nod2-dependent regulation of innate and adaptive immunity in the intestinal tract. *Science* 307:731–734. <http://dx.doi.org/10.1126/science.1104911>.
 25. Travassos LH, Girardin SE, Philpott DJ, Blanot D, Nahori MA, Werts C, Boneca IG. 2004. Toll-like receptor 2-dependent bacterial sensing does not occur via peptidoglycan recognition. *EMBO Rep.* 5:1000–1006. <http://dx.doi.org/10.1038/sj.embor.7400248>.
 26. Müller-Anstett MA, Muller P, Albrecht T, Nega M, Wagener J, Gao Q, Kaesler S, Schaller M, Biedermann T, Götz F. 2010. Staphylococcal peptidoglycan co-localizes with Nod2 and TLR2 and activates innate immune response via both receptors in primary murine keratinocytes. *PLoS One* 5:e13153. <http://dx.doi.org/10.1371/journal.pone.0013153>.
 27. Hashimoto M, Tawaratsumida K, Kariya H, Aoyama K, Tamura T, Suda Y. 2006. Lipoprotein is a predominant Toll-like receptor 2 ligand in *Staphylococcus aureus* cell wall components. *Int. Immunol.* 18:355–362. <http://dx.doi.org/10.1093/intimm/dxh374>.
 28. Schmalzer M, Jann NJ, Ferracin F, Landolt LZ, Biswas L, Götz F, Landmann R. 2009. Lipoproteins in *Staphylococcus aureus* mediate inflammation by TLR2 and iron-dependent growth in vivo. *J. Immunol.* 182:7110–7118. <http://dx.doi.org/10.4049/jimmunol.0804292>.
 29. Zahringer U, Lindner B, Inamura S, Heine H, Alexander C. 2008. TLR2—promiscuous or specific? A critical re-evaluation of a receptor expressing apparent broad specificity. *Immunobiology* 213:205–224. <http://dx.doi.org/10.1016/j.imbio.2008.02.005>.
 30. Stoll H, Dengjel J, Nerz C, Götz F. 2005. *Staphylococcus aureus* deficient in lipidation of prelipoproteins is attenuated in growth and immune activation. *Infect. Immun.* 73:2411–2423. <http://dx.doi.org/10.1128/IAI.73.4.2411-2423.2005>.
 31. Lutz MB, Kukutsch N, Ogilvie AL, Rossner S, Koch F, Romani N, Schuler G. 1999. An advanced culture method for generating large quantities of highly pure dendritic cells from mouse bone marrow. *J. Immunol. Methods* 223:77–92. [http://dx.doi.org/10.1016/S0022-1759\(98\)00204-X](http://dx.doi.org/10.1016/S0022-1759(98)00204-X).
 32. de Jonge BL, Chang YS, Gage D, Tomasz A. 1992. Peptidoglycan composition of a highly methicillin-resistant *Staphylococcus aureus* strain. The role of penicillin binding protein 2A. *J. Biol. Chem.* 267:11248–11254.
 33. Glauner B. 1988. Separation and quantification of mucopeptides with high-performance liquid chromatography. *Anal. Biochem.* 172:451–464. [http://dx.doi.org/10.1016/0003-2697\(88\)90468-X](http://dx.doi.org/10.1016/0003-2697(88)90468-X).
 34. Mizgerd JP, Spieker MR, Doerschuk CM. 2001. Early response cytokines and innate immunity: essential roles for TNF receptor 1 and type I IL-1 receptor during *Escherichia coli* pneumonia in mice. *J. Immunol.* 166:4042–4048. <http://dx.doi.org/10.4049/jimmunol.166.6.4042>.
 35. Strober W, Kitani A, Fuss I, Asano N, Watanabe T. 2008. The molecular basis of NOD2 susceptibility mutations in Crohn's disease. *Mucosal Immunol.* 1(Suppl 1):S5–S9. <http://dx.doi.org/10.1038/mi.2008.42>.
 36. Girardin SE, Boneca IG, Viala J, Chamaillard M, Labigne A, Thomas G, Philpott DJ, Sansonetti PJ. 2003. Nod2 is a general sensor of peptidoglycan through muramyl dipeptide (MDP) detection. *J. Biol. Chem.* 278:8869–8872. <http://dx.doi.org/10.1074/jbc.C200651200>.
 37. Inohara N, Ogura Y, Fontalba A, Gutierrez O, Pons F, Crespo J, Fukase K, Inamura S, Kusumoto S, Hashimoto M, Foster SJ, Moran AP, Fernandez-Luna JL, Nunez G. 2003. Host recognition of bacterial muramyl dipeptide mediated through NOD2. Implications for Crohn's disease. *J. Biol. Chem.* 278:5509–5512. <http://dx.doi.org/10.1074/jbc.C200673200>.
 38. Natsuka M, Uehara A, Yang S, Echigo S, Takada H. 2008. A polymer-type water-soluble peptidoglycan exhibited both Toll-like receptor 2- and NOD2-agonistic activities, resulting in synergistic activation of human monocytic cells. *Innate Immun.* 14:298–308. <http://dx.doi.org/10.1177/1753425908096518>.
 39. Cella M, Sallusto F, Lanzavecchia A. 1997. Origin, maturation and antigen presenting function of dendritic cells. *Curr. Opin. Immunol.* 9:10–16. [http://dx.doi.org/10.1016/S0952-7915\(97\)80153-7](http://dx.doi.org/10.1016/S0952-7915(97)80153-7).
 40. Peluso I, Pallone F, Monteleone G. 2006. Interleukin-12 and Th1 immune response in Crohn's disease: pathogenetic relevance and therapeutic implication. *World J. Gastroenterol.* 12:5606–5610.
 41. Magalhaes JG, Fritz JH, Le Bourhis L, Selge G, Travassos LH, Selvanantham T, Girardin SE, Gommerman JL, Philpott DJ. 2008. Nod2-dependent Th2 polarization of antigen-specific immunity. *J. Immunol.* 181:7925–7935. <http://dx.doi.org/10.4049/jimmunol.181.11.7925>.
 42. Watanabe T, Asano N, Murray PJ, Ozato K, Tailor P, Fuss IJ, Kitani A, Strober W. 2008. Muramyl dipeptide activation of nucleotide-binding oligomerization domain 2 protects mice from experimental colitis. *J. Clin. Invest.* 118:545–559. <http://dx.doi.org/10.1172/JCI33145>.
 43. Macho Fernandez E, Valenti V, Rockel C, Hermann C, Pot B, Boneca IG, Grangette C. 2011. Anti-inflammatory capacity of selected lactobacilli in experimental colitis is driven by NOD2-mediated recognition of a specific peptidoglycan-derived mucopeptide. *Gut* 60:1050–1059. <http://dx.doi.org/10.1136/gut.2010.232918>.

Cutaneous Innate Immune Sensing of Toll-like Receptor 2-6 Ligands Suppresses T Cell Immunity by Inducing Myeloid-Derived Suppressor Cells

Yuliya Skabytska,¹ Florian Wölbing,¹ Claudia Günther,² Martin Köberle,^{1,3} Susanne Kaesler,¹ Ko-Ming Chen,¹ Emmanuella Guenova,^{1,4} Doruk Demircioglu,⁵ Wolfgang E. Kempf,^{1,3} Thomas Volz,^{1,3} Hans-Georg Rammensee,⁶ Martin Schaller,¹ Martin Röcken,¹ Friedrich Götz,⁵ and Tilo Biedermann^{1,3,*}

¹Department of Dermatology, Eberhard Karls University, Liebermeisterstrasse 25, 72076 Tübingen, Germany

²Department of Dermatology, Technical University Dresden, Mommsenstrasse 11, 01069 Dresden, Germany

³Department of Dermatology and Allergy, Technische Universität München, Biedersteinerstrasse 29, 80802 Munich, Germany

⁴Department of Dermatology, University Hospital Zurich, Gloriastrasse 31, CH-8091 Zurich, Switzerland

⁵Department of Microbial Genetics, Eberhard Karls University, Waldhäuser Straße 70/8, 72076 Tübingen, Germany

⁶Department of Immunology, Institute of Cell Biology, and German Cancer Consortium (DKTK), German Cancer Research Center (DKFZ) Partner Site Tübingen, Eberhard Karls University, Auf der Morgenstelle 15, 72076 Tübingen, Germany

*Correspondence: tilo.biedermann@tum.de

<http://dx.doi.org/10.1016/j.immuni.2014.10.009>

SUMMARY

Skin is constantly exposed to bacteria and antigens, and cutaneous innate immune sensing orchestrates adaptive immune responses. In its absence, skin pathogens can expand, entering deeper tissues and leading to life-threatening infectious diseases. To characterize skin-driven immunity better, we applied living bacteria, defined lipopeptides, and antigens cutaneously. We found suppression of immune responses due to cutaneous infection with Gram-positive *S. aureus*, which was based on bacterial lipopeptides. Skin exposure to Toll-like receptor (TLR)2-6-binding lipopeptides, but not TLR2-1-binding lipopeptides, potently suppressed immune responses through induction of Gr1⁺CD11b⁺ myeloid-derived suppressor cells (MDSCs). Investigating human atopic dermatitis, in which Gram-positive bacteria accumulate, we detected high MDSC amounts in blood and skin. TLR2 activation in skin resident cells triggered interleukin-6 (IL-6), which induced suppressive MDSCs, which are then recruited to the skin suppressing T cell-mediated recall responses such as dermatitis. Thus, cutaneous bacteria can negatively regulate skin-driven immune responses by inducing MDSCs via TLR2-6 activation.

INTRODUCTION

The skin is the largest organ at the interface between the environment and the host. The skin plays a major protective role not only as physical barrier but also as the site of first recognition of microbes and orchestrates consecutive immune responses (Naik et al., 2012; Swamy et al., 2010; Volz et al., 2012).

Staphylococcus aureus (*S. aureus*) is one of the most potent skin pathogens and is found to colonize skin of about 30%–

50% of healthy adults, among them 10%–20% persistently (Lowy, 1998). Coming from the skin, *S. aureus* can infect any tissue of the body and cause life-threatening diseases, particularly because of the widespread occurrence of antibiotic-resistant strains, known as methicillin-resistant *Staphylococcus aureus* (MRSA) (Saeed et al., 2014). In atopic dermatitis (AD) patients, there is an approximately 200-fold increase of *S. aureus* colonization with more than 90% of AD patients displaying *S. aureus* in comparison to the healthy skin (Leung and Bieber, 2003).

Microbes are first sensed by the innate immune system through pattern-recognition receptors (PRRs), which recognize microbe-associated molecular patterns (MAMPs) (Kawai and Akira, 2010). Both epithelial cells and resident innate immune cells in the skin express PRRs (Kupper and Fuhlbrigge, 2004; Lai and Gallo, 2008). Among PRRs, Toll-like receptors (TLRs) are a well-characterized family with distinct recognition profiles (Kawai and Akira, 2010). TLR2 has emerged as a dominant receptor for Gram-positive bacteria, especially *S. aureus* (Biedermann, 2006; Lai and Gallo, 2008; Mempel et al., 2003). Among TLR2 ligands, lipoproteins seem to be especially important because the lipoprotein diacylglycerol transferase (*lgt*) deletion mutant of *S. aureus* induces much less proinflammatory cytokines in human cell lines (Stoll et al., 2005) and less TLR2-MyD88 adaptor protein-mediated inflammation in a mouse model of systemic infection (Schmaler et al., 2009). It is now established that there are different classes of lipopeptides that all bind TLR2 (Müller et al., 2010; Schmaler et al., 2009). However, how these TLR2 ligands differ in regard to functional consequences has not been thoroughly investigated. TLR2 is known to form heterodimers with TLR1 and TLR6 to interact with this broad spectrum of ligands (Kang et al., 2009). TLR1 is required as a coreceptor for recognition of triacylated lipopeptides, such as Pam3Cys (Buwitt-Beckmann et al., 2006; Jin et al., 2007), while diacylated lipopeptides, such as FSL-1 or Pam2Cys, interact with TLR2-TLR6 heterodimers (Mae et al., 2007; Mühlradt et al., 1997). Functional properties of *S. aureus* lipopeptides in respect to TLR2 heterodimers have been investigated in several cell types (Buwitt-Beckmann et al., 2006; Hajjar et al., 2001), but evidence demonstrating specific functional

consequences for the activation of different heterodimers *in vivo* is lacking.

Sustained activation of TLRs causes persistent production of proinflammatory cytokines, such as tumor necrosis factor (TNF) or interleukin-6 (IL-6), leading to tissue damage (Kawai and Akira, 2010; Kupper and Fuhlbrigge, 2004; Lai and Gallo, 2008). Consequently, to reconstitute the integrity of the surface organ, mechanisms to limit cutaneous inflammation must be effective (Lai et al., 2009). In recent years, Gr1⁺CD11b⁺ myeloid-derived suppressor cells (MDSCs) have been identified as one cell population responsible for modulating immune responses (Bronte, 2009; Gabrilovich and Nagaraj, 2009; Ostrand-Rosenberg and Sinha, 2009). The most characteristic functional property of MDSCs is to suppress T cell responses (Gabrilovich et al., 2001; Kusmartsev et al., 2000). In the context of inflammation the precise function of MDSCs and the mechanisms of MDSC induction are not well-understood; but in a sepsis model with Gram-negative bacteria their induction has been shown to depend on TLR4-MyD88 activation (Delano et al., 2007), and in tumor models, different innate cytokines, such as IL-6, induce MDSC accumulation (Bunt et al., 2007; Chalmin et al., 2010). However, the suppression of IL-6 also increases susceptibility to bacterial and fungal infections, indicating pleiotropic effects of IL-6 (Hoetzenecker et al., 2012).

In this study, we have identified a pathway of immune regulation that operates in the skin. We mimicked intense cutaneous contact to bacteria in different *in vivo* mouse models by using living bacteria and lipopeptides. We investigated AD as a model for massive cutaneous immune sensing of Gram-positive bacteria in humans. We found that cutaneous infection with *S. aureus* caused immune suppression. The exposure to TLR2-6 ligands was sufficient to cause an almost complete reduction of consecutive cutaneous recall responses. This skin exposure induced accumulation of MDSCs, allowing MDSC recruitment to the skin, and suppression of T cell-mediated recall responses. Signals through TLR2 on skin-resident cells, but not on recruited hematopoietic cells, as well as cutaneous IL-6 induction, were necessary and sufficient for the expansion of MDSCs and consecutive immune suppression. These data demonstrate that cutaneous recognition of TLR2-6 ligands orchestrates a unique pathway of cutaneous immune modulation mediated by MDSCs, indicating a yet unknown level of immune counterregulation.

RESULTS

Cutaneous *Staphylococcus aureus* Induces Immune Suppression

We aimed to characterize the consequences of intense cutaneous innate immune sensing as in the case of colonization or infection with Gram-positive bacteria. We established a mouse model of epicutaneous colonization with pathologically relevant *S. aureus* (Wanke et al., 2013). Mimicking *S. aureus* skin infection by applying living *S. aureus* bacteria onto the skin with disrupted skin barrier, we found a distribution of the bacteria not only in the skin but also in the internal organs (spleen and kidney) (Figure 1A), indicating the importance of the skin as an effective defense immune organ with the potential to impact the whole immune system. To investigate how bacterial infection influences

consecutive immune responses, we combined this model of bacterial colonization and the murine T cell-mediated contact hypersensitivity (CHS) to FITC, in which bacteria were applied epicutaneously during FITC re-exposure of FITC-sensitized mice (see protocol in Figure S1A available online). The application of FITC onto the ear led to FITC-specific dermatitis as determined by ear swelling, which corresponded to the strength of the FITC-specific immune response. The cutaneous application of *S. aureus* 7 days previous to the FITC challenge did not enhance, but significantly reduced ear swelling and immune cell infiltration (Figures 1B and 1C). This immune suppression was completely dependent on immune sensing of bacterial lipoproteins, as lipoprotein-deficient *S. aureus* mutant (Δlgt) (Stoll et al., 2005) failed to induce immune suppression. Injecting *S. aureus* into the sub-epithelial dermis (intracutaneous route) also induced consecutive immune suppression, which, however, tended to be weaker compared to effects of *S. aureus* application onto the epithelium (Figure S1B). To identify underlying mechanisms of *S. aureus*-induced cutaneous immune suppression, we analyzed skin-draining lymph nodes. Only exposure to wild-type (WT) *S. aureus* bacteria and not the lipoprotein-deficient Δlgt *S. aureus* reduced *ex vivo* FITC-specific T cell proliferation (Figure 1D). In the spleen, CD4⁺ and CD8⁺ T cells were also reduced in mice cutaneously exposed to WT *S. aureus*, but not in mice exposed to lipoprotein-deficient Δlgt *S. aureus* (Figure 1E). Only in mice displaying suppressed T cells we detected a strong increase of Gr1⁺CD11b⁺ so-called myeloid-derived suppressor cells (Figure 1E). In contrast to this, accumulation of Gr1⁺CD11b⁺ was not detected in the liver (Figure S1D). At day 3 after FITC challenge, MDSCs were also slightly increased in draining lymph nodes due to cutaneous WT *S. aureus* infection, corresponding to the decrease of proliferating Ki67⁺ T cells (Figure S1E). Further experiments investigating other suppressive cell populations showed no alterations in the number of regulatory T (Treg) cells and IL-10-producing cells (Figure S1F); the numbers of Langerhans cells (LCs, defined as CD11c^{lo}CD205^{hi}) and CD11c⁺MHC-II⁺ cells were also unchanged, and dermal dendritic cells (dDCs, defined as CD11c^{hi}CD205^{lo}) were slightly increased (Figure S1E). These data indicate that MDSCs function independently of Treg cells and do not inhibit migration of DCs into lymph nodes.

In order to further emphasize the functional and clinical relevance of these findings, we investigated atopic dermatitis (AD) patients. AD is a perfectly suited model disease for investigations on immune consequences of skin exposure to bacteria, because AD is an inflammatory skin disease that is nearly always covered with and triggered by *Staphylococci*. In humans, MDSCs are typically described as CD11b⁺CD33⁺HLA-DR⁻CD14⁻ cells (Gabrilovich and Nagaraj, 2009). We observed a significant increase of MDSCs in the peripheral blood mononuclear cells (PBMCs) of AD patients (Figure 1F). The upregulation of human MDSCs was especially consistent in patients, in which severe AD was complicated by eczema herpeticum, which is a severe cutaneous viral infection resulting from immune suppression (Figure 1F, red squares) (Beck et al., 2009; Wollenberg et al., 2003), suggesting suppressive properties of MDSCs also in AD patients.

These data show that cutaneous *S. aureus* is sufficient to induce MDSCs and to cause immune suppression.

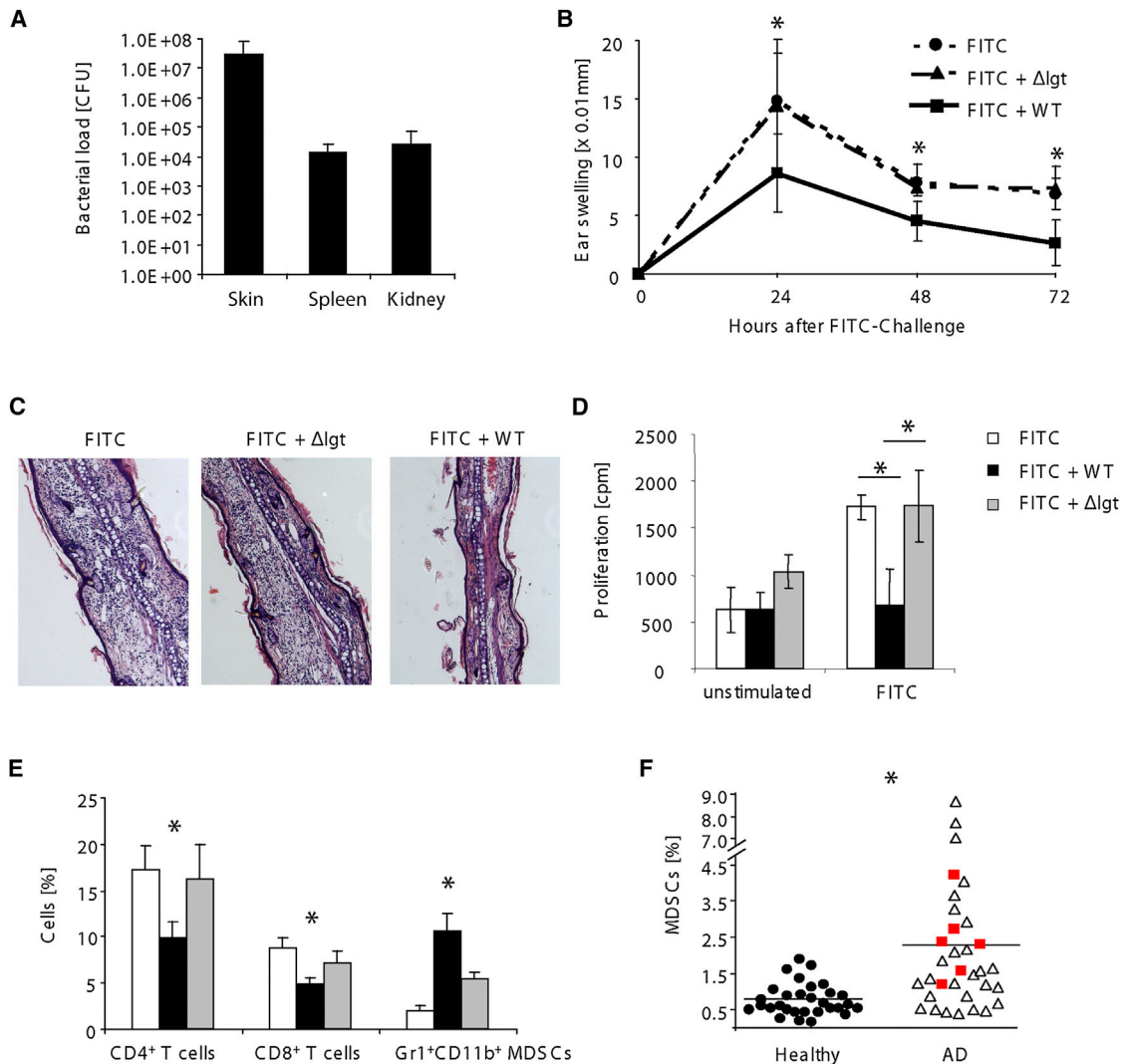


Figure 1. Cutaneous *Staphylococcus aureus* Induces Immune Suppression in Mice and Humans

(A–E) FITC-sensitized WT mice were treated following the protocol in Figure S1A (with living WT or lipoprotein mutant (Δlgt) *S. aureus*). Bacterial load as colony-forming units (cfu) (mean \pm SD, $n = 5$) (A), ear swelling (mean \pm SD, $n = 5$) (B), histology (H&E staining) (C), proliferation of skin-draining lymph node (LN) cells stimulated ex vivo with FITC (detected as counts per minute [cpm] of ^3H -thymidine incorporation) (mean \pm SD of triplicates) (D), and the percentage of cell populations in the spleen (mean \pm SD, $n = 5$) (E) were investigated. * $p < 0.05$.

(F) PBMCs from atopic dermatitis (AD) patients ($n = 33$) and healthy volunteers ($n = 30$) were analyzed for MDSCs, defined as $\text{CD}11\text{b}^+\text{CD}33^+\text{HLA-DR}^-\text{CD}14^-$ cells. The dots represent individual values, and the horizontal bar is the group mean. Red squares represent MDSCs of patients with severe AD and eczema herpeticum. * $p < 0.05$ (Mann-Whitney test). Data are representative of at least two independent experiments. See also Figure S1.

Cutaneous Exposure to TLR2-6 but Not to TLR2-1 Ligands Ameliorates T Cell-Mediated Recall Responses

Next, we investigated the intriguing finding that lipoprotein-deficient *S. aureus* failed to induce immune suppression in our model (Figure 1B). As lipoproteins are sensed by different TLR2 heterodimers (Henneke et al., 2008), we have taken advantage of microbial-derived molecules, which are exclusively bound by one specific TLR2 heterodimer. We selected three lipopeptides for our studies: TLR2-6 ligands diacyl lipopeptides FSL-1 and Pam2Cys and the triacylated lipopeptide Pam3Cys that is often used as a reference compound for TLR2-1 activation. As in our previous model, lipopeptides were applied to the skin during re-exposure of FITC-sensitized mice to FITC (see protocol Fig-

ure S1A). Similarly to the living *S. aureus*, the cutaneous exposure to TLR2-6 ligand FSL-1 almost completely abrogated consecutive FITC-specific recall responses (Figures 2A and 2B), FITC-specific ex vivo T cell proliferation (Figure 2C) and orchestrated splenic reduction of $\text{CD}4^+$ and $\text{CD}8^+$ T cells together with MDSC accumulation (Figure 2D). This result was confirmed with another TLR2-6 ligand, Pam2Cys (Figures 2E–2H). In contrast to Pam2Cys, the TLR2-TLR1 ligand Pam3Cys failed to suppress FITC-specific dermatitis and T cell proliferation (Figures 2E–2G). Accordingly, no reduction of $\text{CD}4^+$ and $\text{CD}8^+$ T cells and no induction of $\text{Gr}1^+\text{CD}11\text{b}^+$ cells could be detected (Figure 2H).

These data show that cutaneous exposure to bacterial TLR2-TLR6 ligands is sufficient to cause immune suppression and that

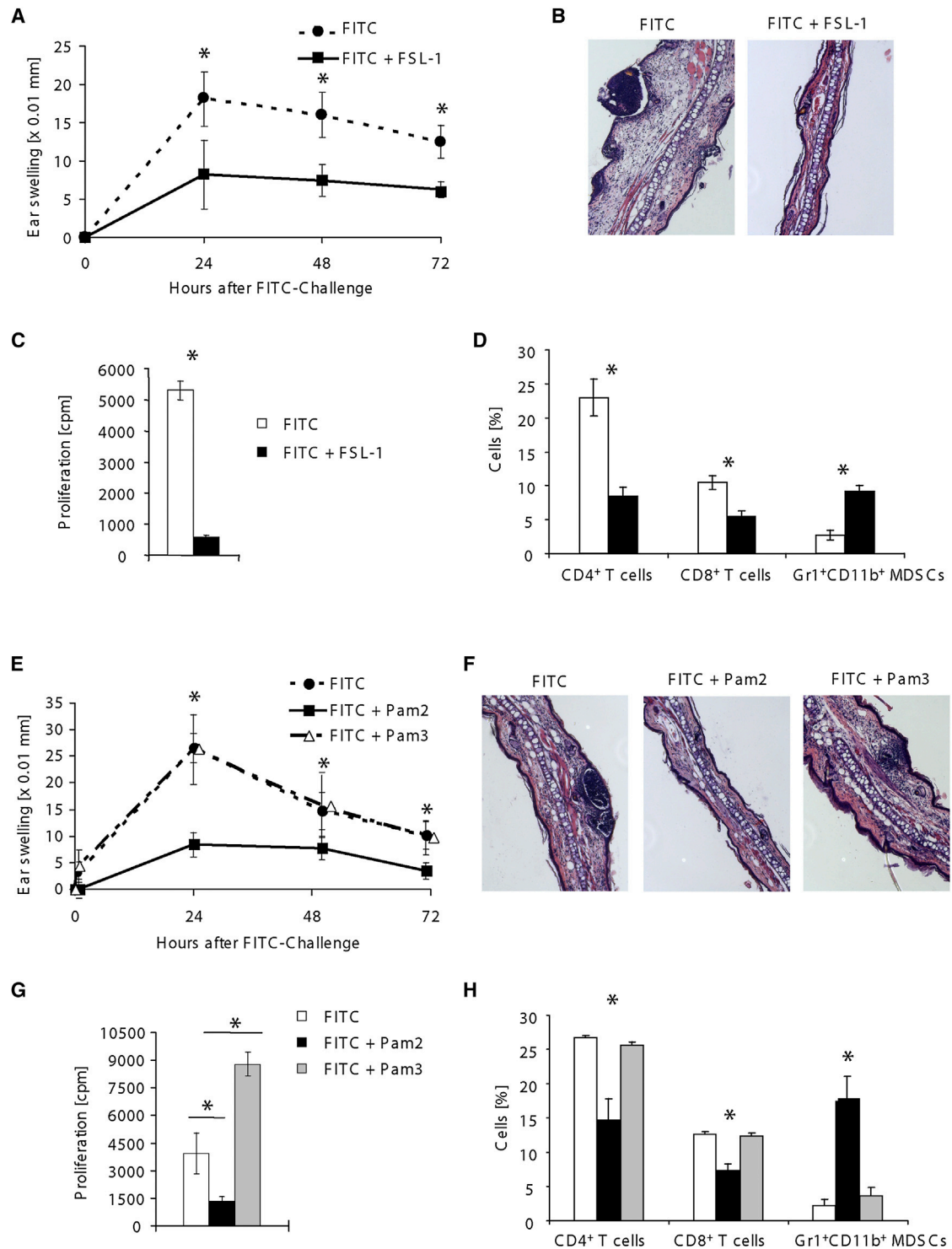


Figure 2. Cutaneous Exposure to TLR2-6 but Not TLR1 Ligands Ameliorates T Cell-Mediated Recall Responses of the Skin

WT mice were treated following the protocol shown in Figure S1A. Mice were cutaneously exposed to FSL-1 in (A)–(D) and Pam2Cys or Pam3Cys in (E)–(H). Ear swelling response (mean \pm SD, n = 5) (A and E), histology (H&E staining) (B and F), proliferation of skin-draining LN cells stimulated ex vivo with FITC (mean \pm SD of triplicates) (C and G), and the percentage of cell populations in the spleen (mean \pm SD, n = 5) (D and H) are shown. Data are representative of at least two independent experiments. Experiments shown in (A) were performed with FSL-1 from two different providers. *p < 0.05.

activation of TLR2-TLR6 heterodimers differs in regard to functional consequences from activation of TLR2-TLR1 heterodimers.

Further, in order to control whether the presentation of the antigen FITC is directly influenced by Pam2Cys exposure, we analyzed the number of FITC positive DCs 14 hr after cutaneous FITC application and Pam2Cys exposure. There were no differences in the numbers of FITC positive CD11c⁺MHC-II⁺ cells and other dendritic cell populations (dDCs, LCs) in draining lymph nodes (Figure S1G). Similarly, the analysis of other cell populations at this early stage of the response revealed comparable numbers of T cells (CD4⁺, CD8⁺), activated T cells (CD4⁺CD25⁺) and proliferating cells (Ki67⁺) (Figure S1H), IL-10 producing cells, and Treg cells (Figure S1I) in both mouse groups. The treatment of mice with cyclophosphamide for Treg cell depletion failed to reverse Pam2Cys-induced immune suppression (Figures S1J–S1L), further indicating that Treg cells are not involved in this type of immune suppression.

Skin-Infection-Induced Immune Suppression Is Mediated by Gr1⁺CD11b⁺ Myeloid-Derived Suppressor Cells

Next, as proof of concept that MDSCs are the responsible cells for the observed immune suppression upon cutaneous Pam2Cys exposure, we depleted Gr1⁺ cells. This depletion caused an abrogation of immune suppression (Figure 3A, right). Inversely, the adoptive transfer of MDSCs, isolated from mice previously exposed to Pam2Cys, resulted in reduction of both FITC-specific dermatitis and T cell proliferation (Figures 3B and 3C). To investigate whether human MDSCs in AD patients with intense cutaneous exposure to lipoproteins were suppressive, we depleted CD11b⁺ cells from PBMCs and analyzed proliferation of activated T cells. The CD11b⁺ population among PBMCs consists of antigen-presenting cells and, in addition, contains MDSCs in AD, but not healthy individuals. Consequently, in seven of eight healthy volunteers, CD11b depletion resulted in reduced T cell proliferation (Figure 3D, left). On the contrary, this was only observed in one out of 7 AD patients (Figure 3D, right). These results demonstrate that MDSCs, which are present among the CD11b⁺ population in AD patients, but not in healthy individuals, are immunosuppressive. Indeed, T cell receptor ζ -chain was significantly downregulated in AD patients (Figure 3E), which is known to be one of the major features of MDSC-mediated T cell inhibition (Zea et al., 2005).

Taken together, these data revealed that skin-infection-induced immune suppression is mediated by MDSCs.

Myeloid-Derived Suppressor Cells Are Recruited to the Skin in Mice and Humans

Detecting MDSCs in human blood and mouse spleen following cutaneous innate immune sensing indicates systemic MDSC expansion. Therefore, we next monitored the kinetics of MDSC induction in mice in (1) the bone marrow (BM), its primary source (Figure 4A, left), and (2) one site of MDSC enrichment, the spleen (Figure 4A, right) at different time points after cutaneous Pam2Cys exposure. Starting on day 2, Gr1⁺CD11b⁺ cells in the BM increased and peaked at day 7 with about 75% of cells being Gr1⁺CD11b⁺. In the spleen, both CD4⁺ and CD8⁺ T cells were strongly reduced. Gr1⁺CD11b⁺ cells increased starting at day 4

with up to 7-fold induction on day 11 following cutaneous Pam2Cys exposure (Figure 4A).

In FITC-CHS, T cells migrate to the skin and elicit dermatitis. Therefore, we analyzed whether MDSCs were also recruited to the skin. Indeed, 8 hr after FITC challenge Gr1⁺CD11b⁺ cells were significantly increased in the skin of mice previously exposed to Pam2Cys (Figure 4B). Similarly, we compared healthy skin with lesional skin from AD patients colonized or infected with *S. aureus*. Flow cytometry analysis confirmed a significant increase of MDSCs in the skin of AD patients compared to healthy skin (Figure 4C), indicating that presence of bacteria and subsequent skin inflammation induce MDSC accumulation in the skin also in humans.

Suppression of T Cell Activation by MDSCs Is Induced by Cutaneous Innate Immune Sensing

Recruitment of MDSCs to the skin suggested MDSC-mediated suppression of T cell activation in the skin in vivo. As first indication, we found that the depletion of CD11b⁺ cells of isolated skin cells caused a stronger T cell proliferation following stimulation with anti-CD3-CD28 in comparison to cells not depleted of CD11b⁺ cells (Figure S2A), confirming a suppressive function of skin MDSCs ex vivo. Moreover, flow cytometry analysis of ear skin tissue following the FITC challenge revealed a significant decrease of CD3⁺ T cells (Figure 5A, right) and IFN- γ production (Figure 5A, left) in previously Pam2Cys-exposed mice. Expression analysis of other cytokines revealed a significant decrease of the Th2 cell cytokine IL-4 (a target for a systemic AD treatment [Beck et al., 2014]), IL-10, and a tendency for IL-17 inhibition (Figure 5B). The investigation of cutaneous chemokines in the skin showed a downregulation of most analyzed chemokines (CCL2, CCL3, CCL4, CCL5, CCL11, CCL13, CCL17, CCL20, CCL27). Only T cell attracting CCL22 (a CCR4 ligand) and CCL28 (CCR3 and CCR10 ligand) were significantly upregulated (Figure 5C). The corresponding chemokine receptors were expressed on the MDSCs in the skin, blood, and bone marrow (Figure 5D), which further indicates that MDSCs are attracted to the site (and by similar mechanism) of T cell migration (Biedermann et al., 2002).

To explore the mechanisms mediating MDSC-induced immune suppression, we isolated MDSCs 10 days after Pam2Cys exposure. Flow cytometry analysis revealed the presence of both Ly6C⁺ and Ly6G⁺ MDSCs. Morphological evaluation of isolated MDSCs confirmed that Ly6G⁺ MDSC were granulocytic, whereas Ly6C⁺ MDSCs were monocytic (Figure S2B). In the skin, Gr1⁺CD11b⁺ cells were further characterized as CD11c⁻, CD15⁻, MHC-II⁻, B220-negative and positive for CD16-32 and partly positive for F4-80 (Figure S2C), and splenic Ly6C⁺ cells had a similar phenotype (Figure S2C). Next, we isolated Gr1^{dim}Ly6G⁻Ly6C⁺CD11b⁺ (Ly6C⁺) and Gr1^{hi}Ly6G⁺CD11b⁺ (Ly6G⁺) MDSCs from Pam2Cys-exposed mice and cocultured them with naive splenocytes (responder cells) activated with anti-CD3-CD28 antibodies (Abs) at different ratios. Following coculture with Ly6C⁺ MDSCs at a ratio of 2:1, almost complete suppression of T cell proliferation was observed, while Ly6G⁺ cells were not suppressive (Figure 5E, left). Investigating the suppressive activity more thoroughly revealed that Ly6C⁺ MDSCs inhibited Th0 CD4⁺ T cells, as well as Th1⁻, Th2⁻, and Th17-polarized cells (Figure S2D). MDSCs' immunosuppressive activity is reported to be a result of the activation of inducible NOS

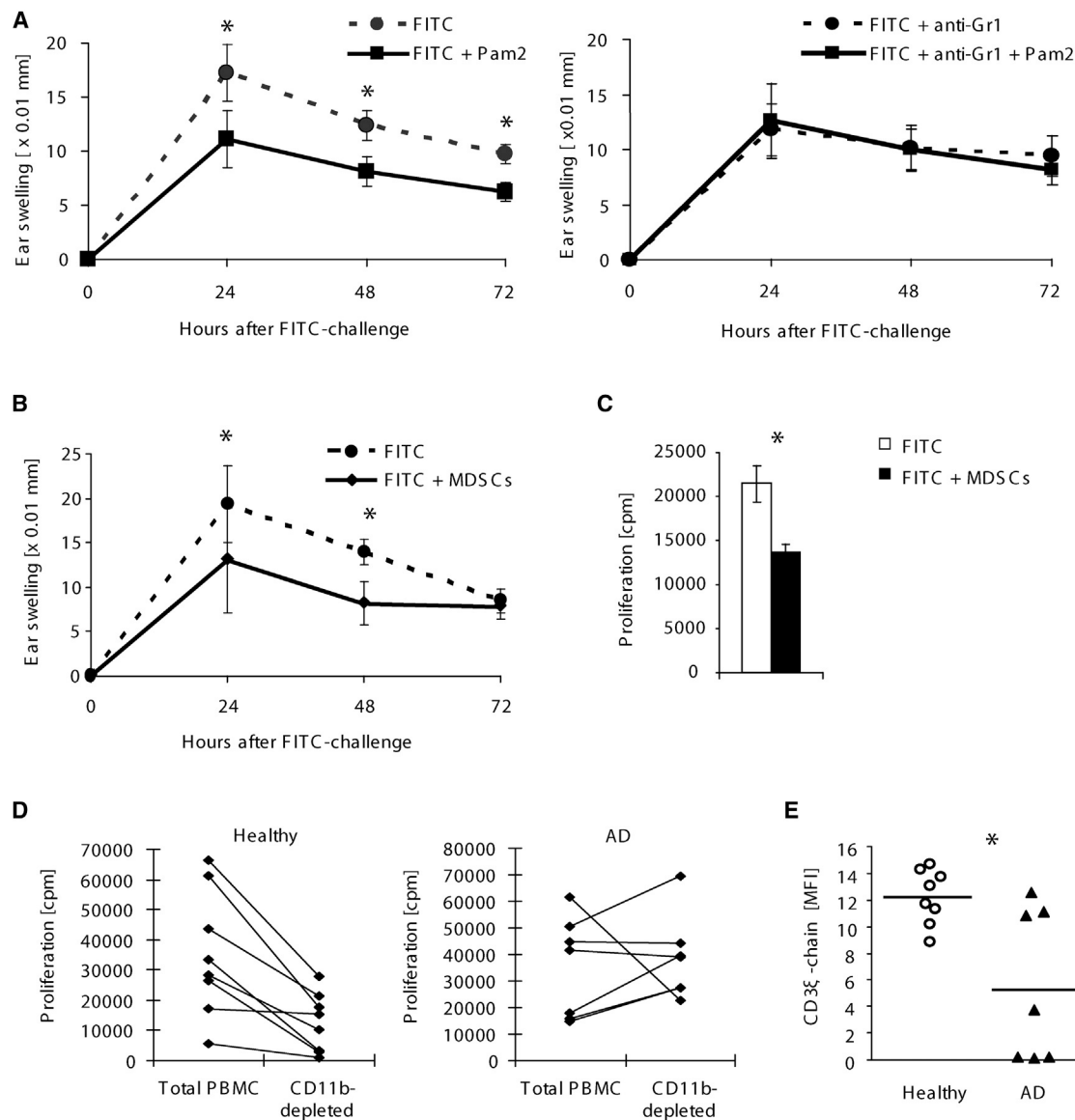


Figure 3. Myeloid-Derived Suppressor Cells Are Responsible for Skin-Infection-Induced Immune Suppression

(A) WT mice were treated with FITC with or without cutaneous Pam2Cys exposure following the protocol in Figure S1A. The mice were additionally treated with Gr1 depleting (right) or with an isotype control antibody (left) at day 2 and 4. Ear swelling response (mean \pm SD, $n = 5$, left) was evaluated. Data are representative of two independent experiments.

(B and C) WT mice were treated following the protocol shown in Figure S1A (without Pam2Cys exposure). One group of mice received Ly6C-Ly6G positive cells from donors that were sensitized with FITC and exposed to Pam2Cys. The control group received spleen cells from naive mice. The ear swelling response (mean \pm SD, $n = 5$) (B) and the FITC-specific proliferation of LN cells (as cpm, mean \pm SD of triplicates) (C) were evaluated.

(D) CD11b⁺ cells of PBMCs from healthy volunteers ($n = 8$, left) and AD patients ($n = 7$, right) were depleted, and remaining PBMCs were stimulated with anti-CD3-CD28-mAbs, and analyzed for proliferation. * $p < 0.05$ (Mann-Whitney test).

(E) PBMCs from healthy donors ($n = 8$) and AD patients ($n = 7$) were analyzed for TCR ζ -chain expression (mean fluorescence intensity [MFI], CD3⁺ gate of living cells) by intracellular flow cytometry. Each dot represents an individual value, and the horizontal bar is the group's mean. * $p < 0.05$ (Mann-Whitney test). See also Figure S2.

(iNOS), leading to increased production of nitric oxide (NO) (Gabilovich et al., 2001). Indeed, we found an increased iNOS expression in the skin after FITC challenge in Pam2Cys-exposed mice (Figure S2E), and Ly6C⁺ MDSCs from Pam2Cys-exposed animals produced high concentration of NO (Figure 5E, middle). NO production and T cell suppression by Ly6C⁺ MDSCs was

completely abrogated in a transwell experiment (Figure 5E middle, Figure S2F), indicating that MDSC activation is a prerequisite for MDSC NO production and MDSC-mediated suppression. Flow cytometry analysis of the coculture confirmed higher expression of iNOS by Ly6C⁺ cells (with a very low expression of arginase and IL-10 by both MDSC subsets) (Figure S2G). In

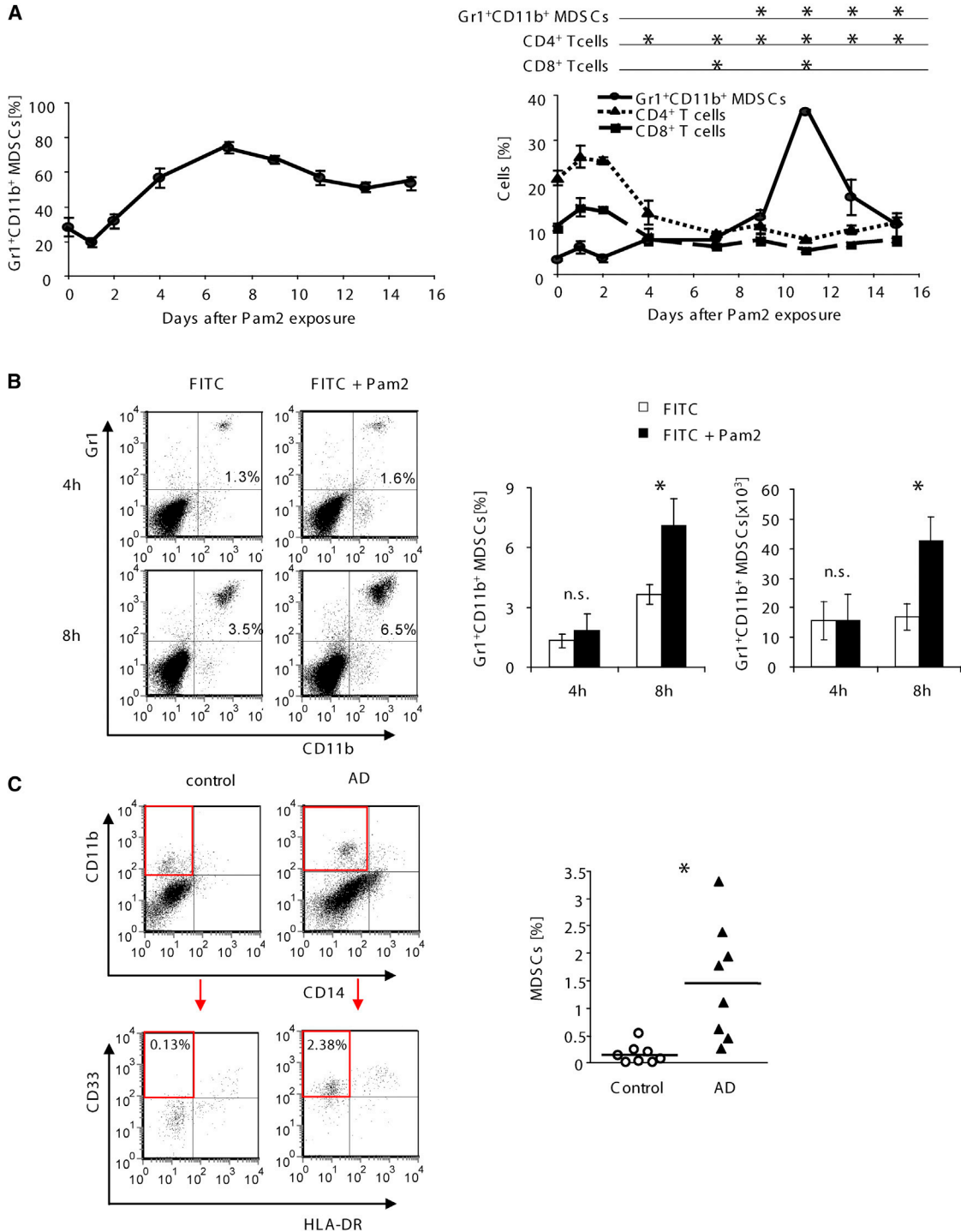


Figure 4. Skin Infection-Induced MDSCs Accumulate in the Skin in Mice and Humans

(A) WT mice were treated following the protocol in [Figure S1A](#). The percentage of CD4⁺, CD8⁺, or Gr1⁺CD11b⁺ cells in Pam2Cys-exposed mice were analyzed by flow cytometry at indicated time points after Pam2Cys exposure in BM (left) and spleen (right) (mean \pm SD, n = 3). Asterisks show significant differences compared with t = 0 determined by one-way ANOVA followed by Dunnett's post test. *p < 0.05. Data are representative of two independent experiments.

(B) Cells from ear skin, isolated 4 hr or 8 hr after FITC challenge, were analyzed by flow cytometry (gate: living cells). A representative flow cytometry plot (left), means \pm SD (n = 5) (middle), and total numbers of Gr1⁺CD11b⁺ cells (mean \pm SD, n = 5) (right) are shown. Data are representative of three independent experiments.

(C) Cells isolated from skin samples of AD patients (n = 9) and non-AD-controls (n = 9) were analyzed by flow cytometry (gate: living cells) for MDSCs, defined as CD11b⁺CD33⁺HLA-DR⁻CD14⁻ cells. A representative flow cytometry plot with the gating strategy first for CD11b⁺CD14⁻ (top) and then CD33⁺HLA-DR⁻ (bottom) and the percentage of the CD11b⁺CD33⁺HLA-DR⁻CD14⁻ cells (left) and cumulative analysis (right) are shown. Each of the dots represents an individual value and the horizontal bar the group's mean. *p < 0.05 (Mann-Whitney test). n.s., not significant.

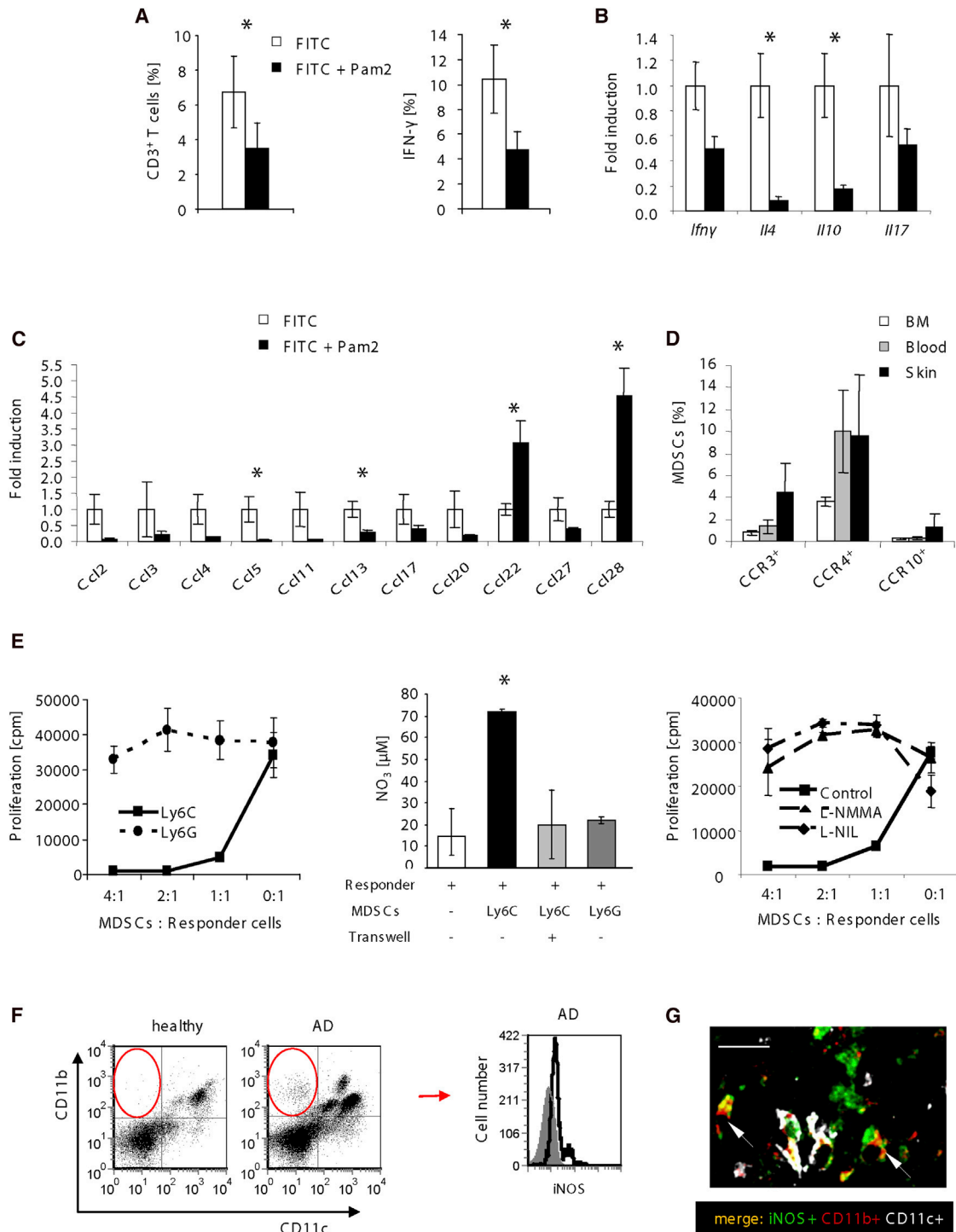


Figure 5. Skin Infection-Induced MDSCs Suppress T Cell Activation through Mechanisms Requiring NO Production

(A) WT mice were treated following the protocol in Figure S1A. 24 hr (A and B) or 8 hr (C and D) after FITC challenge ear tissue cells were analyzed. (A) Flow cytometry for CD3⁺ cells (left) and IFN-γ production (right). A cumulative result (means ± SD, n = 5) is shown.

(B and C) Quantitative RT-PCR analysis for cytokines (B) or chemokines (C) (normalized to housekeeping genes *Actb-Gapdh*) and means ± SEM (n = 5) are shown. Expression of the skin of FITC only-exposed mice was set as 1. *p < 0.05.

(D) Cells isolated from BM, blood, and skin of Pam2Cys-treated mice were analyzed for chemokine receptor expression by flow cytometry (gate: Gr1⁺CD11b⁺ of living cells), shown as percentage of Gr1⁺CD11b⁺ (means ± SD, n = 5).

(E) Spleen cells were cocultured in vitro with Ly6C⁺ or Ly6G⁺ MDSCs as indicated, stimulated by anti-CD3-CD28-mAbs and analyzed for proliferation (left); supernatants (ratio 2:1) were analyzed for NO production by Griess reaction (mean ± SD of experimental triplicates) (middle), and iNOS inhibitors L-NMMA and

(legend continued on next page)

addition, the inhibition of iNOS by L-NMMA or L-NIL completely abrogated MDSC-mediated suppression of T cell proliferation (Figure 5E, right). Similarly, in PBMCs of AD patients we detected a distinct iNOS⁺ population of CD11b⁺CD11c⁻ cells. These cells were completely absent in healthy individuals (Figure 5F). Importantly, we also detected iNOS⁺CD11b⁺CD11c⁻ cells in AD skin (Figure 5G, Figure S2H).

All together, the above results indicate that skin-infection-induced MDSCs are present in the skin in mice and humans, where they inhibit T cell proliferation by means of cell-to-cell contact and iNOS.

Pam2Cys-Induced Immune Suppression Is Dependent on Cutaneous TLR2

Next, we investigated underlying mechanisms how innate immune sensing in the skin initiates MDSCs. Therefore we determined the role of TLR2. *Tlr2*^{-/-} and WT mice were treated as shown in Figure S1A with or without cutaneous Pam2Cys exposure. In contrast to WT mice (Figure 6A, left), *Tlr2*^{-/-} mice failed to inhibit FITC-specific CHS (Figure 6A right) and T cell proliferation (Figure 6B), and no reduction of CD4⁺ and CD8⁺ T cell numbers and accumulation of MDSCs (Figure 6C) was observed following Pam2Cys exposure. Cutaneous innate immune sensing through TLR2 might act through skin resident cells or recruited circulating blood immune cells. Thus, mouse chimeras were generated to distinguish between TLR2 sensing of skin resident or recruited hematopoietic cells, as depicted in Figure S3A. Chimerism was confirmed by PCR of BM cells (Figure S3B). The percentage of MDSCs was analyzed following the protocol shown in Figure S1A. WT mice, reconstituted with WT BM cells (WT + WT-BM) and WT mice, reconstituted with *Tlr2*^{-/-} BM cells (WT + *Tlr2*^{-/-}-BM), upregulated MDSCs following Pam2Cys exposure (Figure 6D, top). In contrast, *Tlr2*^{-/-} mice reconstituted with WT BM (*Tlr2*^{-/-} + WT-BM) failed to accumulate MDSCs, similar to control *Tlr2*^{-/-} mice with *Tlr2*^{-/-} BM (*Tlr2*^{-/-} + *Tlr2*^{-/-}-BM) (Figure 6D, bottom). Thus, TLR2 expression on skin-resident cells, which next to keratinocytes includes radiation-resistant skin-resident Langerhans or mast cells, is necessary and sufficient for MDSC accumulation.

Next, we investigated a functional role of TLR2 on MDSCs. Chimeric mice were generated by reconstitution with 50% CD45.1 WT and 50% CD45.2-*Tlr2*^{-/-} BM (Figure S3C). Following Pam2Cys exposure, approximately 20% of spleen cells were MDSCs irrespective whether WT CD45.1 or *Tlr2*^{-/-} CD45.2 cells were analyzed (Figure S3D), demonstrating that TLR2 is dispensable on MDSC precursor cells for MDSC induction and accumulation.

Cutaneous IL-6 Is Critically Required for MDSC Induction

Our previous experiments showed that cutaneous Pam2Cys sensing through TLR2 is sufficient to induce MDSCs and

consecutive suppression of cutaneous recall responses. To identify underlying mechanisms, we first analyzed which cells in the skin could be responsible for sensing Pam2Cys. Immunofluorescence staining of TLRs after exposure of mice to Pam2Cys or Pam3Cys showed an upregulation of the corresponding TLR on keratinocytes (Figure 7A). Similar analyses of human skin samples showed pronounced TLR2 expression in human skin albeit at lower amount in AD compared to healthy skin (Figure S4A), as known from other studies (Kuo et al., 2013). Next, we analyzed the functional consequences of the TLR upregulation. We exposed mice to different TLR ligands (Pam2Cys, Pam3Cys, CpG, and LPS) and analyzed cutaneous mRNA expression of cutaneous cytokines. All TLR ligands moderately upregulated *Tnf* and the chemokine *Cxcl2* was most dominantly induced by Pam2Cys and Pam3Cys (Figure 7B). Upregulation of *Il6* mRNA in the skin was most pronounced only after Pam2Cys exposure. In comparison to skin following FITC-only or FITC-plus-other TLR-ligands exposure, cutaneous Pam2Cys exposure induced a 400-fold upregulation of *Il6* mRNA (Figure 7B, right). On the protein level, we detected increased IL-6 production by CD45 negative cells (which were also MHC-II negative, Figure S4B) (Figure 7C). To confirm these data, we stimulated primary human keratinocytes with TLR ligands and detected upregulation of IL-6 production exclusively following Pam2Cys treatment (Figure 7D).

To regulate MDSC induction in the bone marrow (Figure 4A), cutaneous IL-6 needs to reach the bloodstream (Chalmin et al., 2010). Indeed, IL-6 concentrations in mouse sera strongly increased 1 day after cutaneous Pam2Cys exposure (Figure 7E). These data suggest that IL-6 plays a crucial role in Pam2Cys-induced MDSC induction; therefore, *Il6*^{-/-} mice were investigated. In contrast to WT mice, cutaneous Pam2Cys exposure in *Il6*^{-/-} mice failed to suppress FITC-CHS (Figure 7F), and no induction of MDSCs could be detected (Figure 7G). Consequently, the injection of IL-6 into the mice caused an increase of MDSCs in the spleen (Figures S4C and S4D), suggesting that IL-6 is responsible for MDSC induction and expansion. To investigate whether IL-6 plays a role in MDSC migration to the skin, we applied anti-IL-6 antibody shortly before challenge and analyzed MDSC numbers in the skin. We found a significant and unequivocal increase of Gr1⁺CD11b⁺ cells in both conditions (Figure S4E), and the adoptive transfer of MDSCs into *Il6*^{-/-} mice showed a suppression of immune responses, comparable to what is observed in WT mice (Figure S4F). To investigate whether IL-6 plays a role for MDSC development, we analyzed MDSCs generation in vitro. BM-derived MDSCs (see Supplemental Experimental Procedures) were treated with IL-6 during development, and their suppressive function was investigated in a suppression assay with responder cells. As shown in Figure 7H, the exposure of MDSCs to IL-6 during generation enhanced their suppressive

L-NIL were added to the coculture (right). Significant differences between experimental conditions were assessed by one-way ANOVA followed by Tukey's post-hoc test (*p < 0.05). Data are representative of at least two independent experiments.

(F) PBMCs from healthy donors and AD patients were analyzed by intracellular flow cytometry (iNOS⁺ in CD11b⁺CD11c⁻ Gate of living cells). A representative result out of seven individuals is shown.

(G) Skin tissue of AD patients was analyzed by immunofluorescence. Arrows indicate cells positive for CD11b and iNOS and negative for CD11c. Scale bar represents 25 μ m. See also Figure S2.

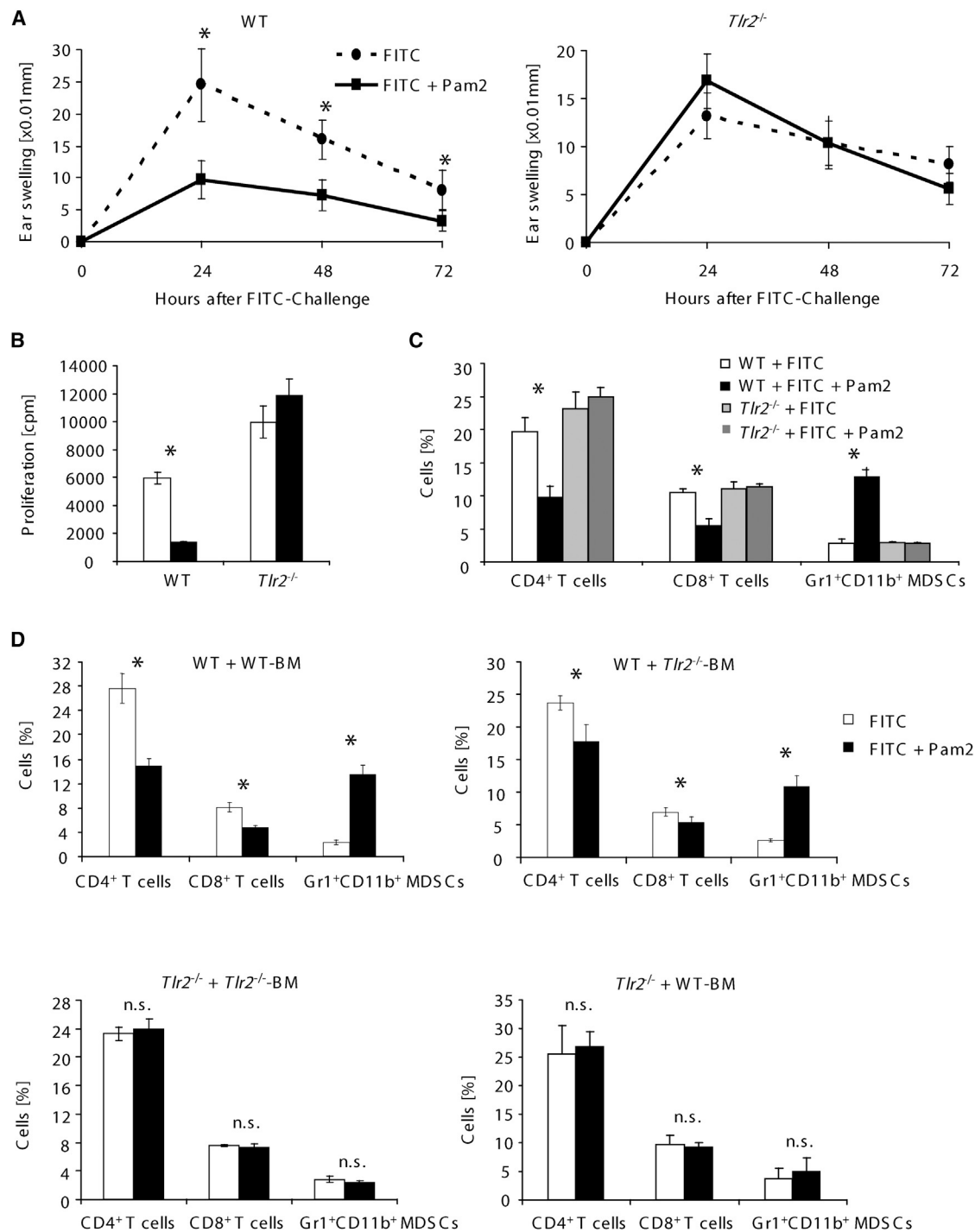


Figure 6. Pam2Cys-Induced Immune Suppression Is Dependent on TLR2

(A–C) WT and *Tlr2^{-/-}* mice were treated following the protocol shown in Figure S1A and ear swelling (mean \pm SD, n = 5) after FITC challenge (A), proliferation of lymph node cells after FITC stimulation ex vivo (mean \pm SD of triplicates) (B), and the percentage of spleen cell populations (mean \pm SD, n = 5) (C) were analyzed. (D) WT or *Tlr2^{-/-}* mice were irradiated and reconstituted with WT or *Tlr2^{-/-}* BM cells (see Figure S3A). Seven weeks later, the chimeric mice were treated following the protocol shown in Figure S1A and their spleen cells were analyzed by flow cytometry. The percentage of Gr1⁺CD11b⁺ cells is shown (mean \pm SD, n = 5). Data are representative of three independent experiments. *p < 0.05, n.s., not significant. See also Figure S3.

function. These data indicate that IL-6 supports induction and development of suppressive MDSCs, but not their migration to the skin.

Taken together, these data suggest a scenario in which Pam2Cys is sensed by TLR2 on skin resident cells, leading to the expression and secretion of IL-6 in such high amounts that

MDSCs expand and accumulate, leading to the inhibition of cutaneous recall responses.

DISCUSSION

In this study, we found that cutaneous exposure to bacteria and bacterial substances known to act as potent MAMPs induced a strong immune suppression mediated by MDSCs. These findings highlight that certain classes of bacterial molecules are able to orchestrate unique pathways that, even after limited cutaneous exposure, are sufficient to induce immune suppression. We found that cutaneous exposure to TLR2-TLR6 but not to TLR2-TLR1 ligands induced MDSCs and consecutive cutaneous immune suppression. Bacteria differ in the acylation patterns of their lipoproteins (Kurokawa et al., 2012b). Our results suggest that they might differ in their potential to activate different TLR2 heterodimers and to regulate immune responses as well. Consequently, acylation properties might characterize bacteria as pathogens or commensals. It was shown recently that the degree of lipoprotein-acylation depends on environmental factors and growth phase. Lipoprotein SitC was triacylated when *S. aureus* was in the exponential growth phase at neutral pH and diacylated in the postexponential phase at low pH (Kurokawa et al., 2012a). At the situation on the skin, where pH is low and chronic *S. aureus* colonization (which is almost always found in AD) is present, a postexponential growth phase of *S. aureus* can be assumed. Consequently, lipoproteins from *S. aureus* on the skin are more diacylated. On the basis of our data and also own recently published data (Kaesler et al., 2014), we hypothesize that diacylation of lipoproteins induces acute inflammation followed by immune suppression as a consequence. Further, one can also assume that pathogenic and nonpathogenic skin microflora might have different acylation properties and therefore different compositions of TLR2 ligands and thus overall differ in regard to their immune consequences.

Previous data obtained using a systemic sepsis model with Gram-negative bacteria derived from the gut described the MyD88 and TLR4 pathway to be most relevant for MDSC expansion (Delano et al., 2007). However, the exact cascade of events was not investigated (Arora et al., 2010; Delano et al., 2007). Our data investigating the common route of cutaneous infection with Gram-positive bacteria show that TLR2 activation on skin-resident cells mediates MDSC accumulation and consecutive immune suppression. Induction of MDSCs by activation of cutaneous TLR2-6 most dominantly involves IL-6. Cutaneous innate immune cells (Blander and Medzhitov, 2004), keratinocytes, and even melanocytes (Stadnyk, 1994; Takashima and Bergstresser, 1996) are all capable of producing innate cytokines, such as IL-6. Indeed, in AD, where keratinocytes act as a critical first line of defense against microbes, early IL-6 production has been described after direct contact of keratinocytes with *S. aureus* (Sasaki et al., 2003). Moreover, IL-6 has been found to be increased in AD skin (Fedenko et al., 2011) and especially in AD skin lesions (Travers et al., 2010), in which the amount of IL-6 correlates with bacterial burden (Travers et al., 2010). Genome-wide association studies recently also identified an IL-6 receptor (IL-6R) variant as a risk factor for AD (Esparza-Gordillo et al., 2013) and a small case series with three patients has

demonstrated therapeutic efficacy of an IL-6R blockade by tocilizumab, an IL-6R antibody (Navarini et al., 2011). These observations confirm the importance of IL-6 production by skin cells in response to microbes; however, the precise immune consequences of cutaneous IL-6 induction had not been elucidated. Our data allow us to propose a model of how the cutaneous innate immune network functions: diacylated lipopeptides activate TLR2-TLR6 on skin resident cells followed by marked IL-6 production leading to the MDSC accumulation, which is a prerequisite of subsequent immune suppression by MDSCs. Our data also indicate that these TLR2-6-induced MDSCs are prototypic MDSCs as characterized in other settings. Moreover, our data have further identified that skin-infection-induced MDSCs suppressed immune responses in mice and humans.

In conclusion, our study reveals a consequence of cutaneous innate immune sensing for adaptive immune functions. The presence of certain lipoproteins on the skin might serve not only as danger signal for the initiation of effective immune responses but also might be able to counterregulate inflammation and potentially control and suppress immune responses.

EXPERIMENTAL PROCEDURES

Animals

Specific-pathogen-free, WT BALB/c mice were purchased from Charles River. *Tlr2*^{-/-} mice (C57BL/6) were from C. Kirschning (Institute of Medical Microbiology, University Duisburg-Essen) and were backcrossed to BALB/c for ten generations. *Ilg6*^{-/-}-BALB/c mice were from Dr. M. Kopf (Swiss Federal Institute of Technology). All mice were kept under specific pathogen-free conditions in accordance with FELASA (Federation of European Laboratory Science Association) in the University of Tübingen. The experiments were performed with the approval of the local authorities (Regierungspräsidium Tübingen HT1/10, HT3/11, HT7/11, HT5/13, HT8/13). Age-matched female mice were used in all experiments.

Epicutaneous Mouse Skin Infection Model

The experimental model is based on epicutaneous application of the *S. aureus* on shaved skin of mice (Wanke et al., 2013). Mice were sensitized with FITC following the protocol as shown in Figure S1A. At days 7 and 10 3×10^8 WT or *Igt* mutant *S. aureus* Newman in 30 μ l PBS or PBS control were added to filter paper discs placed onto the prepared skin and covered by Finn Chambers on Scanpor (Smart Practice). Before application to the skin, barrier was disrupted by tape stripping.

FITC Contact Hypersensitivity and Exposure to TLR2 Ligands

Mice were sensitized by administration of 80 μ l of a 0.37% FITC solution (dissolved in 1:1 acetone:dibutyl phthalate, Sigma Aldrich) on the shaved abdomen on days -8 and -7. TLR2 ligands were applied intracutaneously together with the second epicutaneous application of FITC on days -1 and 0 (Figure S1A) in the following concentrations per mouse: Pam2Cys, 2 μ g; Pam3Cys, 4 μ g; FSL-1, 40 μ g. Control mice obtained PBS instead of TLR2 ligands. At day 7, mice were challenged by epicutaneous application of 0.37% FITC solution on both sides of the ears. Ear thickness was measured with a micrometer (Oditest) as previously described (Volz et al., 2014), and data are expressed as change in ear thickness compared to thickness before treatment. In some experiments, mice were treated with 0.3 μ M CpG 1668 (0.2 μ M, Eurofins Genomics), 1 μ g/mouse LPS (from Salmonella minnesota R595, Alexis Biochemicals), cyclophosphamide (2 mg/mouse, Sigma-Aldrich), 20 μ g/mouse rIL-6 (20 μ g/mouse) or 50 μ g/mouse anti-IL-6 (BioLegend).

Human MDSCs

The study was approved by the local ethics committee of the University of Tübingen, Germany, and written informed consent was obtained from all

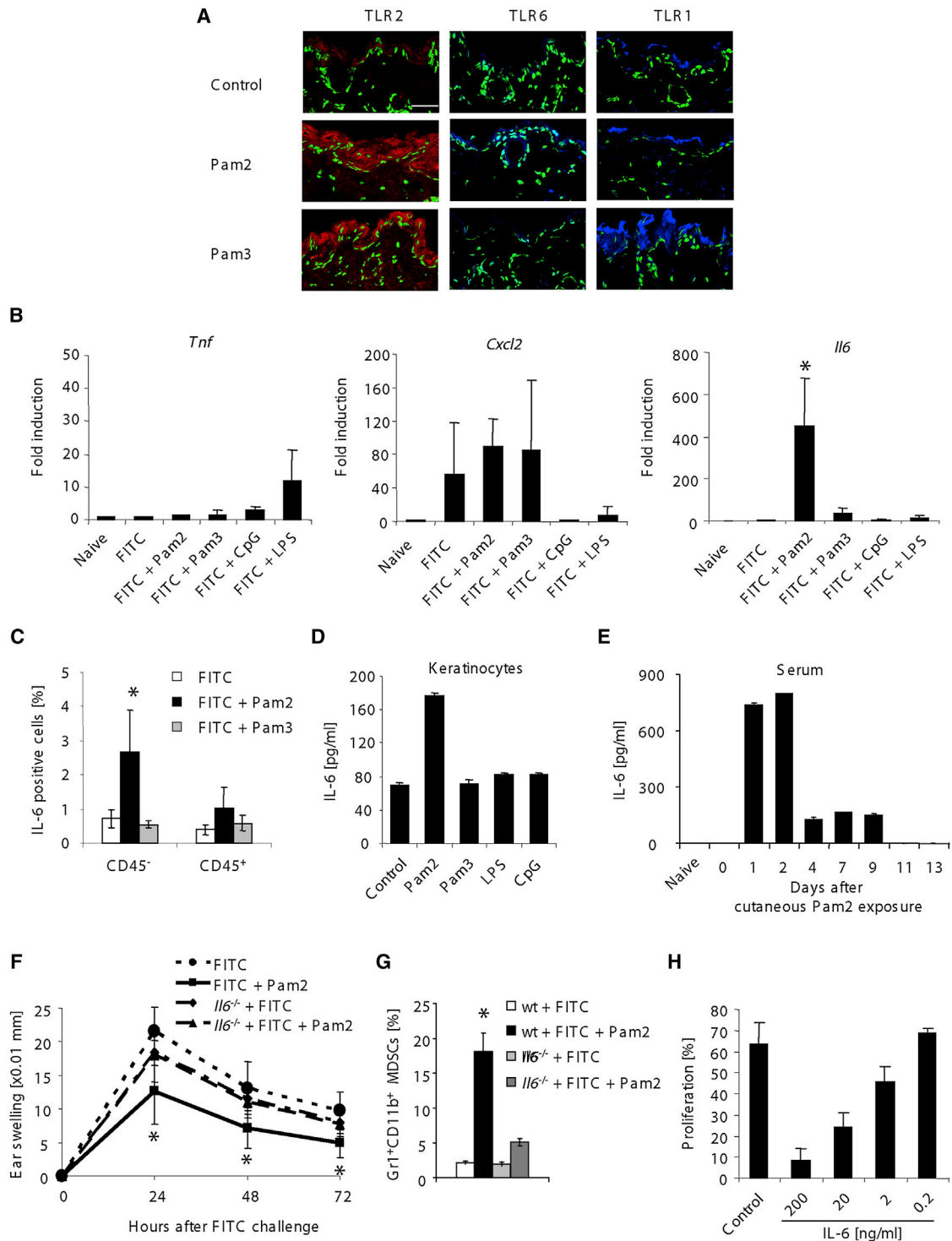


Figure 7. IL-6 Is Required for Induction of Gr1⁺CD11b⁺ Cells and Pam2Cys-Induced Immune Suppression

(A–C) WT mice were treated following a protocol similar to that shown in Figure S1A. 24 hr after cutaneous exposure to TLR ligands or PBS (control), immunofluorescence for TLR2 (red), TLR6 or TLR1 (blue), and nuclei (green) was done in (A), a representative picture (n = 3) is shown. Scale bar represents 30 μm (B). The skin was evaluated for the expression of *Tnf*, *Cxcl2*, and *Il6* mRNA by quantitative RT-PCR analysis (normalized to housekeeping gene *Actb*). Expression in the skin of untreated mice (naive) was set as 1 (mean ± SD, n = 5). (C) Skin cells were isolated and analyzed for IL-6 production by intracellular flow cytometry, and a cumulative analysis (mean ± SD, n = 5) is shown.

(D) Primary human keratinocytes were isolated and treated with TLR ligands for 24 hr, and the production of IL-6 was measured by ELISA (mean ± SD of triplicates).

(legend continued on next page)

subjects (project number 344/2011BO2, 345/2011BO2, 396/2011BO2, 040/2013BO2, 180/2013BO2). PBMCs were obtained from heparinized blood by centrifugation (800 g for 30 min) using Ficoll-Histopaque (Biochrom). MDSCs in the blood or skin of either healthy volunteers or non-AD-controls or atopic dermatitis patients were analyzed by flow cytometry and characterized as CD11b⁺CD33⁺HLA-DR⁻CD14⁻ cells.

Bone-Marrow Chimeras

Recipient mice were lethally irradiated at 7.0 cGy and on the next day BM cells (10⁶ cells per recipient) were intravenously injected into recipient mice. To confirm the chimerism of mice, we conducted genotyping of BM cells by PCR for the WT and the mutated *Tlr2* gene (Figure S3B).

Depletion of CD11b⁺ Cells

CD11b⁺ cells were depleted from PBMCs using the CD11b⁺ Beads (Miltenyi Biotech) according to the manufacturer's protocol.

Statistical Analysis

Unless otherwise stated, quantitative results are expressed as means ± SD and differences were compared by unpaired, two-tailed Student's *t* test (*p* < 0.05 was regarded as significant).

SUPPLEMENTAL INFORMATION

Supplemental Information includes four figures and Supplemental Experimental Procedures and can be found with this article online at <http://dx.doi.org/10.1016/j.immuni.2014.10.009>.

AUTHOR CONTRIBUTIONS

T.B. and Y.S. designed the study, analyzed the data, and wrote the manuscript; Y.S. performed the experiments; C.G. performed histological staining of human samples; F.W., E.G., and T.V. cooperated in regard to human samples and participated in the manuscript preparation; M.K. assisted with data analysis and bacteria preparation; D.D. and F.G. provided WT and Δ *igt* *S. aureus*; S.K., M.S., H.-G.R., and M.R. contributed to project development by fruitful discussions; K.-M.C., W.E.K., D.D., and F.G. participated in the manuscript preparation.

ACKNOWLEDGMENTS

We acknowledge the expert technical assistance of N. Zimmermann (Technical University Dresden), C. Grimmel (FACS core facility, Tübingen), and B. Fehrenbacher (electron microscopy laboratory, Tübingen). We thank F. Eberle, K. Ghor-eschi, C. Hünefeld, K. Belge, and S. Volc for cooperating in regard to the human samples. We appreciate B. Kraft, I. Wanke, J. Holstein, I. Kumbier, and C. Braunsdorf for the help with the keratinocyte culture. M. Kopf (Swiss Federal Institute of Technology, Switzerland) provided *Il6*^{-/-} BALB/c mice, and C. Kirschning (Institute of Medical Microbiology, University Duisburg-Essen) provided *Tlr2*^{-/-} mice. This work was supported by grants from the Baden-Württemberg Stiftung (P-LS-AL2/4 and P-BWS-Glyko/21), the Deutsche Forschungsgemeinschaft (DFG; BI 696/10-1, GU 1271/2-1 and GO 371/9-1, DFG Priority Program 1394 BI 696/5-1, 5-2, KFO 249/GU1212/1-1, and SFB 685; A6) and a MEDDRIVE-grant from the faculty of Medicine, Technical University Dresden.

Received: March 21, 2014

Accepted: October 17, 2014

Published: November 13, 2014

REFERENCES

- Arora, M., Poe, S.L., Oriss, T.B., Krishnamoorthy, N., Yarlagadda, M., Wenzel, S.E., Billiri, T.R., Ray, A., and Ray, P. (2010). TLR4/MyD88-induced CD11b+Gr-1 int F4/80+ non-migratory myeloid cells suppress Th2 effector function in the lung. *Mucosal Immunol.* 3, 578–593.
- Beck, L.A., Boguniewicz, M., Hata, T., Schneider, L.C., Hanifin, J., Gallo, R., Paller, A.S., Lieff, S., Reese, J., Zaccaro, D., et al. (2009). Phenotype of atopic dermatitis subjects with a history of eczema herpeticum. *J. Allergy Clin. Immunol.* 124, 260–269, 269 e261–267.
- Beck, L.A., Thaçi, D., Hamilton, J.D., Graham, N.M., Bieber, T., Rocklin, R., Ming, J.E., Ren, H., Kao, R., Simpson, E., et al. (2014). Dupilumab treatment in adults with moderate-to-severe atopic dermatitis. *N. Engl. J. Med.* 371, 130–139.
- Biedermann, T. (2006). Dissecting the role of infections in atopic dermatitis. *Acta Derm. Venereol.* 86, 99–109.
- Biedermann, T., Schwarzler, C., Lametschwandner, G., Thoma, G., Carballido-Perrig, N., Kund, J., de Vries, J.E., Rot, A., and Carballido, J.M. (2002). Targeting CLA/E-selectin interactions prevents CCR4-mediated recruitment of human Th2 memory cells to human skin in vivo. *Eur. J. Immunol.* 32, 3171–3180.
- Blander, J.M., and Medzhitov, R. (2004). Regulation of phagosome maturation by signals from toll-like receptors. *Science* 304, 1014–1018.
- Bronte, V. (2009). Myeloid-derived suppressor cells in inflammation: uncovering cell subsets with enhanced immunosuppressive functions. *Eur. J. Immunol.* 39, 2670–2672.
- Bunt, S.K., Yang, L., Sinha, P., Clements, V.K., Leips, J., and Ostrand-Rosenberg, S. (2007). Reduced inflammation in the tumor microenvironment delays the accumulation of myeloid-derived suppressor cells and limits tumor progression. *Cancer Res.* 67, 10019–10026.
- Buwitt-Beckmann, U., Heine, H., Wiesmüller, K.H., Jung, G., Brock, R., Akira, S., and Ulmer, A.J. (2006). TLR1- and TLR6-independent recognition of bacterial lipopeptides. *J. Biol. Chem.* 281, 9049–9057.
- Chalmin, F., Ladoire, S., Mignot, G., Vincent, J., Bruchard, M., Remy-Martin, J.P., Boireau, W., Rouleau, A., Simon, B., Lanneau, D., et al. (2010). Membrane-associated Hsp72 from tumor-derived exosomes mediates STAT3-dependent immunosuppressive function of mouse and human myeloid-derived suppressor cells. *J. Clin. Invest.* 120, 457–471.
- Delano, M.J., Scumpia, P.O., Weinstein, J.S., Coco, D., Nagaraj, S., Kelly-Scumpia, K.M., O'Malley, K.A., Wynn, J.L., Antonenko, S., Al-Quran, S.Z., et al. (2007). MyD88-dependent expansion of an immature GR-1(+)CD11b(+) population induces T cell suppression and Th2 polarization in sepsis. *J. Exp. Med.* 204, 1463–1474.
- Esparza-Gordillo, J., Schaarschmidt, H., Liang, L., Cookson, W., Bauerfeind, A., Lee-Kirsch, M.A., Nemat, K., Henderson, J., Paternoster, L., Harper, J.I., et al. (2013). A functional IL-6 receptor (IL6R) variant is a risk factor for persistent atopic dermatitis. *J. Allergy Clin. Immunol.* 132, 371–377.
- Fedenko, E.S., Elisyutina, O.G., Filimonova, T.M., Boldyreva, M.N., Burmenskaya, O.V., Rebrova, O.Y., Yarin, A.A., and Khaitov, R.M. (2011). Cytokine gene expression in the skin and peripheral blood of atopic dermatitis patients and healthy individuals. *Self Nonself* 2, 120–124.
- Gabrilovich, D.I., and Nagaraj, S. (2009). Myeloid-derived suppressor cells as regulators of the immune system. *Nat. Rev. Immunol.* 9, 162–174.
- Gabrilovich, D.I., Velders, M.P., Sotomayor, E.M., and Kast, W.M. (2001). Mechanism of immune dysfunction in cancer mediated by immature Gr-1+ myeloid cells. *J. Immunol.* 166, 5398–5406.

(E) WT mice were treated following a protocol similar to that shown in Figure S1A, and IL-6 concentrations in the sera were analyzed by ELISA (mean ± SD of triplicates).

(F and G) WT and *Il6*^{-/-} mice were treated following the protocol shown in Figure S1A and ear swelling (mean ± SD, n = 5) (F) and the percentage (mean ± SD, n = 5) of Gr1⁺CD11b⁺ cells (G) were analyzed.

(H) BM-derived MDSCs were treated with IL-6 (in indicated concentrations) during generation and their suppressive activity was measured in a coculture with activated spleen cells (responder cells) in ratio 1:4. Proliferation of responder cells without MDSCs was set as 100%. Data are representative of two independent experiments. **p* < 0.05. See also Figure S4.

- Hajjar, A.M., O'Mahony, D.S., Ozinsky, A., Underhill, D.M., Aderem, A., Klebanoff, S.J., and Wilson, C.B. (2001). Cutting edge: functional interactions between toll-like receptor (TLR) 2 and TLR1 or TLR6 in response to phenol-soluble modulin. *J. Immunol.* **166**, 15–19.
- Henneke, P., Dramsi, S., Mancuso, G., Chraïbi, K., Pellegrini, E., Theilacker, C., Hübner, J., Santos-Sierra, S., Teti, G., Golenbock, D.T., et al. (2008). Lipoproteins are critical TLR2 activating toxins in group B streptococcal sepsis. *J. Immunol.* **180**, 6149–6158.
- Hoetzenecker, W., Echtenacher, B., Guenova, E., Hoetzenecker, K., Woelbing, F., Brück, J., Teske, A., Valtcheva, N., Fuchs, K., Kneilling, M., et al. (2012). ROS-induced ATF3 causes susceptibility to secondary infections during sepsis-associated immunosuppression. *Nat. Med.* **18**, 128–134.
- Jin, M.S., Kim, S.E., Heo, J.Y., Lee, M.E., Kim, H.M., Paik, S.G., Lee, H., and Lee, J.O. (2007). Crystal structure of the TLR1-TLR2 heterodimer induced by binding of a tri-acylated lipopeptide. *Cell* **130**, 1071–1082.
- Kaesler, S., Volz, T., Skabytska, Y., Koberle, M., Hein, U., Chen, K.M., Guenova, E., Woelbing, F., Rocken, M., and Biedermann, T. (2014). Toll-like receptor 2 ligands promote chronic atopic dermatitis through IL-4-mediated suppression of IL-10. *J. Allergy Clin. Immunol.* **134**, 92–99.
- Kang, J.Y., Nan, X., Jin, M.S., Youn, S.J., Ryu, Y.H., Mah, S., Han, S.H., Lee, H., Paik, S.G., and Lee, J.O. (2009). Recognition of lipopeptide patterns by Toll-like receptor 2-Toll-like receptor 6 heterodimer. *Immunity* **31**, 873–884.
- Kawai, T., and Akira, S. (2010). The role of pattern-recognition receptors in innate immunity: update on Toll-like receptors. *Nat. Immunol.* **11**, 373–384.
- Kuo, I.H., Carpenter-Mendini, A., Yoshida, T., McGirt, L.Y., Ivanov, A.I., Barnes, K.C., Gallo, R.L., Borkowski, A.W., Yamasaki, K., Leung, D.Y., et al. (2013). Activation of epidermal toll-like receptor 2 enhances tight junction function: implications for atopic dermatitis and skin barrier repair. *J. Invest. Dermatol.* **133**, 988–998.
- Kupper, T.S., and Fuhlbrigge, R.C. (2004). Immune surveillance in the skin: mechanisms and clinical consequences. *Nat. Rev. Immunol.* **4**, 211–222.
- Kurokawa, K., Kim, M.S., Ichikawa, R., Ryu, K.H., Dohmae, N., Nakayama, H., and Lee, B.L. (2012a). Environment-mediated accumulation of diacyl lipoproteins over their triacyl counterparts in *Staphylococcus aureus*. *J. Bacteriol.* **194**, 3299–3306.
- Kurokawa, K., Ryu, K.H., Ichikawa, R., Masuda, A., Kim, M.S., Lee, H., Chae, J.H., Shimizu, T., Saitoh, T., Kuwano, K., et al. (2012b). Novel bacterial lipoprotein structures conserved in low-GC content gram-positive bacteria are recognized by Toll-like receptor 2. *J. Biol. Chem.* **287**, 13170–13181.
- Kusmartsev, S.A., Li, Y., and Chen, S.H. (2000). Gr-1+ myeloid cells derived from tumor-bearing mice inhibit primary T cell activation induced through CD3/CD28 costimulation. *J. Immunol.* **165**, 779–785.
- Lai, Y., and Gallo, R.L. (2008). Toll-like receptors in skin infections and inflammatory diseases. *Infect. Disord. Drug Targets* **8**, 144–155.
- Lai, Y., Di Nardo, A., Nakatsuji, T., Leichtle, A., Yang, Y., Cogen, A.L., Wu, Z.R., Hooper, L.V., Schmidt, R.R., von Aulock, S., et al. (2009). Commensal bacteria regulate Toll-like receptor 3-dependent inflammation after skin injury. *Nat. Med.* **15**, 1377–1382.
- Leung, D.Y., and Bieber, T. (2003). Atopic dermatitis. *Lancet* **361**, 151–160.
- Lowy, F.D. (1998). *Staphylococcus aureus* infections. *N. Engl. J. Med.* **339**, 520–532.
- Mae, M., Iyori, M., Yasuda, M., Shamsul, H.M., Kataoka, H., Kiura, K., Hasebe, A., Totsuka, Y., and Shibata, K. (2007). The diacylated lipopeptide FSL-1 enhances phagocytosis of bacteria by macrophages through a Toll-like receptor 2-mediated signalling pathway. *FEMS Immunol. Med. Microbiol.* **49**, 398–409.
- Mempel, M., Voelcker, V., Köllisch, G., Plank, C., Rad, R., Gerhard, M., Schnopp, C., Fraunberger, P., Walli, A.K., Ring, J., et al. (2003). Toll-like receptor expression in human keratinocytes: nuclear factor kappaB controlled gene activation by *Staphylococcus aureus* is toll-like receptor 2 but not toll-like receptor 4 or platelet activating factor receptor dependent. *J. Invest. Dermatol.* **121**, 1389–1396.
- Mührladt, P.F., Kiess, M., Meyer, H., Süßmuth, R., and Jung, G. (1997). Isolation, structure elucidation, and synthesis of a macrophage stimulatory lipopeptide from *Mycoplasma fermentans* acting at picomolar concentration. *J. Exp. Med.* **185**, 1951–1958.
- Müller, P., Müller-Anstett, M., Wagener, J., Gao, Q., Kaesler, S., Schaller, M., Biedermann, T., and Götz, F. (2010). The *Staphylococcus aureus* lipoprotein SitC colocalizes with Toll-like receptor 2 (TLR2) in murine keratinocytes and elicits intracellular TLR2 accumulation. *Infect. Immun.* **78**, 4243–4250.
- Naik, S., Bouladoux, N., Wilhelm, C., Molloy, M.J., Salcedo, R., Kastenmuller, W., Deming, C., Quinones, M., Koo, L., Conlan, S., et al. (2012). Compartmentalized control of skin immunity by resident commensals. *Science* **337**, 1115–1119.
- Navarini, A.A., French, L.E., and Hofbauer, G.F. (2011). Interrupting IL-6-receptor signaling improves atopic dermatitis but associates with bacterial superinfection. *J. Allergy Clin. Immunol.* **128**, 1128–1130.
- Ostrand-Rosenberg, S., and Sinha, P. (2009). Myeloid-derived suppressor cells: linking inflammation and cancer. *J. Immunol.* **182**, 4499–4506.
- Saeed, K., Marsh, P., and Ahmad, N. (2014). Cryptic resistance in *Staphylococcus aureus*: a risk for the treatment of skin infection? *Curr. Opin. Infect. Dis.* **27**, 130–136.
- Sasaki, T., Kano, R., Sato, H., Nakamura, Y., Watanabe, S., and Hasegawa, A. (2003). Effects of staphylococci on cytokine production from human keratinocytes. *Br. J. Dermatol.* **148**, 46–50.
- Schmalzer, M., Jann, N.J., Ferracin, F., Landolt, L.Z., Biswas, L., Götz, F., and Landmann, R. (2009). Lipoproteins in *Staphylococcus aureus* mediate inflammation by TLR2 and iron-dependent growth *in vivo*. *J. Immunol.* **182**, 7110–7118.
- Stadnyk, A.W. (1994). Cytokine production by epithelial cells. *FASEB J.* **8**, 1041–1047.
- Stoll, H., Dengjel, J., Nerz, C., and Götz, F. (2005). *Staphylococcus aureus* deficient in lipidation of prelipoproteins is attenuated in growth and immune activation. *Infect. Immun.* **73**, 2411–2423.
- Swamy, M., Jamora, C., Havran, W., and Hayday, A. (2010). Epithelial decision makers: in search of the 'epimmunome'. *Nat. Immunol.* **11**, 656–665.
- Takashima, A., and Bergstresser, P.R. (1996). Cytokine-mediated communication by keratinocytes and Langerhans cells with dendritic epidermal T cells. *Semin. Immunol.* **8**, 333–339.
- Travers, J.B., Kozman, A., Mousdicas, N., Saha, C., Landis, M., Al-Hassani, M., Yao, W., Yao, Y., Hyatt, A.M., Sheehan, M.P., et al. (2010). Infected atopic dermatitis lesions contain pharmacologic amounts of lipoteichoic acid. *J. Allergy Clin. Immunol.* **125**, 146–152, e141–142.
- Volz, T., Kaesler, S., and Biedermann, T. (2012). Innate immune sensing 2.0 - from linear activation pathways to fine tuned and regulated innate immune networks. *Exp. Dermatol.* **21**, 61–69.
- Volz, T., Skabytska, Y., Guenova, E., Chen, K.M., Frick, J.S., Kirschning, C.J., Kaesler, S., Röcken, M., and Biedermann, T. (2014). Nonpathogenic bacteria alleviating atopic dermatitis inflammation induce IL-10-producing dendritic cells and regulatory Tr1 cells. *J. Invest. Dermatol.* **134**, 96–104.
- Wanke, I., Skabytska, Y., Kraft, B., Peschel, A., Biedermann, T., and Schittek, B. (2013). *Staphylococcus aureus* skin colonization is promoted by barrier disruption and leads to local inflammation. *Exp. Dermatol.* **22**, 153–155.
- Wollenberg, A., Zoch, C., Wetzels, S., Plewig, G., and Przybilla, B. (2003). Predisposing factors and clinical features of eczema herpeticum: a retrospective analysis of 100 cases. *J. Am. Acad. Dermatol.* **49**, 198–205.
- Zea, A.H., Rodriguez, P.C., Atkins, M.B., Hernandez, C., Signoretti, S., Zabaleta, J., McDermott, D., Quiceno, D., Youmans, A., O'Neill, A., et al. (2005). Arginase-producing myeloid suppressor cells in renal cell carcinoma patients: a mechanism of tumor evasion. *Cancer Res.* **65**, 3044–3048.

Immunity, Volume 41

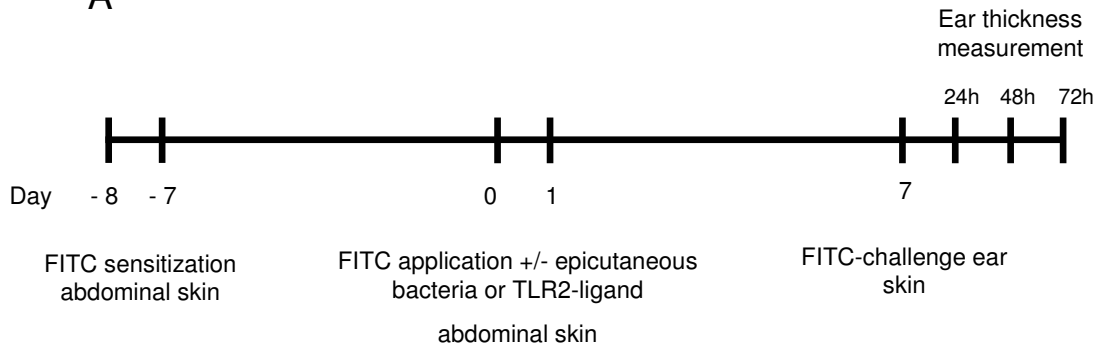
Supplemental Information

**Cutaneous Innate Immune Sensing of Toll-like
Receptor 2-6 Ligands Suppresses T Cell Immunity
by Inducing Myeloid-Derived Suppressor Cells**

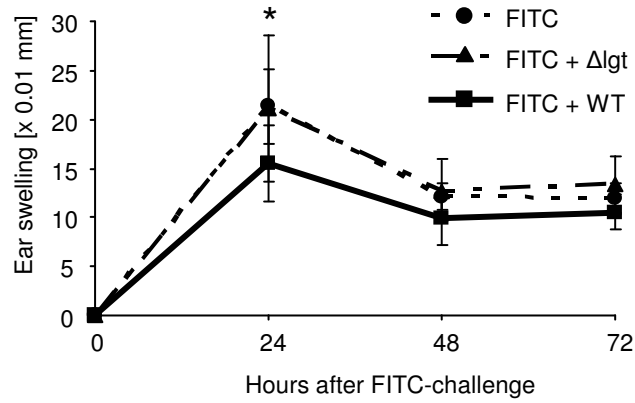
**Yuliya Skabytska, Florian Wölbing, Claudia Günther, Martin Köberle, Susanne Kaesler,
Ko-Ming Chen, Emmanuella Guenova, Doruk Demircioglu, Wolfgang E. Kempf, Thomas
Volz, Hans-Georg Rammensee, Martin Schaller, Martin Röcken, Friedrich Götz, and Tilo
Biedermann**

Figure S1

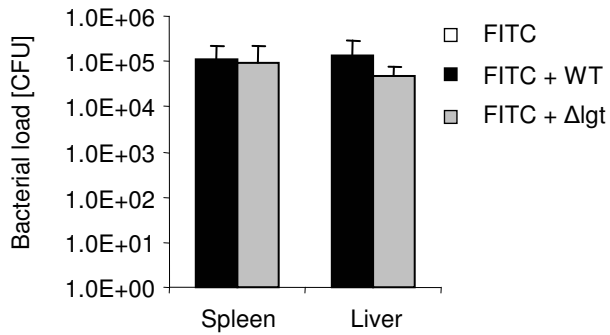
A



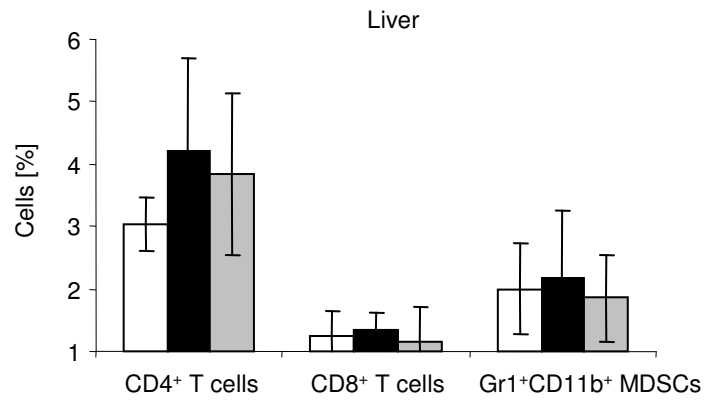
B



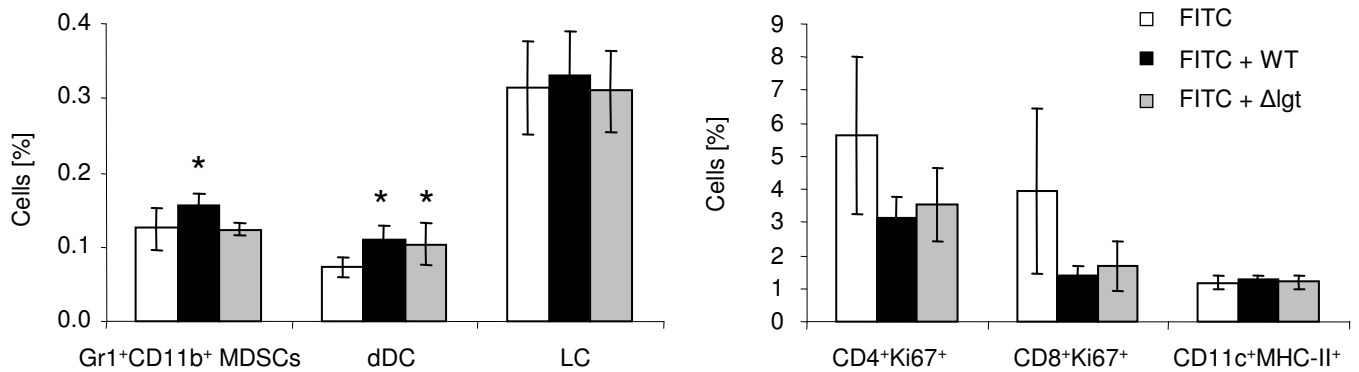
C

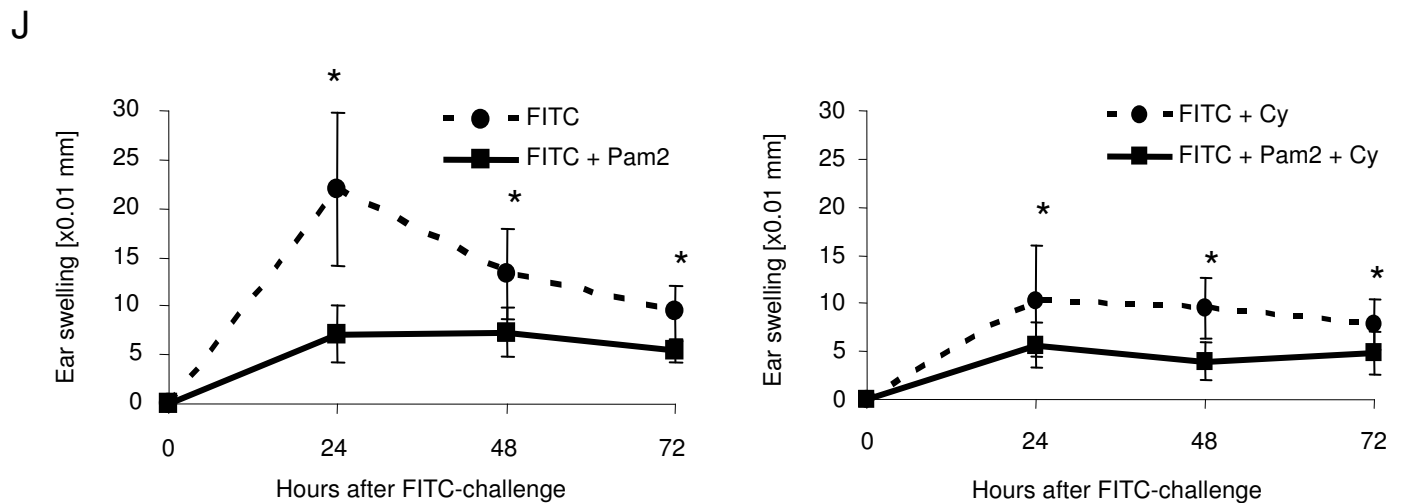
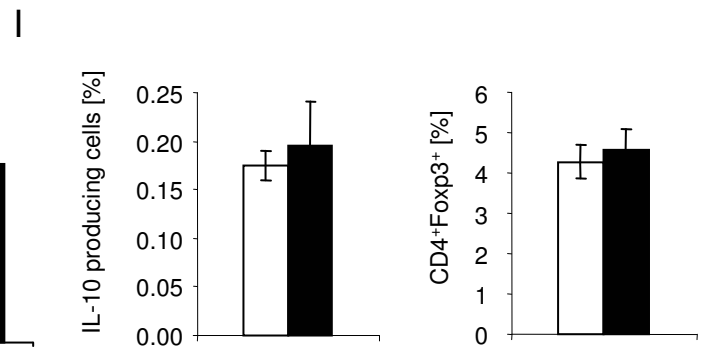
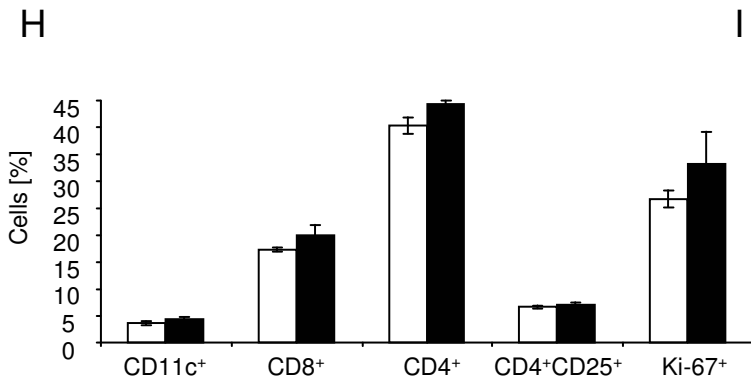
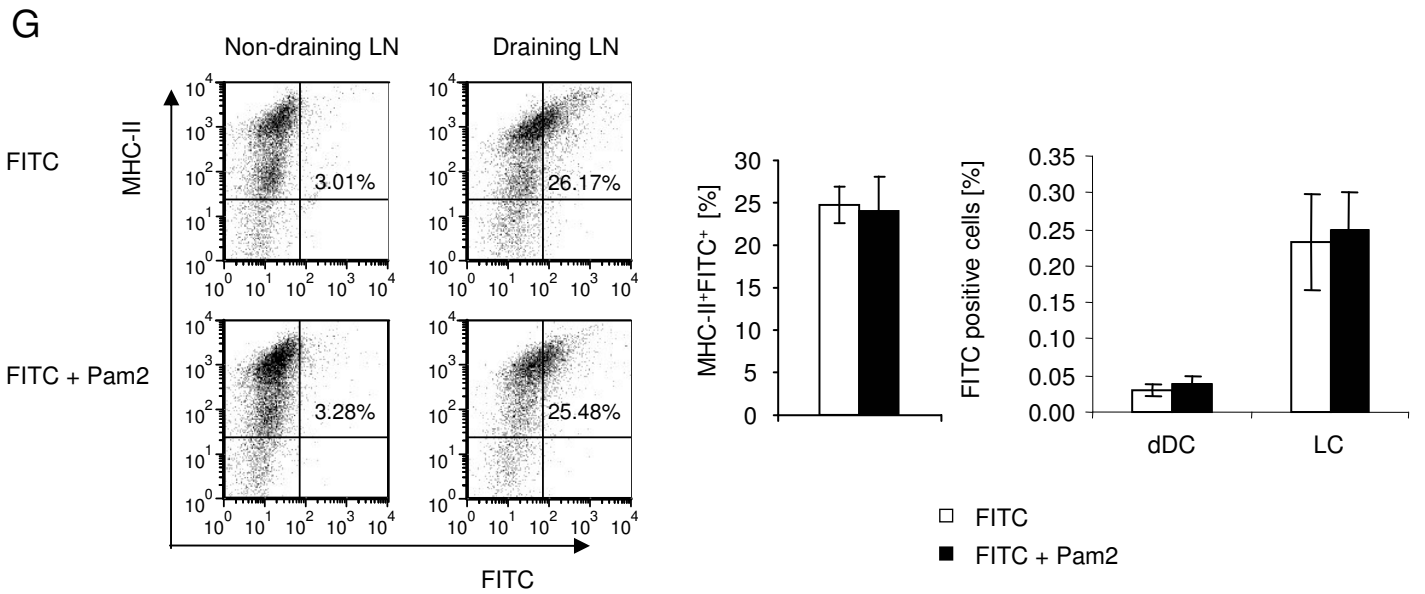
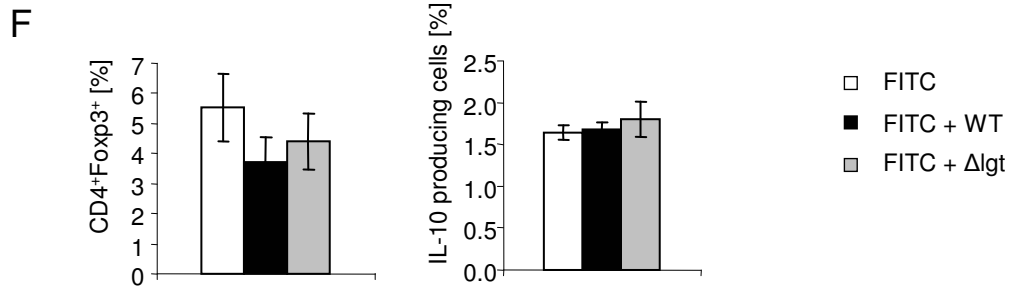


D



E





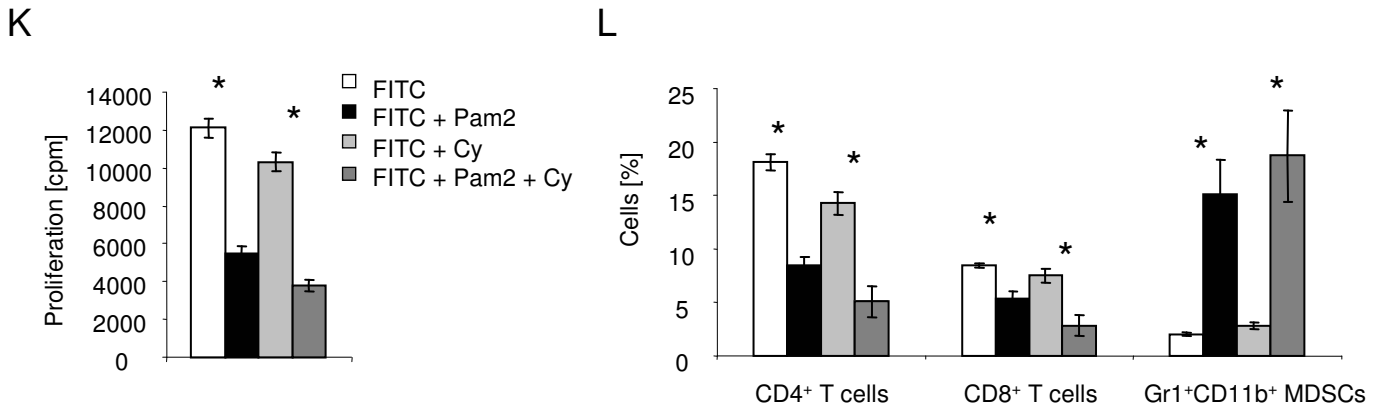


Figure S1. Cutaneous exposure to bacterial lipoproteins induces immune suppression (related to Figure 1).

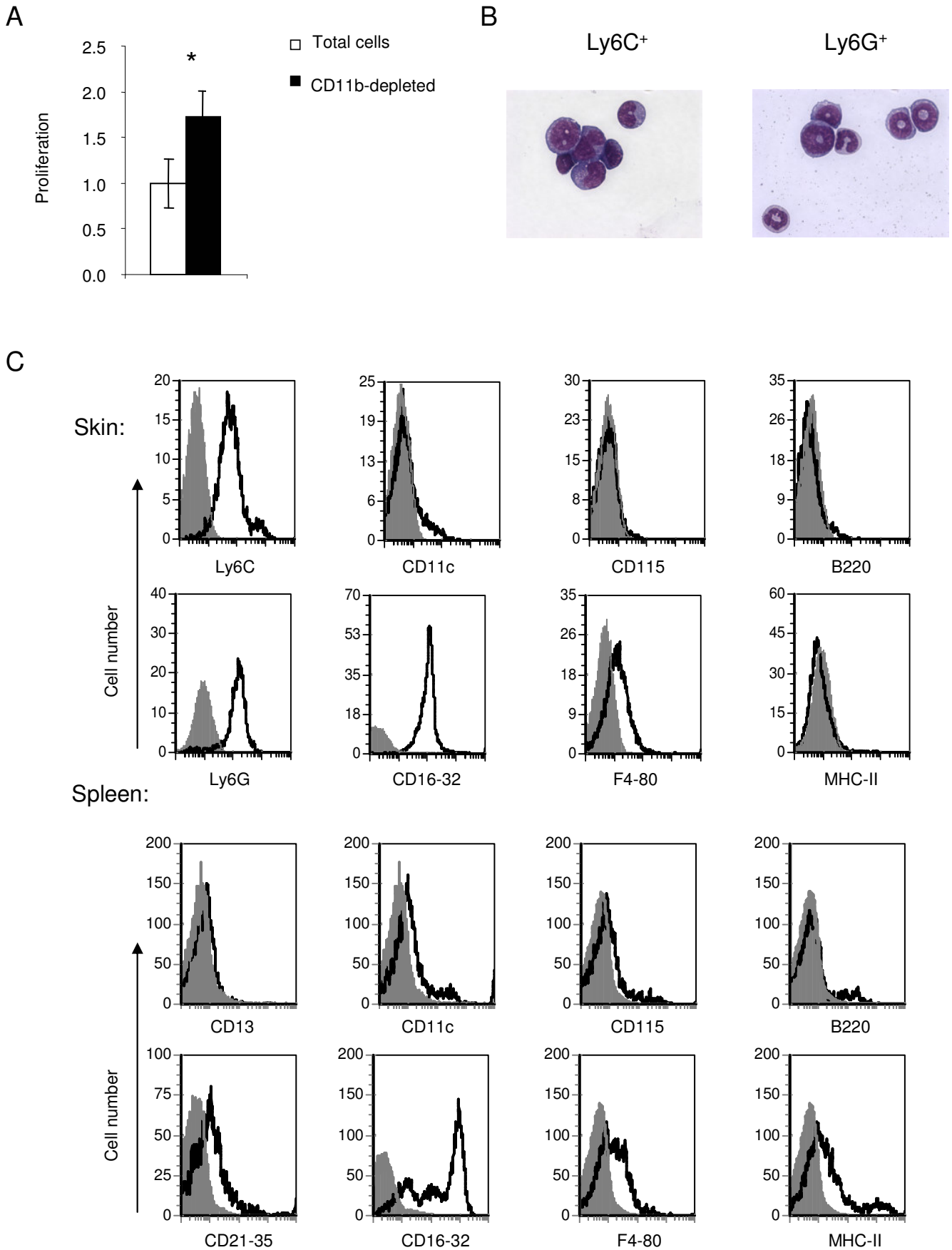
(A) Protocol of FITC-CHS with and without cutaneous exposure to *S. aureus* or TLR ligands. Wild-type (WT) mice were sensitized by administration of FITC solution on the shaved abdomen on days -8 and -7. Together with the second application of FITC on days -1 and 0, some mice were epicutaneously exposed to living WT or lipoprotein deficient (Δlgt) *S. aureus* or TLR ligands in addition. Control mice obtained phosphate-buffered saline (PBS). As read out for the cutaneous recall immune response, FITC was applied to the previously untreated ear skin on day 7 and the increase of ear thickness (ear swelling) was measured over a period of 3 days.

(B) WT mice were treated following a protocol similar to that shown in Figure S1A in which mice were sensitized by administration of FITC solution on the shaved abdomen on days -8, -7. On days -1 and 0 living WT or lipoprotein deficient (Δlgt) *S. aureus* was applied intracutaneously together with the second cutaneous application of FITC. Ear swelling was recorded following a FITC challenge on ear skin five days later (mean \pm SD, $n=5$). Data are representative of two independent experiments.

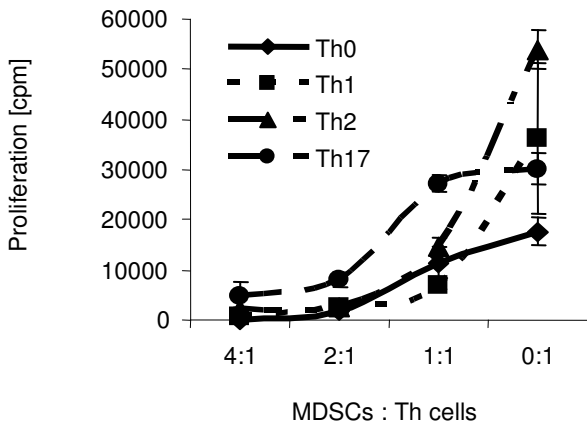
(C-I) FITC-sensitized WT mice were treated following the protocol in Figure S1A (epicutaneous exposure to WT or lipoprotein-deficient Δlgt *S. aureus* in C-F and to Pam2Cys in G-I). C-F) Bacterial load as colony forming units (CFU) (C), cell populations in the liver (D) and in draining lymph nodes (E, F) 3 days after FITC challenge were investigated (mean \pm SD, $n=5$). (G-I) Draining (axillary and inguinal) and non-draining (retroauricular) lymph nodes (LN) were collected at 14 h after the last treatment with FITC and Pam2Cys exposure (14 h after d1 in Figure S1A) and different cell populations were analyzed by flow cytometry. (G) A representative flow cytometry plot (left), means \pm SD ($n=5$) (middle) of MHC-II⁺FITC⁺ (CD11c⁺-Gate), means \pm SD ($n=5$) of dDCs (CD11c^{hi}CD205^{lo}) and LC (CD11c^{lo}CD205^{hi}) (right) and other cell populations (as a percentage of living cells) (H, I) are shown (mean \pm SD, $n=5$).

(J-L) WT mice were treated with FITC with or without cutaneous Pam2Cys exposure following the protocol in Figure S1A. Some mice were treated with 2mg cyclophosphamide (Cy) at d7 for Treg cell depletion. Ear swelling after FITC challenge (mean \pm SD, $n=5$) (J), proliferation of skin-draining lymph node cells stimulated *ex vivo* with FITC (cpm, mean \pm SD of triplicates) (K) and the percentage of cell populations in the spleen (mean \pm SD, $n=5$) (L) were investigated. *: $P < 0.05$ (unpaired, two-tailed Student's t-test).

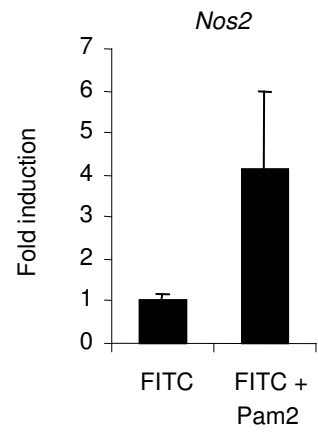
Figure S2



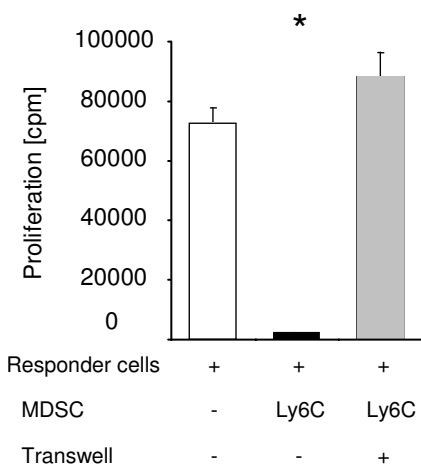
D



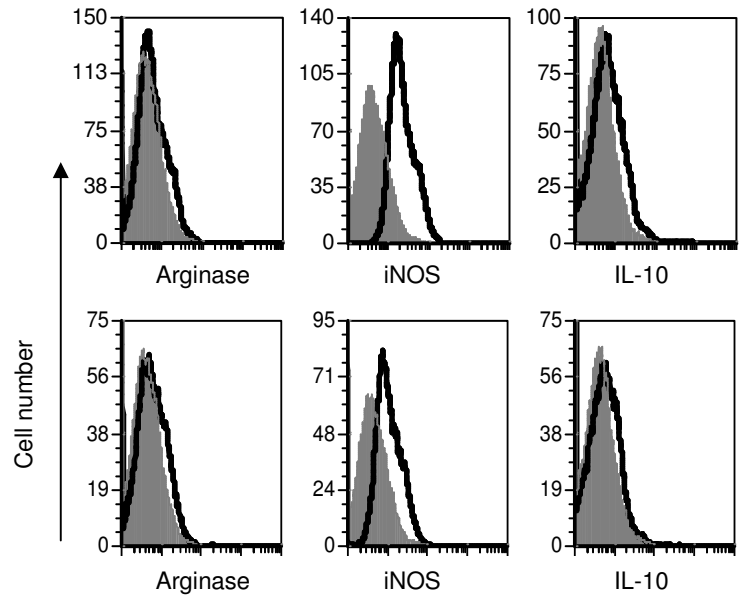
E



F



G



H

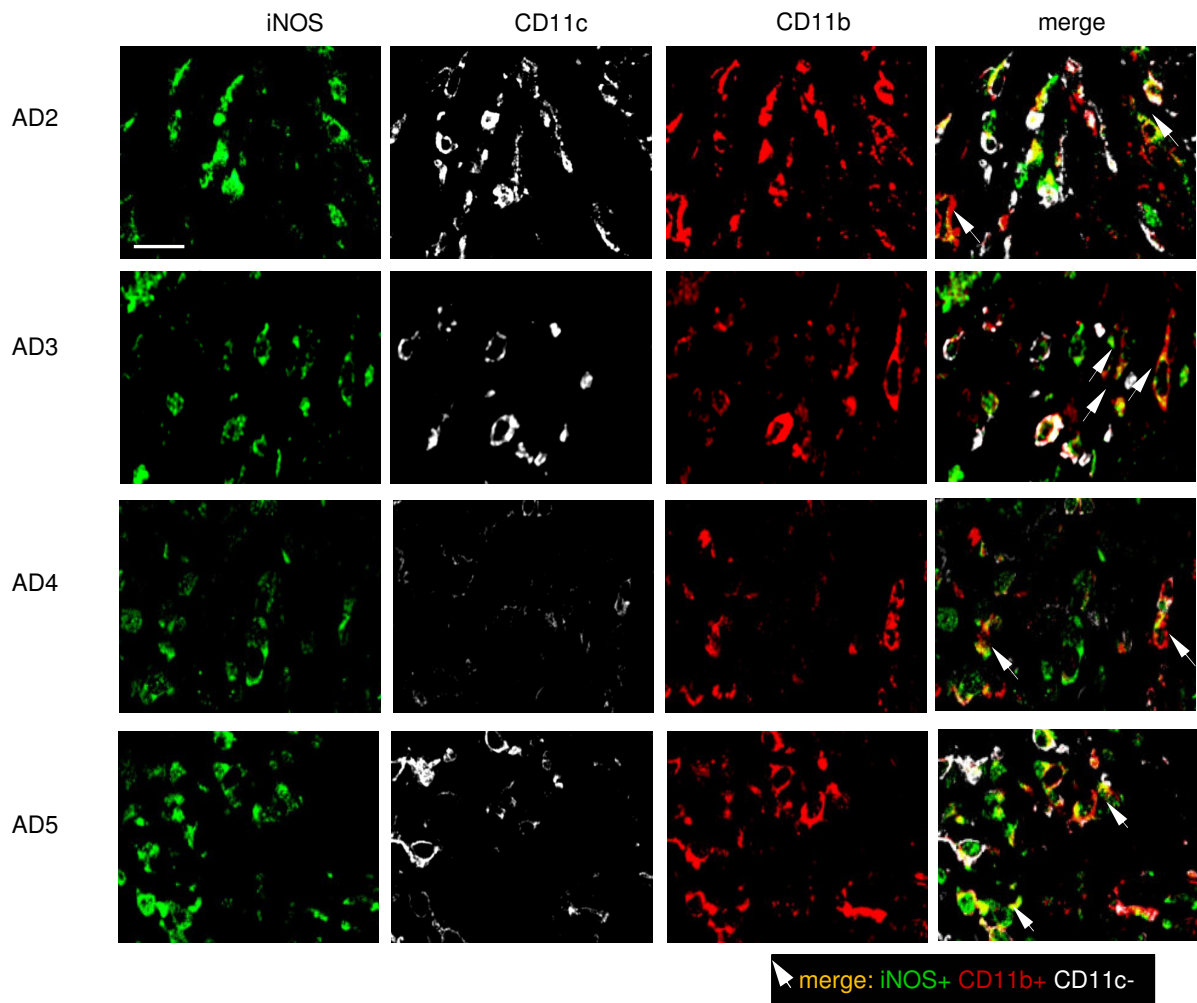
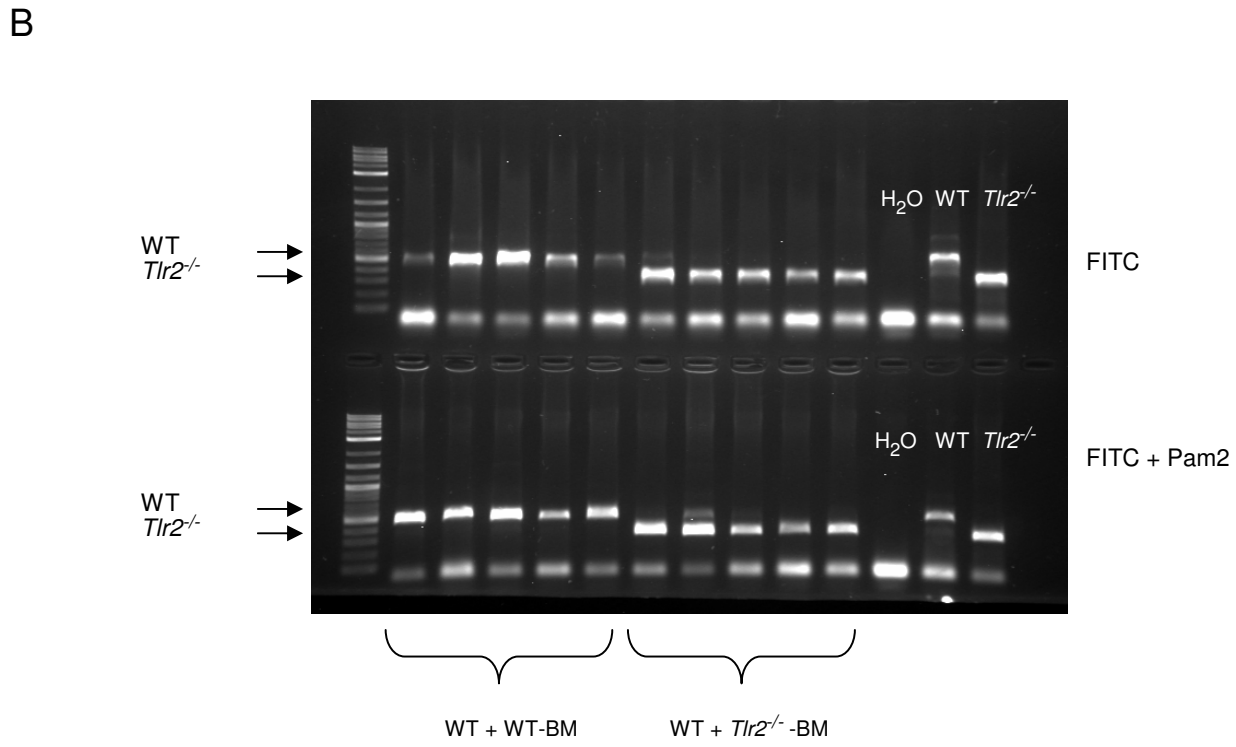
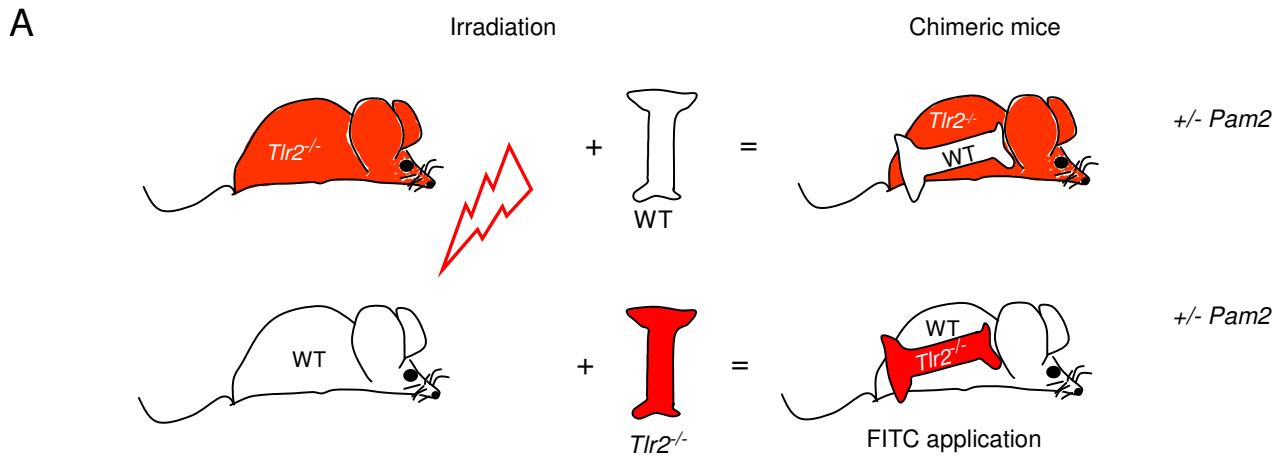


Figure S2. Myeloid-derived suppressor cells are responsible for Pam2Cys-induced immune suppression (related to Figure 3 and Figure 5).

(A-G) WT mice were treated with FITC with cutaneous Pam2Cys exposure following the protocol in Figure S1A. (A) 14h after FITC challenge, skin cells of the ears were isolated, CD11b⁺ cells ($n=5$, right) depleted or not, stimulated with anti-CD3-CD28-mAbs and analyzed for proliferation (as cpm, mean \pm SD, $n=5$). *: $P < 0.05$ (unpaired, two-tailed Student's t-test). (B-D) Gr-1^{dim}Ly6G⁻Ly6C⁺CD11b⁺ (Ly6C⁺) and Gr-1^{high}Ly6G⁺CD11b⁺ (Ly6G⁺) cells were isolated 10 days after Pam2Cys exposure by MACS from spleens of Pam2Cys-exposed mice. Afterwards cytopsin preparations were made from splenic MDSCs and the morphology was analyzed by histological staining (May-Grünwald-Giemsa) in (B). Original magnification was x100, representative images are shown. (C) The phenotype of the Gr1⁺CD11b⁺ cells (skin, 14 h after FITC challenge from Pam2Cys-treated mice) or suppressive Ly6C⁺ MDSCs (spleen) was analyzed for surface marker expression by flow cytometry as indicated (gated for Gr1⁺CD11b⁺ cells in the skin and Ly6C⁺Ly6G⁻ cells in the spleen). One representative result is shown. (D) Polarized T cells were co-cultured *in vitro* with Ly6C⁺ MDSCs as indicated, stimulated by anti-CD3-CD28-mAbs and analyzed for proliferation. (E) 8 h after the FITC challenge ear skin cells were analyzed for *Nos2* expression by qRT-PCR (normalized to housekeeping genes β -actin-GAPDH), mean \pm SEM (right, $n=5$) is shown. Expression of the skin of FITC only-exposed mice was set as 1. (F) Proliferation of anti-CD3-CD28-mAbs stimulated spleen cells was measured with or without the addition of Ly6C⁺ cells (ratio 2:1) (black and white bars, respectively) or in the presence of a transwell membrane (grey bars). Results are expressed as mean \pm SD of experimental triplicates. Significant differences between experimental conditions were assessed by one-way ANOVA followed by Tukey's post hoc test (*: $P < 0.05$). (G) Gr1⁺ cells of the coculture of (F) were stained for iNOS, Arginase and IL-10 by intracellular flow cytometry (Gate for Gr1⁺ cells).

(H) Skin tissue of AD patients was analyzed by immunofluorescence staining for CD11b (red), CD11c (white) and iNOS (green) and visualized by confocal microscopy. Arrows indicate cells positive for CD11b and iNOS and negative for CD11c. Scale bar represents 25 μ m.

Figure S3



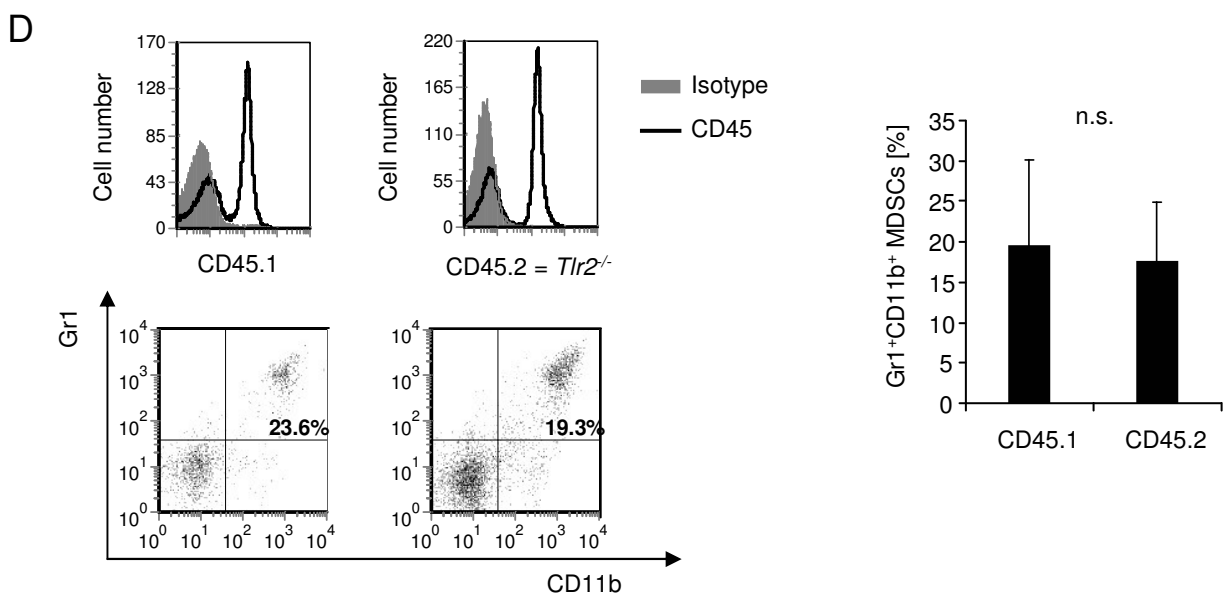
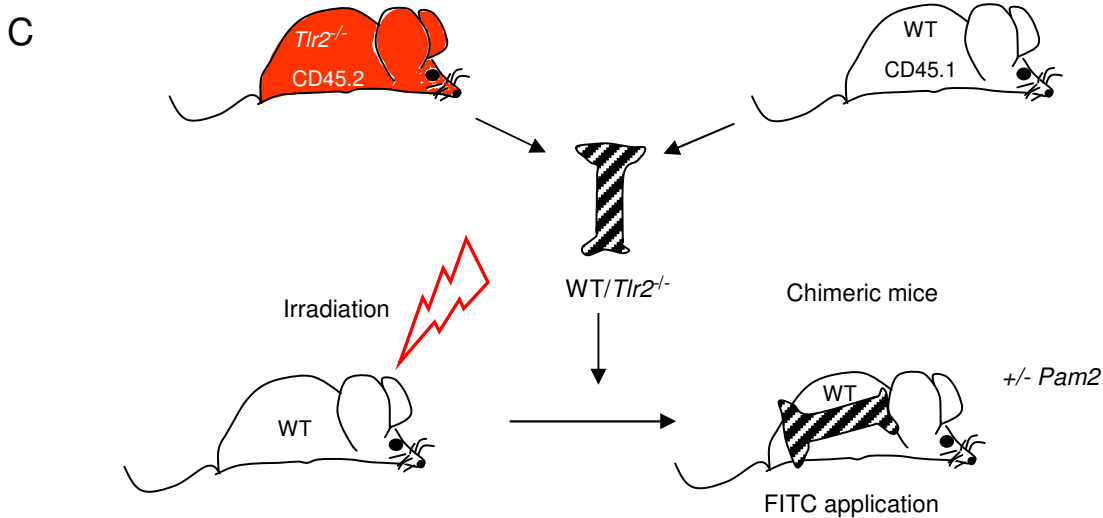


Figure S3. Pam2Cys-induced immune suppression is dependent on TLR2 (related to Figure 6).

(A) Protocol for the generation of chimeric mice. WT mice were irradiated and reconstituted with WT or $Tlr2^{-/-}$ bone marrow (BM) cells. 7 weeks later, the mice were treated following the protocol shown in Figure S1A.

(B) To confirm the chimerism of mice, genotyping of BM cells by PCR for the WT and the mutated TLR2 gene was conducted.

(C) Protocol for the generation of chimera-mix mice. WT mice were irradiated and reconstituted with BM consisting of 50% of CD45.1⁺ wild-type and 50% CD45.2⁺ $Tlr2^{-/-}$ cells. 7 weeks later, the mice were treated following the protocol shown in Figure S1A.

(D) Chimera-mix mice were generated. Representative flow cytometry histograms are shown. Gray filled line: isotype control, black line: respective CD45 allele stain (left, top). Spleen cells were isolated and analyzed by flow cytometry. The percentage of Gr1⁺CD11b⁺ cells in the spleens is shown as a representative flow cytometry plot (left, bottom) or quantification (mean +/- SD, $n=10$) (right). Data are representative of three independent experiments. *: $P < 0.05$ (unpaired, two-tailed Student's t test). n.s., not significant.

Figure S4

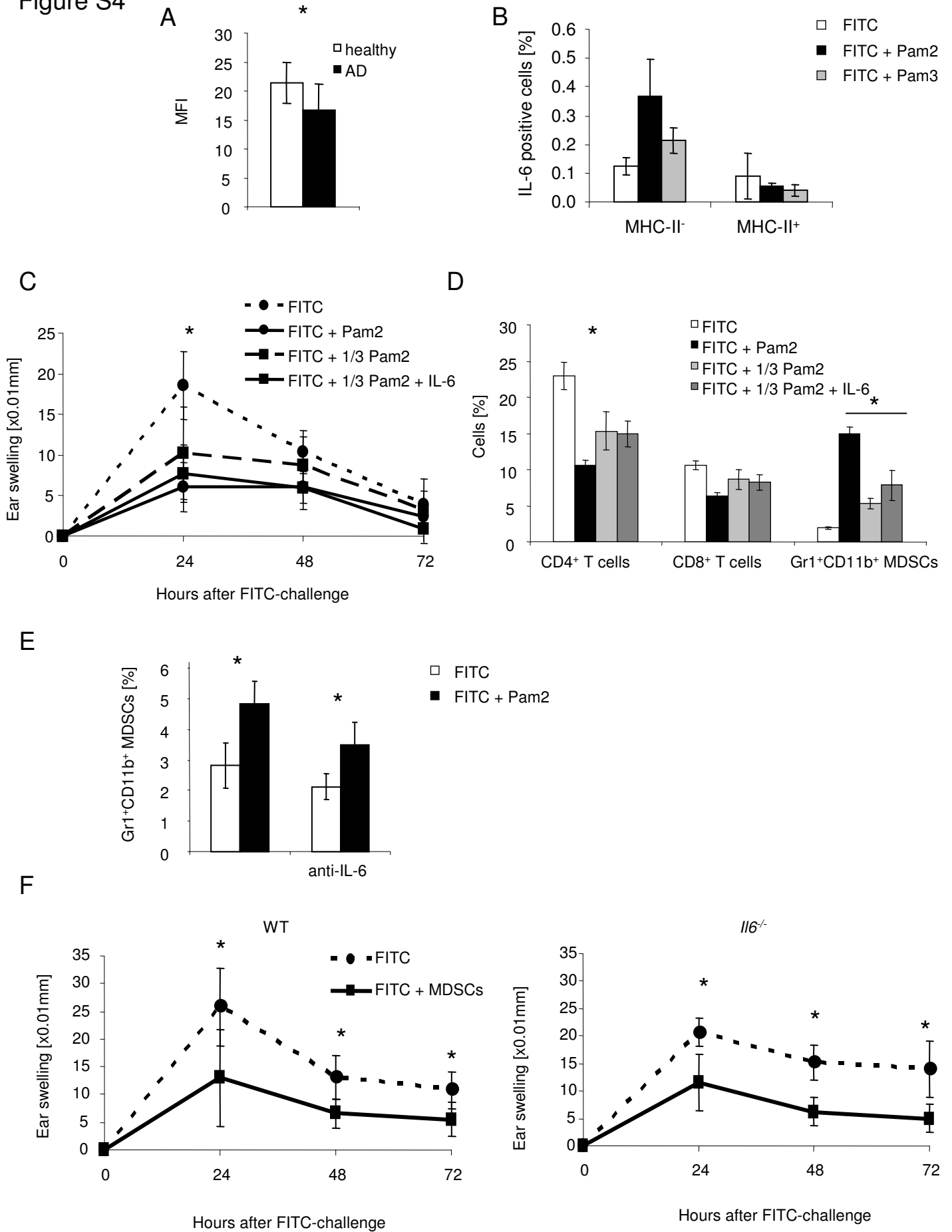


Figure S4. Skin-derived IL-6 is required for induction of Gr1⁺CD11b⁺ cells, but not needed for MDSC migration to the skin and for the suppressive function of developed MDSCs (related to Figure 7).

(A) Skin tissue of AD patients from Figure 4C was analyzed by immunofluorescence staining for TLR2 and visualized by confocal microscopy. A cumulative analysis of mean fluorescence intensity, MFI (mean \pm SD, $n=8$) is shown. *: $P < 0.05$ (Mann-Whitney test).

(B-E) WT mice were treated following a protocol similar to that shown in Figure S1A (with Pam2Cys treatment). (B) 24 h after cutaneous exposure to PBS (control), Pam2Cys or Pam3Cys, skin cells were isolated and analyzed for IL-6 production by intracellular flow cytometry (gate: living cells), a cumulative analysis (mean \pm SD, $n=5$) is shown. (C, D) Some mice were exposed to a lower dose of Pam2Cys (1/3 of dose); some mice were treated with 20 μ g rIL-6 at d 7 and d 8 of the protocol. Ear swelling after FITC challenge (C) and the percentage of cell populations in the spleen (D) (mean \pm SD, $n=5$) were analyzed. (E) 2 h before FITC challenge one group of mice was treated i.p. with anti-IL-6 (50 μ g/mouse). 8 h after FITC challenge cells were isolated from ear skin and the percentage of Gr1⁺CD11b⁺ cells was analyzed by flow cytometry. A cumulative result (mean \pm SD, $n=5$) is shown.

(F) WT and *Il6*^{-/-} mice were treated following the protocol shown in Figure S1A (without Pam2Cys exposure). One group of mice received Ly6C-Ly6G positive cells from donors that were sensitized with FITC and exposed to Pam2Cys. The control group received spleen cells from naïve mice (see Methods, adoptive transfer). The ear swelling response after FITC challenge (mean \pm SD, $n=5$) is shown. *: $P < 0.05$ (unpaired, two-tailed Student's t test).

Supplemental Experimental Procedures

Quantitative real-time PCR

Total RNA was extracted with peqGOLD total RNA Kit (Peqlab, Erlangen, Germany) and reverse-transcribed to cDNA with iScript cDNA Synthesis Kit (Bio-Rad, München, Germany). The real-time PCR assay was carried out with Light-Cycler LC480 (Roche, Basel, Switzerland). Data are presented as normalized to housekeeping genes β -actin and GAPDH.

Primer	Sequence forward	Sequence reverse
<i>Actb</i>	CTGAAGCAGCTATGGCAACT	GGATGCTCTCATCTGGACAG
<i>Gapdh</i>	TGGAGAAACCTGCCAAGTATG	GTTGAAGTCGCAGGAGACAAC
<i>Tnf</i>	CTGTAGCCCACGTCGTAGC	TGGAGATCCATGCCGTTG
<i>Cxcl2</i>	CCAGACTCCAGCCACACTTC	AGGGTCTTCAGGCATTGACA
<i>Il6</i>	GCTACCAAACCTGGATATAATCAGGA	CCAGGTAGCTATGGTACTCCAGAA
<i>Ifny</i>	ATCTGGAGGAACTGGCAAAA	TTCAAGACTTCAAAGAGTCTGAGGTA
<i>Il4</i>	TCAACCCCCAGCTAGTTGTC	TGTTCTTCGTTGCTGTGAGG
<i>Il10</i>	TGGGTGAGAAGCTGAAGACC	TGGCCTTGTAGACACCTT
<i>Il17</i>	AACCGATCCACCTCACCTT	GGCACTTTCCTCCAGAT
<i>Ccl2</i>	GGACCCATTCTTCTTGG	ACAAGAGGATCACCAGCAGC
<i>Ccl3</i>	CCTGCTCAACATCATGAAGGTCTC	GGTCAGTGATGTATTCTTGGACC
<i>Ccl4</i>	AACCCCGAGCAACACCATGAAG	CCACAATAGCAGAGAAACAGCAAT
<i>Ccl5</i>	TCCTTCGAGTGACAAACACGA	TGCTGCTTTCCTACCTCTC
<i>Ccl11</i>	TCCACAGCGTTCTATTCTT	CTATGGCTTTCAGGGTGCAT
<i>Ccl13</i>	GGTGGTGTTGAGTCTAGA	GCACATATGAGGAGATTCCG
<i>Ccl17</i>	AGTGGAGTGTTCCAGGGATG	CTGGTCACAGGCCGTTTTAT
<i>Ccl20</i>	CGACTGTTGCCTCTCGTACA	AGGAGGTTACAGCCCTTTT
<i>Ccl22</i>	GTCCTAGGGAGGAGGACCTG	GAAGGGGATAAGCTGGAAG
<i>Ccl27</i>	CTCCCGCTGTTACTGTTGCT	TCTGGGGATGAACACAGACA
<i>Ccl28</i>	TGGCAAAAGCCACATTCATA	CATGCCAGAGTCGAACAGAA

Immunofluorescence staining

For staining of human samples, primary antibodies (rabbit α -human CD11b (Life Span, Seattle, USA), mouse IgG1 α -human iNOS, rabbit polyclonal α -human TLR2 (Abcam, Cambridge, United Kingdom), mouse IgG2a α -human CD11c (Novocastra, Wetzlar, Germany) were applied to deparaffinized sections at room temperature. After washing, fluorescence-labelled secondary antibodies (goat F(ab')₂ α -rabbit-IgG-AF546, goat α -mouse-IgG1-AF647, goat F(ab')₂ α -mouse-IgG2a-AF488 (Life Technologies, Darmstadt, Germany)) were applied. Sections were mounted with DAPI (4,6 diamidino-2-phenylindole)-containing medium (Vector Laboratories Inc., Burlingame, USA). Stained sections were examined under a LSM confocal microscope (Zeiss, Jena, Germany).

For staining of mouse skin, Pam2, Pam3 or PBS was injected into the skin and 24 h later epidermis was cryofixed in liquid nitrogen, and 5- μ m sections were placed on Silane-Prep slides (Sigma-Aldrich Chemie GmbH, München, Germany). Sections were fixed in periodate-lysine-paraformaldehyde (paraformaldehyde and lysine in PBS) for 2 minutes, followed by incubation with PBS for 5 minutes, PBS/BSA (0.1%) plus Tween 20 (0.1%) for 5 minutes, and PBS plus 10% donkey serum for 30 minutes at room temperature. Anti TLR2 monoclonal rat antibody (1:50), anti-TLR1 or TLR6 polyclonal rabbit antibodies (1:100) (Abcam, Cambridge, Great Britain) were added for 60 minutes at room temperature. Sections were then incubated with donkey anti-rat-Dylight 549 or donkey anti-rabbit-Dylight 649 (1:800; Dianova, Hamburg, Germany) for 60 minutes. All nuclei were stained with YOPRO (Invitrogen, Darmstadt, Germany). All washing and antibody addition steps were performed with a combination of PBS, BSA, and Tween. The sections were analyzed with a confocal laser scanning microscope (Leica TCS SP; Leica Microsystems) at 630 magnification.

Isolation of Gr1⁺CD11b⁺ cells

Gr-1^{dim}Ly6G⁻Ly6C⁺CD11b⁺ and Gr-1^{high}Ly-6G⁺CD11b⁺ cells were isolated from spleens using the MDSCs Isolation Kit (Miltenyi Biotech, Bergisch Gladbach, Germany) according to

manufacturer's protocol. Purity was routinely more than 90% as assessed by flow cytometry analysis.

Gr-1 depletion

200µg/mouse of Ly6G depleting antibody (eBioscience, San Diego, USA) or isotype control was injected to mice i.p. at day 3 and 5 of the protocol shown in Figure S1A.

Skin cell analysis

Skin cell suspensions were generated by incubating skin tissue with dispase-II (Sigma-Aldrich, Taufkirchen, Germany) overnight at 4°C. Afterwards the human skin was incubated in collagenase A (Serva, Heidelberg, Germany) for 30 min at 37°C and then homogenized by GentleMACS (Miltenyi, Biotech, Bergisch Gladbach, Germany). Dermis and epidermis of mice skin was separated and incubated in collagenase A (Serva, Heidelberg, Germany) or trypsin-EDTA (Biochrom Berlin, Germany), respectively, for 30 min at 37°C for the digestion. Afterwards the obtained cell suspensions of epidermis and dermis were pooled, washed twice and analyzed by flow cytometry. For intracellular flow cytometry, ear skin tissue was incubated with Brefeldin A (Sigma-Aldrich, Taufkirchen, Germany) (20 µg/ml) for 2h at 37°C.

Bone marrow-derived MDSCs

BM cells were isolated from naïve BALB/c mice and cultured in medium with 20ng/ml GM-CSF (R&D Systems, Minneapolis, USA) for 4 days. Afterwards the cells were harvested and cocultured with spleen cells (ratio 1:4), activated with anti-CD3 (2µg/ml)/anti-CD28 (1µg/ml) for proliferation. Proliferation was evaluated by ³H-thymidine incorporation (as counts per minute, cpm) during the last 10 hours of culture.

Bacteria preparation

Following 1:100 dilution of an overnight culture in LB medium, *Staphylococci* were grown with shaking at 37°C to an optical density at 600 nm of 0.4-0.6. Culture aliquots were sedimented by centrifugation, and *Staphylococci* were washed and suspended in PBS.

T cell proliferation assay

Splenocytes from naïve BALB/c mice were cultured in the presence of 4 µg/ml anti-CD3 and 2 µg/ml anti-CD28 (Biolegend, San Diego, USA). Gr-1^{dim}Ly6G⁻Ly6C⁺CD11b⁺ (Ly6C⁺) and Gr-1^{high}Ly-6G⁺CD11b⁺ (Ly6G⁺) cells were isolated from the spleens of Pam2Cys-exposed mice (protocol Figure S1A) and added to the cultures at different ratios. Proliferation was evaluated by ³H-thymidine incorporation (as counts per minute, cpm) during the last 10 hours of culture. For some assays iNOS inhibitors N^G-Methyl-L-arginine acetate salt (L-NMMA, 4mM, Sigma-Aldrich, Taufkirchen, Germany) and L-N6-(1-Iminoethyl)lysine dihydrochloride (L-NIL, 0.5mM, Sigma-Aldrich, Taufkirchen, Germany) were used.

Adoptive transfer

A total of 20 x 10⁶ MDSCs (3-4 x 10⁶ Ly6C⁺ and 16-17 x 10⁶ Ly6G⁺) from spleen or BM cells from Pam2Cys-exposed mice were injected i.v. into FITC-sensitized mice on days 2, 4, and 6. As controls, spleen or BM cells from naïve mice were transferred at the same time points.

Primary human keratinocytes

Primary human keratinocytes were isolated from foreskin. Epidermis was dissected from the dermis using dispase-II (Sigma-Aldrich, Taufkirchen, Germany) and cultured in keratinocyte medium (KGM2; PromoCell, Heidelberg, Germany) containing a supplement mix (5mg/l insulin, 0.1mM ethanolamine, 0.1 phosphoethanolamin, 5 x 10⁻⁷M hydrocortison (Sigma-Aldrich, Taufkirchen, Germany), 100mg/l penicillin/streptomycin, 0.4µg/l EFG (Thermo Fisher Scientific Inc, Waltham, USA). To expand cell populations, keratinocytes were grown in low Ca²⁺ (0.06 mM). For experiments, the Ca²⁺ concentration was increased to 1.8 mM to promote differentiation.

The generation of Newman Δlgt mutant

The Newman Δlgt mutant was generated exactly as described in (Stoll et al., 2005) for SA113. For deletion of the *lgt* gene in the genome of *S. aureus* strain Newman, a 1-kb fragment including *hprK* was generated by PCR using Pwo polymerase (Hybaid). An EcoRI restriction site was introduced into the forward primer and a SmaI restriction site into the reverse primer. The fragment was subcloned into pUC18 digested with the same restriction enzymes, yielding pUC18*hprK*. A 1.1-kb fragment including the entire *yvoF* gene and the 5' end of the *yvcD* gene was amplified using SmaI and a BamHI restriction sites, respectively, and ligated into pUC18 *hprK*. The *ermB* gene from Tn551 was removed from pEC2 by 5' cleavage with XbaI and 3' cleavage with HindIII, the ends were filled in with Klenow enzyme, and *ermB* was blunt end ligated into the SmaI site between the *hprK* and *yvoF* genes in pUC18. The inserted fragments were sequenced and introduced into the temperature-sensitive shuttle vector pBT2 harboring the Cm^r marker gene *cat*. The resulting inactivation plasmids were designated pBT-*lgt for* and pBT-*lgt rev*. After construction in *E. coli*, the plasmids were separately electroporated into *S. aureus* RN4220, purified after selection of transformants on Cm-containing BM agar plates, and electroporated into *S. aureus* strain Newman.

Insertional inactivation of *lgt* by homologous recombination was achieved as described in (Bruckner, 1997). Single Em-resistant and Cm-sensitive colonies were presumed to have undergone double crossover and were obtained from cultures harboring the pBT*lgt for* plasmid. The *lgt::ermB* genotype of two colonies was confirmed by PCR analysis and sequencing.

Th polarized culture

To prepare CD4⁺ polarized cells, CD4⁺CD62L⁺ T cells were purified from peripheral LN cells and spleen obtained from naïve BALB/c mice by negative selection using MACS beads (Miltenyi Biotech, Bergisch Gladbach, Germany). Cells were stimulated with 4µg/ml anti-

CD3 (Th17) or 4-2 μ g/ml anti-CD3-anti-CD28 (Th0, Th1, Th2). For Th1 polarizing conditions CpG 1668 (0.2 μ M, Eurofins Genomics, Ebersberg, Germany) and anti-IL-4 (1 μ g/ml, α 11B11) were added at d0. For Th2 polarizing conditions IL-4 (50ng/ml, Promokine, Heidelberg, Germany), anti-IFN- γ (5 μ g/ml, Biolegend, San Diego, USA) were added at d0 and d3. For Th17 polarizing conditions anti-IL-4 (1 μ g/ml), anti-IFN- γ (5 μ g/ml, Biolegend, San Diego, USA), TGF β (2ng/ml, R&D Systems, Minneapolis, USA) and IL-6 (10ng/ml, Biolegend, San Diego, USA) were added at d0; at d4 the cells were restimulated with anti-CD3 and IL-23 (10ng/ml, R&D Systems, Minneapolis, USA) was added. All T cell cultures were supplemented with IL-2 (5 ng/ml) for up to 8 days. Then, the cells were used for the coculture experiment with MDSCs. To prove polarization, the cells were stimulated with PMA/Ionomycin (Sigma Aldrich, Taufkirchen, Germany) in the presence of BD GolgiStop (BD Biosciences, Heidelberg, Germany), then the cells were stained for detection of intracellular cytokines. Supernatants after the stimulation were collected for ELISA.

Flow cytometry

Flow cytometry data were acquired using a LSRII flow cytometer (BD Biosciences, Heidelberg, Germany) and then analyzed using FCS Express V3 Software (De Novo Software, San Diego, USA).

Antibodies: Antibody, Clone, Catalog number

Mouse:

B220-PE, RA3-6B2, BD Pharm. #553090

CD11b-PB, M1/70, Biolegend #101224

CD11b-FITC, M1/70, BD Pharm. #557396

CD4-PB, RM4-5, BD Pharm. #558107

CD8-FITC, 53-6.7, Biolegend #100706

CD3 funct., 145-2C11, Biolegend #100314

CD3-APC, 145-2C11, Biolegend #100312

CD11c-APC, N418, Biolegend #117310

CD13-FITC, R3-242, BD Pharm. #558744

CD16/32 funct., FCR-4G8

CD16/32-PE-Cy7, 93, eBiosc. #25-0161-82

CD21/35-APC-Cy7, 7E9, Biolegend #123419

CD28 funct., 37.51, Biolegend #102112

CD45.1-PerCP, A20, BioLegend #110726

CD45.2-PB, 104, Biolegend #109820

CD115-PE, AFS98, Biolegend #135505

F4/80-PE; BM8, BioLegend #123110

Gr1-APC, RB6-8C5, Biolegend #108411

IFN γ -PE, XMG1.2, BD Pharm. #554412

MHC-II-PE, M5/114.15.2, Biolegend #107608

Ly-6G (Gr-1), Functional Grade Purified, RB6-8C5, eBioscience #16-5931-86

CCR3-Alexa flour 647, J073E5, Biolegend #144507

CCR4-APC, 2G12, Biolegend #131212

CCR10-APC, 248918, R&D #FAB2815A

IL-10-PE, JES5-16E3, BioLegend #505007

Human:

CD11b-PB, ICRF44, Biolegend #301316, Charles N, et al. 2010

CD11c-APC, 3.9, Caltag, #MHCD11c05, Wimazal F, et al. 1999

CD14-FITC, HCD14, Biolegend #325603, Séguier S, et al. 2013

CD33-PE, WM53, Biolegend #303403, Pèrez-Oliva AB, et al. 2011

HLA-DR-APC, L243, Biolegend #307609, Zaba LC, et al. 2007

iNOS-FITC, polyclonal, Biorbyt #orb14179, Guo Z, et al. 2013

References:

Bruckner, R. (1997). Gene replacement in *Staphylococcus carnosus* and *Staphylococcus xylosus*. *FEMS microbiology letters* 151, 1-8.

Stoll, H., Dengjel, J., Nerz, C., and Götz, F. (2005). *Staphylococcus aureus* deficient in lipidation of prelipoproteins is attenuated in growth and immune activation. *Infect Immun* 73, 2411-2423.